

**STUDIES ON THE MICROSTRUCTURE AND MECHANICAL
PROPERTIES OF RECYCLED CAST ALUMINIUM SCRAP**

BY

THOMAS OCHUKU MBUYA

B.Sc. HONS (U.o.N)

**A DISSERTATION SUBMITTED IN PARTIAL SATISFACTION OF THE
REQUIREMENTS OF THE DEGREE**

OF

MASTER OF SCIENCE

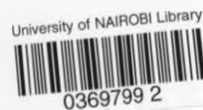
IN

**MECHANICAL ENGINEERING
(INDUSTRIAL ENGINEERING OPTION)**

OF THE

UNIVERSITY OF NAIROBI

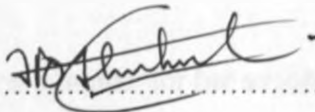
2003



UNIVERSITY OF NAIROBI
EAST AFRICANA COLLECTION

DECLARATION

Except where otherwise stated, this dissertation contains my own work. The work I have presented here has not been submitted in whole or in part at this university or any other institution of learning for examination, or any other purposes.

Mr. Thomas Ochuku Mbuya..........Date.....5/11/2003.....

This dissertation has been submitted for examination with our knowledge and approval as university supervisors:

Eng. B.O. Odera..........Date.....5/11/03.....

Dr. S.P. Ng'ang'a..........Date.....5/11/03.....

Mr. S.K. Ngugi..........Date.....

DEDICATION

I dedicate this work to my mother for her unconditional love and devotion.

ACKNOWLEDGEMENT

I gratefully acknowledge the assistance I received from my supervisors Eng. B.O. Odera, Dr. S.P. Ng'ang'a and Mr. S.K. Ngugi. Throughout the project period, they have provided me with invaluable professional and friendly advice. It has been my greatest pleasure to work with them.

I am thankful to the University of Nairobi for the partial sponsorship and to Jomo Kenyatta University of Agriculture and Technology for providing materials and finances for this research through the Walking Tractor Project, which is headed by Mr. S. K. Ngugi. My gratitude also goes to the several scholars who provided me with relevant reference materials. I am also grateful to the following people:

- Miss Irene for tirelessly typing the manuscript
- Mr. Njue for patiently working with me both in the foundry and metallurgy laboratories
- Mr. Ndulu and Mr. Githome for their assistance in mechanical tests
- Mr. Kingori for his assistance in heat treatment
- Mr. Apondi for his assistance in machining test specimens

Finally, but not least, I wish to thank my parents, relatives, friends and colleagues for all their support.

Thomas Ochuku Mbuya

ABSTRACT

The aluminium casting industry in Kenya is strongly dependent on aluminium scrap recycling. There is, however, little organised information on appropriate recycling procedures and the expected chemical composition of the resulting secondary alloys. Furthermore, little is also known on the expected mechanical properties of castings produced from the secondary alloys under different processing conditions. Consequently, the quality of locally produced castings is poor compared to their imported counterparts as most Kenyan foundries rely on chance to make good castings.

The main objectives of this preliminary study were: (a) to determine the chemical composition of the secondary alloys obtained from recycling various cast aluminium scrap components available in Kenya; and (b) to determine the microstructure, tensile strength, percent elongation and hardness obtainable from these alloys using both green sand and permanent mould casting processes and under different process conditions. The process parameters for both green sand and permanent mould casting processes, whose influence on the said properties was investigated are: the type of mould filling system, melt handling and pouring temperature. The influence of the thickness and initial temperature of permanent moulds on these properties was also investigated.

It was found in this study that the common types of scrap components available in Kenya are automotive engine parts. Most of these components were found to be pistons, cylinder heads, gearbox housings and to a lesser extent, rear axle housings. Pistons and cylinder heads were classified as individual groups while gearbox and rear axle housings were grouped together. The rest of the scrap items, most of which could not be identified, were lumped together to form another separate group. Samples were randomly picked from these scrap groups and individually remelted to obtain secondary alloys. Other secondary alloys were also prepared by blending the above scrap groups in predetermined proportions.

The resulting secondary alloys from these groups of scrap components were all hypoeutectic aluminium-silicon-copper (Al-Si-Cu) based alloys. The samples in similar scrap groups were

fairly equivalent in chemical composition although some minor variations were observed. Some samples from different groups were also found to be fairly equivalent in their chemical composition. Furthermore, all the samples were also fairly equivalent, in their chemical composition, to several common commercial hypoeutectic Al-Si-Cu based alloys.

Permanent mould casting resulted in castings with higher tensile strength, percent elongation and hardness compared to green sand casting in all scrap samples tested. Both quiescent melt handling and quiescent bottom filled mould systems yielded castings with higher aforementioned properties than turbulent melt handling and turbulent top filled mould systems, respectively. In addition, these mechanical properties were found to decrease with increasing pouring temperature and mould preheat. Increasing the mould thickness was, however, found to increase these mechanical properties. Heat treatment of some of the alloys to the T6 condition increased their tensile strength and hardness, but decreased their percent elongation. The microstructure of all the recycled alloys was typically similar and contained α -aluminium matrix, eutectic silicon particles, iron-bearing and copper-bearing intermetallics.

The tensile strength and percent elongation of the recycled alloys did not correlate well with those of their respective commercial counterparts. This was particularly so with top filled green sand castings. The mechanical properties of bottom filled samples were, however, closer to those of their commercial counterparts albeit falling on the lower end in the range of reported mechanical properties of their respective equivalent commercial alloys. The hardness values of the samples, however, correlated well with those of their commercial counterparts.

It is inferred from the results of this study that using the type of scrap component as the sorting criterion is of limited usefulness because some samples cast from different scrap components were fairly equivalent in their chemical composition. Furthermore, some scrap items are either too few to recycle separately and/or difficult to identify. However, in the absence of appropriate facilities to determine the alloy chemistry on-line and make appropriate melt corrections, this sorting criterion together with the chemical compositions of the samples studied in this study can be a useful guide. Also inferred is that blending scrap samples is not useful because no definite trend in the chemical composition was observed with blending.

TABLE OF CONTENTS

Finally the processing conditions strongly influenced the mechanical properties of the samples. It is therefore important to choose the right casting process and to closely control the mould design, molten metal processing and other process parameters like pouring temperature and initial mould temperatures in permanent mould casting. In particular, permanent mould casting should be preferred to green sand casting if maximising mechanical properties is the major factor for process selection. In addition, mould filling systems should be skilfully designed to quiescently introduce molten metal into the mould cavity preferably via bottom filling. The pouring temperature should also be as low as possible.

TABLE OF CONTENTS

Title page.....	i
Declaration.....	ii
Dedication.....	iii
Acknowledgements.....	iv
Abstract.....	v
Table of contents.....	viii
List of tables.....	xii
List of figures.....	xiv
Nomenclature.....	xviii
CHAPTER ONE: INTRODUCTION.....	1
1.1 Casting.....	1
1.2 Aluminium.....	5
1.3 Statement of the problem.....	8
1.4 Objectives of the study.....	10
CHAPTER TWO: LITERATURE REVIEW.....	12
2.1 Aluminium and its alloys.....	12
2.1.1 Aluminium alloy and temper designation.....	12
2.1.2 Aluminium alloy sources and associated problems.....	14
2.1.2.1 Primary and quasi primary metal ingots.....	14
2.1.2.2 Secondary aluminium alloy sources.....	15
2.2 Cast aluminium-silicon alloys.....	24
2.2.1 Overview.....	24
2.2.2 Influence of key elements.....	24
2.2.2.1 Silicon.....	24
2.2.2.2 Copper.....	27
2.2.2.3 Magnesium.....	28
2.2.2.4 Iron.....	31

2.2.2.5	Important minor alloying and impurity elements.....	34
2.3	Liquid aluminium metal treatment.....	38
2.3.1	Overview.....	38
2.3.2	Hydrogen control in molten aluminium and its alloys.....	39
2.3.2.1	Sources of Hydrogen.....	39
2.3.2.2	Hydrogen Solubility.....	41
2.3.2.3	Hydrogen Measurement.....	43
2.3.2.4	Degassing.....	45
2.3.3	Inclusions in molten aluminium and its alloys.....	51
2.3.3.1	Sources of Inclusions.....	52
2.3.3.2	Inclusion Removal Techniques.....	57
2.3.3.3	Inclusion Detection and Measurement Methods.....	63
2.3.4	Melt chemistry control.....	65
2.3.4.1	Alloying Addition Methods.....	66
2.3.4.2	Removal of Impurity Elements.....	67
2.3.5	Treatment of molten aluminium with fluxes.....	68
2.3.5.1	Flux Ingredients.....	68
2.3.5.2	Uses of Fluxes.....	71
2.4	Casting process selection.....	74
2.5	Mould design.....	77
2.5.1	Parting line generation.....	82
2.5.2	Pouring basin design.....	83
2.5.3	Sprue design.....	85
2.5.4	Well design.....	88
2.5.5	Runner design.....	89
2.5.6	Ingate design.....	91
2.5.7	Riser design.....	94
2.5.8	Using chills.....	96
2.6	Microstructure of cast aluminium-silicon alloys.....	98
2.7	Tensile properties of cast aluminium-silicon alloys.....	100
2.7.1	Effect of casting defects and microstructure on tensile properties.....	100

2.8	Comments on the literature review.....	106
-----	--	-----

CHAPTER THREE: EXPERIMENTAL METHODOLOGY.....107

3.1	Introduction.....	107
3.2	Scrap sorting and classification.....	107
3.3	Mould design.....	109
3.3.1	Design of gating and risering systems.....	109
3.3.2	Fabrication of the moulds.....	116
3.4	Melting and pouring.....	116
3.5	Chemical composition analysis.....	117
3.6	Mould thickness and preheat.....	118
3.7	Heat treatment.....	118
3.8	Tensile and hardness testing.....	119
3.8.1	Tensile testing.....	119
3.8.2	Hardness testing.....	120
3.9	Microstructure characterization.....	120

CHAPTER FOUR: RESULTS AND DISCUSSIONS.....122

4.1	Chemical composition.....	122
4.1.1	The silicon content.....	123
4.1.2	The copper content.....	123
4.1.3	The magnesium content.....	124
4.1.4	The iron content.....	125
4.1.5	The manganese content.....	125
4.1.6	The content of other elements.....	126
4.1.7	Comparison with commercial alloys.....	127
4.2	Mechanical properties.....	132
4.2.1	Effect of type of casting process.....	142
4.2.2	Effect of mould filling system design and melt handling.....	142
4.2.3	Variation of mechanical properties with casting location.....	143
4.2.4	Effect of mould thickness and preheat.....	144

4.2.5	Effect of pouring temperature.....	150
4.2.6	Effect of heat treatment.....	154
4.2.7	Correlation with the chemical composition.....	155
4.2.8	Comparison with equivalent commercial alloys.....	159
4.3	The microstructure.....	164
CHAPTERS FIVE: CONCLUSIONS AND RECOMMENDATIONS.....		176
5.1	Conclusions.....	176
5.2	Recommendations.....	178
5.3	Future work.....	179
REFERENCES.....		180

LIST OF TABLES

Table 2.1 Table 2.1 The AA alloy specification for wrought and cast aluminium alloys.....	13
Table 2.2 Examples of typical remelt chemistry derived from three different aluminium alloy scrap classifications.....	20
Table 2.3 Composition limits for aluminium-silicon alloys.....	21
Table 2.4 Composition of common aluminium-silicon casting alloys.....	22
Table 2.5 Characteristics of aluminium-silicon casting alloys.....	23
Table 2.6 Typical mechanical properties of some common cast aluminium alloys.....	23
Table 2.7 Examples of the various Fe-bearing phases that form in aluminium-silicon alloys.....	32
Table 2.8 Review of degassing methods.....	50
Table 2.9 Classification and characteristics of inclusions in molten aluminium.....	53
Table 2.10 Inclusion Detection Methods.....	63
Table 2.11 Characteristics of flux compounds.....	69
Table 2.12 Properties of selected compounds used in fluxes.....	70
Table 4.1 Chemical composition of the experimental Alloys.....	122
Table 4.2 Comparison of scrap samples with equivalent commercial alloys.	129
Table 4.3 As-cast mechanical properties of sand and permanent mould cast piston scrap samples-turbulently filled.....	132
Table 4.4 As-cast and T6 mechanical properties of sand and permanent mould cast piston scrap sample (P4)-quiescently filled.....	133
Table 4.5 As-cast mechanical properties of sand and permanent mould cast housing scrap samples-turbulently filled.....	133
Table 4.6 As-cast and T6 mechanical properties of sand and permanent mould cast housing scrap sample (H5)-quiescently filled.....	134
Table 4.7 As-cast and T6 mechanical properties of sand and permanent mould cast housing scrap sample (H5) -quiescently filled mould, but turbulently handled melt.....	134
Table 4.8 As-cast mechanical properties of sand and permanent mould cast cylinder head scrap samples-turbulently filled.....	135

Table 4.9 As-cast and T6 mechanical properties of sand and permanent mould cast cylinder head scrap sample (C4)-quiescently filled.....	135
Table 4.10 As-cast mechanical properties of sand and permanent mould cast miscellaneous scrap samples - turbulently filled.....	136
Table 4.11 As-cast and T6 mechanical properties of sand and permanent mould cast miscellaneous scrap sample (M4)-quiescently filled.....	136
Table 4.12 As-cast mechanical properties of sand and permanent mould cast blended scrap samples-turbulently filled.....	137
Table 4.13 Effect of mould thickness and preheat on mechanical properties.....	145
Table 4.14 Effect of mould thickness and preheat on SDAS and grain size.....	145
Table 4.15. Effect of pouring temperature on mechanical properties.....	151
Table 4.16 Effect of pouring temperature on SDAS and grain size.....	151
Table 4.17 Weighted contributions of elements to tensile strength of the samples.....	158
Table 4.18 Weighted contributions of elements to percent elongation of the samples.....	159
Table 4.19 comparison of mechanical properties of scrap samples with typical properties of their equivalent commercial.....	162

LIST OF FIGURES

Fig. 2.1 Aluminium-silicon binary phase diagram with the composition ranges for wrought and foundry alloys indicated.....	25
Fig. 2.2 Micrographs of binary Al-16 silicon alloy showing primary Silicon refinement with increasing the melt overheating temperature	26
Fig. 2.3 The hydrogen solubility in aluminium and two of its alloys, illustrating the abrupt fall in solubility on solidification	42
Fig. 2.4 A schematics showing the effect of increasing height on a falling stream of liquid.....	55
Fig. 2.5 The schematic view of a splash of molten aluminium showing the formation of a folded (double) film that might consist of thick old film, or new thin film, or both, all likely to occlude air in the	55
Figure 2.6 Standard Gibbs energy of formation of several sulphides, oxides, chlorides and fluorides. The data are given at 723 °C per mole of S, O, Cl ₂ , and F ₂ , respectively	72
Fig. 2.7 Unstable advance of a film-forming alloy, leading to the formation of laps as the interface intermittently stops and restarts by bursting through and flooding over the surface film	79
Fig. 2.8 Illustration of the most common defect in castings - bubble damage as a mixture of oxide cracks and residual entrapped bubbles.....	79
Fig. 2.9 A "core blow" - a trapped bubble containing core gases. Shown at the bottom of the illustration is a bubble trail, ending in an exfoliated dross defect as the result of a passage of copious volumes of core gas	80
Fig 2.10 A design of an offset pouring basin	84
Fig 2.11 Conical pouring basin tested in an investment casting filling system for an aluminium alloy	84
Fig 2.12 A nomogram for the calculation of running systems for aluminium alloys	87
Fig 2.13 (a) Offset Sprue/Runner junction and (b) conventional in-line sprue/runner junction	88

Fig 2.14 Vortex-Flow Runner design	90
Fig 2.15 Expanding runner designs	91
Fig 2.16. A schematic illustrating metal flow in longitudinal and transverse gates	92
Fig 2.17 A typical design of a longitudinal and an expanding transverse gates	92
Fig 2.18 A schematic illustrating metal flow in a gating system (a) without a filter and (b) with a filter	93
Fig 2.19. A schematic illustrating (a) a poor filling system and (b) a good filling system.	93
Fig 2.20 Good filling systems illustrating two ways of locating filters and the use of (a) chills and (b) cooling fins.	94
Fig. 2.21 SDAS as a function of freezing rate	98
Fig 3.1 Turbulent top filled mould system	111
Fig 3.2 Turbulent top filled mould design assembly used in the current study for green sand casting.....	111
Fig 3.3 Turbulent top filled mould design assembly used in the current study for permanent mould casting.....	112
Fig 3.4 Quiescent bottom filled mould design assembly used in the current study for green sand casting.	113
Fig 3.5 Quiescent bottom filled mould design assembly used in the current study for permanent mould casting.	114
Fig 3.6 A DIN 50 125-A8X40 standard tensile test piece with a diameter d_0 of 8mm and an original gauge length L_0 of 40mm.	120
Fig 4.1 As-cast and T6 ultimate tensile strength of sand and permanent mould cast piston scrap sample P4-quiescently filled.	138
Fig 4.2 As-cast and T6 per cent elongation of sand and permanent mould cast piston scrap sample P4-quiescently filled.	138
Fig 4.3 As-cast and T6 hardness of sand and permanent mould cast piston scrap sample P4-quiescently filled	138

Fig 4.4 As-cast and T6 ultimate tensile strength of sand and permanent mould cast housing scrap sample H4 (quiescently filled) and sample H5 (quiescently filled mould, but turbulently handled melt).	139
Fig 4.5 As-cast and T6 per cent elongation of sand and permanent mould cast housing scrap sample H4 (quiescently filled) and sample H5 (quiescently filled mould, but turbulently handled melt).	139
Fig 4.6 As-cast and T6 hardness of sand and permanent mould cast housing scrap sample H4 (quiescently filled) and sample H5 (quiescently filled mould, but turbulently handled melt).	140
Fig 4.7 As-cast and T6 ultimate tensile strength of sand and permanent mould cast cylinder head scrap sample C4-quiescently filled.	140
Fig 4.8 As-cast and T6 per cent elongation of sand and permanent mould cast cylinder head scrap sample C4)-quiescently filled.	140
Fig 4.9 As-cast and T6 hardness of sand and permanent mould cast cylinder head scrap sample C4-quiescently filled.	141
Fig 4.10 As-cast and T6 ultimate tensile strength of sand and permanent mould cast miscellaneous scrap sample M4-quiescently filled	141
Fig 4.11 As-cast and T6 per cent elongation of sand and permanent mould cast miscellaneous scrap sample M4-quiescently filled	141
Fig 4.12 As-cast and T6 hardness of sand and permanent mould cast miscellaneous scrap sample M4-quiescently filled	142
Fig 4.13 Effect of mould thickness and initial mould temperature on ultimate tensile strength.	146
Fig 4.14 Effect of mould thickness and initial mould temperature on hardness.	146
Fig 4.15 Effect of mould thickness and initial mould temperature on percent elongation	147
Fig 4.16 Effect of pouring temperature on ultimate tensile strength.	152
Fig 4.17 Effect of pouring temperature on hardness.	152
Fig 4.18 Effect of pouring temperature on percent elongation	153
Fig. 4.19 Micrographs for (a) sand cast P1, (b) Permanent mould P1, (c) sand cast P2, (d)	

Permanent mould P2, (e) sand cast P3, and (f) Permanent mould P3.....169

Fig. 4.20 Micrographs for (a) sand cast P4 in as-cast condition, (b) permanent mould P4 in as-cast condition, (c) sand cast P4 – T6, (d) permanent mould P4 – T6.....170

Fig. 4.21 Micrographs for (a) sand cast H1, (b) Permanent mould H1, (c) sand cast H2, (d) Permanent mould H2, and (e) sand cast H3.....171

Fig. 4.22 Micrographs for (a) sand cast H4 in as-cast condition, (b) permanent mould H4 in as-cast condition, (c) sand cast H4 – T6, (d) permanent mould H4 – T6.....172

Fig. 4.23 Micrographs for (a) sand cast H5 in as-cast condition, (b) permanent mould H5 in as-cast condition, (c) sand cast H5 – T6, (d) permanent mould H5 – T6.....173

Fig. 4.24 Micrographs for (a) sand cast C1, (b) Permanent mould C1, (c) sand cast C2, (d) Permanent mould C2, and (e) sand cast C3.....174

Fig. 4.25 Micrographs for (a) sand cast C4 in as-cast condition, (b) permanent mould C4 in as-cast condition, (c) sand cast C4 – T6, (d) permanent mould C4 – T6.....175

Fig. 4.26 Micrographs for (a) sand cast M1, (b) Permanent mould M1, (c) sand cast M2, (d) Permanent mould M2, (e) sand cast M3, and (f) Permanent mould M3.....176

Fig. 4.27 Micrographs for sand cast M4 in (a) as-cast condition, and (b) T6 condition.....177

Fig. 4.28 Micrographs for (a) sand cast B1, (b) Permanent mould B1, (c) sand cast B2, (d) Permanent mould B2, (e) sand cast B3, and (f) Permanent mould B3.....178

Fig. 4.29 As-cast micrographs for (a) sand cast B5, and (b) permanent mould.....179

LIST OF SYMBOLS

A	Area
AA	Aluminum Association
AFS	American Foundrymen Society
Al-Si	Aluminium silicon
B1	A sample of a mixture of equal amounts of pistons and cylinder heads.
B2	A sample of a mixture of equal amounts of pistons and housings.
B3	A sample of a mixture of equal amounts of cylinder heads and housings.
B4	A sample of a mixture of equal amounts of pistons, cylinder heads and housings.
B5	A sample of a mixture of equal amounts of pistons, cylinder heads, housings and miscellaneous scrap.
BHN	Brinell hardness number
C1 to C4	Cylinder head scrap samples
°C	Degrees centigrade
DAS	Dendrite arm spacing
ρ	Density
g	Gravitational acceleration
H1 to H5	Housing scrap samples
HIPping	Hot isostatic pressing
LIBS	Laser induced breakdown spectroscopy
L	Length
Q	Mass flow rate of molten metal
M1 to M4	Miscellaneous scrap samples
E1	Percent elongation
P1 to P4	Piston scrap samples
SDAS	Secondary dendrite arm spacing
C_p	Specific heat
w	Specific weight of the molten metal
K	Thermal conductivity

LIST OF SYMBOLS

A	Area
AA	Aluminum Association
AFS	American Foundrymen Society
Al-Si	Aluminium silicon
B1	A sample of a mixture of equal amounts of pistons and cylinder heads.
B2	A sample of a mixture of equal amounts of pistons and housings.
B3	A sample of a mixture of equal amounts of cylinder heads and housings.
B4	A sample of a mixture of equal amounts of pistons, cylinder heads and housings.
B5	A sample of a mixture of equal amounts of pistons, cylinder heads, housings and miscellaneous scrap.
BHN	Brinell hardness number
C1 to C4	Cylinder head scrap samples
°C	Degrees centigrade
DAS	Dendrite arm spacing
ρ	Density
g	Gravitational acceleration
H1 to H5	Housing scrap samples
HIPping	Hot isostatic pressing
LIBS	Laser induced breakdown spectroscopy
L	Length
Q	Mass flow rate of molten metal
M1 to M4	Miscellaneous scrap samples
EI	Percent elongation
P1 to P4	Piston scrap samples
SDAS	Secondary dendrite arm spacing
C_0	Specific heat
w	Specific weight of the molten metal
K	Thermal conductivity

- t Thickness
- UTS Ultimate tensile strength
- h Vertical height
- VHC₀ Volumetric heat capacity

1.1 CASTING

In casting, a molten metal is poured into a mould and solidified to form a cast part. This operation is the first stage of the casting process. The design of the mould is very important. It must be able to hold the metal at the required temperature and to allow the metal to flow into the desired shape. The solidification of the metal in the mould is a complex process and is affected by many factors such as the geometry of the mould, the pouring temperature, the cooling rate, etc.

As in any manufacturing process, the quality of the cast part is dependent on the quality of the mould. The quality of the mould is determined by the design and the material used. The design of the mould must be such that it allows the metal to flow into the desired shape and to solidify at the required rate. The material used for the mould must be able to withstand the high temperature of the molten metal and to maintain its shape during the casting process. The quality of the cast part is also affected by the pouring temperature, the cooling rate, etc.

The design of the mould is very important. It must be able to hold the metal at the required temperature and to allow the metal to flow into the desired shape. The solidification of the metal in the mould is a complex process and is affected by many factors such as the geometry of the mould, the pouring temperature, the cooling rate, etc.

CHAPTER ONE

INTRODUCTION

1.1 CASTING

In casting, a molten metal is poured into a preformed mould or cavity that approaches the shape of the finished part. Heat is extracted through the mould (made from sand, metal or some other refractory material) and the molten metal solidifies into the final solid shape. This seemingly simple process can be quite complex to control in terms of both process variables and metallurgy.

As in any manufacturing process, the laws of nature are at work in the casting of metals [1]. As the molten metal is processed in the furnace and during its subsequent excursion from the furnace to the mould cavity, its constituents interact aggressively both amongst themselves and with the surrounding environment as the system strives to equilibrate. This inevitably leads to contamination of the melt with various unwanted elements and/or phases. For examples, some of the common unwanted elements introduced in aluminium melts are hydrogen and iron, while the unwanted phases may include adsorbed gases, oxides, sludge and other extraneous particles.

The flotation, suspension or settling of particles in the liquid metal is described by Stoke's Law. The result is determined through a balance between viscous drag forces and buoyancy forces and is a function of particle density, shape and size, liquid density and temperature, degree of agitation and time available [2]. This phenomenon is invaluable during melt cleaning, which is usually achieved through fluxing, filtration and/or sedimentation methods. Hydrogen removal, from aluminium melts, is achieved through degassing, which also removes some inclusions. The degassing methods developed for aluminium alloys are based on Sievert's Law and the most widely used degasser has been hexachloroethane (which releases chlorine) although the use of inert gases such as nitrogen and argon for degassing is increasingly being preferred due to

environmental concerns.

As the metal cools from the superheated molten state to the solid state, transient heat spills down temperature gradients in accordance with Fourier's Law. The molten metal moves in response to inertial and body forces according to the Navier-Stokes equations. Tensile strains develop in the solidifying shell subject to changing cooling conditions, the constitutive behaviour of the metal and the Prandtl-Reuss relations. Solutes segregate as thermodynamics compete with diffusion to create a heterogeneous solid from a fairly homogeneous liquid [1].

Solidification models have been developed to simulate and control the behaviour of the metal during solidification. The accuracy of these models depends on the boundary conditions, initial conditions and material property data used in the heat-flow equations. The boundary conditions between the casting and the mould are dependent on a number of factors. These include; the temperatures near the interface; interfacial contact pressures; the casting and mould materials; the mould-coating type, thickness, density and roughness; mould-preheat temperature; the pouring temperature; and the geometry of the casting.

Solidification control requires three distinct metallurgical processes: constitution control, nucleation control and growth control. Each stage is equally important and only when the foundryman regulates each stage can a uniform and consistent macrostructure be obtained in a casting alloy. The melt constitution is the state of nucleation of a melt, including its inherited foreign and heterogeneous nuclei, and the cumulative effect of all reactions occurring in the melting environment during the entire melting cycle, which influences the development of these nuclei. The as-melted constitution may be affected by any of the molten metal treatments used to produce quality castings [3]. Once the as-melted constitution is established in the alloy, it is necessary to establish the proper nucleation potential in the melt. This may be accomplished by adding an inoculant or grain refiner to the melt. An inoculant is a material added to the liquid melt just prior to casting to produce alterations in the solidification structure of the alloy far greater than

those which can be obtained by an alloying addition of a like amount [3]. Once the proper nucleation potential has been established in the melt, the growth of the individual crystallites must be restricted to allow sufficient undercooling of the melt ahead of the solid-liquid interface for the activation of the heterogeneous nuclei. Additions of certain elements promote an equiaxed grain structure in alloys that normally solidify with columnar grains.

The critical parameters that influence molten metal processing are chemistry, time and temperature. These parameters, which make up the environment of molten metal processing, all exert significant effects on our ability to produce the products that meet quality specifications. Gross or major element chemistry has well-documented effects. In contrast, there is relatively little organized information available on the effects and interactions of minor elements. This is potentially a critical weakness in the casting industry it is largely dependent on scrap recycling. Minor element effects are important factor in all cast materials. Some studies have shown that there are only small variations in the average analyses of scrap materials [4]. However, what is crucial is the fact that there are significant local variations in scrap analyses. It is therefore important to intelligently specify and control minor element chemistry in the materials that are recycled. Materials are also significantly influenced by their thermal history. For example, phase diagrams and time-temperature-transformation (TTT) curves are based on the influence of temperature. Furthermore, the solidification control of metals is sensitive to the solidification rate. As all the metals we deal with are melted and processed at elevated temperatures, reactions tend to occur more rapidly and their impact is significant.

Solid metal shrinks on solidification. Thus, the casting and mould must be so designed that a supply of molten metal is available to compensate for the shrinkage and avoid formation of shrinkage pores. Allowance for shrinkage and thermal contraction must be provided in the design to prevent defects such as hot tearing. Also, since the solubility of dissolved gases in the liquid decreases suddenly as the metal solidifies, castings are subject to the formation of gas porosity unless proper preventive steps are taken. In film

forming alloys such as aluminium alloys, oxide films can and do get incorporated into the casting structure. Other non-metallic inclusions such as various forms of oxides, sand, refractory material fragments and other extraneous particles can also be trapped into the structure of the final casting. Properly controlled melt treatment and handling in concert with proper maintenance of melting and laundering equipment serve to reduce the amount of these inclusions in the melt. Additionally, ingenious filling system design, to enhance quiescent filling has for many years been shown to be particularly effective and salutary in combating casting defects.

Grain size and other microstructure features such as secondary dendrite arm spacing (SDAS), intermetallic compounds and eutectic particles are influenced by alloy chemistry and casting conditions. It has been observed experimentally that increasing the cooling rate results in a finer microstructure; reduced SDAS; smaller and globular second phases; fine eutectic particles; and uniformly distributed microporosity of reduced size. The factors that seem to control the final microstructure of a casting are: heat transfer during solidification, cooling rates, mould materials, pouring conditions and the flow of liquid metal into the mould, and microstructure refiners and modifiers [5].

The microstructure of the casting is therefore determined by the alloy chemistry and processing conditions. In turn the physical and mechanical properties of the casting are determined by its microstructure. Casting defects and certain microstructure features have deleterious effects on the properties of castings such as fatigue resistance, fracture toughness, tensile strength, tensile ductility, hardness and leak-tightness. The degree of seriousness depends on the size, form and location of these defects and microstructure features, with some having precedence over others in initiating and propagating cracks that lead to failure [6-7].

Good foundry engineering is thus needed to produce quality castings. This can be achieved by applying modern technology and careful quality control. The founders must of necessity possess a good understanding of the essential features of the casting process in order to manipulate the relevant variables to attain the desired casting structure.

Several casting processes have been developed and continue to be improved while fresh ones are being developed with advancements in technology. The large number and variety of casting and moulding processes available currently offers design engineers and component users enormous flexibility in meeting their metal casting needs. Selecting the right process to produce a particular part is an essential facet of foundry practice. Each process offers distinct advantages and benefits when matched with the proper alloy and application.

Controlled post-casting operations are also applied to improve the performance of castings. One of the intended purposes of post-casting operations is to enervate the potency of casting defects and microconstituents by removing or reducing them and/or changing their size, morphology and distribution. A notable example is the recently invented hot isostatic pressing (HIPping), which is applied to castings to remove or reduce the number and size of porosity [8-10]. Others include the various types of controlled heat treatments such as the most commonly used T6 and T7 tempers for aluminium castings.

1.2 ALUMINIUM

Aluminium has grown rapidly from just but a chemical curiosity in the early nineteenth century to be the world's second most commonly used metal after iron [11]. The rapid growth in the aluminium industry is attributed to its unique combination of properties, which makes it one of the most versatile engineering and construction materials. Aluminium is light, non-toxic, ductile, corrosion resistant, has good electrical and thermal conductivity and can be strengthened by alloying.

Pure aluminium is a relatively weak material. For applications requiring greater mechanical strength, it is alloyed with other metallic elements. Most of the metallic elements readily alloy with aluminium although only a few are important major alloying ingredients in commercial-based alloys. Nevertheless an appreciable number of other elements serve as supplementary alloying additions for improving other alloy properties

and characteristics. For applications requiring strengths greater than those achieved through alloying, the alloys are work-hardened or precipitation hardened to increase their strengths. These controlled treatments also relieve residual stresses and improve other properties such as ductility, fracture toughness, thermal stability and resistance to corrosion or stress corrosion cracking [11-13].

Aluminium alloys can be cast, drawn, rolled, forged and extruded into almost any shape, and aluminium products vary from large aircraft components to thin foil for food wrappers. The major uses of aluminium and its alloys are in building and construction, containers and packaging, transportation, and electrical conductors. Aluminium's light weight and high specific modulus and the ability to obtain high strengths by simple alloy additions and subsequent heat treatments make it especially attractive for transportation systems where strength to weight ratio is of primary importance in engineering design. Since aluminium is light, abundant, versatile and easily recyclable retaining its original quality, new markets may be created by shortages of other materials, and by economic, environmental, and safety considerations [14].

Aluminium castings have been used to produce various automobile parts for a long period. It has been used in automotive intake manifolds and transmission housings for more than 50 years; aluminium cylinder heads have been used for about 20 years while the widespread use of aluminium in engine blocks is more recent. As a key trend the material for engine blocks, which is one of the heavier parts, is being switched from cast iron to aluminium resulting in significant weight reduction. Aluminium castings have been used for almost 100% of pistons, about 75% of cylinder heads, 85% of intake manifolds, 40% of wheels and 100% of transmission cases [15]. Other applications include valve bodies and channel plates (90%), rear axle and differential housings, driveshafts, brackets, master brake cylinders, suspension components (control arms and supports), steering components (air bag supports, steering shafts, knuckles, housings and wheels), instrument panels and electric motor, alternator and pump housings. With the escalation of fuel costs and environmental concerns, aluminium is being increasingly used for other components of ground transportation systems.

Casting alloys of the 3xx.x series are replacing cast iron in engine blocks as well as in other components such as intake manifolds, valve lifter carriers and suspension systems.

These alloys are some of the most widely used because of the flexibility provided by the high silicon content and its contribution to castability. They also respond well to heat treatment after casting to obtain the required combination of ductility and strength. Cast wheels, gearbox casings and rear axle housings are among the applications of these alloys. The commonly used alloys in the 3xx.x series are 319.0 and 356.0/A356.0 for sand and permanent mould casting, 360.0, 380.0/A380.0 and 390.0 for die-casting and 357.0/A357.0 for many types of castings including the squeeze/forged cast technologies. Alloy 332.0 is also among the workhorse alloys because it can be made exclusively from scrap recycling [13-18].

Landing flap mountings and other aircraft components are made from alloys of the 201.0 or A356 types. Alloy 203.0 is a special alloy used in particular components such as engine piston heads, integral engine parts, or bearings. The 4xx.x series alloys are used in typewriter frames, dental equipment, marine and architectural applications. The 5xx.x alloys find applications in cooking utensils, food handling equipment, aircraft and highway fittings. The 7xx.x alloys are used in furniture, garden tools, office machines, farm machinery and mining equipment while the 8xx.x are used in bearings and bushings of all types. The 7xx.x and 8xx.x alloys are relatively hard to cast and are used only when their unique machining and bushing characteristics are essential [16-17].

Cast aluminium alloys are also used in a wide variety of other engineering applications. For example, they are used in oil tanks and pans, machine tool parts, marine hardware, pump parts, valve bodies, bridge railing parts, rudder control supports, aircraft wheels, fuselage fittings and fuel tank elbows for airplane and missiles and compressor bodies. The list is by no means exhaustive.

Aluminium alloys are designed for both properties and processes. Where strength requirements are low, as cast properties are employed. High strength castings usually require the use of an alloy that can be subsequently heat treated. Sand casting has the

least process restrictions. The aluminium alloys used for permanent mould casting must be designed to have lower coefficients of thermal expansion (or contraction) because the moulds offer restraint to the dimensional changes that occur upon cooling. Alloys used for sand and permanent mould castings are frequently selected from compositions that respond to solution heat treatment and quenching. Such is the case with squeeze casting and semi-solid material forging (thixocasting). High-pressure die casting alloys require high degrees of fluidity because they are often cast into thin sections. Moreover, as high-pressure diecastings are ordinarily not heat-treated, the alloys are designed to produce high as cast strength under rapid cooling conditions. High-pressure diecastings are not normally solution heat treated because heating to the required solution temperature of between 480°C to 540°C causes blistering, hence producing a grossly disfigured surface. This is due to the expansion of internal porosity, initially trapped and compressed under high pressures during solidification, which is made possible by the reduced strength of the product at the high temperatures. New improvements in high-pressure diecasting (e.g. vacuum die-casting and the Japanese patented "Pore Free" die casting system) have resulted in internal quality that is compatible with solution heat treatment. This has permitted the use of T6 and T7 tempers [19-20]

1.3 STATEMENT OF THE PROBLEM

Previous studies [21] have shown that the Kenyan foundry sector uses about 23 percent of its available capacity. The possible explanations for this poor industrial performance are the limited range of foundry products coupled with a poor marketing strategy, and the poor quality of the local products as compared with their imported counterparts. The poor product quality has been attributed to poor foundry practice including the following [22]:

- (i) The use of low quality raw materials.
- (ii) The use of low levels of casting and moulding technology.
- (iii) Lack of trained personnel beyond the craft courses for the foundry industry.
- (iv) Lack of continued research in foundry.
- (v) Lack of cooperation among foundry stakeholders.

Cast aluminium alloy products are widely used in Kenya. After their service life is over, some of the scrap is exported while the rest is usually ploughed back for recycling by the Kenyan foundry shops for use in casting other products. Most of the scrap available in Kenya is from automotive components and is relatively cheap (approximately Kshs 70 per kg). The number of alloys being used for the automotive applications is very large. The problems become more difficult to manage when we appreciate that cast aluminium alloys from foreign vehicles entering the scrap stream have not been exposed to the same processing methodologies. For example, antimony is often used to control the eutectic silicon structure in Europe and Japan, but this acts as an impurity in the strontium-modified alloy castings produced in North America and Australia [2]. In addition, different alloys are often used to produce similar vehicle components depending on the vehicle model and the manufacturer's preferences. The mix of alloy chemistries for effective recycling consequently requires study to ensure adequate control of impurities.

It is common practice to find foundry shops in Kenya melting scrap obtained from different components together without regard to their varied chemical compositions and impurities. This sorting practice is likely to be a major setback to the successful recycling of aluminium alloy, particularly in cases where facilities for on-line chemical composition analyses are not available. Most large foundries, especially in industrialised countries have developed and implemented new technologies that facilitate accurate and economical sorting especially. These technologies have been particularly effective in segregating between cast and wrought aluminium alloys and even between different wrought alloys. In most of these foundries, cast scrap is normally not segregated further because it would be uneconomical. Most Kenyan foundry shops segregate between wrought and cast aluminium alloys using inaccurate and crude methods such as by visual inspection. The cast scrap is usually not segregated further. However, there are differences between the practice elsewhere and that in Kenya in recycling the segregated cast scrap that significantly influence the quality of the resulting secondary alloys. These include the fact that whereas in most commercial enterprises in other countries the alloy chemistry of the recycled scrap is controlled via on-line facilities (e.g. spectrometers) and correcting additives, this is seldom practiced in Kenyan shops. This leads to a high

degree of uncertainty in the expected properties of the products cast from these alloys due to uncertainty of the resulting alloy chemistry. The situation is worsened when the alloy chemistry of the resulting secondary alloys cannot be determined even after the castings have been poured because of lack of reliable and economical laboratories for chemical composition analyses.

It is therefore readily inferred that the level of technology in aluminium foundry operations in this country is low. This, in concert with the possible concomitant inept, injudicious or even crass workmanship, which is due to a general lack of skill and possibly inattention to detail, explains the poor quality of castings produced locally. It is a practical truism that in such operating environment, castings with various forms of defects and deleterious microconstituents are likely to result.

The foregoing indicate that it is necessary to carry out studies on the recycling of cast aluminium scrap so as to develop better practices that will contribute to the improvement of the quality of locally produced aluminium castings. That will, however, be solving just but one facet of the problem. It is necessary to tackle the other aspects of the poor foundry practice including those listed above in order to strengthen the aluminium casting industry as a whole in this country. This preliminary study on the recycling of cast aluminium scrap is based on these observations.

1.4 OBJECTIVES OF THE STUDY

The objectives of this preliminary investigation on the recycling of cast aluminium scrap are:

- (i) To determine the typical chemical composition of recycled alloys obtained from different cast aluminium scrap components and analyse its variation from sample to sample
- (ii) To determine the microstructure, tensile strength, percent elongation and hardness obtainable from the recycled alloys using both green sand and permanent mould casting processes and under different process conditions. The process parameters

for both green sand and permanent mould casting processes, whose influence on the said properties are investigated include: the type of mould filling system, melt handling and pouring temperature. The influence of the thickness and initial temperature of permanent moulds on these properties is also investigated.

2.1. RESEARCH OBJECTIVES

The main objective of this research is to investigate the influence of the pouring temperature, the thickness of the permanent mould and the type of mould filling system on the properties of the cast parts. The research objectives are: to study the influence of the pouring temperature on the properties of the cast parts; to study the influence of the thickness of the permanent mould on the properties of the cast parts; to study the influence of the type of mould filling system on the properties of the cast parts. The research objectives are: to study the influence of the pouring temperature on the properties of the cast parts; to study the influence of the thickness of the permanent mould on the properties of the cast parts; to study the influence of the type of mould filling system on the properties of the cast parts.

2.2. LITERATURE REVIEW

The literature review is divided into three parts: the first part is a general review of the casting process; the second part is a review of the properties of the cast parts; the third part is a review of the influence of the pouring temperature, the thickness of the permanent mould and the type of mould filling system on the properties of the cast parts. The literature review is divided into three parts: the first part is a general review of the casting process; the second part is a review of the properties of the cast parts; the third part is a review of the influence of the pouring temperature, the thickness of the permanent mould and the type of mould filling system on the properties of the cast parts.

The literature review is divided into three parts: the first part is a general review of the casting process; the second part is a review of the properties of the cast parts; the third part is a review of the influence of the pouring temperature, the thickness of the permanent mould and the type of mould filling system on the properties of the cast parts. The literature review is divided into three parts: the first part is a general review of the casting process; the second part is a review of the properties of the cast parts; the third part is a review of the influence of the pouring temperature, the thickness of the permanent mould and the type of mould filling system on the properties of the cast parts.

CHAPTER TWO

LITERATURE REVIEW

2.1 ALUMINIUM AND ITS ALLOYS

Aluminium and its alloys are classified into two major groups based on their processing routes to the finished products [11, 13, 23]. These are wrought and cast aluminium alloys. Wrought aluminium alloys are usually first cast into ingots and subsequently deformed into final products. Examples of common deformation processes include drawing, rolling, forging and extrusion. On the other hand, cast aluminium alloys are cast directly into the final product. There are many casting processes through which the casting alloys can be converted to the final product. Examples include green sand casting, investment casting, permanent mould casting, low-pressure permanent mould casting, high-pressure diecasting, squeeze casting and thixocasting.

2.1.1 ALUMINIUM ALLOY AND TEMPER DESIGNATION

The Aluminium Association (AA) alloy and temper designation system is recognised by the American National Standards Institute (ANSI) as the United States national standard and as such is incorporated into ANSI standards H35.1 and H35.2 [24]. The nomenclature for wrought alloys has been accepted by most countries and is now called the International Alloy Designation System (IADS). The first digit indicates the alloy group and the last two digits identify the alloy or indicate the aluminium purity (Table 2.1). The second digit indicates modifications of the original alloy or impurity limits. A prefix X identifies experimental alloys.

Although the first digit for cast alloys is essentially the same as for wrought alloys, the second two digits serve to identify a particular composition. The zero after the decimal point identifies the product as a casting while other numerals (1, 2) are used to designate ingots. A letter prefix is used to denote either an impurity level or the presence of a secondary alloying element. These letters are assigned in alphabetical order starting with

A but omitting O, Q, X, and I. X is reserved for experimental alloys.

Unlike wrought alloys, cast aluminium alloys are not identified internationally according to the single AA designation system. The system is, however, widely used together with other national specifications published by several major industrial countries.

Table 2.1 The AA alloy specification for wrought and cast aluminium alloys is as follows:

Cast Aluminium alloys	
1xxx	pure Al (99.00% or greater)
2xxx	Aluminium-Copper alloys
3xxx	Aluminium -Manganese alloys
4xxx	Aluminium -Silicon alloys
5xxx	Aluminium -Magnesium alloys
6xxx	Aluminium -Magnesium-Silicon alloys
7xxx	Aluminium -Zinc alloys
8xxx	Aluminium + other elements
9xxx	unused series

Wrought Aluminium alloys	
1xx.x	pure Al (99.00% or greater)
2xx.x	Aluminium-Copper alloys
3xx.x	Aluminium -Silicon + Copper and/or Magnesium alloys
4xx.x	Aluminium -Silicon alloys
5xx.x	Aluminium -Magnesium alloys
7xx.x	Aluminium -Zinc alloys
8xx.x	Al-Tin alloys
9xx.x	Aluminium + other elements
6xx.x	unused series

The heat treatment or temper nomenclature system developed by the AA has also been adopted as part of the IADS by most countries. It is used for all forms of wrought and

cast aluminium alloys with the exception of ingot. The system is based on the treatments used to develop the various tempers and takes the form of letters added as suffixes to the alloy number. One or more digits following the letter indicate subdivisions of the tempers, when they significantly influence the characteristics of the alloy. Alloys supplied in the as-fabricated or annealed condition are designated with suffixes F or O, respectively. The letters H and W designate those supplied in the strain-hardened and solution heat treated conditions, respectively. Those in the heat treated condition are designated by T. Digits following H represent the degree of strain hardening and those following T, the type of aging treatment.

2.1.2 ALUMINIUM ALLOY SOURCES AND ASSOCIATED PROBLEMS

There are several sources of aluminium alloys utilised by foundries. These sources provide a variety of combinations for different products, depending upon a range of factors including cost, availability, practicality, alloy specification and the required final product.

2.1.2.1 Primary and Quasi-Primary Metal Ingots

Primary metal ingots made at a smelter from molten potline metal include commercial purity aluminium ingots (with various grades from 99.5% to 99.85% aluminium) or alloy ingots (with alloying element additions). The chemical composition of potline metal varies from smelter to smelter as a result of their different raw material sources and process operating parameters. However, it is possible to assign some typical average values to impurity levels as reported by Mondolfo [23].

Quasi-primary metal ingots can also be made by remelting commercial purity primary ingots and making further alloying additions. The main drawback is the introduction of an additional remelt/holding/casting cycle. This means greater potential for producing more entrained oxides, hydrogen pick-up and contamination with non-metallic and intermetallic inclusions.

Foundries that are situated in close proximity to either a smelter or a secondary metal producer may have the option of receiving their metal in the molten form. This may be delivered in securely sealed and heavily insulated transport crucibles, loaded onto semi-trailers and transported on the public road system. Alternatively, potline transfer crucibles loaded onto hot metal carriers can deliver molten metal to foundries located at or near smelter sites. The advantage of this form of metal supply over the in-house remelt of ingots is that a complete remelt cycle is eliminated from the process, resulting in potential dross reduction and decreased furnace energy costs [2].

2.1.2.2 Secondary Aluminium Alloy Sources

Secondary metal by definition is made from recycled alloy scrap. The distinct advantage gained with the use of secondary metal is reduced cost. Remelting aluminium scrap consumes only about 5% of the total amount of energy required to produce the same tonnage of primary aluminium by the electrolytic reduction process [2]. All foundries produce some scrap (new-scrap) in the course of their casting processes. This includes furnace scrap (dross, skimmings and metal spills), reject castings, cast trimmings (rigging system) and machine swarfs. Each foundry has to decide which scrap will be used in-house and for which products. It must also decide which scrap to dispose off. In general, only heavy gauge scrap can be used effectively in-house, with lighter gauge scrap being sold. This is because light gauge scrap requires the use of dedicated flux-covered melting furnaces to avoid excessive melt losses [25].

Old scrap, which is composed of aluminium components discarded by consumers after expiry of their service life, is purchased in various forms and compositions. It is then checked and sorted either manually or through the use of sophisticated techniques such as the recently introduced Laser Induced Breakdown Spectroscopy (LIBS) [26]. The LIBS technique has been used successfully to improve automotive scrap sorting. Other techniques only allow separation of aluminium from other materials in scrapped vehicles. The LIBS however, separates cast aluminium from wrought, and even differentiates between wrought alloys. LIBS uses a laser to first clean the surface of the scrap by laser

ablation, and then employs a laser pulse to hit the same spot on the scrap. This second laser pulse vaporizes a small amount of material from the metals surface creating a small, highly luminescent plume of plasma, or ionised gas. The plume is then analysed by optical emission spectroscopy for the scrap's alloy chemistry. Once the verification is made, the scrap is sorted by alloy on piece-by-piece basis. The sorted scrap is then blended, melted and alloyed to the required customer specification.

Each recycled product type has its own elemental mix and therefore its own potential problems. In addition, recycled scrap is sometimes highly oxidized or surface-contaminated. Sorting is never completely reliable and separated piles often contain some unwanted material. Special care has to be taken in separating and utilizing iron and steel containing items. This may involve additional use of magnetic separation units and/or sweating/raking furnaces. Due to these inherent process limitations, secondary metal is permitted to contain higher levels of impurities than primary metal. Most of the AA specifications permit the presence of 0.05 wt.% each (0.15 wt% total) of impurity elements. These general impurity limits are lower in some alloys, but are set higher for some specified elements, particularly iron and silicon, in most alloys [2, 13].

One of the major problems in recycling is the build-up of impurities. These impurities originate from four main sources [13]:

- Mixed alloys due to poor scrap segregation, recovery of metal from furnace dross, and remelting of multi-alloy products.
- Contamination of the scrap by extraneous materials such as iron, sand, painted sheet, and coatings.
- Incorporation of non-metallic inclusions such as oxide films and aluminium-magnesium spinel into the metal during melting and casting.
- Contamination from furnace tools, refractories and hydrogen from furnace atmosphere.

As previously noted, each time aluminium is remelted, there is a consequent oxidation loss of aluminium to dross. Another important factor is that other reactive elements (e.g.,

magnesium and sodium) can also be oxidized and lost on remelt, while the more stable elements (iron, manganese, chromium, zinc) are not. Instead, these stable elements gradually build up in concentration, making it progressively more difficult to make alloys within specification without resorting to the addition of purity metal for “sweetening” purposes [2].

Further complications in secondary metal production can arise from unwanted carryover effects of minor elements that are added to particular products for specific purposes. Grain refiners have been demonstrated to provide some residual grain refining effect. This effect may last for a few remelt cycles before fading. It has also been shown that even small extra additions are able to rejuvenate them to full potency. Eutectic silicon modifiers may also carryover through remelt. Antimony is able to reproduce its full modifying effect even after numerous remelt cycles, whereas sodium and strontium lose their effect on remelt more rapidly. Antimony, lithium and phosphorus are significant and troublesome in remelt streams because their chemical analysis is difficult in the 5-500 ppm range, and they can interfere with the modification of eutectic silicon by strontium and sodium [2].

The effects of the impurities associated with recycling aluminium alloy can be summarized as follows [13]:

- Explosion hazards: A major safety problem when the furnace charge contains water, rust or certain chemicals.
- Increased melt loss: An increase in melting dross results from organic or anodic coatings on the scrap and from the presence of alloying or impurity elements such as lithium, sodium, calcium, magnesium, bismuth, and zinc.
- Inclusions in castings: Potential inclusions include: aluminium oxide, $MgAl_2O_4$ spinel, titanium and vanadium diboride, aluminium carbide, as well as miscellaneous materials such as pieces of furnace refractory, flakes from tool washes, and fragments of filter media. In alloys containing relatively large amounts of magnesium or zinc, primary intermetallic particles can crystallize from the melt if the level of transition metal impurities is too high.

- **Gas porosity:** Hydrogen that is readily picked up by molten aluminium from water vapour and hydrogen-containing compounds such as in paints can lead to gas porosity in ingots and castings if the melt is not properly degassed
- **Hot-shortness and embrittlement:** In aluminium-magnesium (manganese) alloys such as 5182, a few ppm of sodium or calcium can lead to cracking during hot rolling. Small amounts of low melting point metals such as indium, tin, bismuth, cadmium, and lead can lead to hot cracking in some alloys as well.
- **Recovery and recrystallisation:** Small amounts of zirconium and chromium, and to a lesser extent vanadium and manganese, can reduce the rate of recovery during annealing and increase the recrystallisation temperature and final grain size.
- **Heat treatment:** Increased amounts of chromium and manganese increase the quench sensitivity of precipitation-strengthened alloys. Small amounts of cadmium, indium, or tin change the precipitation kinetics of aluminium-copper alloys.
- **Reduced ductility, strength and fracture toughness:** Increasing amounts of iron and silicon increases the volume fraction of insoluble intermetallic phases, which in turn decrease the strain to fracture. Other elements that can form intermetallic particles such as nickel, cobalt, or combinations of iron with manganese or copper have similar detrimental effects.
- **Reduced electrical conductivity:** All elements in solution will reduce conductivity, but vanadium, chromium, titanium and manganese are particularly deleterious.
- **Weld arc instability.** As little as 10 ppm calcium or lithium in 5xxx welding wire causes the weld arc to be unstable.
- **Reduced vacuum brazeability:** As little as 10 ppm lithium or calcium in the cladding layer of brazing sheet can interfere with vacuum brazing process.
- **Toxicity:** Welding wire and alloys to be welded should not contain more than a few ppm beryllium to avoid exposure to toxic beryllium oxide fumes. In alloys intended for food containment, the concentration of toxic metals such as lead, arsenic, cadmium and thallium are also restricted to avoid possible contamination.

To overcome some of the inherent problems in recycling aluminium alloy scrap, controlled melt treatment can be used in order to maintain the best possible quality. These

practices include inert degassing and various forms of melt filtration (including use of ceramic foam filters) [2]. New technologies have been developed that allow aluminium dross to be processed on site at the melting furnaces to recover available metallic values. These systems are capable of economically processing dross quantities ranging from about 80 kg down to 10 kg per cycle, recovering up to 90 % of the aluminium with a combination of agitation and chemical reactions in less than five minutes. While at elevated temperature, the recovered alloy may then be returned to the original furnace to save remelting energy [25].

Despite these limitations with utilizing secondary metal in the foundry, there are several advantages besides reduced cost. Impurity elements are free and are sometimes beneficial. Two examples are; firstly, the high levels of iron, which are desirable in high-pressure die casting to alleviate the die soldering tendency of the melt, and secondly, high zinc and magnesium levels compensate for the loss of corrosion resistance in aluminium-silicon alloys resulting from the presence of copper and iron [2].

Some of the main classifications of recycled materials that are utilized are [2]:

- Beverage cans: 3004 and 5182 type alloy mix.
- Extrusions: 6xxx series alloys, containing magnesium, silicon and copper plus the grain refining elements.
- Swarf/millings: This is a mixture of alloys with a variety of surface contaminants. If these products are obtained from known workshops and stored separately, the alloy mix may be predicted with accuracy.
- Domestic: This material is too difficult to sort.
- Electrical wire: Purity aluminium with boron additions.
- Aeronautical: Mainly 7xxx alloys containing high levels of zinc and magnesium. Aluminium-lithium alloys also fall in this category.
- Castings: These normally contain high silicon levels. Many die cast alloys also contain copper as another major element and high levels of iron (>1%). Sodium, strontium and even antimony can be present in small amounts as modifiers. If grain refined hypereutectic alloys are included in the mix, then phosphorus may also be

present. Occasionally, zinc and magnesium alloy diecastings are accidentally included.

A simpler classification system for recycled aluminium alloy materials is also reported [27] as shown in Table 2.2, which also indicates the typical chemical analyses of the classifications.

Table 2.2 Examples of typical remelt chemistry derived from three different aluminium alloy scrap classifications

SCRAP SOURCE	ELEMENT (wt %)						
	Silicon	Iron	Copper	Manganese	Magnesium	Zinc	Aluminium
Municipal	0.80	0.50	2.40	0.60	1.70	2.00	balance
Automotive	5.00	0.80	2.00	1.0/0.30	0.10	0.60	balance
Used Beverage Cans	0.2	0.60	0.15	0.90	1.1/1.3	-	balance

2.2 CAST ALUMINIUM SILICON ALLOYS

2.2.1 OVERVIEW

Aluminium silicon alloys are the most commonly used group of cast aluminium alloys, constituting 85% to 90% of the total cast aluminium parts produced [28]. The reason for this change is because aluminium-silicon alloys offer excellent fluidity, good corrosion resistance, and can be machined and welded. They are also less prone to shrinkage, hot tearing and porosity defects than aluminium-copper alloys [23, 28]. These alloys have therefore generated great interest and have been under extensive investigation from as early as 1920 [29, 30]. They generally fall in the groups of (3xx.x) and (4xx.x) alloys. Their general composition is within the limits given in Table 2.3 [13, 23].

Table 2.3 Composition limits for aluminium silicon alloys (wt. %)

Element	Composition range (wt. %)
Silicon	5 - 25
Copper	0 - 5.0
Magnesium*	0 - 2.0
Zinc	0 - 3.8
Iron	≤ 3.0
Manganese, Chromium, Cobalt, Molybdenum, Nickel*, Beryllium and Zirconium	≤ 3.0 (total)
Phosphorus	≤ 0.01
Tin	0 - 0.25
Lead	0 - 0.35
Titanium	0 - 0.25
Aluminium	Balance

*The composition limit of Mg is normally 1.0%.

*Compositions of Ni alone can be up to 2.5% in certain alloys (e.g., for the 336 alloy).

The most commonly used of the cast aluminium-silicon alloys belong to the 3xx.x group of alloys and their equivalents in other designations. Some alloys in the 4xx.x group and

their equivalents are also used especially in intricate, thin walled castings of moderate strength and high ductility. The composition, characteristics and mechanical properties of some of the workhorse alloys belonging to these two groups are summarized in Tables 2.4, 2.5 and 2.6, respectively.

Table 2.4 Composition of common cast aluminium silicon alloys [13].

Alloy	Casting Method ^(b)	Silicon	Copper	Magnesium	Zinc	Iron	Others ^(a)
319	S, P	6.0	3.5	<0.10	<1.0	<1.0	
A319	S,P	6.0	<3.5	0.3	<1.0	<1.2	
332	P	9.5	3.0	1.0	1.0	<1.2	
355	S, P	5.0	1.25	0.5	<0.35	<0.6	
356	S,P	7.0	<0.25	0.35	<0.35	<0.6	
A356	S, P	7.0	<0.20	0.35	<0.1	<0.2	
357	S,P	7.0	<0.05	0.55	<0.05	<0.15	
A357	S, P	7.0	<0.20	0.55	<0.1	<0.2	0.05 Beryllium
380	D	8.5	3.5	<0.10	<3.0	<2.0	
383	D	10.5	2.5	0.10	<3.0	1.3	0.15 Tin
384	D	11.3	3.75	<0.10	<3.0	<1.3	0.35 Tin
390	D	17.0	4.5	0.55	<0.1	<1.3	<0.1 Manganese
393	S,P,D	22	0.9	1.0	-	<1.3	2.25Nickel, 0.12Vanadium
413	D	12.0	<0.1	<0.10	-	<2.0	
443	S, P	5.25	<0.6	<0.05	<0.5	<0.8	

(a) Remainder: Aluminium and other impurities

(b) S, Sand casting; P, Permanent Mould Casting; D, High Pressure Die casting

Table 2.5 Characteristics of cast aluminium silicon alloys [28]

Alloy (1)	Met hod	Resistance to tearing	Pressure tightness	Fluidity	Shrinkage Porosity	Corrosion Resistance	Machin ability	Welda bility
319	S, P	2	2	2	2	3	3	2
332	P	1	2	1	2	3	4	2
355	S, P	1	1	1	1	3	3	2
A356	S, P	1	1	1	1	2	3	2
A357	S, P	1	1	1	1	2	3	2
380	D	2	1	2	-	5	3	4
390	D	2	2	2	-	2	4	2
413	D	1	2	1	-	2	4	4
443	P	1	1	2	1	2	5	1

(1) Ratings: 1, best; 5, worst

Table 2.6 Typical mechanical properties of some common cast aluminium alloys [13]

Alloy	Sand Casting				Permanent Mould Casting			
	UTS (MPa)	YS (MPa)	Elongat ion (%)	BHN	UTS (MPa)	YS (MPa)	Elongat ion (%)	BHN
319-F	186	124	2.0	70	234	131	2.5	85
319-T6	250	164	2.0	80	276	186	3.0	95
355-F	159	83	3.0	-	-	-	-	-
355-T6	241	172	3.0	80	-	-	-	-
C355-T6	269	200	5.0	85	-	-	-	-
356-F	164	124	6.0	-	179	124	5.0	-
356-T6	228	164	3.5	70	262	186	5.0	80
A356-F	159	83	6.0	-	-	-	-	-
A356-T6	278	207	6.0	75	-	-	-	-
357-F	172	90	5.0	-	193	103	6.0	-
357-T6	345	296	2.0	90	359	296	5.0	100
A357-T6	317	148	3.0	85	359	290	5.0	100
A390-F	179	179	<1.0	100	200	200	<1.0	110
A390-T6	278	278	<1.0	140	310	310	<1.0	145
443-F	145	62	8.0	40	159	62	10.0	45

Table 2.6 Continued

Alloy	Die Casting			
	UTS (MPa)	YS (MPa)	Elongation (%)	BHN
360-F	324	172	3.0	75
A360-F	317	165	5.0	75
380-F	331	165	3.0	80
A380-F	324	159	4.0	75
390-F	279	241	1.0	120
413-F	296	145	2.5	80
A413-F	241	110	3.5	80
443-F	228	110	9.0	50

F - As-cast condition; T6 - Heat treated to the T6 condition

2.2.2 INFLUENCE OF KEY ELEMENTS

2.2.2.1 Silicon

Silicon is the main alloying element in aluminium-silicon alloys (Fig. 2.1 [31]). Silicon is fairly inexpensive and is one of the few elements that are added to aluminium to reduce its weight to volume ratio (and increase its strength to weight ratio) because of its low density (i.e., 2.33 g/cm^3 for silicon cf. 2.698 g/cm^3 for aluminium) [18, 23, 32, 33]. The coefficient of thermal expansion of aluminium is also appreciably reduced by the addition of increasing amounts of silicon [32]. Silicon is inert to most corrosive environments, and thus the corrosion resistance of aluminium-silicon alloys in most electrolytes is as good as, or better than, that of pure aluminium [34]. Increasing the silicon content generally increases the yield strength, tensile strength and hardness, but decreases the ductility of aluminium [34]. The modulus of elasticity increases with increasing silicon content [35]. The increased hardness imparts high wear resistance, but leads to poor machinability.

The strength and hardness properties, however, strongly depend on the size shape and distribution of the silicon particles (eutectic or primary). Alloys in which the silicon

particles are small, round and evenly distributed usually have higher ductility and better machinability. On the other hand, alloys in which the silicon particles are large, faceted and acicular are usually less ductile, but exhibit slightly higher strength. The ductility and machinability are improved by the addition of chemical modifiers, such as Strontium, sodium or antimony, that change the shape, size and distribution of the eutectic silicon particles in hypoeutectic and eutectic aluminium-silicon alloys [23, 28, 36]. The primary silicon in hypereutectic alloys, on the other hand, is refined by melt superheating [37](Fig. 2.2) or by the addition of phosphorus to improve ductility and machinability [28]. Modification also produces a limited increase in strength [23]. At higher cooling rates, normal in die-casting, the silicon is already somewhat refined without modification and the improvement from chemical modification is reduced [23].

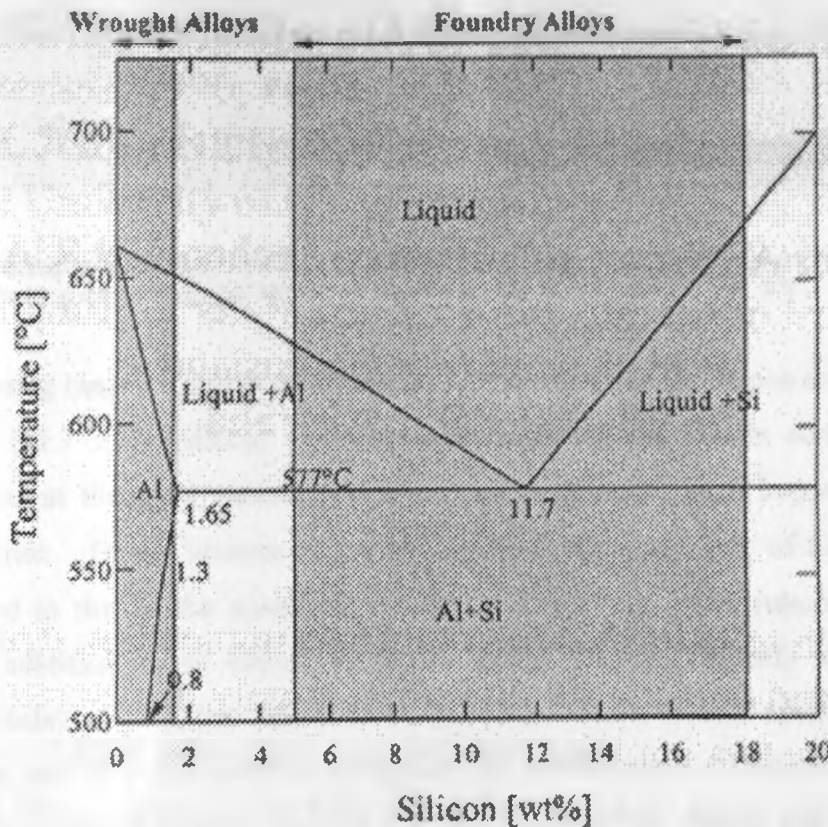


Fig. 2.1 Aluminium-silicon binary phase diagram with the composition ranges for wrought and foundry alloys indicated. Hypoeutectic cast aluminium silicon alloys have a maximum of 11.7% silicon (the eutectic composition), while hypereutectic alloys have Silicon contents of above 11.7% silicon. Silicon contents of up to 25% have been used, but the maximum indicated in the phase diagram (18%) applies to most common commercial cast aluminium silicon alloys [31].

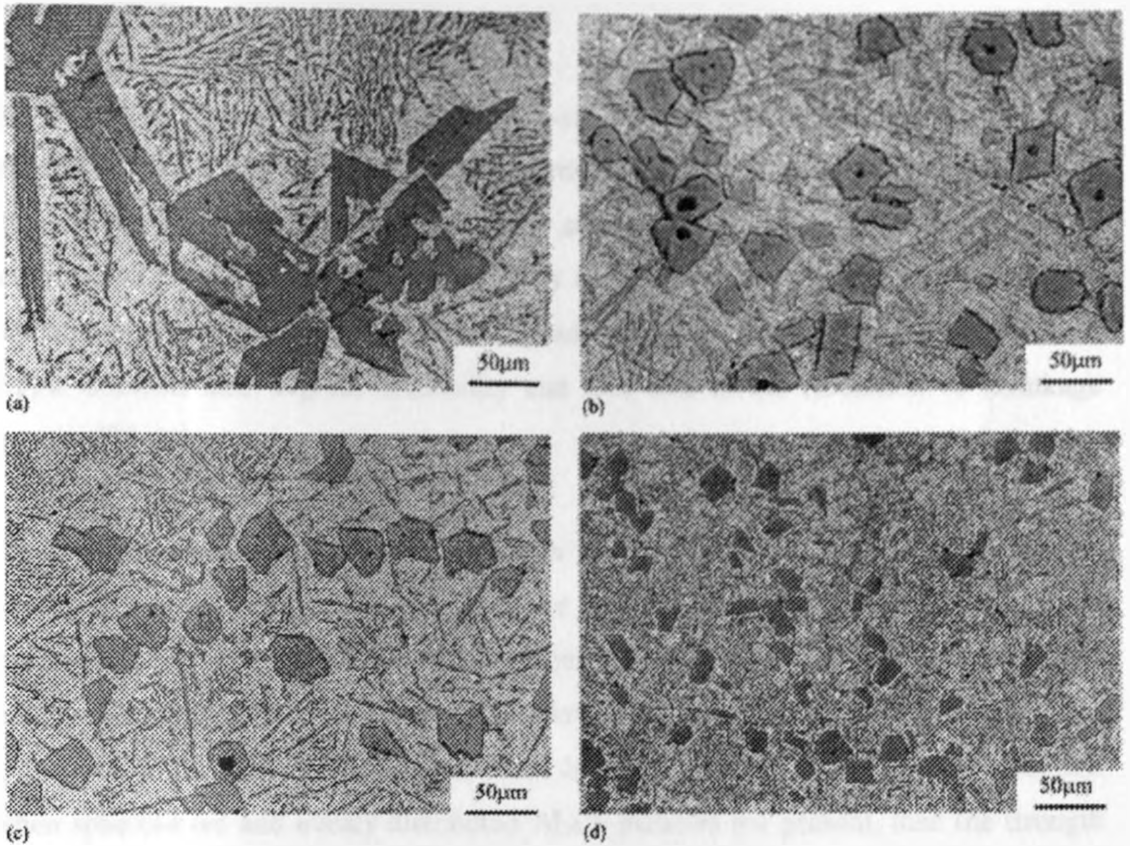


Fig. 2.2 Micrographs of binary Al-16silicon alloy showing primary Silicon refinement with increasing the melt overheating temperature. (a) 720 °C; (b) 880 °C; (c) 960 °C; (d) 1050 °C [ref. 37]

The freezing range of aluminium decreases with increases in the silicon content up to the eutectic (11.7 wt.% silicon). Furthermore, increasing the silicon content results in reductions in the alloy viscosity at a constant temperature even beyond the eutectic composition. This is because of the ~ 4.5 times higher latent heat of fusion of silicon compared to that of the equivalent volume of aluminium. The volumetric shrinkage during solidification of aluminium-silicon alloys decreases linearly with increasing silicon content and reaches zero at 25 wt. % silicon. This is because silicon expands as it solidifies and thus compensates for part of the solidification shrinkage of aluminium. The narrow freezing range, coupled with low viscosity are mostly responsible for the excellent fluidity of aluminium-silicon alloys, particularly those with silicon in the range of 7-18 wt. %. The low shrinkage and narrow freezing range of aluminium-silicon alloys are also responsible for their resistance to hot tearing, their good weldability and casting soundness [34].

2.2.2.2 Copper

Increasing the copper content in aluminium-silicon based alloys up to a maximum of between 4 and 5 wt. % improves their hardness, yield and tensile strength (at both ambient and elevated temperatures), fatigue strength, creep resistance, heat treatability and machinability, but degrades their ductility and corrosion resistance [32, 34]. Copper contents in excess of 5 wt% generally degrade mechanical properties [32]. Increased copper contents also degrade feedability and thus lead to the formation of shrinkage porosity [38-40].

The strength and ductility depend on whether the copper is present in solid solution, as evenly distributed spheroidised particles or as a continuous network at the grain boundaries [34]. Alloys with dissolved copper have the largest increase in strength and retain substantial ductility. Conversely, alloys where copper is present at the grain boundaries do not show appreciable increase in strength, but do show a loss of ductility. When spheroidised and evenly distributed Al_2Cu particles are present, then the strength of the alloy becomes a function of the mean free path between the particles.

Zhang and StJohn [41] reported that copper influences the strength of the aged aluminium silicon based alloy matrix through several possible mechanisms. These are:

- Copper atoms may be taken into the Mg_2Si precipitates leading to an increase in their volume fraction, which gives a higher strength. This mechanism is only possible if substantial magnesium is present for the Mg_2Si to precipitate.
- Copper atoms may combine with aluminium to form Al_2Cu precipitates, which increase the yield strength.
- Copper atoms may combine with magnesium, aluminium and perhaps also silicon atoms to form a new phase. The higher strain hardening rate that is usually associated with alloys containing copper might be due to the existence of this type of precipitate which may be stronger than Mg_2Si precipitates and can probably only be bypassed by moving dislocations.
- A substantial fraction of the copper atoms may continue to stay in solid solution in

the fcc aluminium causing a solution hardening effect. This solution hardening effect may also be partly responsible for an increase in the strain hardening rate.

Samuel [42] expressed the yield strength, ultimate tensile strength and percent elongation of 319 type alloys as a function of the copper concentration in the aluminium matrix after solutionising in the temperature range of 480-515°C. These expressions are: $YS \text{ (Mpa)} = 81.1 + 24.9 \times Cu \text{ (wt. \%)}$; $UTS \text{ (Mpa)} = 154.5 + 36.6 \times Cu \text{ (wt. \%)}$; and $El \text{ (\%)} = 0.023 + 1.01 \times Cu \text{ (wt. \%)}$.

A recent electronmicroscopy study by Reif et al [43] observed that the strengthening in the ternary aluminium-silicon-copper alloy after ageing is attributed to the formation of Al_2Cu plates while no silicon-containing precipitates could be identified. This is in line with the observations by Krol [44]. Reif et al [43] also observed that the precipitation hardening in the quaternary aluminium-silicon-copper-magnesium alloy can be ascribed to the simultaneous formation of relatively large Al_2Cu plates and small Al_2CuMg , again without contributions from Mg_2Si or other silicon-containing precipitates.

2.2.2.3 Magnesium

In some alloys such as the 380, magnesium is specified to be below a certain level, a maximum of 0.1% in the USA. Wang et al [34] attributed this low limit to the strong tendency of magnesium to react with other elements to form inclusions and intermetallic particles such as $Al_8FeMg_3Si_6$ and $Al_5Cu_2Mg_8Si_6$. For example magnesium can easily oxidize in the melt to form MgO . At high holding temperatures (i.e., $>745^\circ C$) magnesium can form spinel. Magnesium can also react with refractories and oxides, and by doing so may introduce finely dispersed inclusions in the melt. These inclusions and intermetallics reduce the alloys fluidity and castability in general and the subsequent mechanical properties of the alloy especially ductility. Furthermore, high magnesium-containing alloys are sensitive to the solutionising temperature, which varies between 490 to $540^\circ C$ depending on the melting point of the precipitates present (e.g., $505^\circ C$ for $Al_5Cu_2Mg_8Si_6$) [42, 45].

The low limits of magnesium imposed on the 380 alloy and other alloys have, however, been questioned by Wang et al [34] based on the rationale that significant data is not available to support the set limits. Furthermore, allowing higher magnesium content in the alloy can substantially reduce the cost of damaging (magnesium removal) and enhance hardness and tensile strength [34, 56]. It is perhaps because of this reason that the limits on magnesium set for alloys similar to the 380 alloy in other countries are considerably higher. For example, the Canadian SC84R alloy (0.45-0.75 %), the German 226/D alloy (0.3 %), the French A-S9U3A alloy (0.3 %), and the Japanese ADC10 and ADC12 alloys (0.3 %), are all equivalent to the US alloy 380, and allow higher magnesium contents.

Magnesium addition to aluminium-silicon based alloys increases the base alloys' strength, hardness and creep resistance, but decreases its ductility. Magnesium also improves corrosion resistance, machinability and the alloy's response to age hardening. It is, however, said to increase the coefficient of thermal expansion [34]. Magnesium contents in excess of 1 wt. % generally degrade mechanical properties [32].

Reif et al [43] appreciated that the mechanism of strengthening by magnesium is not clear due to the several alloying additions and the resulting complexity of phase transitions. The Al_2Cu phase usually precipitates when copper is present while Al_2CuMg and Mg_2Si phases form when magnesium and silicon are added. The best combination of mechanical properties corresponds to the presence of all possible hardening phases.

According to Caceres et al [46], the hardening precipitates (Mg_2Si) in the aluminium-magnesium-silicon system are coherent or semi-coherent with the aluminium matrix and produce a large increase in the yield strength. When the material is plastically deformed, these precipitates are relatively easy to cut by the dislocations. This results in a relatively low strain hardening rate. In contrast, the precipitation of Al_2CuMg plates in aluminium-silicon-copper-magnesium alloys leads to increased strain hardening rate at low strains due to Orowan looping around the plates. The precipitation of hard non-shearable Al_2Cu precipitates also exhibit similar deformation characteristics. It is, however, important to

note that studies on A356/357 alloys indicate that at low strains, the hardening rate is higher for a material with elongated silicon particles and higher magnesium content [47]. An increase in the hardening rate at low strains is actually observed whenever particles are added to a ductile matrix.

Researchers [41, 46, 48-49] have demonstrated that increasing the magnesium content in aluminium-silicon based alloys increases the maximum achievable strength and at the same time decreases the ductility. Simultaneous additions of magnesium and copper lead to a larger increase in strength, especially after heat treatment, but with a corresponding decrease in ductility [49]. Copper tends to form Al_2Cu in grain boundaries in as-cast structures, while the presence of magnesium leads to formation of $\text{Al}_5\text{Mg}_8\text{Cu}_2\text{Si}_6$ in addition to the Al_2Cu phase. The Al_2Cu phase occurs in both the blocky and eutectic forms in the as-cast condition depending on the local concentration of copper in the matrix. The addition of magnesium leads to segregation and increase of the copper phase away from the silicon eutectic regions and thus favours the blocky type Al_2Cu [45, 50].

A higher magnesium content leads to the formation of a higher volume fraction of magnesium-containing precipitates, which may be Al_2CuMg , $\text{Al}_4\text{Cu}_2\text{Mg}_8\text{Si}_7$, $\text{Al}_4\text{CuMg}_5\text{Si}_4$, $\text{Al}_5\text{Cu}_2\text{Mg}_8\text{Si}_6$ and/or Mg_2Si . This gives a greater strengthening effect. The presence of the silicon-containing precipitates in heat treated aluminium-silicon-copper-magnesium alloys has, however, been questioned by Reif et al [43] and Krol [44]. For a given magnesium and copper content, both strength and ductility can be altered by changing the ageing conditions.

The high strain hardening rate at low strains presumably due to the precipitates (whether in as-cast or heat treated condition) allows the matrix to shed enough load onto the second phase particles (eutectic silicon and iron-intermetallic particles) thus leading to lower ductility. Furthermore, it is reported that aluminium-silicon-copper-magnesium alloys with 0.5 wt. % magnesium contain $\pi\text{-Al}_8\text{FeMg}_3\text{Si}_6$ phase particles [46]. The π -phase particles tend to be large and brittle and are known to lower the ductility of alloy 357 in comparison with alloy 356 [48-49, 51]. It is thus reasonable to assume that the π -

phase would also reduce the ductility of the aluminium-silicon-copper-magnesium alloys.

2.2.2.4 Iron

Iron is the main impurity in most cast aluminium-silicon alloys and is generally kept as low as is economically possible because of its deleterious effects on mechanical properties and corrosion resistance [23]. There are reports that iron may slightly increase strength, but it drastically decreases ductility and fatigue resistance [23]. It is invariably present in aluminium die casting alloys where it is either intentionally added in order to mitigate the tendency to die soldering, or it is inadvertently introduced into the molten alloy from steel tools used during melt handling and from charge materials that contain it.

Iron is a relatively insoluble element in aluminium and its alloys. The maximum solubility of Fe in solid aluminium is between 0.03 % and 0.05 % at 655°C. Consequently, it segregates during solidification and forms intermetallic compounds with aluminium and several of the other elements present in the alloy. For high strength and ductility castings such as those cast through sand and permanent mould casting, iron levels are limited to a maximum of 0.7 wt.%. In some piston alloys and die castings, up to 3 wt.% iron may be tolerated [23].

The iron-bearing intermetallic compounds can occur in a variety of morphologies; large or small needles; Chinese script; globular; rosettes; hexagonal; polyhedral; star-like; and indefinite forms [2, 23, 38, 50, 52]. Table 2.7 outlines examples of the various iron-bearing phases that can form in aluminium-silicon alloys. The two most common iron-containing intermetallic phase forms in hypoeutectic cast aluminium-silicon alloys are β -Al₃FeSi phase with a needle or platelet morphology, and α -Al₁₅Fe₃Si₂ phase with Chinese script morphology. An additional phase, known as π -Al₈Mg₃FeSi₆, may also form in the presence of magnesium, and may form with independent Chinese script morphology or else grow from the surfaces of β -Al₃FeSi platelets. The α -phase can also appear as polyhedral if it solidifies as a primary phase [2, 38, 52].

Table 2.7 Examples of the various Fe-bearing phases that can form in aluminium-silicon alloys [2, 23, 48, 50, 53]

Morphology	Fe-bearing phase	Necessary composition conditions
β -Platelets	Al_3FeSi (eutectic)	$0.05\% < \text{iron} < 0.7\%$
β -Platelets	Al_3FeSi (primary)	$\text{Iron} > 0.7\%$
α -Chinese script or globular	$\text{Al}_{15}(\text{Fe}, \text{Mn})_3\text{Si}_2$	Manganese $> 0.2\%$ when iron is present
Star-like or polyhedral	$\text{Al}_{13}(\text{Fe}, \text{Cr})_4\text{Si}_4$ $\text{Al}_2(\text{FeCr})_5\text{Si}_8$	Chromium $> 0.1\%$ when iron is present
Chinese script or globular	$\text{Al}_8\text{FeMg}_3\text{Si}_6$	$\text{Iron} > \text{magnesium}$
Chinese script or globular	$\text{Al}_9(\text{Fe}, \text{Co})_2$	Cobalt $> 0.1\%$ when iron is present
Acicular	Al_9FeNi	Nickel $> 0.1\%$ when iron is present
Needles	$\text{Al}_8\text{CuMg}_8\text{Si}_6$	copper $> 1\%$, magnesium > 2 copper
Particle clusters	$\text{Al}_5\text{Cu}_2\text{Mg}_8\text{Si}_6$	When magnesium, copper and strontium are present
Chinese script	(Be-Fe)- $\text{Al}_8\text{Fe}_2\text{SiBe}$	When Beryllium is present
Chinese script	$\text{Al}_9\text{FeMg}_3\text{Si}_5$	When strontium and magnesium ($\sim 0.7\%$) are present
Chinese script	$\text{Al}_5\text{Fe}_2\text{Si} / \text{Al}_8\text{Fe}_2\text{Si}$	When magnesium, copper or zinc is present
Acicular	Al_7FeCu_2	When copper is present
Chinese script	$\text{Al}_{15}\text{Fe}_3\text{Si}_2$	Can form as long as iron is present

The phases that form depend on cooling rate, the presence of elements soluble in the iron phases (such as manganese or chromium), and the melting-holding temperatures used. The cooling rate affects the time available for the iron intermetallics to form; thus, the kinetics of the iron-based reactions become important. High cooling rates, such as experienced in die casting, suppress the segregation of iron and therefore the formation of the β -phase. This reduces the size and amount of this phase in the solidified structure.

High cooling rates also favour the formation of α -Chinese script over the β -phase [2, 38, 52]. The β -phase has been associated with a coarsening of the grain size and a decrease in the SDAS in a 319 alloy, especially at low cooling rates [38]. Also, the β -Al₃FeSi phase may nucleate eutectic silicon even in strontium-modified alloys [38].

The morphology of the iron-bearing intermetallic compounds play a deciding role in the alloys' mechanical properties, particularly ductility and strength. The β needle-shaped iron-bearing phase is most detrimental, mainly because of the more severe stress concentration effect that the higher aspect ratio of the needles introduce into the alloy's matrix [52].

One way of controlling the deleterious effects of iron is to control the size and morphology of the iron-bearing phases through the addition of iron-correcting elements. Various elements have been proposed and tried. Some of these are manganese, chromium, beryllium, cobalt, molybdenum, vanadium, tungsten, copper, nickel, yttrium, neodenum, lanthanum and cerium [2, 23, 32, 48, 50, 52-55]. The most common iron-controlling addition used commercially is manganese, which favours the formation of the α -phase. Chromium is also used occasionally, often in conjunction with manganese, though it has a tendency to form sludge by peritectic precipitation on holding [2,13]. The ratio of iron:manganese:chromium has significant effect on the morphology and size of the iron-bearing phase. At low manganese and chromium levels, the iron-bearing phase is in the form of needles. With the addition of higher levels of manganese and chromium, the needles are replaced by Chinese script, polyhedral or star-like particles. Manganese addition favours the formation of Chinese script while chromium addition favours the formation of star-like and polyhedral particles [52]. Mondolfo [23] favours the use of cobalt and molybdenum, while beryllium has been suggested to have the most profound iron-neutralizing effect (optimum level is 0.26% beryllium per 1% iron) [2, 55]. Beryllium with manganese, or beryllium with chromium, provide even greater improvement in mechanical properties over beryllium additions alone [2]. There are other reports, however, which claim that at low iron contents, beryllium additions reduce strength [55].

Reducing the iron content of an alloy can also be used to control the amount and size of the β -platelets. Another technique is the application of high temperature melt heat treatments prior to casting. This favours the formation of α phase over β phase [2].

2.2.2.5 Important Minor Alloying and Impurity Elements

Apart from silicon, copper and magnesium, which are the major alloying elements in aluminium-silicon based alloys, an appreciable number of other elements are normally added as minor alloying elements. These supplementary alloying additions are normally made to improve specific alloy properties and casting characteristics. Furthermore, commercial cast aluminium alloys almost always contain impurity elements. Most of these elements, because of their low concentrations, dissolve in the aluminium and have a minimal influence on alloy properties. Under certain conditions, however, impurity elements may form intermetallic compounds that may have appreciable effects on the alloy properties. The minor and impurity elements most common in cast aluminium-silicon alloys together with their effects on the alloy properties are briefly described in this subsection.

Manganese: The solubility of manganese in aluminium is 1.8% at 657°C, 1.0% at 627°C, and 0.2% at 427°C [34]. The solubility of manganese in aluminium is reduced by the presence of iron and silicon, leading to the formation of some intermetallic compounds, such as $Al_{15}(Fe,Mn)_3Si_2$. Manganese is usually added to wrought alloys to improve their strength through work hardening, and as an iron corrector.

Aluminium-silicon alloys always contain high levels of manganese brought into the melt through contamination with wrought scrap [27]. In these alloys, manganese offers no significant strengthening benefits as they are not work hardened. However, the presence of manganese may slightly improve the alloys high temperature properties, enhance its fatigue resistance, reduce its shrinkage and enhance corrosion resistance [34]. At higher contents and at certain holding temperatures, manganese may form sludge especially when chromium is present. For example, primary $Al_{15}(Fe,Mn)_3Si_2$ (Sludge), may form in alloys with compositions exceeding 0.6% iron, 0.5% manganese and 8% silicon at holding temperatures of around 610-660°C [56]. Sludge reduces the alloy's mechanical properties and machinability [23]. Sludge reduces the alloy's fluidity, castability and hence casting soundness [34]. Manganese, together with iron and nickel,

is strongly related to hot tearing [27]. Manganese is usually added to cast aluminium alloys in amounts that do not exceed half the alloy's iron content to act as an iron corrector as discussed earlier.

Chromium: Chromium is also usually used as an iron corrector and it slightly increases the room and elevated temperature strength of aluminium-silicon alloys. Chromium may form sludge with manganese and iron as mentioned earlier and may therefore reduce the alloys castability, mechanical properties and machinability [34].

Nickel: Nickel also increases both room and elevated temperature strength of aluminium-silicon alloys. It is also said to improve their ductility when it acts as an iron corrector. Otherwise, it reduces their ductility. Nickel reduces the coefficient of thermal expansion of aluminium based alloys. Nickel and iron together in aluminium-silicon alloys enhance their resistance to attack by high temperature water and steam [34].

Zinc: When present in aluminium-silicon alloys, zinc decreases high temperature strength, tends to increase the tendency for hot tearing, but improves the alloy's machinability. In secondary alloys, zinc and manganese compensate for copper and nickel and enhance the alloys corrosion resistance. The detrimental effects of zinc are not pronounced and for this reason, it is specified in many alloys at higher levels than other impurities, e.g. up to 3% in some aluminium-silicon alloys [34].

Tin and Lead: Tin and lead, if present together with magnesium in aluminium-silicon alloys, tend to enter into the Mg_2Si phase. They decrease the alloys high temperature strength, but improve the alloys machinability. Tin is, however, deleterious to corrosion resistance [34].

Titanium: Titanium is added alone as Al-Ti master alloy or normally with boron as Al-Ti-B master alloys to grain refine aluminium alloys. Grain refinement means facilitating the formation of small equiaxed grains ($\sim 200 \mu m$ in diameter) instead of large columnar grains [57]. Titanium-based grain refiners are usually added within their solid solubility limit of 0.1-0.15% although higher contents of up to 0.25% may be specified for cast alloys as shown in Table 2.3 in Section 2.2.1. Grain refinement has been reported [58-61] to cause the following:

- Better feeding of the casting. However, excessive addition of grain refiner has been reported [59] to decrease the size of interdendritic channels during feeding thus leading to increased

external shrinkage especially at hot spots.

- Better dispersion of second phases
- Reduced and evenly distributed microporosity
- Uniform macrostructure throughout the casting (i.e. better homogeneity of the casting)
- Improved and more uniform mechanical properties throughout the casting (the improved mechanical properties include tensile properties, fracture toughness and fatigue resistance.
- Reduced hot tearing
- Improved machinability
- Improved surface finish and response to anodising
- Improved response to heat treatment due to the shorter diffusion paths of solutes
- Better fluidity

Misra and Oswalt [62] reported that titanium forms TiA_3 precipitates, which besides acting as a grain refiner also affects the normal ageing kinetics in A356 and A357 alloys. According to these authors, the complete precipitation of the equilibrium phase (Mg_2Si) is delayed and a secondary peak in elongation occurs after long ageing times and corresponds to the best combination of strength and elongation. Shankar and Apelian [63] also reported recently that an addition of 0.125 % Ti to A380 alloy reduces die soldering.

Titanium does work in synergy with other alloying and impurity elements such as magnesium, lead, tin. Chromium, nickel and iron to enhance grain refinement by, for example, increasing the growth restriction factor of the alloy among other mechanisms.

Other important minor alloying elements that are commonly encountered in aluminium-silicon based alloys are strontium, sodium, antimony and calcium for modification of the eutectic silicon. Most of these elements are depleted on remelting except antimony, which is retained even after several remelts. Antimony and calcium are, however, less frequently used for this purpose. Other elements that may be present in aluminium-silicon based alloys are beryllium, vanadium, cobalt, molybdenum, lithium, phosphorus, tungsten among others. Some rare earth impurity elements such as lanthanum may also be introduced as constituents of fluxing agents. Beryllium is an excellent iron corrector,

improves the precipitation kinetics of strengthening precipitates and even acts as a grain refiner of aluminium. It also raises the melting temperature of the Al_2Cu phase from $\sim 515^\circ C$ to $\sim 522^\circ C$ [64]. This allows a higher solutionising temperature to be used for aluminium-silicon-copper based alloys without the danger of incipient melting. This element, its benefits notwithstanding, is toxic and its addition is rare and limited to a small group of alloys such as A357, C357, 358, B358 and 364 [13].

2.3 LIQUID ALUMINUM METAL TREATMENT

2.3.1 OVERVIEW

In order to consistently produce high quality castings, it is necessary to optimise the metal quality prior to casting. The aspects of molten metal processing important to cast aluminium-silicon alloys are [65]:

- Control of melt composition
- Degassing of the liquid melt
- Inclusion removal
- Grain refinement
- Modification of the eutectic silicon

Each of these areas is important and all have been under extensive research. As a result, a number of innovative techniques aimed at improving the casting quality have emerged in recent years. A number of reviews have been published that discuss to some degree of detail the various molten metal processing practices. To mention some of them: Samuel and Samuel [66] reviewed the various aspects involved in the gassing and degassing of molten aluminium alloys; Utigard et al. [67] reviewed the properties and uses of various fluxes in molten aluminium processing; Makarov et al. [68] reviewed the various aspects involved in the detection and removal of inclusions in molten aluminium; Murty et al [57], reviewed grain refinement while Gruzleski [69] reviewed modification. Shivkumar et al. [70], Gruzleski and Closset [28] and Sigworth et al. [65] presented a more comprehensive review of molten aluminium processing. The last two reviews also cover thermal analysis, which is an equally important molten aluminium processing practice that is used to non-destructively control the microstructure, particularly in relation to grain refinement and modification. The use of electrical conductivity to control modification is also considered by Gruzleski and Closset [28]. In the following subsections, the various aspects of molten aluminium processing that are of particular relevance to the current study are briefly discussed. Grain refinement, eutectic modification, and the use of thermal analysis and electrical conductivity for

microstructure control are not considered.

2.3.2 HYDROGEN CONTROL IN MOLTEN ALUMINIUM AND ITS ALLOYS

Liquid aluminium metal is a highly reactive chemical. It will react with both the gases surrounding it and the solid material of the crucible that contains it. If there is any kind of slag or flux floating on top of the melt, it will probably react with it too. These reactions take place throughout the duration of melting in the furnace, laundering, pouring and mould filling [6]. However, the two most important interactions between liquid aluminium and its environment are the dissolution of hydrogen into the melt and the instantaneous formation of an alumina oxide film on the surface exposed to air.

Porosity or microporosity in castings is inevitable to a certain extent and can be very detrimental to surface quality, mechanical properties, leak tightness and corrosion resistance. Porosity in castings occurs mainly because of the rejection of gas from solution during solidification and/or the inability of the liquid metal to feed through the interdendritic regions to compensate for the volumetric shrinkage associated with solidification [66]. Hydrogen is the only gas with any appreciable solubility in molten aluminium and is usually present in molten aluminium alloys constituting from 70 to 80% of the total gas content in the melt. It therefore plays a major role in causing porosity in aluminium castings and considerable effort is expended in controlling its dissolution and in removing it from the molten aluminium alloy. In addition to causing porosity, hydrogen has also been reported to cause blistering and high temperature deterioration or advanced internal gas precipitation during heat treatment [13]. It also probably plays a role in grain boundary decohesion during stress corrosion cracking that occur normally in wrought alloys [13].

2.3.2.1 Sources of Hydrogen

Aluminium castings in industry are generally produced in environments where hydrogen is invariably present in the form of water vapour, obtained in large quantities from

various sources. Most hydrogen, which finds its way into molten aluminium, therefore, comes from the dissociation of water vapour at the surface of molten aluminium according to the reaction [2, 28];



From the reaction, a little metal is sacrificed to form alumina and the hydrogen is released to equilibrate itself between the gas above the melt surface and the molten aluminium. Whether it will, on average, enter the melt after dissociating from molecular hydrogen or enter the gas above the melt will depend on a number of variables. These include the relative partial pressure of hydrogen already present in both of these phases, the melt temperature and the alloy composition, which directly affects the chemical activity of hydrogen in the melt. This reaction is highly favoured at foundry operating temperatures, and it is safe to assume that all water vapour coming into contact with molten aluminium will dissociate in this way. The contact must, however, be with metallic aluminium and not the oxide. The reaction cannot proceed if the molten bath is protected by the oxide film on its surface [2, 6, 28].

The potential sources of water vapour (and hence hydrogen) in a foundry are numerous. Examples are:

- High atmospheric humidity: This is considered to be the most important source of water vapour [28].
- Foundry fluxes and/or fluxing gases contaminated with water: Fluxes are generally hygroscopic salts that naturally pick up water from the atmosphere. Some fluxes also contain water of crystallisation, which is bonded into their crystal structure.
- Damp foundry tools such as plungers and ladles.
- Damp or recently installed crucibles and refractories: The usual clay/graphite materials for crucibles are quite permeable to water vapour and/or hydrogen, since they are designed to be approximately 40 per cent porous [6]. Most refractories are also hygroscopic and will absorb water up to 5 to 10 per cent of their weight [6].
- Combustion gases: The products of combustion of most fuels contain 10 to 20 per

cent water vapour [28].

- **Charge materials:** Charge materials may contain moisture on their surface or in pores and crevices. Scrap may also be contaminated with grease, cutting oil, corrosion products and oxide layers. Oxide layers often hold water and partly corroded aluminium can add hydrogen by decomposition of the corrosion product, aluminium hydroxide ($2\text{Al}(\text{OH})_{3(s)} + 2\text{Al}_{(l)} \rightarrow 2\text{Al}_2\text{O}_{3(s)} + 3\text{H}_2$) [28]. Alloying materials may also contain significant hydrogen levels [2].

2.3.2.2 Hydrogen Solubility

The levels of hydrogen which can be dissolved and exist at equilibrium with the melt depend on the melt temperature, the partial pressure of water vapour in the immediate vicinity of the melt, the degree of protection afforded to the melt by the integrity and nature of the oxide skin, and the alloy composition.

The following empirical equation describes the equilibrium hydrogen concentration in a melt (C_H) [2]:

$$\ln C_H = -A/T + B \ln P_{\text{HsubO}} - \ln \gamma_H + C \quad (2.2)$$

Where A, B and C are empirically determined constants, T is the melt temperature, P_{HsubO} is the partial pressure of water vapour above the melt and γ_H is the activity of hydrogen in a particular melt composition.

Hydrogen in solution is governed is governed by Sievert's law, which allows prediction of the partial pressure of hydrogen that will be in equilibrium with a given concentration of hydrogen in solution. Sievert's law is given stated as:

$$[\text{H}]^2 = k P_{\text{Hsub2}} \quad (2.3)$$

Where the constant k is experimentally determined and is affected by the alloy chemistry

[71] and temperature.

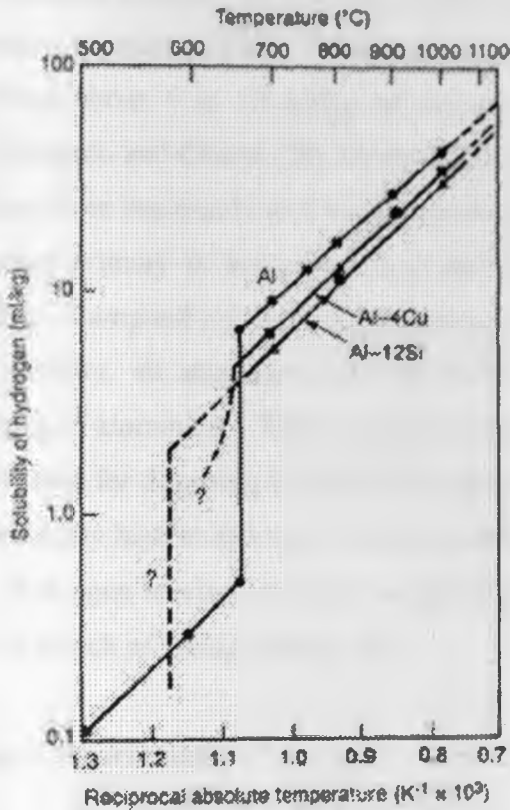


Fig. 2.3 The hydrogen solubility in aluminium and two of its alloys, illustrating the abrupt fall in solubility on solidification (After Campbell [6]).

The solubility of hydrogen in pure aluminium at one atmosphere pressure is shown in Fig. 2.3 together with that of aluminium copper and aluminium silicon alloys at different temperatures [6, 28]. It is evident from the figure (Fig 2.3) that hydrogen solubility in aluminium and its alloys has a strong temperature dependence, especially in the liquid state. It is reported that the hydrogen solubility in pure aluminium doubles for each 110°C increase in superheat [28]. It is also observed that hydrogen has a low solubility in solid aluminium and that there is a large change in the solubility at the melting point. This means that virtually all of the hydrogen in molten aluminium is unable to dissolve in the solid on freezing. Hydrogen, therefore, accumulates in the liquid at the solidifying interface and may eventually assist in porosity formation.

Addition of alloying elements to aluminium changes the hydrogen solubility, although the solubility curves retain the same basic shape as shown in Fig. 2.3. Silicon, Zinc, copper and manganese decrease the solubility, while others such as magnesium, titanium, nickel and lithium increase it [28]. The equilibrium hydrogen solubilities in foundry alloys range from about 6 to 10 ml/Kg of aluminium depending on the alloy and temperature. Gruzleski and Closset [28], however, reports that it is extremely rare to find melts, which have been reasonably well handled containing these levels of hydrogen. For example, remelted primary or secondary ingot will usually contain between 2 and 3 ml/Kg aluminium. Campbell [6] has also demonstrated that on a normal day with 30 per cent relative humidity, an aluminium melt at 750°C should have 1 ml of dissolved hydrogen per 1 kg of aluminium. This is respectively low for most commercial castings and thus the rationale for degassing by just leaving the melt to settle for 30 to 60 minutes. If the melt is originally high in hydrogen, it will equilibrate by losing the hydrogen to its environment. Hydrogen levels in the melt of less than 0.1ml/kg are attainable through this degassing approach of 'doing nothing' [6].

2.3.2.3 Hydrogen Measurement

It is necessary to accurately assess the amount of hydrogen in the melt to be able to control it. Many techniques have been developed for this purpose, each geared towards greater improvement in the ease of measurement and its accuracy. Of the available methods, three (recirculating gas, sub-fusion analysis and vacuum fusion) provide a direct measurement of the hydrogen concentration. The others are indirect techniques in that they involve the measurement of some physical property usually related to density or bubble formation, and from this the hydrogen concentration is inferred.

The simplest and cheapest, but unfortunately the most inaccurate method involves deducing the hydrogen level from density measurements of standard samples using the Archimedes Principle. The volume of hydrogen is given by:

$$\text{ml H}_2/\text{Kg Al} = 1000 (1/D_s - 1/D_t) \quad (2.4)$$

Where D_s = Sample density and D_t = theoretical density of the alloy.

The theoretical density can be determined by a simple calculation based on the alloy chemistry or by measuring the density of a chill cast sample poured from a well degassed metal or one subjected to HIPping. The major source of inaccuracy in this method is the assumption that all of the porosity in the sample is due to hydrogen volume. Other sources of inaccuracy are related to density measurement errors and differences in pore nucleation phenomena associated with melt cleanliness [28].

Among the earliest tests known is the Straube – Pfeiffer Test, where the hydrogen content is estimated by from the density of a metal solidified under reduced pressure. It is for this reason that it is also called the “Reduced Pressure Test”. A variation of the test involves solidifying a sample in an isolated vacuum chamber and measuring the pressure increase in the chamber due to evolution of hydrogen. The hydrogen level is calculated from the pressure rise. Another variation is the ‘Initial Bubble Test’, which involves noting the pressure at which the first bubble is observed in the molten sample kept in a chamber in which the pressure is slowly reduced. The hydrogen concentration is then calculated from Sievert’s Law, assuming that the chamber pressure at which the first bubble occurs equals the partial pressure of hydrogen in the melt. There are several varieties of commercial equipment based on the principal of the Reduced Pressure Test. Examples include the Hydro Tester, Alu-Melt Tester and the Hyscan series equipment (e.g. Hyscan 11).

The recirculating gas method forms the basis for two types of commercial equipment: Telegas and Alscan and this method measures directly the hydrogen content in molten aluminium and its alloys. The apparatus recirculates a small volume of nitrogen through the molten alloy bath. As the nitrogen contacts the bath, it picks up hydrogen, until eventually the hydrogen content of the nitrogen stream comes into equilibrium with the hydrogen concentration in the bath. The partial pressure of hydrogen in the molten alloy is determined by measuring the thermal conductivity of the nitrogen-hydrogen mixture.

Calibration is done beforehand using a premixed hydrogen nitrogen gas. Once the partial pressure is known, the hydrogen concentration in the melt is determined using Sievert's Law.

Sub-fusion and Vacuum Fusion techniques are capable of providing very accurate hydrogen analysis and are often used to calibrate the other methods. A commercial version of the vacuum fusion method is the Leco (RH series).

In both sub-fusion and vacuum fusion, the hydrogen is extracted under vacuum from a reheated sample (to about 50°C below melting point for sub-fusion and melted for vacuum fusion), which was highly chilled to retain all hydrogen in solid without porosity formation. The extracted hydrogen is separated from other gases by allowing it to diffuse through a heated palladium tube and measured.

2.3.2.4 Degassing

The first and most important control of hydrogen in molten metal is, naturally, to avoid as much as possible all the sources and conditions that introduce it and/or accelerate its dissolution. As mentioned previously, the level of dissolved hydrogen in molten aluminium depend on the degree of protection afforded to the melt by the integrity and nature of the oxide skin. If the oxide skin on the melt is of high integrity and low permeability then the reaction between aluminium and water vapour, the subsequent breakdown of molecular hydrogen to atomic hydrogen and its diffusion into the melt will be limited. This can be achieved by minimising turbulent operations that will break the surface of the metal. It can also be achieved by using cover fluxes and by avoiding holding the melt at high temperatures (>60°C superheat) for extensive periods of time. Low temperature holding is essential because the oxide layer losses its tenacity through a change in its crystal structure [28]. Furthermore, the solubility of hydrogen in molten aluminium also increases with temperature as previously discussed.

Initially, the aluminium oxide layer formed on an aluminium melt is amorphous alumina,

which subsequently transforms to a crystalline γ -alumina film after about 5-10 minutes at about 750°C [72]. The crystalline γ -alumina is more stable and protective than the amorphous oxide, but after longer incubation time, it converts to α -alumina (corundum) with an associated volume reduction of 24%. This leads to oxide rupture and exposure of molten aluminium to the atmosphere [2]. In alloys with high magnesium levels (>0.2%), the amorphous MgO that forms subsequently transforms to crystalline MgO. This transformation can impose stresses sufficient to rupture the protective γ -alumina skin [2]

It is however, helpful to note that recent work by Li and Bian [73] indicated that just as hydrogen content increases in molten aluminium and its alloys with increasing temperature, it is also lost to the atmosphere when the temperature is decreased. This is, however, possible only if the high temperature is rapidly quenched to the normal operating temperature. This can be achieved by adding a predetermined cold amount of a similar material (referred to by the authors as thermal-rate treatment).

Other preventive steps include the following:

- Fluxes should be stored in sealed containers, which are impermeable to air and should probably be heated to above 100°C to drive off absorbed water before use [28].
- New crucibles and refractories and/or those that have not been in use for several days should be preheated prior to charging. Foundry tools should also be clean and sufficiently preheated.
- Dirty Scrap or other charge materials should be avoided. Some charge materials can be preheated to drive off water from their surfaces.
- Stirring actions or melt additions should be made as gently as possible and any form of surface turbulence should be avoided.

Various methods have been developed over the years for removing hydrogen from molten aluminium. They all involve either gas purging or vacuum degassing. Hydrogen removal has also been achieved through natural degassing. Gas purging is used most extensively and different methods based on it differ basically in the type of purge gas

used and the method of its introduction into the melt

Natural Degassing

If the melt is originally high in hydrogen (supersaturated), It will naturally try to equilibrate by losing some of this hydrogen to its environment if the melt surface is not prohibitive (i.e. no protective oxide or cover flux is present) and the original hydrogen content in the environment is lower. Natural degassing is slow and requires several hours depending on the holding temperature and tenacity of the melt surface. This method is favoured by low holding temperatures and dry atmospheres or inert gas atmospheres over the melt (i.e., free of hydrogen) [6, 28].

Vacuum Degassing

This involves creating a vacuum above the melt surface that accelerates the hydrogen removal in three steps; (i) by diffusion from the immediate melt surface that is continuously being renewed by convection, (ii) by free evaporation at the surface, and (iii) by diffusion through the gas phase [71]. Degassing is also provided through provision of a completely hydrogen-free atmosphere. The rate of degassing with this method is, however, slow and requires 30 to 60 minutes [6]. This time can be reduced to a few minutes if the melt is simultaneously flushed with pure, dry nitrogen. This stirs the melt and helps the rising bubbles to overcome the metallostatic head [6, 28, 66].

Although vacuum degassing is not yet widely used in the foundry industry because of the high costs involved, it is capable of attaining hydrogen levels in the melt of as low as 0.1 ml/kg aluminium [6]. It also has the benefit that other aspects of the environment of the melt, such as the refractories are also dried and therefore do not affect degassing results [6, 66]. It is also environmental friendly like natural degassing because no harmful gases are released to the atmosphere.

Gas Purging

This is the treatment with an inert gas, a reactive gas or a combination of these. As the stream of gas bubbles passes through the melt the hydrogen in the liquid metal diffuses into these bubbles and is removed to the atmosphere when the bubbles break at the surface of the melt. Differences between the various degassing techniques lie in the type of gas, which is introduced, and in how the bubbles are formed.

Among the common gases used include pure dry nitrogen or argon (inert gases), chlorine, freon, sulphur hexafluoride or hexachloroethane (reactive gases). Pure chlorine was used extensively in the past, but has now been largely discontinued due to its toxicity and corrosive effects on equipment [28]. Reactive gases work more effectively than inert gases due to the chemical reactions that result when such gases are introduced into the melt, and the rate of removal is therefore faster. They also have the advantage of removing inclusions from the melt and controlling the alloy chemistry by removing certain elements (usually alkali and alkali earth-metals). However, in certain cases, some of these elements are added intentionally to impart certain properties to the alloy (e.g. Sr and Na for modification of eutectic silicon) and the use of some of the reactive gases will result in their removal depending on the melt treatment procedure. Furthermore, fume evolution associated with reactive gases is a major environmental problem. Inert gases are environmental friendly although their degassing efficiency is somewhat lower. There is also a possibility for the formation of nitride inclusion if pure nitrogen is used.

To combine the advantages of reactive and inert gases and reduce their disadvantages, gas mixtures are used instead. Examples include a mixture of nitrogen or argon and chlorine, freon-12 (CC_2F_2), or sulphur hexafluoride (SF_6) with the reactive gas concentration varying from 1 % to 30 %. A mixture of 80 % nitrogen, 10 % chlorine and 10 % carbon monoxide has also been used.

The treatment gas can be introduced into the melt through the use of tablets, lances, porous plugs or rotary impellers. In tablet degassing, tablets containing hexachloroethane

(C_2Cl_6), which decompose above $700^\circ C$ are plunged into the melt and held therein using a perforated bell. Hexachloroethane decomposition releases hydrogen, which react with aluminium to form aluminium chloride ($AlCl_3$ is gas above $183^\circ C$). As aluminium chloride gas bubbles rise through the melt, they pick up hydrogen. The fumes evolved are due to a reaction of aluminium chloride with water vapour to form a fine white fume that is a mixture of hydrochloric acid and aluminium oxide. Tablet degassing is the least controllable method of degassing since decomposition is rapid and dross formation is promoted. Despite these disadvantages, it is often quite suitable for small melts and finds application where precise control of degassing is not required [28].

Introducing gas through a lance (usually graphite) with an inside diameter of about 0.3 cm is also simple but not very effective. Such a lance produces large bubbles with diameters of the order of 2-3 cm, which rise close to the lance surface, and so contact a minimum of melt. A much finer dispersion of gas bubbles can be achieved with the use of a porous plug screwed at the end of a lance. The porous plug can be made of alumina, silicon carbide [74] or graphite [28]. The most effective is the rotary impeller degasser which introduces the gas into the melt through a special impeller head which rotates rapidly, chops the gas stream into very fine bubbles (3-6mm) and then disperses them throughout the body of the melt. The final hydrogen levels achieved depend on the initial hydrogen content, purge gas flows, impeller rotation speed, size of melt and treatment time employed [28].

There is also another method, which involves automated flux injection into the melt. The process eliminates hydrogen as well as oxides and can also be used to modify and refine the alloys being treated. Flux is mixed with nitrogen gas, which acts as a carrier for the flux and is introduced below the surface of the melt using a lance [66]. This method has faster treatment times, gives consistent quality of final cast product, is environmental friendly and is economical [66]. The various gas purging methods described together with vacuum degassing are summarised in Table 2.8.

Table 2.8 Review of degassing systems [66]

System	Purge gas	Efficiency of removal	Fume evolution	Degassing rate	Capital Cost	Operate Involvement
Tablets	Reactive	High	High	Moderate	None	High
	Inert	Moderate	None	Moderate	None	High
Lance	Reactive	High	High	Moderate	Low	Moderate
	Mixed	Moderate	Moderate	Low	Low	Moderate
	Inert	Low	None	Low	Low	Moderate
Rotary devices	Mixed	High	Moderate	High	Moderate	Low
	Inert	High	None	High	Moderate	Low
Vacuum	None	High	None	Low	High	Low

Hydrogen removal through gas purging can be thought of as a process requiring several successive steps [28]:

- Hydrogen transport in the molten alloy to the surface of a purge gas bubble, usually by a combination of diffusion and convective motion.
- Transport of hydrogen atoms by diffusion through a thin stagnant boundary layer of liquid at the bubble surface.
- Chemical absorption of hydrogen atoms onto the bubble surface.
- Reaction of hydrogen atoms to form hydrogen gas molecules and desorption of these molecules from the bubble surface.
- Diffusion of gaseous hydrogen into the main volume of the bubble.
- Removal of the hydrogen containing bubbles from the melt surface.

Depending on the degassing arrangement, the first four steps can control the efficiency. The single most important factor in determining the degassing efficiency is the bubble size. High efficiencies of even up to 100 % can be achieved at small bubble sizes (<5 mm in diameter). Larger bubbles (> 10 mm in diameter) result in very poor efficiencies (20 % to 30 %) [28, 66]. A large number of small bubbles will be close together and hydrogen atoms will have only a short distance to travel in the melt to arrive at a bubble surface. Liquid phase transport is no problem, but the small volume bubbles quickly

become saturated with hydrogen (100 % efficiency) and an increase in the gas flow rate is required to increase the degassing rate. Small bubbles also float more slowly and have a longer contact time during which they can absorb hydrogen. Large bubbles are more buoyant and therefore rise rapidly and so have shorter contact time with the melt.

Of the four commonly used methods for introducing degassing agents into aluminium melts, lance degassing and tablets are the most inefficient. Lance degassing produces large bubbles, which rise only in the vicinity of the lance and tend to collide and coalesce, thus becoming even larger. Decomposition of tablet degassers is uncontrolled, bubble size is variable and the bubbles are confined to a volume of melt around the plunger, which is used to introduce the degasser. A considerable refinement of the bubble size occurs with use of a porous plug. However, bubbles again tend to rise only in a plume above the plug. The volume of melt contacted is limited, and bubble coalescence occurs reducing efficiency. By far the most uniform pattern of fine bubbles is obtained with a rotary impeller degasser, which also if properly sized can disperse the bubbles throughout the melt to achieve maximum contact.

The degassing efficiency is improved at lower melt temperatures. In view of this, degassing should always be carried out at the lowest temperatures possible. Other factors being constant, the time to degas to certain level of hydrogen doubles for each 70°C increase in melt temperature [65].

2.3.3 INCLUSIONS IN MOLTEN ALUMINIUM AND ITS ALLOYS

Several types of inclusions can be present in the melt. These inclusions lead to several problems, which include [28, 65, 68]:

- A reduction in mechanical properties of the casting, especially tensile strength, ductility and fatigue resistance that are drastically affected. The yield strength is relatively unaffected. Inclusions, which help to initiate fracture under both tensile and fatigue loads are also a major contributor to scatter in properties.
- Poor machinability and high tool wear. Some of the inclusions such as α -alumina

(usually known as hard spots) are brittle and extremely hard. Small amounts of these inclusions in the casting lead to extensive tool wear during machining.

- Loss of fluidity and feeding properties of the alloy.
- Increased porosity. Inclusions act as sites for nucleation of gas bubbles.
- Poor surface quality, which is unsuitable for anodising and perhaps even for painting or varnish. The sheen and luster that are characteristic of machined aluminium are lost in the presence of inclusions.
- Lack of pressure tightness, thus requiring weld repair or impregnation.
- Reduced corrosion resistance, especially flux inclusions.
- Increase in the modulus of elasticity.

The critical size of inclusions that may be tolerated depends on the end application. In most cast components, inclusions with sizes greater than 10 to 20 μm may have drastic effects on the quality of the part.

2.3.3.1 Sources of Inclusions

Inclusions in molten aluminium can be classified according to their size, chemical content and phase (i.e. solid or liquid). These inclusions can be exogenous and/or indigenous. Exogenous inclusions originate from outside the melt itself and include refractory particles such as alumina, silica, and silicon carbide, which result from the wear and erosion of crucible materials. These are found as discrete particles and may range in size from about 1 μm up to several millimetres. Indigenous inclusions arise from either chemical reactions within the melt itself, or else remain from some deliberate melt treatments such as fluxing or grain refinement [28, 68]. According to Shivkumar et al. [70], inclusion concentrations of unprocessed aluminium melts range from 0.005 to 0.2 vol. %. Even at low inclusion concentrations (by volume), a substantial number of inclusions may be present in the melt. For example, if the average inclusion size is about 40 μm , an inclusion concentration of 1 ppm would mean that 1 kg of metal would contain approximately 11, 000 particles. Table 2.9 summarises data for various inclusion types. The table shows that inclusions may be present in several physical forms such as discrete

particles, clusters of particles, or as films.

Table 2.9 Classification and characteristics of inclusions in molten aluminium [68]

Type	Form	Density ρ , g/cm ³	Dimensions, μm	MP, °C
OXIDES				
MgAl ₂ O ₄ (Spinel)	Particles, skins, flakes	3.60	0.1-100, 10-5000	2825
Al ₂ O ₃ (Corundum)	Particles, skins	3.97	0.2-30, 10-5000	2047
MgO	Particles, skins	3.58	0.1-5, 10-5000	2115
SiO ₂	Particles	2.66	0.5-30	1650
CaO	Particles	3.37	<5	2630
CARBIDES				
Al ₄ C ₃	Particles, clusters	2.36	0.5-25	2100
SiC	Particles	3.22	0.5-5	2540
BORIDES				
TiB ₂	Particles, clusters	4.5	1-30	2790
AlB ₂	Particles	3.19	0.1-3	2160
NITRIDES				
AlN	Particles, skins	3.26	10-50	2227
OTHER				
Chlorides and salts (CaCl ₂ , NaCl, MgCl ₂)	Liquid droplets	1.9-2.2	0.5-1	712-800
Fluorides (cryolite)		2.9-3.0		1000
Sludge Al(FeMnCr)Si		>4.0		-
ULTRAFINE GAS BUBBLES			10-30	
Argon bubbles				
N ₂ bubbles				
INTERMETALLICS (TiAl ₃ , TiAl, NiAl, Ni ₃ Al)	Particles, clusters	-	10-100	-

The free energy of formation of alumina ($\Delta G^\circ = -324$ Kcal/mol of Al₂O₃ at 1000 K) is such that it is practically impossible to prevent film formation at exposed surfaces [6, 72]. Because of its strong affinity for oxygen, aluminium can form more than 15 different oxides, ranging in specific gravity from 2.3 to 4 [70]. The concentration of oxygen in commercial aluminium is in the range of 0.1 to 100 ppm. Oxide films and clusters of oxide particles are, therefore, the major source of inclusions [70]. Fortunately, the Pilling-Bedworth ratio for aluminium is 1.27, indicating that the oxide film is dense, continuous and protective [70]. Most group 1A and 11A elements, if present in aluminium, also readily form very stable oxides. Examples are Na₂O, Li₂O, MgO, CaO, BeO and MgAl₂O₄ (spinel). When most of these oxides are present (except for BeO), the melt may be unable to maintain its continuous protective Al₂O₃ skin, even when it is

quiescent. Instead it will be subject to the rapid and continuous production of more oxides.

Alumina films are usually suspended on the melt surface and/or entrapped within it due to turbulence. Despite their greater density, oxide inclusions tend to remain on the surface due to the surface tension, but once entrained into the melt, they have a slow sedimentation to the bottom [72]. Oxide inclusions also have a tendency to agglomerate because they are poorly wetted by molten aluminium. Spinel inclusions originate from melting scrap as well as magnesium additions into the holding furnace. Since magnesium oxide has a lower free energy of formation than alumina, it tends to form preferentially, particularly in alloys containing more than 0.5 % magnesium [68].

The melt transference and mould pouring are the most turbulent foundry operations, and the most damaging to the aluminium melt. During these operations, a large quantity of the melt surface is exposed to air, resulting in enormous oxide film generation (Figs 2.4-2.5). Surface turbulence also provides conditions for breaking the oxide into numerous small films, incorporation of these oxide films into the bulk liquid, and introduction of some air bubbles into the liquid. The passage of air bubbles through the melt also promotes aluminium oxidation, and the remaining oxide tubes form bubble trails [6, 72].

It is noteworthy that these oxides are entrained into the melt as double oxide films, folded dry side to dry side. Even if a thick oxide film is pushed into the melt in an effort to create a single immersed inclusion, it will be surrounded by two new non-wetting films. The microscopic surface roughness of these solid films results in point contact at the asperities on the surface and, therefore, gas entrapment between the contacting films. The defect constitutes a crack in the liquid. The existence of shear-type forces due to bulk turbulence or stirring within the melt may then distort or compact these double films into highly contorted structures but still retaining the characteristics of convoluted cracks [75].

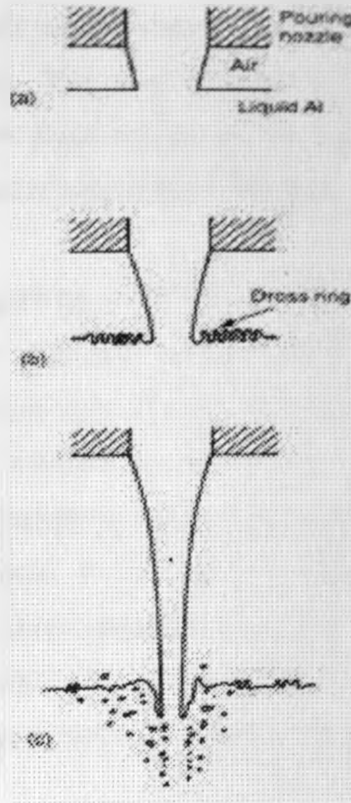


Fig. 2.4 A schematics showing the effect of increasing height on a falling stream of liquid, illustrating: (a) the oxide film remaining intact; (b) the oxide film being detached and accumulating to form a cross ring; (c) the oxide film and air being entrained in the bulk melt (After Campbell [6]).

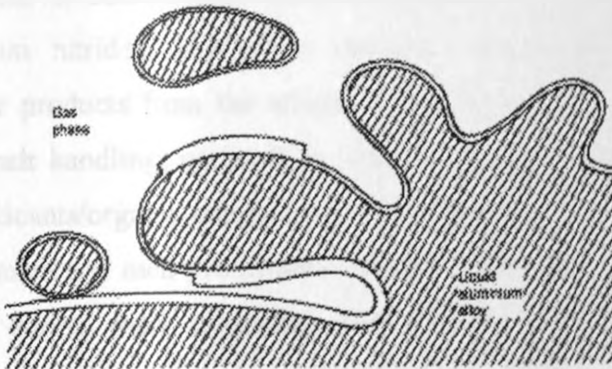


Fig. 2.5 The schematic view of a splash of molten aluminium showing the formation of a folded (double) film that might consist of thick old film, or new thin film, or both, all likely to occlude air in the folds (After Campbell [6]).

Elements within melts may combine to form various intermetallic phases during

solidification. Under special conditions of holding time and temperature, certain phases may also form within the melt prior to casting or at least prior to solidification. These are termed as "primary" phases. This may be used to advantage to remove unwanted impurities, but may also work disadvantageously by causing losses of important elements and/or promoting entrainment of undesirable inclusions.

High specific gravity and melting point iron-containing intermetallics usually form in aluminium die-casting alloys. These are referred to as sludge, which has a composition of either $Al_{15}(Fe,Mn)_3Si_2$ or $Al_{15}(Fe,Mn,Cr)_3Si_2$. These are approximate compositions and may actually include small amounts of other elements such as copper and zinc. The formation of sludge occurs mainly as a result of poor melt handling of die-casting alloys containing high levels of iron. At low holding temperatures (e.g. 610-650°C), iron, manganese and chromium form sludge when present above certain critical levels in aluminium-silicon alloy melts. These intermetallics are very dense relative to the aluminium melt and therefore settle to the bottom of furnaces and ladles [2].

Alloying additions can also be a source of inclusions. Magnesium can contain 10-40 ppm oxides, 15-60 ppm nitrides and 1.5-7 ppm carbides. Silicon is also reported to contain up to 0.1 % Al-Si-Ca oxides and 120 ppm SiC [2]. Elements can also exist as constituents of non-metallic inclusions trapped within the metal during solidification. Aluminium nitrides, aluminium carbides, cryolite and fluoride salts are potential carryover products from the smelter reduction process. Carbides can also be created during melt handling, particularly when scrap with carbon-based surface contaminants (e.g. lubricants/organic coatings) are introduced into the melt due to use of inadequate pre-treatment and melt procedures. Nitrides formed through the introduction of nitrogen bubbles during inert degassing and borides introduced via grain refiners added deliberately or in scrap, can agglomerate and settle in quiescent melts. Chlorides and fluorides of group IA and IIA elements may also form due to fluxing. These include, liquid phase inclusions of $CaCl_2$, $NaCl_2$, $MgCl_2$ and KCl_2 and solid phase inclusions of NaF_3 and CaF_2 [68]. Reaction products between salt fluxes and refractories can form deposits on furnace walls. These may become dislodged and transferred into the melt

when disturbed through erosion or mechanical means. Refractory particles can also originate from furnace and ladle linings, launders and refractory washes [2]. These refractories can agglomerate and complex compounds such as $\text{Al}_2\text{O}_3 \cdot \text{SiO}_2 \cdot \text{CaO}$ can form [68].

2.3.3.2 Inclusion Removal Techniques

It has been reported in the literature [2] that it is not possible to completely eliminate the production of dross (mixture of aluminium oxide, molten and/or solid aluminium droplets and other reaction compounds) during the industrial handling of aluminium melts. It is therefore more appropriate to direct our attention to dross and hydrogen minimization rather than complete removal. The first step towards inclusion control is to minimise their introduction into the melt.

A number of factors that influence dross and gas generation, and which, therefore, require strict attention in the operations in foundries include the following [2]:

- Chemical composition of the metal.
- Effect of time and temperature.
- Gauge of scrap and its degree of surface contamination.
- Charging and melting methods employed.
- Furnace combustion characteristics.
- Melt turbulence during holding, transfer, pouring and casting.

Charging ingots or scrap should as much as possible be of high quality and free of any surface contamination. Good melt handling practice involves carrying out all alloying procedures, melt degassing and fluxing treatments at suitable temperatures in minimum times with minimum degree of agitation required to achieve melt homogeneity. The melt should then be allowed to stand for sufficient time to permit flotation of any entrained particles. Care should be taken to avoid holding times and temperatures that encourage sludge formation. The dross layer should then be skimmed off immediately prior to pouring. The melt transference and pouring should be done quiescently to minimize

surface turbulence. Furnaces, ladles and other laundering systems should be properly maintained. Build-ups of oxides on the walls are commonly contaminated with a variety of adsorbed elements (e.g. silicon, iron, potassium sodium and calcium). The oxides can subsequently enter the melt through mechanical perturbances. Adsorbed elements may also diffuse back into melts if concentration gradients are favourable [2]. These build-ups should therefore be avoided by cleaning the furnace walls regularly using cleaning fluxes. Furnace heels are often repositories for high specific gravity inclusions. It is therefore desirable to maintain furnace heels of at least 5-10 % between casts in order to minimize disturbance and carryover [2]. If these agglomerated deposits are disturbed, they may be transferred to castings.

A number of methods exist for the removal of inclusions from melts prior to casting. The basic mechanisms of these methods are based on one or more of the following principles: sedimentation, flotation, interception (filtration), electromagnetic forces or ultrasonic absorption [28, 68, 76]. An effective unit for inclusion removal must separate inclusions down to the smallest sizes from the melt (5 μm or less), as smaller inclusion particles are preferable to the larger ones in regard to pore nucleation [77].

Gravity sedimentation may be effective for inclusions larger than 90 μm , while the flotation technique may be effective up to about 30 to 40 μm . Removal of inclusions of less than 30 μm may be accomplished by filtration, but with limited and controversial filtration efficiency. Electromagnetic separation can, by comparison, remove even micrometer-sized inclusions in principle by using high-intensity force fields [76].

Gravity Sedimentation

It is well known that holding the melt in a furnace for long periods is beneficial to metal cleanliness. This is attributed to the settling of inclusions, due to their larger density than that of the melt. It is, however, believed that natural settling is not a practical technology for inclusion removal. This is because most inclusions range from 1 to 30 μm in size and their ultimate settling velocity is at most 0.5 mm/s. Even for inclusions of about 100 μm

in size, the actual settling velocity is less than 3 mm/s. This is uneconomical in terms of time and energy requirements due to long holding times. Moreover, most of the oxides formed are very similar to molten aluminium in density, and increasing holding time would lead to increased oxidation, especially in the case of magnesium-containing alloys [77].

Nevertheless, it has been reported that under appropriate conditions, inclusion levels could be dramatically reduced after holding for only 5 to 15 minutes [78]. In a recent report, Cao and Campbell [79] showed that gravity sedimentation of a significant quantity of oxide films and iron-rich primary intermetallics is possible within relatively short times. The iron-rich intermetallics nucleate and grow on the wetted side of suspended oxide films and cause them to sediment by increasing their density. This is possible at low holding temperatures and is limited to alloys having high iron equivalent factors (sludge factors). The iron equivalent factor (IEV) is given by $IEV = 1(\%Fe) + 2(\%Mn) + 3(\%Cr)$. The authors observed that holding an Al-11.5Si-0.4Mg alloy with an iron equivalent value at 600°C for 10 minutes resulted in moderate improvement in tensile properties. The particularly attractive feature of this technique is that it removes both iron and oxides films.

Flotation

Removal of inclusions by flotation is one of the most commonly used treatment methods in the aluminium foundry industry. In the flotation treatment process, either an inert gas, or a mixture of an inert and a reactive gas, is bubbled into the molten metal. While the bubbles rise to the surface, they come into contact with inclusions and dissolved hydrogen and carry them to the melt surface. The addition of chlorine or other halogens affects the surface tension of the bubbles in such a way as to make the particles stick to the bubbles more efficiently [65].

The methods of introducing the purge gas are similar to those described earlier for degassing. Just as in degassing, the rotary impeller is the most effective flotation method

of inclusion removal. The inclusion removal efficiency largely depends on the contact time between the bubbles and the metal. It also depends on the ratio between the interfacial gas-metal surface and the volume of gas injected into the melt [80-82]. The interaction between inclusions and gas bubbles depends on the flow field inside the melt created by the flow of the bubbles as well as the impeller rotation and the size and number of bubbles. Particle removal also depends on the agglomeration of the particles caused by turbulence in the flow field.

Historically, the optimisation of melt-treatment processes relied largely on operator experience, but better understanding of processes has been achieved through mathematical modelling and computer simulations. In addition, simulations have been used to optimise existing processes and design new processes. An example of useful mathematical modelling and computer simulation work in inclusion removal by flotation is the work of Maniruzaman and Makhlof [80-82]. This work has shown that by employing periodical reversal of rotation, there is improvement in the melt flow field and the possibility of top slag ingestion into the melt, which is normally observed in a conventional rotary impeller, is reduced [82].

Filtration

Filtration technologies offer an effective way of removing inclusions in the size range less than 30 μm [68]. The inclusions are transported to the filter surface as a result of bulk fluid flow and, subsequently, the inclusions are captured in the filter material due to interfacial or surface forces. Materials such as fibreglass cloths, steel gauze screens, wirewool and other sieves and strainers have been utilized although they are only useful for the removal of large inclusions. Ceramic foam filters, extruded monoliths, or porous tubes are normally used in the foundry while deepbed filters are used in virtually all primary production plants [28, 68]. Filters are placed either in the furnace or melting crucible or in the gating system. The choice of location is dictated by the casting operation and by the cost per unit weight of metal filtered. In die casting, the metal is filtered as it leaves the melting furnace or as it is held in a ladle or crucible. The nature

of sand and permanent mould casting permits inclusion of filters in the running system, which also minimizes turbulence during mould filling.

Filtration processes can be either through deep bed filtration or cake filtration. In deep bed filtration, the inclusions are trapped within the body of the filter itself as the melt flows through it. The effective pore size of the filter is much larger than the diameter of the particle that it will retain. Cake filtration occurs on the filter surface and is essentially a sieving action. The pore size of the filter determines the size of inclusions to be removed. Inclusions of 30 μm and larger can be separated by this technique. Deep bed filters can be effective at inclusion sizes less than 30 μm . In ceramic foam filters, apart from filtration within the filter, the build up of the cake on the filter surface also contributes to the overall effect. This phenomenon also affects the flow of the liquid metal through the ceramic foam filter. The metal does not flow through the filter until sufficient pressure is created by the metallostatic head. An initial surge of metal is observed until the cake builds up on the filter surface. Subsequently, steady state flow is formed until blockage of the filter occurs. The running system should be so designed as to fill the mould cavity before the filter is blocked. Although the efficiency of various filters is surrounded by controversy, it appears that filters that utilize both cake and depth modes provide the best results [65]. Some authors [83] have, however, reported that the most important benefit of ceramic foam filters placed in the running system is to control the metal flow velocity. In their work, the authors did not find any evidence to link the action of the filter with filtration. The authors actually suggested that ceramic foam filtration is only effective when working with excessively dirty melts.

Electromagnetic Separation

In electromagnetic techniques, an externally applied electromagnetic (Lorentz) force acts on the melt (conducting) and as a reaction to this externally applied force, the inclusions (non-conducting) move in the opposite direction – as a result of Newton's third law and thus become separated. This force acting on the inclusions is called the Archimedes electromagnetic force [68, 84]. The sources of the Lorentz force and, consequently, the

Archimedes electromagnetic force depend on the manner in which the electric and magnetic fields in the melt are produced. These include inductions coil, travelling magnetic field, pinch-effect and super imposed magnetic field. The first two are referred to as induction current separation while the latter two are injection current separation techniques. Large force densities in large melt volumes are difficult to achieve, mainly due to the complexity of producing strong, highly homogenous fields. For this reason, separation efficiencies are quite low when the inclusion size is below 50 μm . This method is therefore, not widely used.

The use of high DC magnetic fields generated by modern superconducting coils can considerably improve separation efficiency and move the sizes limits towards smaller inclusions as discussed by Makarov and co-workers [84-85]. These authors have shown that this method can remove inclusions of the order of 10 μm in size. For large force densities, the main problem remains the homogeneity of the force distribution throughout the volume. If the force is not uniform, very strong electromagnetically driven motion and turbulence may result.

Ultrasonic Treatment

Ultrasonic absorption in many liquid metals, including molten aluminium, is relatively small giving rise to the opportunity for ultrasonic treatment of the melt. The ultrasonic treatment includes acoustic degassing of the aluminium melt and fine filtration of molten aluminium in the cavitation field. The application of ultrasound to the melt has been shown to affect the wettability of the inclusions [68].

Separation of inclusions from molten aluminium may be enhanced by the use of filters and ultrasonics. The use of fine filters or use of multilayered filters is limited by the capillary permeability of these filters. However, the situation is radically improved when a cavitation field is formed above the filter surface as the sonocapillary effect comes into effect. The melt then freely passes the labyrinth of capillaries and dispersed inclusions subsequently settle at the surface of the filter [86].

2.3.3.3 Inclusion Detection and Measurement Methods

To effectively monitor inclusions during molten aluminium processing, it is necessary to have a rapid and inexpensive technique for measuring the level of inclusions in the melt in terms of their volume content (or numbers) and their type and size distribution. The aluminium foundry industry is, however, still struggling to develop such technique. Nevertheless, a number of inclusion detection and measurement techniques have so far been developed. These techniques are summarized in Table 2.10 and some of them are discussed below.

Table 2.10 Inclusion Detection Methods [68]

DETECTION METHODS	<i>Sample weight, g</i>	<i>Particle size affected, μm</i>	<i>Operation</i>
PRESSURE FILTER TESTS PdDFA LAIS Prefil Footprinter	≤ 2000 ≤ 1000	All sizes	Off-line Off-line On-line
ELECTRIC RESISTIVITY TEST LIMCA, LIMCA II	≤ 100 per minute	> 15	On-line
ACOUSTIC DETECTION Signal-noise technique Pulse-echo technique		> 10	On-line
ELECTROCHEMICAL DISSOLUTION	≤ 100	All sizes	Off-line
CHEMICAL ANALYSYS Emission spectroscopy; Hot extraction; Combustion analysis; Neutron activation; Gas chromatography	0.5-30	All sizes	Off-line
EDDY CURRENT METHOD	-	-	On-line
CAPACITANCE PROBE	-	-	On-line
X-RAY DETECTION			Off-line
ELECTROMAGNETIC DETECTION TECHNIQUE	≤ 200 per minute	> 10	On-line

Pressure filtration Techniques

These involve filtering a molten aluminium sample (of a known amount) under pressure through an ultrafine filter, resulting in a build up of inclusions on the filter surface. The inclusions collected are then analysed metallographically. The method is tedious, labour intensive and therefore off-line. The Porous Disk Filtration Apparatus (PoDFA), Liquid Aluminium Inclusion Sampler (LAIS) and the Prefil Footprinter, are based on this principle. In the Prefil Footprinter, the filtration rate is recorded during a standardized pressure filtration test and it is compared with pre-programmed information. In spite of their shortcomings, these tests are quantitative and have been used quite effectively to assess inclusion levels in most foundry shops [28, 68].

Resistivity Tests

LIMCA (or LIMCA II) is based on the electrical resistive pulse principle. Its probe consists of a heat-resistant sampling tube that draws molten aluminium under vacuum through a small orifice. A constant current is maintained through the orifice with a DC power supply and two electrodes, one placed inside the sampling tube, the other located in the surrounding melt. Any passage of inclusion (non-conducting) through the orifice causes a drop in the electrical resistance, resulting in a voltage pulse. The number of pulses and their amplitudes are then calculated using a signal processing program to assess the inclusion density and size distribution. LIMCA is considered to be reliable for on-line detection of small inclusions (15-20 μm in size). It can be used either alone or together with PoDFA or LAIS for larger inclusions [68]. The system is, however, too expensive and is suited for continuous casting.

Qualiflash

The qualiflash determines melt cleanliness through the clogging of an extruded ceramic filter by inclusions (usually alumina skins). Molten metal enters at a temperature-controlled shell (420-430°C) with a filter at the bottom. The passing metal then flows

into a nomograph (a 10 – stepped ingot mould. Once the metal has stopped flowing through the filter, the degree of cleanliness is quantified by the quantity of metal that fills the ingot mould. The dirtier the melt, the faster the clogging and thus less metal in the mould. Prior calibration makes it possible to judge the melt cleanliness. The test can be complete in only 10 minutes and is therefore on-line. The test can be used by relatively unskilled personnel and the only consumable is the filter [87].

K-Mould

The K-Mould produces a flat plate casting, with four notches cast into its cope surface. The notches serve as fracture points in the final shape, and the knife edges in the mould seem to improve the collection efficiency to capture the inclusion matter in the fracture zone through some eddy effect. Multiple samples of the plates are poured in a preheated mould from the metal being evaluated. They are then fractured immediately and the inclusions on the fracture surfaces are counted and metallographically identified. Each fracture surface that contains inclusions is considered an event and the K-value is quantified by expressing the events as a ratio of total fractures examined. For example if two fractures with inclusions are found in a total of 20 fractures, the K-value is 0.1. Allowable K-values are normally established prior to the test. Typically, a thin-wall casting that has pressure tightness requirements may not exceed values of 0.05 [88].

2.3.4 MELT CHEMISTRY CONTROL

Chemical analysis of aluminium alloy melts is usually carried out routinely prior to casting, using chill samples and spark emission spectroscopy [2]. The results detail the concentration of particular elements present in the metal but do not give information regarding the form in which the element is present, either in the melt or in the casting. In molten aluminium alloys, elements are typically present in solution, provided there is adequate time and temperature for dissolution. Liquids may also contain elements present as constituents of high melting point solid phases.

The importance of getting the right alloy chemistry prior to casting cannot be overemphasized. Established foundries have found it imperative to purchase spectrometers for in-house analysis, others use outside laboratories. In many markets, casting buyers won't consider buying a product from a foundry that does not have a spectrometer. They use it to measure the level of technology in the foundry and hence the quality of their products [77]. Often, foundries have customers who demand that their castings conform to specified chemical limits. Since the time it takes to send samples to a commercial laboratory or the use of in-house wet/combustion chemical analysis could delay the delivery of castings to the customer, foundries utilize in-house spectrometers to provide analysis before the castings are out of the mould [89]

In addition, spectrometers have a major impact on cost reduction when their information is used to reduce the cost of additions to the melt. An accurate chemical analysis of a sample provides a foundry with the chemical composition of its base alloy. From the analysis, and depending on the computer software and the customized information database incorporated, the spectrometer can make calculations to determine the exact and lowest-cost charge correction required to produce the specified chemical composition of the castings. Many physical properties of metallurgical interest such as theoretical tensile strength, hardness or density of an alloy may be calculated directly by the spectrometer using the chemistry of the alloy. If a foundry knows from its spectrometer that an element's concentration has changed, it can have a system in place to compensate for those changes. Control charts for the chemistries can be generated and process capability monitored [77, 89].

2.3.4.1 Alloying Addition Methods

Several methods of alloying are practiced in the industry. The choice of method is dictated by cost effectiveness, ease of use, quality, packaging and health and safety considerations. Elements such as silicon and magnesium, which melt or dissolve readily in aluminium, are added as the pure metal. The other alloying additive types which are most readily dissolved in aluminium are the master alloys. These generally contain a

mixture of aluminium and the aluminide of the alloying element. The rapid dissolution of the aluminide at normal melting or holding furnace temperatures make it relatively simple to use and to ensure high and rapid recoveries. They are, however, expensive. Concentrated additives can also be used and are a mixture of alloying element powder (typically 75 or 80%), aluminium powder and/or a flux. For high dissolution rates and maximum yield, the addition practice should follow additive manufacturer's guidelines [90].

2.3.4.2 Removal of Impurity Elements

It is sometimes necessary to reduce the content of certain elements in the molten alloy. This may be achieved by making proportionate additions of the other elements, thus reducing the level of the elements in question. Whereas this method is useful in controlling the level of major and minor alloying elements, it may not be very effective in controlling the level of impurity elements. The use of scrap leads in many cases to an undesirable final level of metallic impurities in the melt due to the diversity of recycled materials. Among the most harmful impurities depending on the application are iron, magnesium, zinc, manganese, chromium, tin, zirconium, titanium, antimony, strontium, sodium, calcium and lithium. Some of these elements, particularly group IA and IIA elements (i.e. sodium, calcium, lithium, magnesium and strontium) can be removed by flushing the melt with a reactive gas or by using refining fluxes [67]. Cooper and Kearns [91] reported that some transition metal impurities, particularly titanium, vanadium, chromium and zirconium can be removed by adding boron to form borides of these elements. These borides are then removed by a suitable inclusion removal technique. Flores-V. et al [92] have also reported that precipitation and segregation of intermetallic compounds is a suitable method of removing iron, manganese, chromium, Zirconium, titanium and vanadium. This is achieved by adjusting the alloy chemistry so as to allow precipitation of intermetallic compounds in the melt that contain these elements. The inclusions are then removed either by gravity sedimentation or by using any other suitable inclusion removal technique. The removal of iron, manganese and chromium can actually be done by encouraging sludge formation by adjusting their content in the

melt and holding at a suitable temperature for sufficient time. The sludge can then be removed by gravity sedimentation, electromagnetic separation or some other technique [79, 92-94].

2.3.5 TREATMENT OF MOLTEN ALUMINIUM WITH FLUXES

Fluxing refers to addition and treatment of molten aluminium with chemical compounds. These compounds are usually inorganic and may perform several functions, such as degassing, damping, cleaning, metal refining and alloying. Solid fluxes are mainly blends of chloride and fluoride salts and most of them are based on a mixture of potassium chloride (KCl) and sodium chloride (NaCl), which forms a low temperature 665°C eutectic. Other fluxes are based on MgCl₂-KCl, which forms a low melting eutectic at 424°C, or carnalite (MgCl₂.KCl), which melts at 485°C. MgCl₂ is, however, fairly expensive and is therefore primarily used in sodium free fluxes for alloys containing more than 2 % magnesium and which have very low limits of sodium and calcium [67].

2.3.5.1 Flux Ingredients

Many flux ingredients are available as shown in Table 2.11. These additives affect properties such as fluidity, wettability and reactivity as shown in Table 2.12. Alkali – fluoride salts (e.g. NaF, Na₃AlF₆, and KF) are common ingredients which act as surfactants - they decrease the surface tension both between the flux and the metal and between the flux and the oxides. Chloride salts as well as AlF₃ and MgF₂ exhibit this property, but to a much lesser extent. Fluxes may contain fluoride salts such as Na₃AlF₆, CaF₂, and Na₂SiF₆ in amounts up to 20 %. These fluorides have some solubility of aluminium oxide that improves wettability, which in turn favour separation of oxide inclusions from the metal and metallic aluminium from dross [67].

Table 2.11 Characteristics of flux compounds [67].

Chemical	Molecular Mass (g/mol)	Solid Density (g/cm ³)	Melting Point (°C)	Boiling Point (°C)
LiCl	43.39	2.068	605	1325
NaCl	58.44	2.165	801	1413
KCl	74.56	1.984	770	1500
CaCl ₂	110.99	2.15	782	1600
MgCl ₂	95.22	2.32	714	1412
AlCl ₃	133.34	2.44	190	177.8
BaCl ₂	208.25	3.92	963	1560
LiF	25.94	2.635	845	1676
NaF	41.99	2.558	993	1695
KF	58.1	2.48	858	1505
CaF ₂	78.08	3.18	1423	2500
MgF ₂	62.31		1261	2239
AlF ₃	83.98	2.882		s 1291
Na ₃ AlF ₆	209.94	2.9	1010	
LiNO ₃	68.94	2.38	264	d 600
NaNO ₃	84.99	2.261	307	d 380
KNO ₃	101.11	2.109	339	d 400
Li ₂ SO ₄	109.94	2.221	859	High
Na ₂ SO ₄	142.04		897	
K ₂ SO ₄	174.27	2.66	1069	1689
CaSO ₄	136.14	2.61	1450	High
MgSO ₄	120.37	2.66		d 1124
Li ₂ CO ₃	73.89	2.11	723	1310
Na ₂ CO ₃	105.99	2.532	851	High
K ₂ CO ₃	138.21	2.42	894	High
MgCO ₃	84.32	2.96		d 350
CaCO ₃	100.09	2.71	1339	850

s: sublimes; d: decomposes

Oxygen-containing compounds, such as KNO₃ release oxygen, which reacts with metallic aluminium to yield Al₂O₃ and considerable heat. This locally increases the fluidity, which enhance the recovery of metallics suspended in the oxide. In cleaning fluxes, the reaction increases penetration of the flux into oxides. Certain compounds decompose into chlorine, CO₂ or metal halide gases (AlCl₃). If these are introduced beneath the melt surface, they create bubbles that can degas and remove inclusions. The most notable gas-releasing compound is hexachloroethane (C₂Cl₆), which generates Cl₂ and gaseous AlCl₃ as discussed previously. Finally, compounds that react with aluminium and its impurities can be used to add certain elements to the melt or reduce the concentration of others. For

example, NaF will add traces of sodium to the melt, K_2TiF_6 can add titanium and KBF_4 can add boron. To some extent, AlF_3 removes calcium, strontium, sodium and magnesium and compounds releasing chlorine can also remove calcium, strontium, lithium and magnesium [67].

Table 2.12 Properties of selected compounds used in fluxes [67]

Formula	Fluidity	Wettability	Chemical Active	Exothermic	Gas Release	Element Added
AlF_3	↑		Yes			
$CaCl_2$	↑					
$MgCl_2$	↑		Yes			
$MnCl_2$	↑		Yes			Mn
KF	↑		Yes			K
NaF	↑		Yes			Na
NaCl	↑					
KCl	↑					
$NaAlF_4$			Yes			
CaF_2	↓	↑				
Na_3AlF_6	↓	↑	Yes			
Na_2SiF_6	↓	↑	Yes	Yes		
KNO_3	↑	↑	Yes	Yes	N_2, NO_x	
C_2Cl_6			Yes		Cl_2-AlCl_3	
K_2CO_3			Yes	Yes	CO_2	
Na_2CO_3			Yes	Yes	CO_2	
K_2TiF_6			Yes			Ti
KBF_4			Yes			B

The choice of specific flux compounds depends on the specific purpose(s) of the flux.

The various constituents serve to [67]:

- Form low-melting, high fluidity compounds, as is the case with NaCl –KCl mixtures.
- Decompose to generate anions, such as fluorides, chlorides, nitrates, carbonates and sulphates that are capable of reacting with impurities in aluminium.
- Act as fillers to lower the cost per kg or to provide a matrix or carrier for active ingredients.
- Absorb or agglomerate reaction products from the fluxing action.

2.3.5.2 Uses of Fluxes

The uses of fluxes fall into five categories: cover, cleaning, drossing, refining, and wall-cleaning.

Cover fluxes: These fluxes prevent oxidation of the molten metal and promote the separation of metal and oxide by agglomeration of metal droplets allowing them to sink back into the bath. Cover fluxes (NaCl-KCl + CaCl₂ and some fluorides) provide a physical barrier to oxidation of the metal. They may also serve as a cleanser for alloys or scrap foundry returns, protective cover under highly oxidizing conditions (melt temperature >775°C), melting of fines and chips, or making alloys containing more than 2 % magnesium. There is a wide range of possible flux compositions. While many of these fluxes can be used with a variety of alloys, it is important that those containing sodium salts not be used with alloys containing >2 % magnesium. Magnesium will replace sodium in the salt according to a reaction of the type.



The result is that some magnesium is lost to the dross and the alloy picks up sodium, which may be deleterious [28]. This reaction is possible because the magnesium-halides are more stable than those of sodium because of their higher Gibbs energy of formation as shown in Fig. 2.6. The stability of compounds increases with increasing negative value of the Gibbs energy of formation [67].

Cleaning fluxes: Cleaning fluxes are designed to remove particles of alumina, from the melt and to facilitate keeping furnace or crucible walls free of build up. Build-up begins as a composite of metallic aluminium and oxide, so that it initially can be loosened and dispersed by exothermic fluxes. It often originates from wet dross sticking to the furnace walls and gradually forming corundum. A jackhammer may be needed if it is not removed at an early stage. The active ingredient in cleaning fluxes is usually Na₂SiF₆ [28, 67].

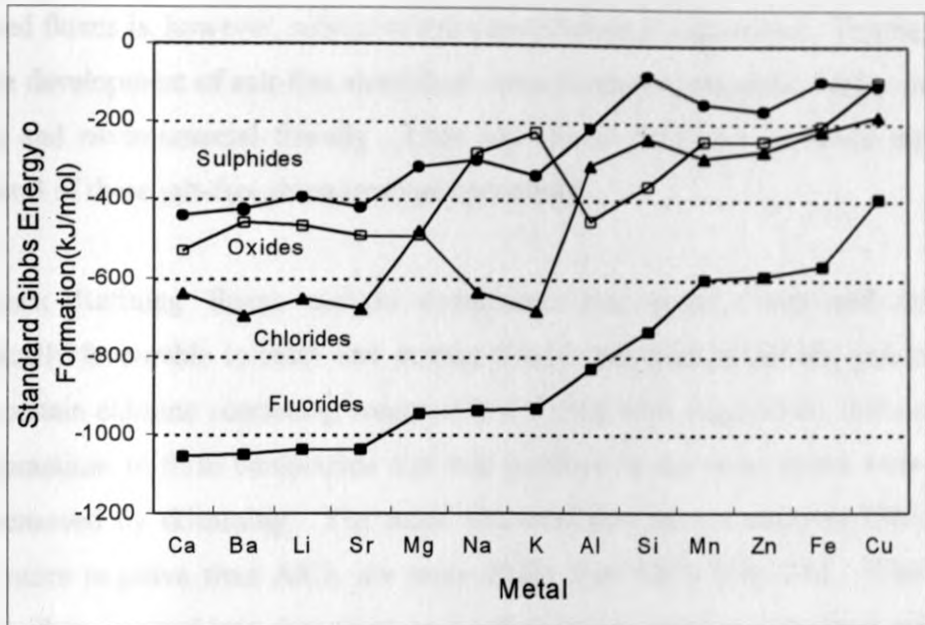


Figure 2.6 Standard Gibbs energy of formation of several sulphides, oxides, chlorides and fluorides. The data are given at 723 °C per mole of S, O, Cl₂, and F₂, respectively.

Drossing fluxes: Drossing fluxes promote separation of the dross from the molten metal. These fluxes usually contain compounds that can react exothermically with metallic aluminium or Al₂O₃ in the dross, giving heat and improved wettability. The fluorides wet and slightly dissolve oxide films, which with mechanical agitation, may be broken to release entrapped aluminium. Possible active ingredients include Na₂SiF₆ and KNO₃ [67].

Drossing fluxes are used to great advantage to lower the metallic content of drosses that may contain up to 60-80 % free metal. Considerable cost savings result because proper fluxing will recover perhaps over 50 % metal directly back to the melt. Drossing fluxes are added either by weight (about 0.2-1% of metal charged) or by surface area (2.5 kg/m², corresponding to a thickness of about 1 mm). Too little exothermic combustion reduces fluxing efficiency, while too much flux burns excessively, creating excessive fume and loss of metallic aluminium.

Separate dross reclamation systems have also been developed and are currently in use.

These systems can recover up to 90% of the aluminium in dross using salt fluxes [25]. Disposal of used fluxes is, however, subject to strict environmental regulations. This has encouraged the development of salt-free aluminium dross treatment processes, which are more efficient and environmental friendly. Unlu and Drouet [95] have reviewed and compared several of these salt-free dross treatment processes.

Refining fluxes: Refining fluxes contain compounds that break down and are thermodynamically favourable to react with certain metallic elements in the aluminium. For example, certain chlorine containing compounds will react with magnesium, lithium, sodium and potassium to form compounds that will partition to the dross phase where they can be removed by skimming. The metal chlorides that have a standard Gibbs energy value more negative than AlCl_3 are more stable than AlCl_3 (Fig 2.6). When chlorine is, therefore, injected into aluminium containing various metallic elements it will react preferentially with these metallic impurities. The same also applies to fluorides. Lithium, sodium, potassium, calcium magnesium and barium all form stable chlorides and fluorides than aluminium (Fig. 2.6) and can therefore, be removed by chlorine, fluorine or sulphur hexafluoride (SF_6) injection. The removal of other impurities such as zinc, manganese, silicon, iron and copper by chlorine or fluoride treatment is basically impossible. Similarly, if the flux used contains compounds of such metals, they will react with the melt and contaminate the aluminium. This can, however, be used to advantage in other cases where these elements need to be added to the alloy [67].

2.4 CASTING PROCESS SELECTION

The versatility of metal casting is demonstrated by the large number and variety of casting and moulding processes currently available. This wide range of choices offers design engineers and component users enormous flexibility in meeting their metal forming needs. Selecting the best one to produce a particular part depends on several basic factors, such as cost, size, production rate, finish, tolerance, section thickness, physical and mechanical properties, intricacy of design, machinability and weldability [96-100]. Each process offers distinct advantages and benefits when matched with the proper alloy and application.

These processes can be classified either by the type of mould and or by the pressure or force used to fill the mould with molten metal. In all these processes, metal is introduced into a cavity in a sand mould or a steel/cast iron die. The main factor controlling the solidification rate is the heat flow across the metal/mould interface. This is generally described by means of a heat transfer coefficient. Therefore, the nature of the mould surface, and the pressure applied to the metal during solidification are the major factors, which distinguish the main casting processes.

An in-depth review and comparison of all the available casting and moulding processes is adequately covered in existing literature (6, 19, 20, 96-101) and will not be considered here. As mentioned at the beginning of this thesis, selecting the right process is invariably salutary and essential for both the component designer and the foundry. A vocabulary straddles the two disparate groups of component designers and manufacturers. This constraint is resolved by process selection procedures, which have been developed to provide a common language that allows an interpretation of the component requirements, matched against process capabilities and, thus appropriate process selection. For instance, the manufacturer of a high quality cast aluminium component relies on selecting the correct alloy composition, process and heat treatment. In order to determine the best manufacturing route, designers need a systematic and robust method of addressing the many different and often conflicting issues considered

during the design process. Selection procedures provide just such a method, ensuring that all the available options are considered in an unbiased manner as well as capturing and making accessible, expert information, which might otherwise be lost.

Several techniques for process selection, especially at conceptual stages of design have been proposed and implemented in software or otherwise. The conceptual level process selection tools are generic (i.e. casting processes form only a small subset of the processes covered in these tools, and hence are only some of the possible choices), while those that are designed for selection at a more specific level of design detail are task based. Specifying a subset of materials (e.g. cast aluminium alloys) and processes (e.g., casting processes) may be considered to define a manufacturing task (e.g., casting an aluminium alloy) [102].

The Cambridge Process Selector (CPS) discussed by Esawi and Ashby [103] and the Manufacturing Advisory Service (MAS) described in detail by Smith [104] are some of the most elaborate software for generic preliminary process selection at the conceptual stages of design. The CPS is used in conjunction with the Cambridge Materials Selector (CMS) in a combined software package, the Cambridge Engineering Selector (CES) developed and distributed by Granta Design Ltd. (<http://www.grantadesign.com>) [105]. The MAS is a complete web based unit (<http://cvbercut.berkeley.edu/mas2/>), which contains both the processes and materials databases. Both software (CES and MAS) are built on massive relational databases of engineering, design and manufacturing information. Other conceptual level process selection tools, which have been reviewed by Smith [104], are Computer Aided Material/Process Selection (CAMPS), Material and Process Selector (MAPS), Process Sequencing Expert Shell (PSES), Rapid Prototype System Selector (RPSELECT), Design Advisor (DA), and Material and Manufacturing Process Selection (MAMPS).

The general problem of creating selection procedures for individual tasks, with just enough detail to work within the scope required, has recently been described by Lovatt [106]. The creation of a task-based procedure for aluminium casting formed one of the

case studies of this work. Similar work on process and alloy selection for aluminium casting was reported by Lovatt et al [102]. The paper illustrated how selection techniques can be used to help determine suitable combinations of aluminium alloy, process and heat treatment for a given design. It also illustrated the use of standard tests and process models in augmenting the selection procedure and demonstrated how such a procedure could be enhanced by the use of fuzzy logic algorithms in a software implementation - The FuzzyCasting Selector. In addition to the above contributions, Akarte et al [107] recently proposed a systematic approach for evaluating product-process compatibility for casting processes using linear weighting and fuzzy logic models, and Analytical Hierarchy Process (AHP). Darwish and El-Tamimi [108] also proposed an expert system for selecting a casting process for a given part.

- 2.5 MOULD DESIGN

Mould design is dependent on both the alloy to be cast and the casting process that will produce the part. It involves the design of the gating and risering systems, patterns, cores, chills and/or cooling fins, and the mould assembly as a whole. The mould assembly includes the placement of the above items in the mould system as well as designing the part orientation and the parting line.

The driving force in the design of a moulding system is to produce a casting with maximum accuracy, a minimum of defects, excellent surface and sub-surface structure and hence excellent properties (physical and mechanical). The other aspect of consideration, which is equally important, is the casting yield. These aspects are highly dependent on the methods engineer's ingenuity in designing the mould system. The surface finish is as well enhanced through the avoidance of melt penetration into the mould. This can be achieved by using fine sand or applying a mould wash in addition to controlling the pouring temperature (or the degree of superheat).

A critical look at the ten rules for good castings proposed by Campbell [109] reveals that the majority are greatly dependent on the adroit design of the moulding system. This basically underpins the potency of the moulding system on the quality of castings. Campbell [109] emphasizes the provision of a good quality melt. Melt quality is dependent on the melting equipment, quality of the charge, melt handling (while in the melting and holding furnaces, during transfer, and pouring), and melt treatment. This has little to do with the moulding system. Most of the other rules, however, have something to do with controlled filling or feeding, so as to avoid surface turbulence, bubble damage, liquid front arrest and/or damage, shrinkage and convection. Core outgassing (leading to core blows) and residual stresses are major considerations during the design of cores and patterns (and/or feeding systems) respectively. The effect of segregation due to poorly designed gating and filling systems may as well not be underestimated.

Avoiding liquid metal front (the meniscus) from damage is essential to avoid oxide films,

dross and gas from being entrained into the bulk of the melt. The occlusion of air leads to porosity and oxide film defects in the final cast product. Maximum meniscus velocity is suggested to be not more than 0.5 m/s to avoid surface turbulence [6, 109-111]. This is made possible through proper rigging system design. Guidelines for rigging system design are extensively reported in existing literature [6, 101, 110-116] and the subject is still under investigation.

The liquid metal front should not go too slowly, nor should it stop at any point during filling. The advancing liquid metal meniscus should be kept “alive” and free from the thick oxide film, which can be incorporated into the casting (Fig. 2.7). This is achieved by ensuring that the liquid front only advances uphill (in the case of gravity poured casting processes, from the base of the sprue onwards). This implies that only bottom gating is permissible, and no falling or sliding downhill of liquid metal is allowed. Arrest of pouring and extensive horizontal sections or waterfall effects should also be avoided through proper rigging system design and mould orientation. This will avoid oxide laps and/or cold laps.

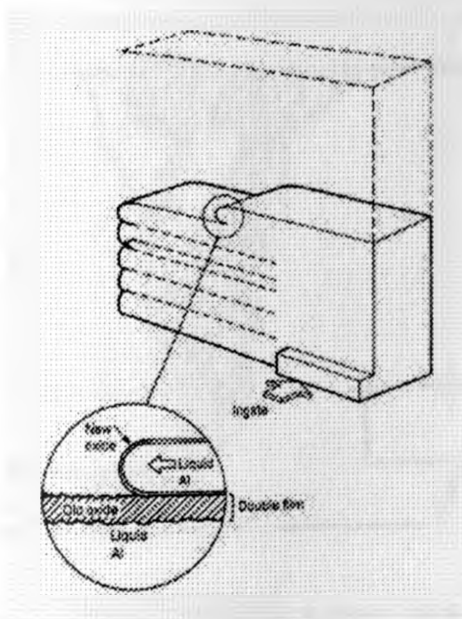


Fig. 2.7 Unstable advance of a film-forming alloy, leading to the formation of laps as the interface intermittently stops and restarts by bursting through and flooding over the surface film (After Campbell [109]).

Surface turbulence produces non-reproducible castings. This is the result of the nature of turbulence (chaos; unpredictability) [6]. The effect of randomness of surface turbulence on the reliability of castings has been quantified by the use of Weibull Statistics [117-119].

No air bubbles should be entrained by the running system. If they are entrained, then they should not be allowed to pass through the liquid metal in the mould cavity. If this happens, then a mixture of oxide bubble trails, together with residual misshapen bubbles in the casting will result (Fig. 2.8). This severe defect may be avoided by a fast backfill of the filling system by virtue of properly designed sprue and pouring basin [6, 101, 110, 112-115]. Sometimes additional use is made of a stopper in small castings [110], ceramic foam filters [6, 101, 115, 120] placed close to the sprue/runner junction, and bubble traps. Whenever possible, any solutions should be demonstrated as effective using some suitable technique such as real-time x-ray radiography and/or computer modelling [113-117, 119, 121]. Uninterrupted pouring alleviates the problem as well.

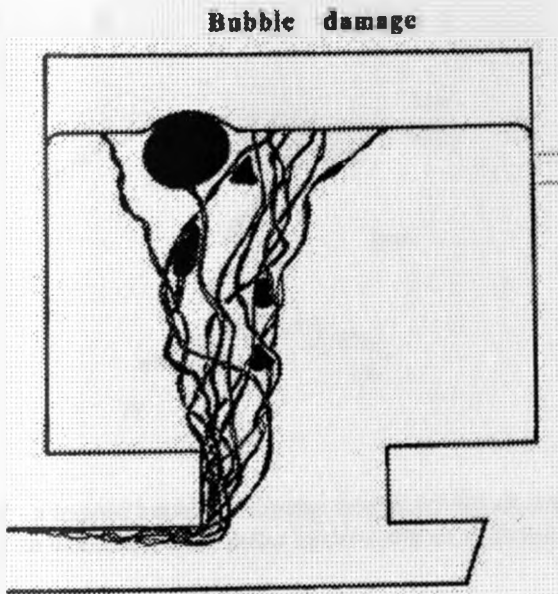


Fig. 2.8 Illustration of the most common defect in castings - bubble damage as a mixture of oxide cracks and residual entrapped bubbles (After Campbell [109]).

Gases from cores or even occasionally from parts of the mould should not be allowed to

penetrate the liquid metal. Core or mould blows cause a rather different type of defect than the entrained air bubbles as described by Campbell (Fig. 2.9) [6]. They are characterized by huge size (up to 100 mm in diameter) and are usually located some distance beneath the top of the casting above the highest point of the core, especially if it is sharply pointed. In film forming alloys like Al alloys, the passage of core bubbles through the melt naturally creates a bubble trail. The passage of a large number of bubbles can be highly damaging, leading to leakage paths through the casting, and exfoliation type defects where the bubbles break the surface of the casting. Cores should be demonstrated to be of sufficiently low gas content and/or adequately vented to prevent bubbles from core blows. This can be done by a video recording of the filling of the mould without a cope, for instance [122].

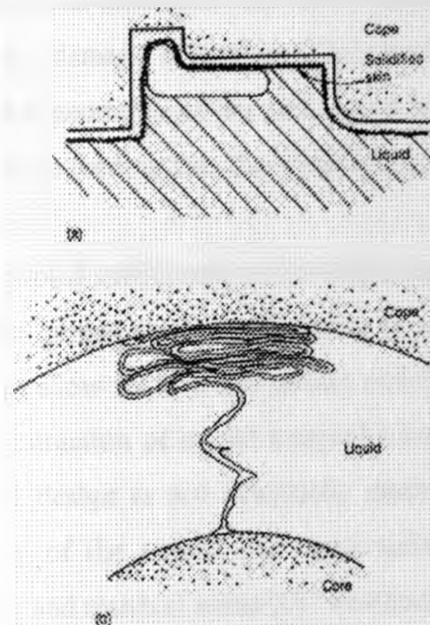


Fig. 2.9 A "core blow" - a trapped bubble containing core gases. Shown at the bottom of the illustration is a bubble trail, ending in an exfoliated cross defect as the result of a passage of copious volumes of core gas (After Campbell [6]).

Feeding should be designed to avoid shrinkage cavities. Feeding should be controlled through ingenious riser design based on accepted rules governing the dimensioning and locating of risers [6, 101, 112, 123-125]. Chills and/or cooling fins are also used to

control solidification shrinkage [6,153-154]. Shrinkage cavities can also be avoided by controlling the level of flash at mould and core joints, mould coats and mould temperatures. Random flash, mould coats, and mould temperatures can give random feeding effectiveness by unpredicted changes to the temperature distribution in the casting [109].

Thin or thick section castings automatically avoid convection problems. Thin section castings freeze quickly before convection builds up. In thick section castings, convection helps redistribute hot metal into the risers on the top of the casting, since there is plenty of time before freezing starts. However, intermediate sections, which represent the great majority of castings, have a freezing time commensurate with the time taken for convection to operate (in a few minutes) and can cause damage. Unsuitable temperature gradients in the casting can undermine the effectiveness of risers, and lead to segregation and apparent shrinkage damage in castings. This problem can be alleviated by avoiding convection loops in the geometry of the casting and by rigging. 180-degree rollover after mould filling and bottom feeding can also eliminate convection [6, 109].

When a casting has cooled sufficiently to develop some coherence as a solid, then further cooling will cause the casting to start contracting as a whole. Patterns and hence moulds should be designed to allow for this contraction which depends on the alloy. Allowance for expansion and contraction of mould material (metal or sand) is equally essential. If this aspect of mould design is not adequately dealt with, it will lead to problems of dimensional accuracy of the casting and more seriously, casting defects such as hot tearing, cold cracking and residual stress [6]. Residual stress is exacerbated if quenching, especially for big castings is done by dipping into water following high temperature solution treatment [6, 109, 122]. Another consideration during mould design is the provision for location points for dimensional reference and clamping points to be used during machining [6, 109].

Real time x-ray radiography is increasingly being used to study the flow of molten metal in filling systems and within the mould cavity. The Weibull statistical technique has

been used to quantify the effect of the running system on the reliability of castings [117-118]. Rezvani et al [117] reported that castings made using poorly designed running systems can give an average tensile strength of 230 MPa for cast Al-7Si-Mg and are as unreliable as engineering ceramics. On the other hand, those made using adroitly designed running systems can give an average strength of over 300 MPa and have a reliability that can equal or exceed that of forgings. Similarly, for the same alloy, turbulently filled (poor gating design) castings have been shown to have lower fatigue lives than the quiescently filled (optimised gating design) castings [118]. Bottom filling systems are widely preferred to top filling systems [6] because they have greater potential for less surface turbulence. Cox et al [119, 128] have shown that bottom filling of aluminium investment castings reduces the scatter in tensile strength and hence improved reliability when compared with top filling.

To mitigate the effects of oxide film formation, clean metal programs have been in place in many foundries since the mid-1980s. Useful innovations, such as metal filtration, disposable ladle liners, direct pouring through risers with filters and metal treatment in ladles, have been incorporated with varying degrees of success. A new development apart from real-time x-ray radiography has been software for computational numerical modelling of metal flow in the mould. These programs are capable of illustrating flow conditions quickly, inexpensively and in great detail. In addition, these simulations provide an unlimited number of iterations with varying geometry and pouring conditions, allowing designers to determine the validity of a design without expensive shop trials and inspections [121]. There are several simulation software available in the market today, such as MAGMAsoft, PROCAST, Flow-3D and AFS Solidification System (3-D) [129].

2.5.1 PARTING LINE GENERATION

The design of the rigging system starts with the determination of part orientation and the parting plane. Identification of the gate location to allow uniform feeding of the casting is the next step. Having decided where the gates are located, an appropriate runner geometry is selected. The sprue location is determined so that it will be as far from the

nearest gate as possible. Sizing of the elements of the rigging system is done using the geometry of the part and some common rules of thumb. It is not uncommon for several trial rigging designs to be required in producing a sound casting.

Orientation of the part should be such that the large part of the casting is relatively low, the height is minimized and in such a way that top risers can be placed on high points on the castings for the heavy sections. Open spaces of the part should be placed facing down to enhance bottom gating. In general, runners and gates are placed in the drag so that the parting line forms the top of these channels and cavities. The parting line should be placed as low as possible relative to the casting and at the cross section of the largest area of the casting [6, 109]. The location of the parting line should be such that the number of cores is minimized and undercuts are avoided. It should also minimize excessive depth in the cope and drag, and reduce the draft required. Irregular parting lines should be avoided. The parting line should also enhance the final dimensional accuracy [19, 130].

2.5.2 POURING BASIN DESIGN

The pouring basin should be kept full during pouring of the metal to prevent vortex formation in the sprue. An offset rectangular pouring basin with a rounded weir step has been reported to be the best design so far (Fig 2.10) [6, 110, 113]. The offset feature is important to arrest and reverse the flow, giving some opportunity for lighter phases such as slag and bubbles to separate prior to entering the sprue. The weir is essential to eliminate the fast horizontal and vertical component of the momentum for the molten aluminium entering the sprue, thus reducing surface turbulence and controlling the filling. Basins without the weir give an effective discharge coefficient of 0.5 for the sprue as they are usually partially filled (approximately half full). The discharge coefficient of a sprue attached to an offset weir basin is commonly near 0.9 or more. The provision of radii to the weir step and the entrance into the sprue further aid the smooth flow of metal. The lack of any one of these three features causes the smooth functioning of the basin to be impaired, and lead to slag, dross and air entrainment into the metal.

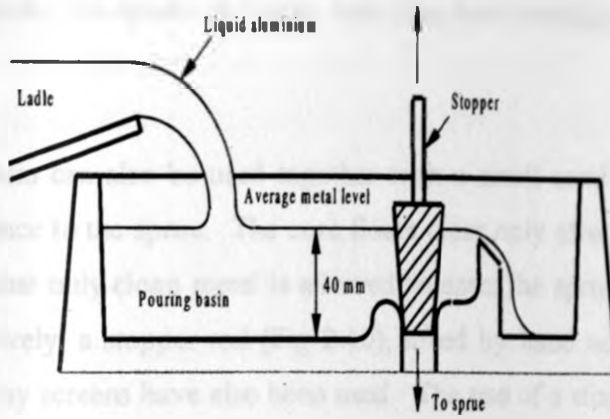


Fig 2.10 A design of an offset pouring basin [111].

The in-line conical basin (Fig 2.11) has been reported [6, 110, 128] to do very poorly because the metal enters at an unknown and unchecked velocity. The conical pouring basin, however, is simple and economical and providing the sprue fills quickly, it works fairly well for small castings [6]. Dross, slag or bubbles are necessarily taken down the sprue and the small volume of the basin makes it difficult for the pourer to keep the basin full and hence, the sprue is partially full.

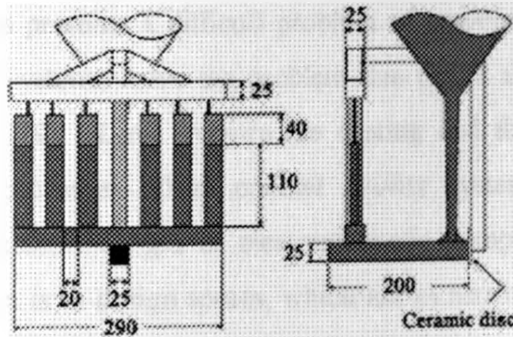


Fig 2.11 Conical pouring basin tested in an investment casting filling system for an aluminium alloy [128]

Finally, computer simulations have demonstrated that the mould cavity fills differently depending on precisely where in the basin the pourer directs the pouring stream [110]. It is important for the caster to pour the metal into the blind end, or the offset part of the basin, so that the fall of the stream is arrested, thus allowing bubbles and slag to float and separate prior to falling down the sprue [6, 112]. The pouring basin should be kept full of metal during the whole duration of the pour. If it is allowed to empty at any stage then

air and dross will enter the sprue. A vortex may also form leading to surface turbulence [6,112].

The offset weir basin can also be used together with a small sand core (skimmer core) placed in the entrance to the sprue. The core floats clear only after the basin is full, and therefore ensures that only clean metal is allowed to enter the sprue and air aspiration is avoided. Alternatively, a stopper rod (Fig 2.10), lifted by hand accomplishes the same task. Filters or delay screens have also been used. The use of a stopper greatly improves the filling of the sprue giving a discharge coefficient higher than 0.9. This operation is however highly inconvenient and is only recommended where excellent quality castings are required [6,110].

2.5.3 SPRUE DESIGN

The fundamental problem with the design of sprues is that the critical fall height under gravity at which the critical velocity is reached is usually very small. For aluminium, this is about 13 mm. Since sprues are typically 100 to 1000 mm long, the critical velocity is greatly exceeded. This presents a difficult problem of preventing damage to the metal front. Counter gravity systems solve the problem due to the absence of free falling of liquid metal [6, 110, 119]. Low pressure die casting and the Cosworth process are examples of casting processes where counter gravity systems are applied. These processes use either pressurized gas or electromagnetic pumps to control the flow of metal. Another solution is to design sprues, which are as narrow as possible, so that the metal has no opportunity to break and entrain its surface during the fall. The concept of protecting the liquid from damage is either to prevent it from going over its critical velocity, or, if the critical velocity has to be exceeded, then to protect it by constraining its flow in channels as narrow as possible. The large volume of the channel allows the metal to jump and splash when it hits the base of the sprue causing severe turbulence in the runner. This is caused by the delay in filling the sprue during the initial pouring stages [110].

The turbulent flow may also cause erosion of the sand mould. The hot liquid ricochets and sloshes about, its high speed and agitation punishing the mould surface with a hammering and scouring action. This action is exacerbated by the presence of aspirated air, which oxidizes away the binder material [6].

Rectangular cross-section sprues have been reported to do better than circular ones with the same sectional area, since the critical velocity for turbulence is much less for circular sections. In addition, vortex formation tendency in a sprue with circular cross section is higher. However, round sprues with small heights and radii do not cause vortex problems, are easier to make and, thus, are more economical for small castings (up to 50 kg) [6, 112].

It is first necessary to decide on an average filling rate for the casting. Guidelines for approximating this rate have been reported by Campbell [6]. In general, a tolerance guide is to check the thinnest section on the casting, and from this find its corresponding solidification time, using embedded thermocouples. The rate of pouring is then chosen to ensure that the mould is filled before freezing is complete. This may not be easy but a fairly reasonable arbitrary filling rate can be obtained; this can later be modified. The sprue dimensions are then calculated.

The sprue exit area can be calculated using the following equation [112]:

$$A = \frac{Q}{w\sqrt{2gh}} \quad (2.6)$$

Where;

Q is the mass flow rate

w is the specific weight of the molten metal

A is the cross-sectional area

g is gravitational acceleration

h is the vertical height of molten metal within the sprue

The height of the sprue is determined by the height of the casting and the top riser height.

The entrance area of the sprue is made slightly larger than the exit area providing a taper of approximately 5% minimum [112] or a 20% safety factor oversize [6,110]. Sometimes it is advisable to provide the sprue with a slightly larger taper than required [112]. Using a tapered sprue results in a lower height sprue than an untapered sprue, while retaining the same flow rate. For most practical purposes, however, nomograms (Fig 2.12) can be constructed to assist in determining the sprue dimensions [6].

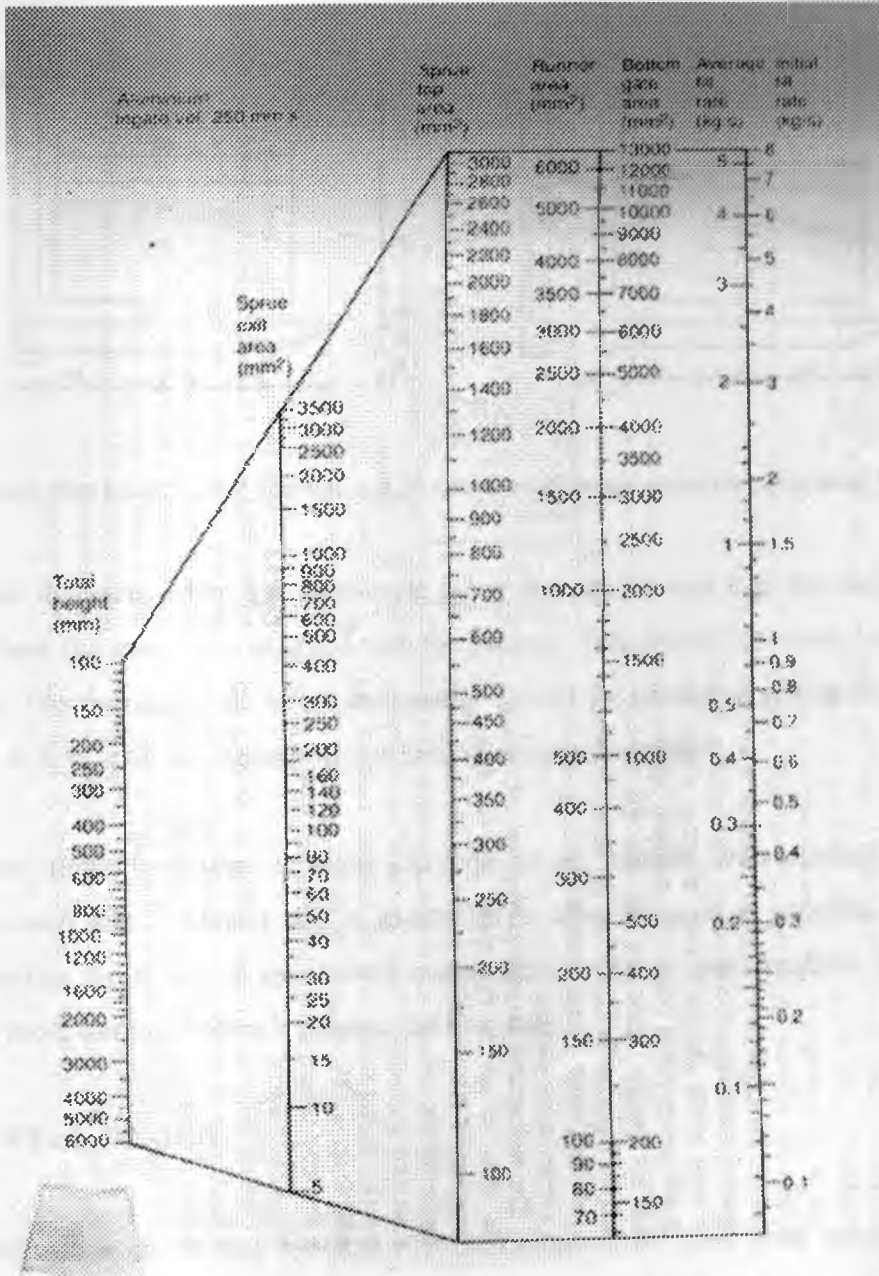


Fig 2.12 A nomogram for the calculation of running systems for aluminium alloys [6]).

In practice, the important dimension of the sprue for controlling the precise rate of flow is the area of the exit. It is vital to appreciate the importance of this area; it acts as a choke. Yang et al. [114] have shown that a sprue/runner junction with a sprue offset relative to the runner (Fig 2.13a) results in ingate velocities in the range of 0.3 to 0.4 m/s. The conventional in-line sprue/runner junction (Fig 2.13b) gives ingate velocities in the range of 0.5 to 0.7 m/s. Greater strength and consistence is also achieved with the offset sprue indicating an overall reduction in damage for the castings.

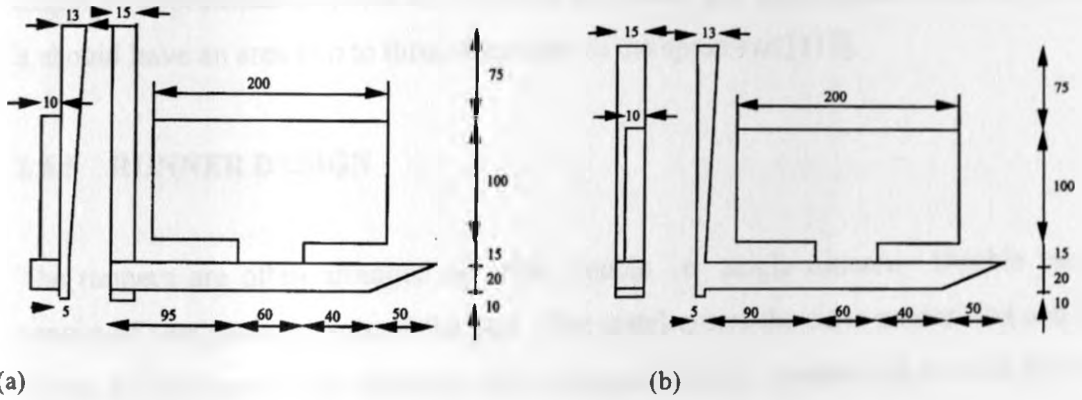


Fig 2.13 (a) Offset Sprue/Runner junction and (b) conventional in-line sprue/runner junction [14].

There are instances when a reverse-taper sprue is used because it is the only option in cases where the sprue is to be fixed with the pattern. This should, however, be avoided if possible. The runner should be so designed to correct the damaging effects of such sprue design. A filter can also be used if this kind of design is adopted.

The sprue should be located centrally along the runner distance, with an equal number of gates on each side. It should also be located as far from the gates as possible. Often, the flow leaving the sprue or sprue well is turbulent; a longer path enables the flow to become more laminar before it reaches the first gate.

2.5.4 WELL DESIGN

Most authorities on running systems such as Campbell [6] give great emphasis to the provision of a well at the base of the sprue. The argument is that the metal is somehow

cushioned in its fall, and the right angle turn of the metal from the sprue into the runner is facilitated, avoiding the worst effects of the first splash (perturbances) and the vena contracta. Recent research has, however, shown that the best designs of the well operate no better than having no well at all [110, 121]. Thus wells could safely be abandoned without any threat to the quality of the casting [110].

For those who still prefer to use the well, it is recommended that its diameter and its length be approximately twice the depth of the runner [6]. Other writers recommend that it should have an area two to three times that of the sprue exit [112].

2.5.5 RUNNER DESIGN

The runners are often arranged as either double or single runners. Double runners consist of two passages around the part. The metal enters the outer runner first and then moves to the inner runner through short passages. Single runners can as well be either tapered or untapered. The selection of the runner type depends on the filling complexity of the part and the designer's preference. Double runners are usually used for more difficult parts; thin-walled sections in particular. Tapered runners are preferred when more than one gate is attached to the runner. The taper can either be stepped or smooth and straight. Tapering ensures simultaneous uniform flow of metal through all the gates by avoiding pressure differences among them [6,112].

Rectangular cross-section runner is preferred in sand castings [112]. Yang et al. [111], however, used both computer modelling and real-time x-ray radiography techniques to demonstrate that a vortex-flow runner filling system (Fig 2.14) gives ingate velocities in the range of 0.3 to 0.4 m/s, thus greatly reducing the occurrence of surface turbulence in the cavity. Conventional rectangular bar runner systems give ingate velocities in the range generally above the critical value of 0.5 m/s. A vortex-flow runner can also eliminate the rolling back-wave (a constrained hydraulic jump) normally encountered in the priming of conventional runners.

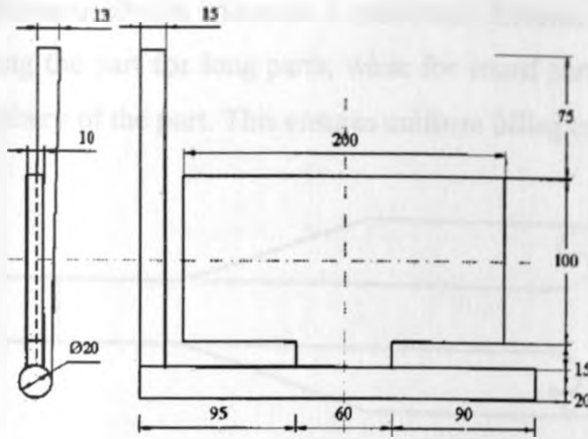


Fig 2.14 Vortex-Flow Runner design

For deep rectangular runners, the metal flows as a fast jet along the floor of the runner. Thus in most runners, the metal does not fill the runner. The consequence is that when the jet reaches the end of the runner, the reflected wave rides back as a rolling wave over the top of the jet entraining air along the boundary between the two juxtaposed and opposite streams (2.15). Increasing the horizontal width of the runner has been shown to help. Expanded runner designs are therefore recommended with the expansion starting from the runner origin (sprue base) (Fig 2.17). If expansion starts at any distance away from the sprue origin, then the flow continues along the original runner direction, filling the expanded sides of the runner later by countercurrent flows reflected back from the end of the runner (re-introducing the same deleterious problem of flow juxtaposition) (Fig 2.17) [110]. Abrupt changes in the direction of runners should be avoided. If the change in direction is more than about 15 degrees, the joint needs to be filleted. A large radius, at least as large as the diameter of the sprue exit (for circular sprues), at the sprue/runner junction is found to aid the filling of the runner with little entrainment of air because the presence of the vena contracta is suppressed [110].

It is best to keep part of the runner above and part of it below the gate levels. The part of the runner above the gate level will trap the entrained gas and other inclusions in the cope portion of the casting, and the part below will act as a surge reservoir to feed the gates. The metal will be levelled before it enters the gates. Runner extensions (blind ends) are also used in most castings to trap any dross or bubbles that may occur in the molten metal

stream [6,112]. Runners should maintain a minimum distance from the part. They should also run along the part for long parts, while for round parts, two runners usually run around the periphery of the part. This ensures uniform filling of the cavity [6,112].

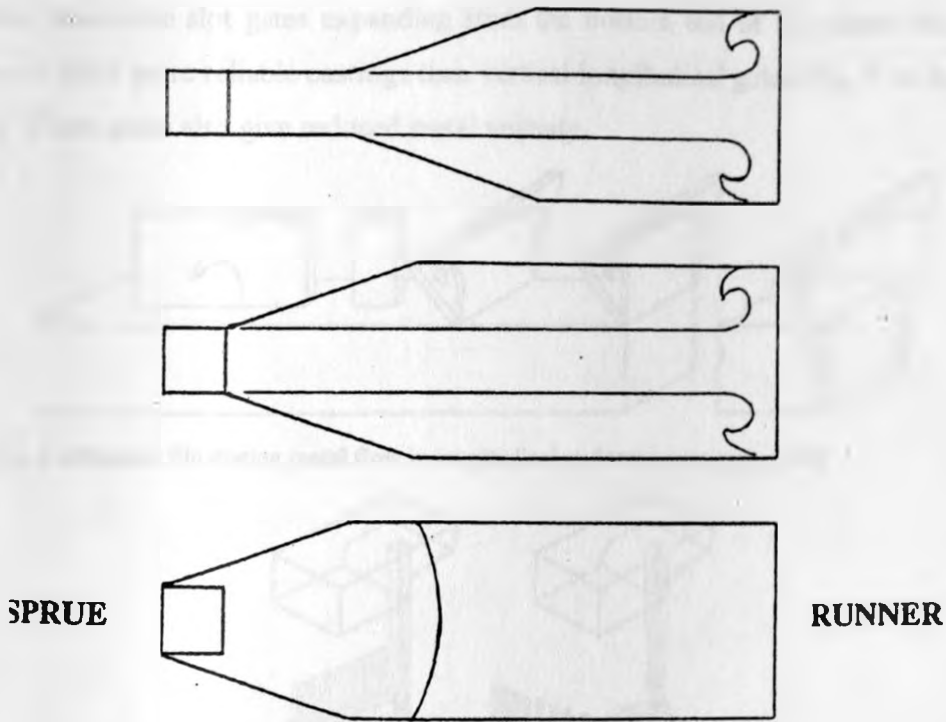


Fig 2.15 Expanding runner designs [110].

Campbell [6] has reported that the runner should have an area which is at least twice the sprue exit area and half the gate area. We should choose whichever is the larger when optimising quality. Runners are sized using a gating ratio, usually prescribed for the type of metal used in the casting [112]. Campbell [6], however, strongly discourages the use of gating ratios as they are not always appropriate. He asserts that the real parameter which requires control is the velocity of metal entering the mould. He recommends the use nomograms such as those reported in the same reference and illustrated in Fig 2.12.

2.3.6 INGATE DESIGN

Gates are the passages between the runners and the part. It is important that the liquid metal flows through the gates so as to enter the mould cavity smoothly. Bottom gating,

in which the gates are placed at the lowest level of the mould cavity but above the runners has been reported to be quite effective [6, 109-110, 117]. Gates are best arranged vertically, though, because of enhanced moulding difficulties and associated costs, horizontally arranged gates at the bottom of the mould cavity are preferred [110]. Vertical transverse slot gates expanding from the bottom end of the runner have been shown to yield more reliable castings than vertical longitudinal gates (Fig 2.16 and 2.17) [117]. These gates also give reduced metal velocity.

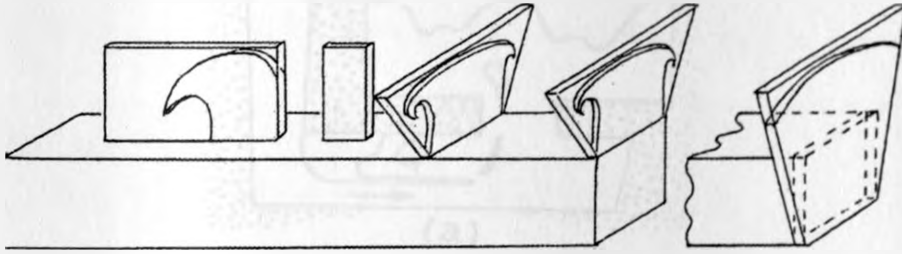


Fig 2.16. A schematic illustrating metal flow in longitudinal and transverse gates [110]

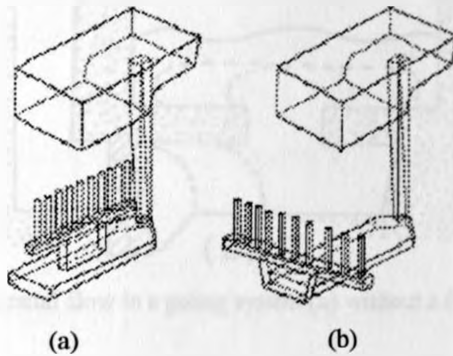


Fig 2.17 A typical design of a longitudinal and an expanding transverse gates [117]

Gates should be placed at the thick regions of the castings and in such way that they minimize agitation and avoid erosion of the sand mould by the metal stream. This may be achieved by orienting the gates in the direction of the natural flow path [112]. Multiple gating is frequently desirable. This has the advantage of lower pouring temperatures, which improve the metallurgical structure of the casting. In addition, multiple gating helps to reduce the temperature gradients in the casting. Fillets between the gates and the casting are desirable especially where gates form a T-junction with the casting [6, 112]. Other T-junction design requirements have been described by Campbell [6]. T-junction is associated with shrinkage porosity because they are susceptible to the formation of hot spots.

For small and medium-sized castings, the use of filters or screen placed at the runner just next to sprue/runner junction have been reported to offer some resistance to the flow, allowing the sprue to fill, thus reducing problems of entrainment of copious volumes of air at this point (Fig 2.18). The velocities downstream of the runner are reduced to near the critical velocity, thus perfectly filling the runner [6, 101, 110, 116, 120]. In harsher conditions, however, filters can break down, causing the creation of deleterious dross downstream [110].

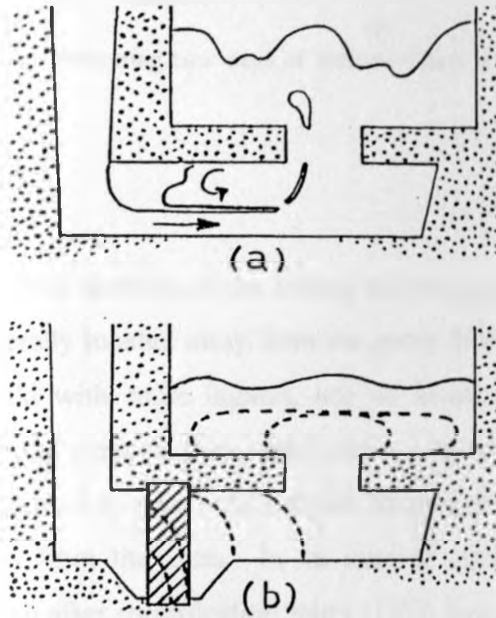


Fig 2.18 A schematic illustrating metal flow in a gating system (a) without a filter and (b) with a filter [110]

Examples of poor and good filling designs are shown in Figs 2.19 and 2.20

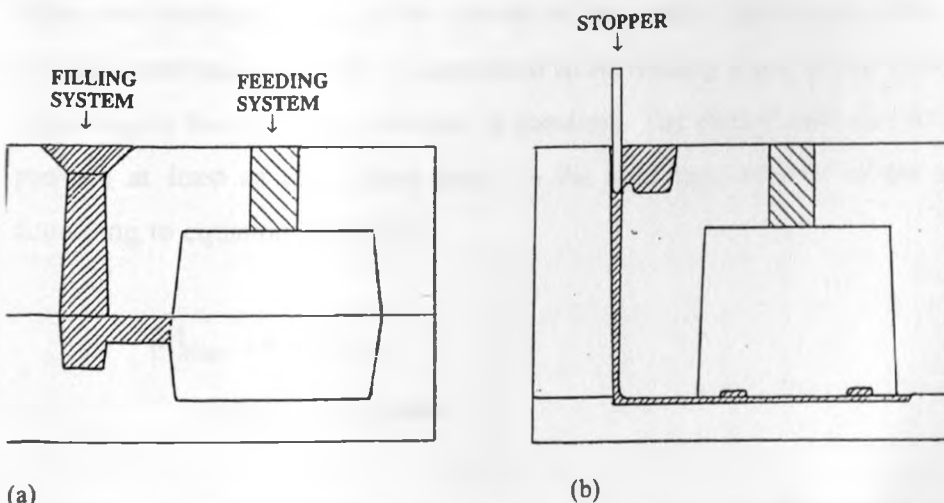
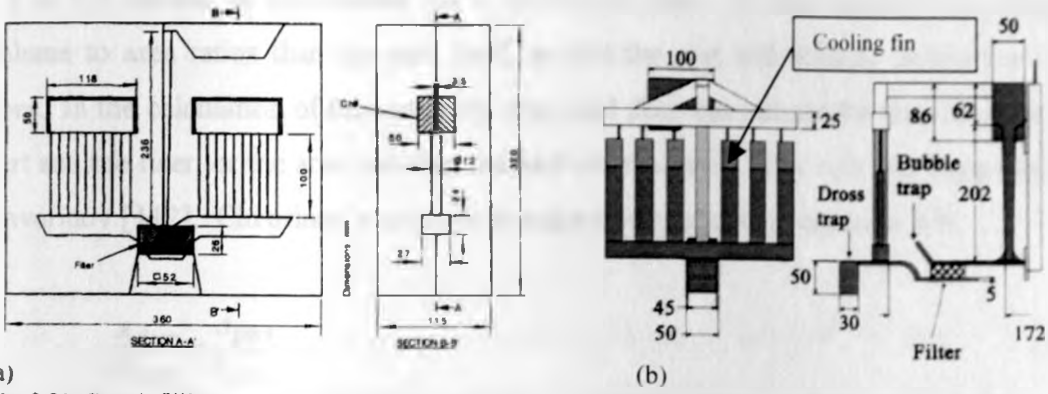


Fig 2.19. A schematic illustrating (a) a poor filling system and (b) a good filling system.



(a)
 Fig 2.20 Good filling systems illustrating two ways of locating filters and the use of (a) chills and (b) cooling fins.

2.5.7 RISER DESIGN

Risers are located near thick sections of the casting and are generally placed high to feed downhill. They are generally located away from the gates. If the casting is bottom gated, fast filling of the mould with more ingates, use of insulated exothermic risers, and chilling the gate area (using external (Fig 2.20a) and/or internal chills and/or cooling fins (Fig 2.20b)) are safe practices to cure unfavourable temperature gradients. Top risers are located on bosses, away from the gates. In the case of open risers, hot metal can be poured into the riser often after solidification starts [112]. External risers are preferred to internal ones because of easy removal and cleanup after production.

Risers are sized according to the volume of the casting section to be fed. In the case of multiple risering, each riser is considered to be feeding a part of the casting and is sized according to the volume of that part in question. The riser should also be large enough to provide at least as much feed metal as the shrinkage volume of the section it feeds according to equation 2.7 [124].

$$[V]_{Riser} \geq 0.5[V]_{casting} \quad (2.7)$$

Where V is volume.

If the top of the riser is not open to atmospheric pressure, the height to diameter ratio of

1:1 to 3:1 should be maintained for a cylindrical riser. A riser should have greater volume to area ratios than the part itself, so that the part will solidify before the riser does. In the calculation of this ratio, the area used does not include the area between the part and the riser, or the area between the part and the gates. This rule was suggested by Chvorinov [112]. Chvorinov's rule can be expressed as shown in equation 2.8.

$$\frac{A_{riser}}{V_{riser}} < \frac{A_{part}}{V_{part}} \quad (2.8)$$

Assuming that a cylindrical riser is used, equation 2.8 can be simplified to the expression shown in equation 2.9, where r is the radius of the riser and, h , the riser height.

$$\frac{1}{h} + \frac{2}{r} < \frac{A_{part}}{V_{part}} \quad (2.9)$$

The height obtained using equation 2.9 is usually multiplied with a factor of safety of about 1.2. Alternatively, this factor of safety can be incorporated in equation 2.8 to give the following expression [124]:

$$\left[\frac{V}{A} \right]_{Riser} \geq 1.2 \left[\frac{V}{A} \right]_{Casting} \quad (2.10)$$

On parts that have cylindrical bosses, the radius of the riser selected is slightly less than that of the boss to ease the removal of the riser from the part after solidification. The best riser shape is a sphere because of its high volume-to-area ratio, but it is not easy to work with spherical risers. Circular cylinders are frequently used as risers, as they are the second best, as far as the volume to area ratio is concerned. If two nearby thick sections are risered, the thin section in between may contain porosities. The problem may be avoided by risering one thick section and chilling the other.

The maximum feeding distance depends upon whether the alloy is a short-freezing range or a long-freezing range alloy. Maximum feeding distance for an aluminium plate of

thickness 't' varies from 8t to 3t as the thickness of the plate varies from 1.27 to 5.1 cm [139]. The riser junction should be heavier than the section to be fed. Ideally, the cross section of the riser is slightly larger than the section it feeds.

For horizontal plates, it is best to use side risers. Side risers are usually located on top of the gates. Use of side risers is also common for thin-walled sections. Since the first metal to enter the casting will warm the bottom of the side riser and cool down, and side risers will be filled with hot metal, use of side risers promotes sequential solidification [112]. However, side risers are not strictly speaking considered as part of the feeding system, nor do they fall entirely in the category of filling systems. They possess the dual function of filling and feeding.

Insulating and/or exothermic materials are also frequently used to improve the feeding efficiency of risers. However, computer simulation programs are finding widespread application in the engineering of risers.

2.5.8 USING CHILLS

Chills are metal inserts placed in the mould to hasten solidification of regions of the casting inaccessible to risers or enhance directional solidification. External and/or internal chills can be used to enhance this localized cooling. The effectiveness of chills depend on their heat diffusivity (ρCK) and volumetric heat capacity (ρCV), where; ρ , is the density of the chill; C , the specific heat; K , the thermal conductivity of the chill; and V , the volume of the chill [6, 126].

External chills are placed against the outside of the casting (Fig 2.21a). They need not be of the same material as that of the casting as fusion (through some kind of diffusion bonding process) must not occur. The most common materials used for external chilling of aluminium alloy castings are steel, cast iron, graphite and copper [6, 126]. In contrast internal chills are placed in the mould cavity where they are cast in, becoming integral with the casting. They are necessarily of the same alloy chemistry as that of the casting

and some surface melting is required in order to fuse the chill into the body of the casting over its entire surface. This requires careful selection of size and shape of the chills. Chaplets, used to support cores, can be used as internal chills as well, but they should remain strong enough to support the core during surface fusion [6].

Internal chills are seldom used for aluminium alloys because of the difficulty introduced by the presence of the oxide film. They can, however, be applied with care and deserve more frequent consideration for feeding or chilling problems in castings, which are difficult to tackle by other techniques [6]. Chills are also known to cause blow defects. This is due to condensation, rust spots and/or other impurities such as oil or grease on the chill surface. Deposition of debris (e.g. eroded sand and dross) on the chill during turbulent filling can also present problems [6].

Sand blasting of the chills before use is good practice if metal chills are used. A layer of cellophane over the chill surface will protect against rusting or condensation of moisture when left in a green sand mould overnight.

2.6 MICROSTRUCTURE OF ALUMINIUM-SILICON ALLOYS

The microstructure of hypoeutectic cast aluminium-silicon alloys are mainly composed of primary aluminium dendrites, eutectic or primary silicon, and iron-rich and copper-bearing intermetallic particles. The volume fraction of dendrites and the second phase particles is determined by alloy chemistry, whereas the size and distribution of the dendrites and second phase particles are dominated by both the solidification conditions and alloy chemistry. For a given alloy, the matrix and eutectic structure can also be affected by the heat treatment. Therefore, the size, volume, and morphology of microstructure constituents are functions of alloy chemistry, solidification conditions, and heat treatment.

SDAS provides a convenient means of linking the mechanical properties to the solidification conditions [48, 131]. The SDAS is a function of solidification rate as illustrated in Fig. 2.21.

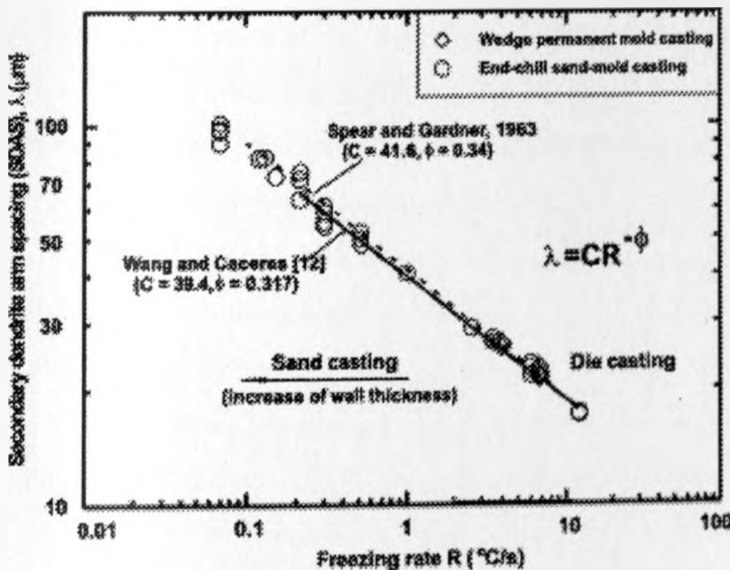


Fig. 2.21 SDAS as a function of freezing rate (After Wang et al. [133]). Note that λ stands for SDAS (μm), R for freezing rate ($^{\circ}\text{C/s}$), and C and ϕ are material constants whose values are given in the graph as obtained from the quoted references. The references are Wang et al's [i.e., ref 133].

Finely spaced dendrite arms reduce the size and promote a uniform distribution of the interdendritic microconstituents (micropores, eutectic or primary silicon, non-metallic

and intermetallic inclusions) [48, 131-133]. This in turn improves mechanical properties [131-132]. The effect of SDAS on size and shape of strontium-modified eutectic silicon particles is, however, not pronounced, but increasing SDAS does worsen the heterogeneous distribution of eutectic silicon particles even in strontium-modified alloys [133].

2.7 TENSILE PROPERTIES OF CAST ALUMINIUM-SILICON ALLOYS

The presence of casting defects in the form of, for example, gas or shrinkage porosity formed during solidification as well as dross or oxide films entrapped during the filling of the mould, can make mechanical properties of casting alloys unpredictable through their detrimental effects. Casting defects, generally, deteriorate mechanical properties to various degrees depending on their size, shape and location in the casting and the individual property in question.

Campbell [6] reported that the size of a defect is often of much less importance than its form and location. For instance, a large pore in a low-stressed area of the casting may be far less detrimental than a small region of layer porosity in a sharp corner subjected to high tensile stresses. To have blanket specifications requiring elimination of all types of defects from every area of the casting is therefore not appropriate, and can result in scrapping of many serviceable castings. The most logical and effective control over casting performance is achieved by specifying separate designated regions of the castings, each separate region being required to contain no defects above the critical size appropriate to that location. Mechanical properties and fracture behaviour of aluminium-silicon based cast alloys depend on casting defects (such as porosity (gas or shrinkage) and oxides), SDAS, and the size and shape of eutectic or primary silicon particles and iron-rich intermetallics that are present in the interdendritic regions. Deformation and fracture of these alloys is usually associated with gradual microstructure damage accumulation. It is generally recognised that these alloys fail due to a ductile fracture process in three classical failure stages of ductile materials: the initiation of microcracks in the silicon and iron-rich intermetallics, the growth of microcracks into cavities and the subsequent coalescence of cavities by the collapse of the resisting matrix ligaments.

2.7.1 EFFECT OF CASTING DEFECTS

Porosity is commonly the single most important parameter affecting the tensile strength

and ductility. Castings with thin sections are especially vulnerable to the effects of porosity since a single macropore, may cover a significant fraction of the load bearing area. The effect of porosity on the tensile properties of castings has been studied by several researchers [134-136]. Caceres and Selling [134] considered the effect of gas porosity, a combination of gas pores, entrapped dross and oxides, and artificial holes on the tensile properties of an Al-7%Si-0.4%Mg - T6 casting alloy. They found that the ductility and tensile strength show little or no correlation with the bulk porosity content, especially in the samples containing dross and oxide films. In contrast, the mechanical performance decreases monotonically with an increase in the area fraction of defects in the fracture surface of the samples. The projected area fraction of defects in a given cross section of the sample seemed to determine the effect of casting defects on the tensile behaviour. Whether the defect was single or multiple, or whether it was cylindrical, near-spherical (gas porosity), or two-dimensional (dross or oxide film), did not seem to be significant.

These results are in agreement with those of Surappa et al [135] and with predictions based on models for the growth of plastic instability in a tensile sample, such as that by Caceres [136], which was based on Surappa et al's results. Surappa et al pointed out that the ductility and strength of the Al-7Si-0.3Mg-T6 alloy depend mainly on the size of the pores on the fracture surface, rather than on volume percent porosity. They showed that the decrease in tensile strength and ductility could be related to the projected area of the pores in the fracture surface, which reduce the load bearing area. Caceres [136] also reported that the shape of the voids and the degree of clustering, when several voids coexist in a section of the sample, are significant parameters that affect ductility. The defect containing regions thus yield first, leading to the concentration of stress and plastic strain. The concentration of the strain results in the cracking of silicon particles near the voids, which increase the local damage and eventually premature failure. Caceres concluded that even low levels of localized porosity may have significant effect on both ductility and tensile strength of the material.

Lee et al [137] also recently reported that yield and tensile strengths, and elongation of

HIPped specimens are much greater than that for non-HIPped specimens. However, in a marked departure from the previous arguments, they associated the improved properties with the significant reduction in the volume fraction of pores by HIPping. The previous explanation, however, still seems plausible; HIPping not only reduced the volume fraction of pores but also considerably reduced the size of pores that remained. Lee et al actually reported a complete elimination of large pores after HIPping. The reduced number and size of defects may have resulted in the reduction of the area fraction of the defects at any given cross section of the samples; thus the improved tensile properties.

Recent detailed studies using the Bauschinger effect [138] and quantitative metallography [139-141] have shown that the rate of particle cracking or debonding is determined by the SDAS and the size and shape of the particles. Tensile fracture has generally been observed [134] to occur at a roughly constant level of damage in the form of cracked second phase particles (mostly silicon particles but also with an increased number of iron-rich intermetallics at higher iron-contents especially if the silicon particles are modified). This has been reported [140-141] to be about 15-20% of the total population of second phase particles. The differences in the fracture strain of sound material with different dendrite cell size are due to the different rates at which damage develops with microstructure orchestrated by the differences in the interactions between the slip bands and the particles at cell or grain boundaries [139-142]. It has also been reported by Dighe and Gokhale [143] that fracture related material properties are often sensitive to the fracture path, and that the relevant fracture path often senses and goes through the largest microstructural features. In the A356 alloy studied, the fracture path of the tensile test specimens was seen to primarily go through the largest silicon particles.

In short, plastic deformation results in the cracking of silicon particles [48, 139-145] and iron-rich intermetallics [48, 140]. When the dendrite cell size is small for a sound material, the cracking is concentrated in the eutectic along the grain boundaries so that fracture is intergranular. On the other hand, when the cell size is large, the final fracture occurs by microcrack nucleation and growth along the dendrites' cell boundaries leading to transgranular fracture.

There exists an intermediate cell size value that coincides with the transition between transgranular and intergranular fracture. Increasing or decreasing the cell size from this intermediate value leads to increased tensile ductility as long as the silicon particles are chemically modified (Fig. 2.22a) [48, 139, 142, 144]. In unmodified alloys, it has been reported [48, 141-142] that, at intermediate cell sizes, the size (equivalent diameter) and shape (aspect ratio) of the silicon particles remains constant while the strain hardening rate decreases with increasing SDAS and this causes an increase in the elongation to fracture (i.e., the upturn in ductility observed in Fig. 2.22b). The low ductility of the large SDAS in unmodified alloys is usually ascribed to the presence of large and elongated silicon particles. These particles tend to crack early during plastic deformation, lowering the ductility of the alloys [48, 140-142].

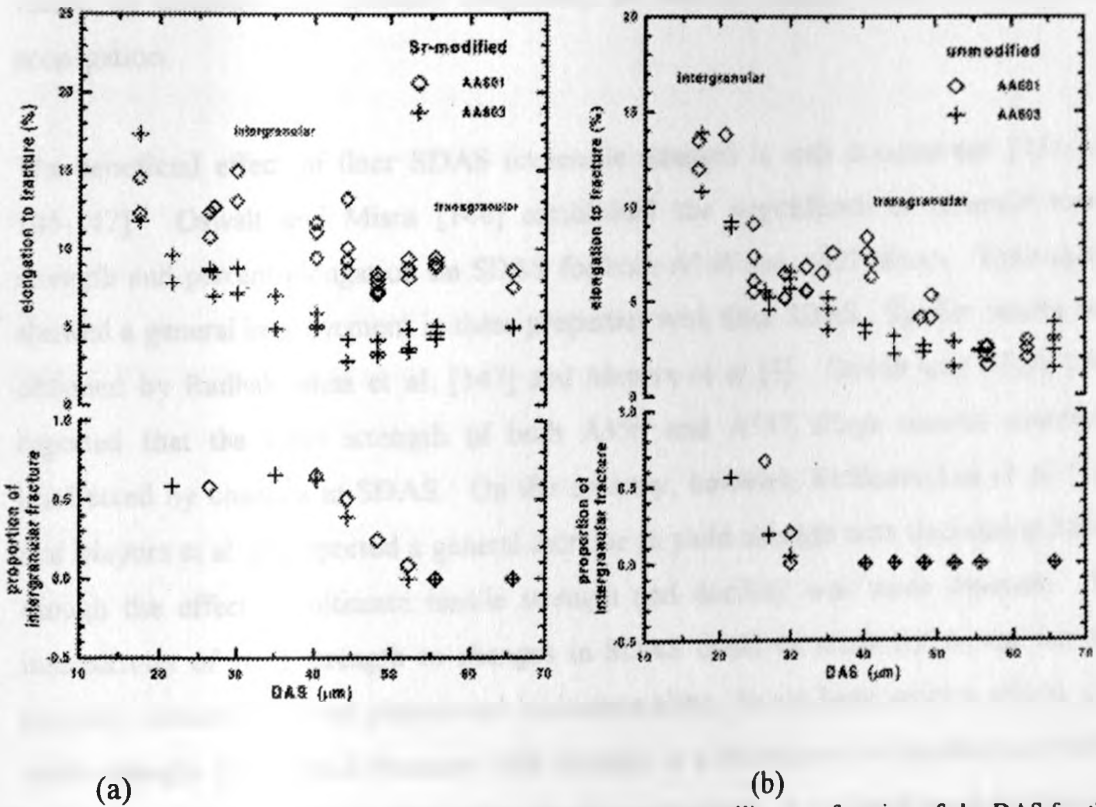


Fig. 2.22 The proportion of intergranular fracture and the tensile ductility as a function of the DAS for the (a) Sr-modified alloys and (b) unmodified alloys (After Wang and Caceres [139]).

Meyers et al [5] also witnessed this subtle upturn in ductility-SDAS relationship for an A357 – T6 premium casting. The work by Caceres and co-workers just discussed maintain that, over this small range, the size and shape of silicon particles remain

constant and that the ductility upturn is an effect of increase in as-cast SDAS. In a marked departure from this understanding, Meyers et al [5] ascribed this upturn to the decrease in the volume fraction of silicon particles with SDAS. They correlated their results with extant theories at the time using a schematic that superimposed the expected ductility-SDAS pattern with that of ductility-volume fraction of silicon particles. The resultant curve gave a similar ductility trough.

The phenomenon of local variation in silicon particle volume fraction, witnessed by Meyers et al, has also been reported recently [145]. The segregation of eutectic composition liquid to areas associated with the last stages of feeding is sometimes seen in commercial permanent mould castings. This segregation effect will influence local values of ductility and fracture toughness, as well as fatigue crack initiation and propagation.

The beneficial effect of finer SDAS on tensile strength is well documented [131-132, 145-147]. Oswalt and Misra [146] established the dependence of ultimate tensile strength and percent elongation on SDAS for both A356 and A357 alloys. Their results showed a general improvement in these properties with finer SDAS. Similar results were obtained by Radhakrishna et al. [147] and Meyers et al [5]. Oswalt and Misra [146] reported that the yield strength of both A356 and A357 alloys remain essentially unaffected by changes in SDAS. On the contrary, however, Radhakrishna et al. [147] and Meyers et al. [5] reported a general increase in yield strength with decreasing SDAS, though the effect on ultimate tensile strength and ductility was more dramatic. The insensitivity of yield strength to changes in SDAS could be attributed to the fact that porosity, insoluble second phases and inclusions alike, do not have serious effects upon yield strength [5]. This is because yield strength is a function of dislocation movement and pinning on precipitates within the aluminium matrix. It is therefore determined by the type, size and distribution of precipitates. The improvements reported are generally associated to the improved response to heat treatment with decreasing SDAS due to shortened diffusion-path lengths [5, 6].

The effect of heat treatment on tensile properties is very strong as evidenced by previous reports [132, 148]. Atxaga et al. [148] reported that A356 alloy specimens in the T6 condition exhibit tensile strength and yield strength values that are significantly higher than those in as-cast specimens with just a slight decrease in ductility. Siaminwe and Clegg [132] also reported an 81 and 212 % increase in ultimate tensile strength and yield strength respectively for an equivalent alloy (LM25). Ductility is adversely affected by artificial ageing treatment, which always results in a loss of ductility [46]. Averaging, however gives higher ductility but lower strength than peak ageing.

Just as asserted by Campbell [7], it seems to be clear from the foregoing discussions that cast aluminium alloys generally fail by the initiation of cracks from their most serious defects (e.g., large pores and, to a lesser extent, oxide films). If these defects are eliminated by, for instance, careful and/or appropriate processing, then the performance of the material is likely to be improved. Strength and fatigue properties in service are then limited by the next most serious family of defects. When each family of defects has been removed, the alloy will fail from microstructural features such as eutectic silicon particles, Fe-rich intermetallic compounds and/or other large brittle phases that might be present. Finally, if in turn, the potency of these microstructural features is minimized, we then have the ultimate resistance to failure of the material. This ultimate resistance is now dictated by the metallurgy of the alloy, for instance, the ability of the alloy to resist slip and once slip has been initiated, the slip distance as dictated by the cell/grain size as enshrined in the Hall-Petch relation. The metallurgy of the alloy is dictated by the atomic arrangement including the inherent crystal defects.

2.8 COMMENTS ON THE LITERATURE REVIEW

It is evident that the quality of aluminium castings depends on a complex interaction of many parameters. Those that are considered to be of major concern have been reviewed in this chapter. They include the following:

- (i) The type and quality of the metal or alloy being cast.
- (ii) The melt handling and treatment practices.
- (iii) The type of casting process used and the actual processing conditions.
- (iv) The mould system design.
- (v) The post-casting operations such as HIPping and heat treatment.

The final structure and soundness of the resulting casting strongly depend on these parameters. The casting structure and soundness in turn determines its mechanical properties, which consequently determine its suitability for the intended application.

In this project, a preliminary study was conducted to investigate the microstructure, hardness, ultimate tensile strength and per cent elongation of several recycled cast aluminium alloys under different processing conditions. The remainder of the thesis reports the experimental methodology and the results obtained.

CHAPTER THREE

EXPERIMENTAL METHODOLOGY

3.1 INTRODUCTION

The main objective of this study was to determine the chemical composition, ultimate tensile strength (UTS), percent elongation (El) and hardness values (BHN) that can be obtained from recycled cast aluminium alloy components. The emphasis in this study was to determine the UTS, El and BHN obtainable from castings produced from various types of cast aluminium scrap under operating conditions typical of those customarily used in the Kenyan aluminium casting shops. It is, however, evidently clear from the literature survey in chapter two and other extant literature that alloy chemistry is just but one of the many variables that influence mechanical properties. Others include process variables, casting and mould design, and melting practices. It would therefore be foolhardy to associate mechanical properties with alloy chemistry without considering the conditions under which the alloy is processed. To illustrate this salutary casting tenet, some of these parameters were varied in this study. The details of the experimental methodology are presented in the sections that follow.

3.2 SCRAP SORTING AND CLASSIFICATION

Pools of approximately 100 kg of assorted cast aluminium scrap were purchased from six different vendors chosen randomly. This was done to determine the common scrap components available in the Kenyan market (at least within Nairobi). The scrap was then sorted component-wise and the scrap components identified were, pistons, cylinder heads, gearbox housings, rear axle housings, alternator covers, exhaust manifolds, oil sumps, other assorted scrap items. The assorted items are those that could be identified to be cast aluminium by comparative visual inspection of their cross-sections (a primitive method but considered to suffice in the absence of better cheap options), but were either too few in number and/or could not be readily identified.

The above scrap components are mostly motor vehicle parts, usually from cars, light trucks (including public transport vehicles), and heavy trucks. The most common of these components were found to be pistons, cylinder heads, gearbox housings and, to a lesser extent, rear axle housings. Pistons and cylinder heads were classified as individual groups while gearbox and rear axle housings were grouped together as housings. The rest were not as common and were collectively lumped together under miscellaneous scrap as the group name. These groups were coded as follows: P for pistons, C for cylinder heads, H for housing (gearbox and rear axle housings), and M for miscellaneous scrap. The miscellaneous scrap included the remaining scrap items (i.e. alternator covers, exhaust manifolds, oil sumps and assorted scrap)

It is true as stated in section 1.3 that different alloys are often used to produce similar automotive components depending on the vehicle model and the preferences of the manufacturer. It is, however, also true that the performance requirements of similar components vary within a limited range. This implies that the alloys to be used are also likely to have properties that do not vary significantly. The probability of using alloys whose chemical compositions vary within a limited range is therefore high. This provides the basis for sorting the scrap component-wise because it is hypothesized that the chemical composition of the resulting alloys will not vary significantly. On the other hand, it is also hypothesized that if cast aluminium alloy scrap components were to be cast together without further sorting, the resulting alloys are likely to have significantly varied chemical compositions. This is because different components have different performance requirements and although some alloys may be able to meet the requirements of two or more components, it is likely that most will not. Therefore several different alloys whose chemical compositions vary significantly will be used for the different components. The alloy chemistry of the resulting alloys are therefore likely to vary significantly depending on the components recycled and the alloys they were originally made from.

To determine typical chemical compositions and mechanical properties of the scrap groups, it was found necessary to melt at least four samples randomly picked from each group. These were coded as follows:

- P1, P2, P3 and P4 for pistons.
- C1, C2, C3 and C4 for cylinder heads.
- H1, H2, H3, H4 and H5 for Housings.
- M1, M2, M3 and M4 for miscellaneous scrap.

To determine the effect on alloy chemistry and mechanical properties when the different groups are blended, the following samples were also prepared and coded as indicated below:

- B1 - A mixture of equal amounts by weight of pistons and cylinder heads.
- B2 - A mixture of equal amounts by weight of pistons and housings.
- B3 - A mixture of equal amounts by weight of cylinder heads and housings.
- B4 - A mixture of equal amounts by weight of pistons, cylinder heads and housings.
- B5 - A mixture of equal amounts by weight of pistons, cylinder heads, housings and miscellaneous scrap.

3.3 MOULD DESIGN

3.3.1 DESIGN OF GATING AND RISERING SYSTEMS

To illustrate the effect of the type of process on mechanical properties, two types of casting processes were used in this study, namely, green sand and permanent mould casting processes. These processes were chosen in this study because they seem to be the most commonly used in Kenyan foundry shops. For both green sand and permanent mould casting processes, test castings were produced using two types of gating methods. This was done to evaluate the effect of the gating system design on mechanical properties. The gating systems used were:

- The turbulent top filled system in which no precautions were taken to prevent entrainment of gases and oxide films. The system was designed to be similar in principle to that used by Cox et al. [128] in which a comparison was also made between top filling and bottom filling of investment castings. Cox et al's system is illustrated in Fig 3.1 and the mould designs used in this study are given in Fig 3.2 for

green sand casting and Fig 3.3 for permanent mould casting. For turbulent top filled green sand casting, nine wooden patterns were used to make six cast specimens in each mould assembly as shown in Fig 3.2. There was no need for the use of a two-part mould assembly (i.e. cope and drag). Turbulent top filled permanent moulds were designed to have cavities, which run through the height of the mild steel rod used as the mould. The cavity was covered at the bottom during pouring by a movable 100mm by 100mm by 50mm mild steel plate. Several moulds were fabricated with a similar mould cavity (cast specimen size) but differing mould thickness. The mould thickness used were 15, 20, 25, 30 and 35mm. Fig 3.3 gives the mould assembly for the mould with 25mm thickness.

- Optimised quiescent bottom filled system that were designed according to current best practice guidelines to prevent entrainment of gases and oxide films. The practical guidelines discussed in chapter two, together with the details in other recent publications [6, 110, 112, 115, 117] were used in dimensioning the filling system. It is important to note that the ideal case would have been to place filters within the running system and optimise the system using a combination of computer modelling of fluid flow (using simulation software such as MAGMAsoft) and real-time x-ray radiography observations as used in most recent work on running systems [113-117, 119]. These facilities were, however, not available. The next best practice was therefore employed. It involves designing the filling system by a trial and error method documented by Campbell [6] using stopwatch measurements and a nomogram given in Fig 2.12 in section 2.5.3. The first trial design is then improved iteratively in an effort to achieve ingate velocities of less than 0.5 m/s. The mould designs used in this study are given in Fig 3.4 for green sand casting and Fig 3.5 for permanent mould casting. They were both designed to be similar in principle to that used by Rezvani et al. [117] (Fig 2.17b).

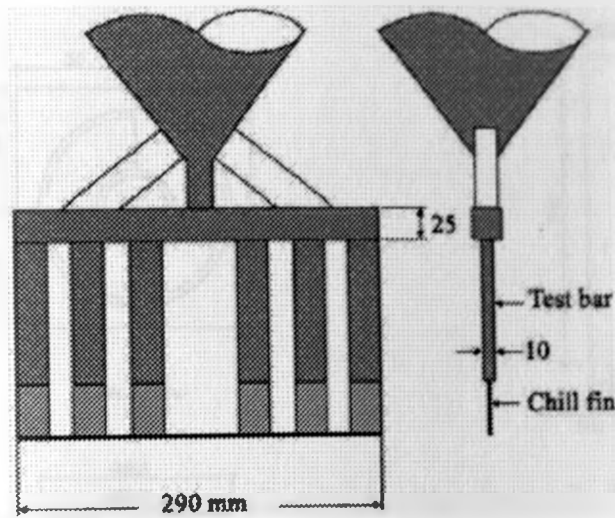


Fig 3.1 Turbulent top filled mould system used by Cox et al. [128]

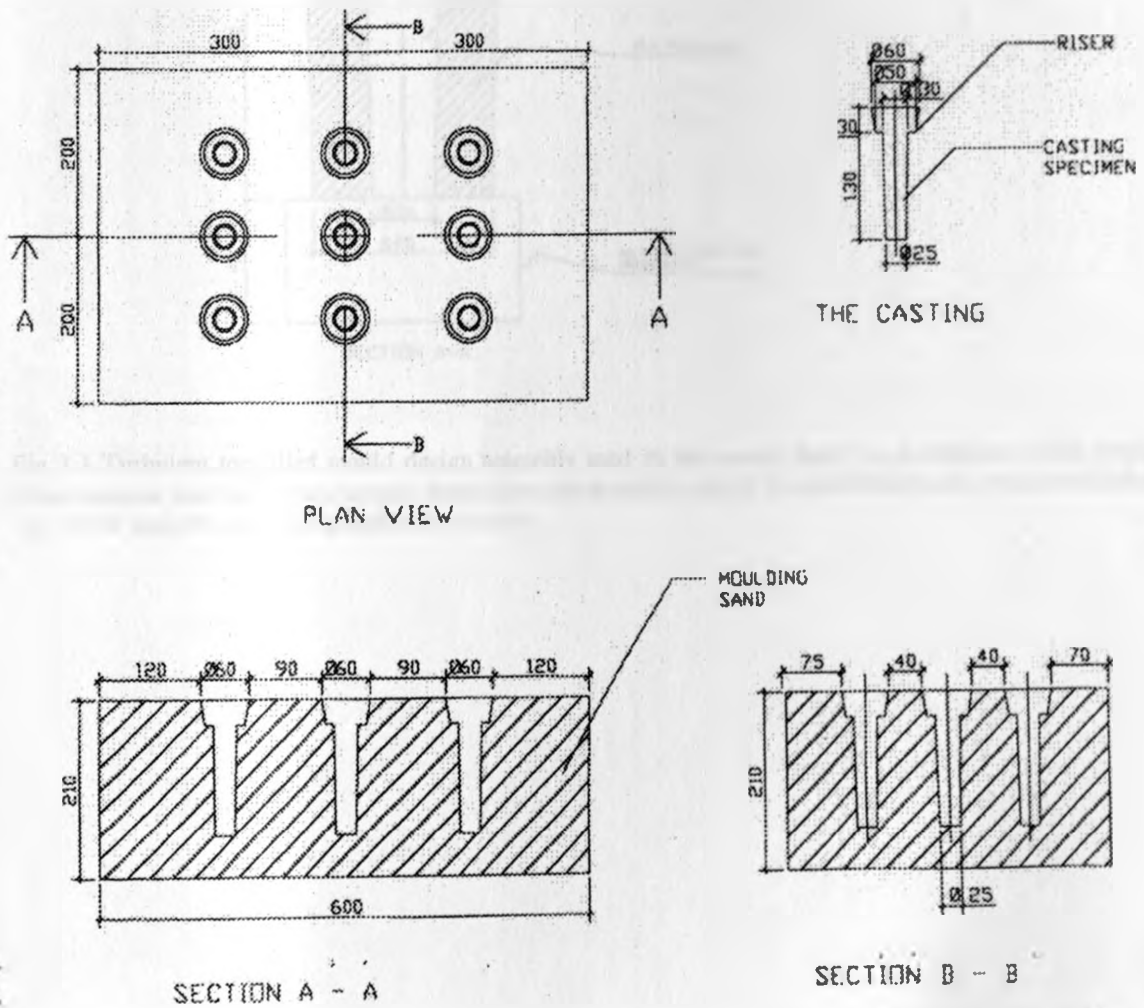


Fig 3.2 Turbulent top filled mould design assembly used in the current study for green sand casting. All dimensions are in mm

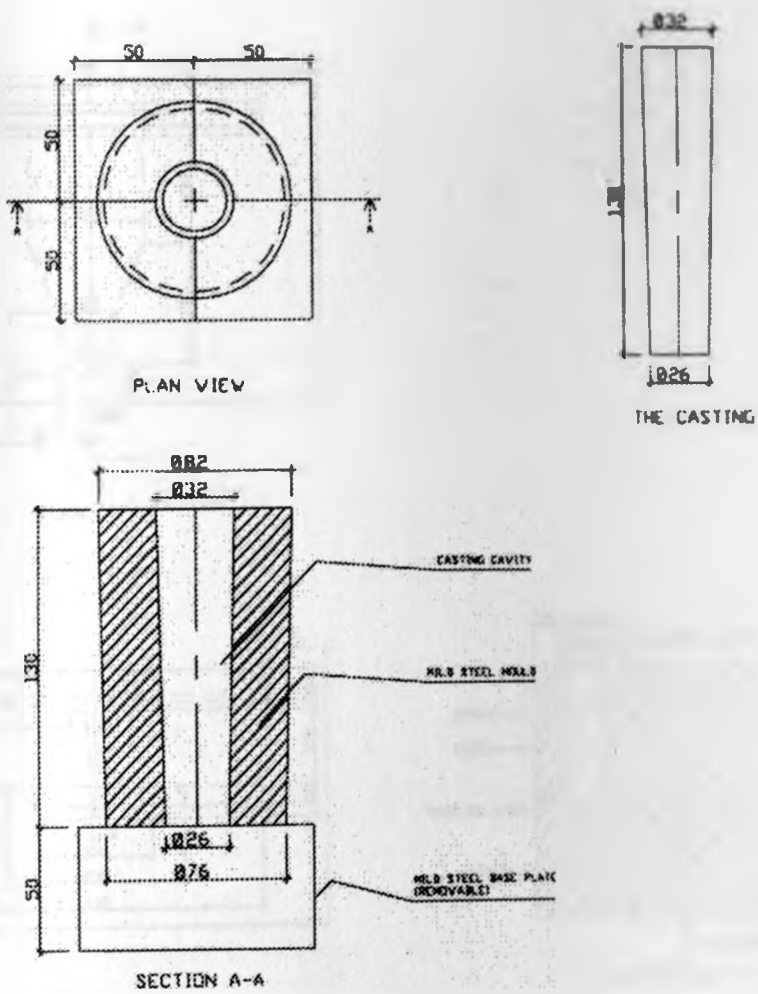


Fig 3.3 Turbulent top filled mould design assembly used in the current study for permanent mould casting. Other moulds used had similar mould dimensions and assembly except the mould thickness, which varied from 15, 20, 30, and 35mm. All dimensions are in mm

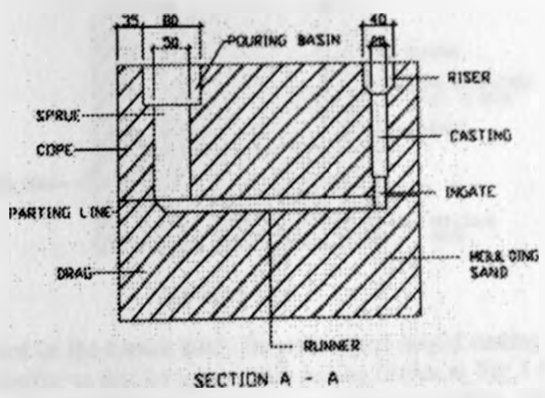
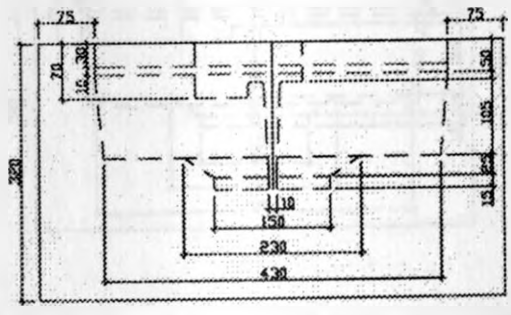
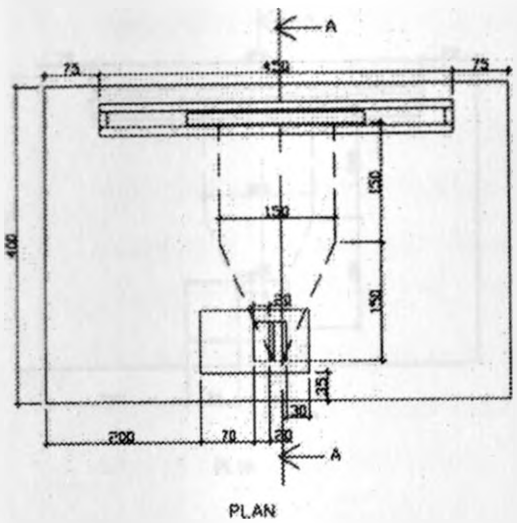


Fig 3.4 Quiescent bottom filled mould design assembly used in the current study for green sand casting. All dimensions are in mm

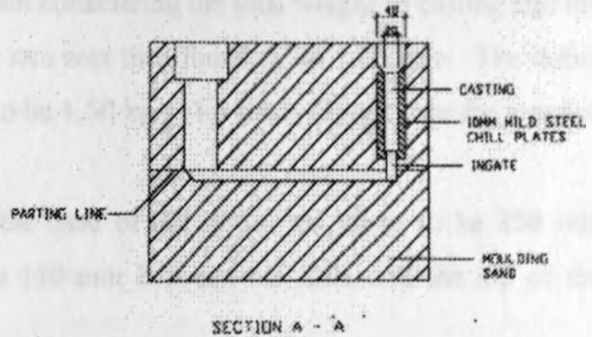
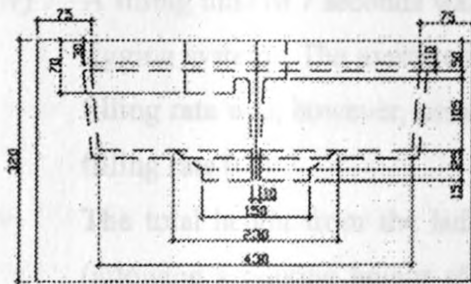
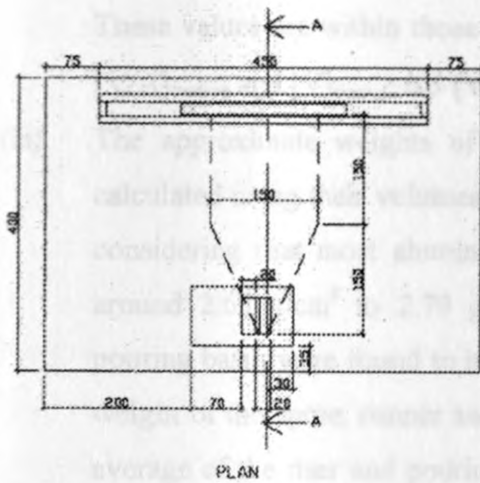


Fig 3.5 Quiescent bottom filled mould design assembly used in the current study for permanent mould casting. Note that all the dimensions and the mould assembly are similar to that for green sand casting shown in Fig 3.4 except for the 10 mm mild steel chill plates placed around the casting bar to simulate permanent moulding. All dimensions are in mm

The following procedure was followed in designing the quiescently filled system:

- (i) An offset weir pouring basin was designed and dimensioned as shown in Figs 3.4 and 3.5. The size of the basin was chosen so as to control the pouring operation. The generous dimensions provided allow the sprue to be kept full throughout the pour, especially at the start of pouring.
- (ii) Considering the modulus of the casting (volume to surface area) calculated as 9 mm ($918750 \text{ mm}^3/104670 \text{ mm}^2$), the riser was dimensioned so as to give a riser modulus calculated as 11 mm ($489500 \text{ mm}^3/44500 \text{ mm}^2$). This gives a modulus ratio (modulus of the riser to that of the casting) of 1.22 (11 mm/9 mm) and a volume ratio (ratio of the volume of the riser to that of the casting) of 0.53 ($489500 \text{ mm}^3/918750 \text{ mm}^3$).

These values are within those usually recommended in practice (i.e., $[V/A]_{\text{riser}} \geq 1.2 [V/A]_{\text{casting}}$ and $[V]_{\text{riser}} \geq 0.5 [V]_{\text{casting}}$) [124].

- (iii) The approximate weights of the casting, riser and the pouring basin were then calculated using their volumes and an approximate density of the alloy of 2.70 g/cm^3 considering that most aluminium silicon alloys have densities that range between around 2.65 g/cm^3 to 2.79 g/cm^3 [13,101]. The weight of the casting, riser and pouring basin were found to be 2.64 kg, 1.32 kg and 1.74 kg respectively. The total weight of the sprue, runner and ingate was tentatively taken to be about 1.53 kg (an average of the riser and pouring basin weights). The total weight of the casting and the rigging system was thus taken to be 7.23 kg.
- (iv) A filling time of 7 seconds was chosen considering the total weight of casting and the rigging system. The average filling rate was then found to be 1.00 kg/s. The initial filling rate was, however, assumed to be 1.50 kg/s (1.5 times higher than the average filling rate [6]).
- (v) The total height from the ladle to the base of the sprue was taken to be 250 mm (allowing a pouring height of about 110 mm between the ladle and the top of the pouring basin).
- (vi) Using the nomogram in Fig. 2.12 for aluminium alloys, the sprue entrance and exit areas were estimated to be 800 and 400 mm^2 respectively. A rectangular sprue was preferred and was dimensioned as shown in Figs 3.4 and 3.5.
- (vii) Expanding runner and vertical expanding end gate designs were adopted in this study to increase the cross-section areas and thus reducing the ingate velocity. The runner and ingate dimensions were calculated and are shown in Figs 3.4 and 3.5, giving a bottom ingate area of 2250 mm^2 . This gives an ingate velocity of about 0.25 m/s.
- (viii) During the first trial, the filling was timed with a stopwatch and was found to take 6 seconds. Together with the actual total casting weight of 6.9 kg, the average filling rate was found to be 1.15 kg/s and thus giving an initial filling rate of 1.725 kg/s, which gives an ingate velocity of about 0.3 m/s. The system was thus confirmed to be quiescent as the ingate velocity was much less than the recommended maximum of 0.5 m/s.

Note that the sprue well is not incorporated in the designs as it has been found [110] to contribute little to alleviate turbulence.

3.3.2 FABRICATION OF THE MOULDS

The permanent moulds were fabricated from mild steel at the Jomo Kenyatta University of Agriculture and Technology workshops. The sand moulds were prepared on site at the department of Mechanical Engineering foundry workshop in the University of Nairobi where melting was done. 14 wt. % bentonite (the binder material) was added to silica sand, which was then mixed thoroughly while slowly adding up to 15 wt.% water. The sand mixture was then rammed manually around wooden casting patterns in metal flasks. The wooden patterns were fabricated at the department of Civil Engineering workshop in the University of Nairobi. The metal flasks used in this study were already available in the foundry workshop.

For the quiescent bottom gating system, fabrication of a complete permanent moulding system using mild steel would require excessive material because of the geometry of the gating system. Therefore, it would be inconvenient to operate besides being unnecessarily expensive. To alleviate this problem, permanent moulding was simulated by making a mould similar to the one used for quiescent green sand filling, but with the casting chilled at all sides with 10mm mild steel plates.

3.4 MELTING AND POURING

Scrap samples of 25 kg each were charged into a diesel fired crucible furnace located at the department of Mechanical Engineering foundry workshop in the University of Nairobi and melted under COVERAL 11* (purchased from Allparts Castings ltd). This fluxing agent is highly exothermic and acts as a covering flux to protect the melt from excessive oxidation and hydrogen pick-up during melting. It also acts as a drossing-off flux by agglomerating the oxides and other inclusions to allow easy removal from the melt surface. At melt

* COVERALL 11 and DEGASER 190 are trademarks of Foseco International Ltd.

temperatures of around 750°C, the dross was skimmed off and the melt degassed with DEGASER 190 tablets for hydrogen removal (also purchased from Allparts Castings Ltd). DEGASER 190 tablets contain hexachloroethane which releases chlorine gas when they are plunged into the melt. Quiescent melt handling was exercised for all samples (except for the H5 scrap sample) throughout the whole process of melt treatment and laundering to minimize entrainment of oxide films and other extraneous materials such as dross remnants into the bulk of the melt. An extra sample of housings, coded as H5 was, however, turbulently handled to assess the effect of melt handling on properties. The samples were not subjected to chemical modification or grain refinement. One of the reasons why the alloys were not modified or grain refined is because the emphasis of the project was to determine the mechanical properties of the recycled alloys using casting practices typical of those customarily used in Kenyan casting shops. Modification and grain refinement is seldom done in most Kenyan foundry shops and therefore modifiers and grain refiners are not sold in the Kenyan market. It is, however, recommended that further research be done using modifiers and grain refiners to assess the improvement in the mechanical properties of the recycled scrap.

The metal was poured to the moulds at pouring temperatures of between 730°C and 750°C save for the case where the effect of pouring temperature on properties was to be assessed. In this case, sample H4 was poured at temperatures of 750°C, 800°C, 850°C and 900°C to both green sand and permanent moulds.

3.5 CHEMICAL COMPOSITION ANALYSIS

For each secondary scrap alloy, small cast samples were poured and quenched in unpreheated mild steel moulds for chemical analysis. The chemical composition of the samples was then determined at Booth Manufacturing Africa Ltd at the Aluminium Extrusion Division located in Thika. The analysis was done using an OES-5500 optical emission spark spectrometer manufactured by Shimadzu Corp. The spectrometer is equipped with a system that has enhanced analytical precision including: minimised influence of discontinuity (e.g. cracks and pinholes) on the sample during measurement because of statistical processing;

improved analytical sensitivity to trace elements (down to 10 ppm) due to the system's element measurement method; and excellent analytical precision because it measures frequency distribution of light intensities and uses the median value as representative.

3.6 MOULD THICKNESS AND PREHEAT

To determine the effect of mould thickness and preheat on mechanical properties, sample B5 was poured into steel moulds of 15, 20, 25, 30 and 35 mm thickness whose initial temperatures were varied from room temperature (approx. 25°C), to 200°C and subsequently to 350°C.

3.7 HEAT TREATMENT

The green sand and permanent mould castings produced in quiescent bottom filled mould systems using samples P4, H4, H5, C4 and M4 were each sectioned into two portions, one of which was subjected to heat treatment to the T6 condition. The other portion together with all the other castings produced in turbulent top filled systems were tested while in the as-cast condition.

The procedure for heat treatment was as follows:

For solution treatment, the samples were put into an ELSKLO manufactured electric resistance furnace of type LNT20. The furnace has an automatic temperature measurement and control device (Commander 50). The furnace was first heated to 540°C before inserting the specimens into the heating chamber. The specimens were held at that temperature (with fluctuations of $\pm 2^\circ\text{C}$) for 24 hours. The specimens were then quenched in cold water and put into another electric resistance furnace for artificial aging.

Though solution treatment times of less than 24 hours may be possible and adequate [149], 24 hours was chosen to ensure complete fragmentation and spheroidization of eutectic silicon particles considering that the alloys were not modified, and perhaps modification of some of

the soluble intermetallic phases. Pre-ageing at room temperature was avoided to ensure that peak T6 strengths were achieved. Although pre-ageing improves ductility, it decreases ultimate tensile strength.

The furnace used for artificial aging was an ELSKLO manufactured electric resistance furnace of type JN 200R. The furnace also has an in built automatic temperature measurement and control system (Commander 50). It also has an air circulating fan which can be switched on or off during heat treatment. The specimens were put into the furnace after preheating it to 170°C with the fan on and they were held at this temperature (with fluctuations of $\pm 2^\circ\text{C}$) for 6 hours. The specimens were then removed and left to cool in air.

Both furnaces used for heat treatment are located at department of Mechanical Engineering workshop in the University of Nairobi.

3.8 TENSILE AND HARDNESS TESTING

3.8.1 TENSILE TESTING

Standard tensile test specimens were prepared from the as-cast cylindrical top filled castings. For as-cast and heat treated plate castings, tensile test specimens were sectioned at 20 mm intervals systematically from the ingate end to the riser end. This was done to investigate the variation of mechanical properties with location in the casting. The dimensions of the tensile test specimens were according to the Germany standard DIN 50 125-A8x40 as illustrated in Fig 3.6.

Tensile tests were carried out at a strain rate of $5 \times 10^{-5} \text{ s}^{-1}$ using a TORSEE's SENSTAR Universal Tensile Testing Machine type SC-10CS N^o 6044. The equipment is located at department of Mechanical Engineering workshop in the University of Nairobi.



Fig 3.6 A DIN 50 125-A8X40 standard tensile test piece with a diameter d_0 of 8mm and an original gauge length L_0 of 40mm. Other dimensions are: d_1 - diameter of gripped ends (approx. $1.2 d_0 = 10\text{mm}$), L_c - parallel length ($L_0 + d_0 = 48\text{mm}$), h - length of gripped ends (30mm), and L_t - total length (115mm)

3.8.2 HARDNESS TESTING

The AVERY Brinell Hardness Tester N^o 6403 was used to obtain hardness values of specimens excised from every tensile test specimen before machining. The specimens were machined into small discs of 20mm diameter and 20mm height. They were then subjected to fine grinding using a series of silicon carbide papers of increasing fineness up to 1200 grit. This was to ensure that artificial machining defects did not affect test results. A ball diameter of 10mm and load of 1000 kg were used for making indentations on specimens for a period of 20 seconds. For every hardness test, six indentations were made on the specimen and an average of three diameter measurements were taken for each of the six indentations. A standard chart was then used to interpret these diameters into Brinell Hardness Number values. The hardness value was then taken as the average of the six values. All tests were carried out three months after casting to allow for natural ageing of the as-cast specimens.

3.9 MICROSTRUCTURE CHARACTERISATION

Specimens for microstructural characterisation were sectioned from both the as-cast and heat treated castings. The specimens were then subjected to grinding using a series of silicon carbide papers (220, 320, 360, 400, 500 and 600 grit) mounted on a flat plate under running water. They were then polished to obtain a mirror finish on polishing cloth attached onto a rotating wheel using diamond paste up to 1 micron. The specimens were then etched in an aqueous solution of NaOH (25g of NaOH in 100 ml of distilled water [150-151]).

The microstructures were studied using a light optical microscope and representative micrographs were taken at various magnifications using a Zeiss Ikon camera attached to the microscope.

The phases in the microstructure were identified by comparing their shapes with those of similar phases reported in the literature and by comparing their colour before and after etching with the NaOH aqueous solution with the chart reported by Vander Voort [151].

The SDAS measurements were carried out using the linear intercept method. The procedure followed is similar to that described by Caceres and Wang [144]. Measurements were carried out on micrographs taken at a magnification of 54X. This was done by drawing an edge to edge line over a small group of well defined cells and then dividing the length of the line by the number of cells. Ten such groups of cells were measured and the SDAS value was taken as the average of the ten measurements.

For grain size measurements, the specimens were etched for 2 minutes in the Modified Murakami's etch. This etchant was prepared by mixing 10 g of sodium hydroxide (NaOH) and 5 g of potassium ferricyanide ($K_3Fe(CN)_6$) in 60 ml of water. The grain sizes were also measured using the linear intercept method by counting the number of grains intercepted by two lines running along diagonals of the micrographs taken at a magnification of 54X.

CHAPTER FOUR

RESULTS AND DISCUSSIONS

4.1 CHEMICAL COMPOSITION

The chemical compositions of the experimental scrap (secondary) alloys representing the various scrap categories investigated in this study are shown in Table 4.1.

Table 4.1 Chemical Compositions of the Experimental Alloys (wt.%).

Co de	Al	Cu	Si	Fe	Mg	Mn	Ni	Zn	Cr	Pb	Sn	Ti
P1	86.618	1.607	7.881	0.900	0.472	0.084	1.833	0.110	0.016	0.055	0.101	0.101
P2	85.997	2.052	8.563	0.610	0.700	0.074	1.733	0.083	0.021	0.043	0.062	0.061
P3	87.768	3.052	6.169	0.674	0.141	0.236	0.279	1.399	0.026	0.105	0.111	0.040
P4	85.814	2.307	8.022	0.841	0.841	0.256	1.726	0.099	0.023	0.053	0.066	0.052
H1	86.816	3.298	7.142	0.818	0.084	0.138	0.137	1.142	0.032	0.130	0.155	0.050
H2	87.782	3.024	7.087	0.849	0.064	0.191	0.101	0.658	0.031	0.094	0.079	0.042
H3	87.089	3.208	7.277	0.860	0.055	0.214	0.117	0.858	0.032	0.118	0.085	0.058
H4	85.648	3.488	8.125	0.900	0.069	0.261	0.146	0.749	0.045	0.128	0.180	0.043
H5	85.799	3.072	8.446	0.900	0.058	0.234	0.112	0.678	0.029	0.149	0.180	0.043
C1	91.362	1.737	5.818	0.383	0.064	0.206	0.059	0.170	0.005	0.097	0.083	0.016
C2	89.970	2.931	5.858	0.514	0.059	0.248	0.040	0.182	0.009	0.064	0.060	0.063
C3	89.837	3.088	5.460	0.710	0.038	0.286	0.044	0.273	0.012	0.120	0.078	0.056
C4	91.593	1.216	6.055	0.430	0.078	0.277	0.017	0.156	0.008	0.072	0.052	0.045
M1	86.738	3.537	6.745	0.713	0.126	0.202	0.233	1.318	0.018	0.146	0.180	0.043
M2	88.539	2.038	7.142	0.715	0.147	0.219	0.290	0.615	0.017	0.107	0.118	0.054
M3	89.734	1.900	5.619	0.669	0.131	0.238	0.129	1.203	0.026	0.097	0.180	0.062
M4	87.540	2.347	7.339	0.900	0.184	0.188	0.588	0.475	0.019	0.088	0.092	0.048
B1	89.367	2.851	6.049	0.670	0.088	0.248	0.302	0.205	0.011	0.087	0.063	0.057
B2	86.076	3.242	7.855	0.900	0.089	0.237	0.224	0.544	0.028	0.166	0.180	0.089
B3	86.764	3.784	6.981	0.900	0.046	0.326	0.080	0.570	0.024	0.132	0.140	0.074
B4	89.081	2.615	6.594	0.726	0.046	0.211	0.130	0.343	0.013	0.090	0.108	0.044
B5	87.891	2.388	7.246	0.900	0.123	0.219	0.478	0.439	0.020	0.087	0.124	0.074

Significant observations that can be discerned from the chemical composition results are discussed below.

4.1.1 THE SILICON CONTENT

The silicon content in the samples varies between 5.460 to 8.563 wt %. This indicates that the majority of the scrap components were originally produced from a range of hypoeutectic aluminium-silicon based foundry alloys.

The silicon composition range of 5.460-8.563 wt. % for the experimental scrap samples is well within the composition range that exhibit excellent castability, weldability, machinability and tensile strength. The ductility will, however, depend on the eutectic silicon particle modification by chemical additives, control of cooling rate and/or solution heat treatment.

4.1.2 THE COPPER CONTENT

The copper content in the samples varies between 1.216 to 3.784 wt %. This indicates that most of the scrap components were originally produced from aluminium-silicon-copper based alloys. It is, however possible that some components (very few) made from aluminium-copper based alloys may have been included in the samples. This is particularly possible for piston samples because pistons are sometimes made from these alloys. If this was the case, then these components may have contributed to the higher copper contents in the piston samples. It is highly likely that sample P3 experienced such a scenario given its significant difference from the other piston samples.

The copper contents in the scrap samples (1.216-3.784 wt. %) are below the maximum limit of 5 wt. % normally recommended for commercial aluminium-silicon-copper based alloys and are capable of bringing about significant hardening to the alloys. The alloys with lower copper contents (e.g. P1, C1, C4 and M3) would be expected to have relatively improved castability and ductility at the expense of hardness and tensile strength compared to their

counterparts with higher copper contents (e.g., those with copper >3 wt %).

4.1.3 THE MAGNESIUM CONTENT

The magnesium content in the housing, cylinder head and blended scrap samples is generally low and is in the range of <0.1 wt. %. This implies that these scrap components were originally produced from aluminium-silicon-copper based alloys containing only trace amounts of magnesium. This inference may, however, not hold for the blended scrap samples as their composition depends on the mix of the different types of scrap components, whose magnesium contents are not necessarily of trace amounts. For example, samples B1, B2 and B4 contain substantial amounts of piston scrap (i.e., 50 % of pistons for B1 and B2 and 33.3 % of pistons for B3) whose magnesium content varies from 0.141 to 0.841 wt. %. Furthermore, B5 contains 25% of miscellaneous scrap (whose magnesium content varies from 0.126 to 0.184 wt%) in addition to another 25% of piston scrap. It is thus possible that significant amounts of magnesium may have been lost during melt handling because magnesium oxidizes easily. Degassing with hexachloroethane is also known to remove substantial amounts of magnesium [28]. Hexachloroethane releases chlorine, which reacts with aluminium to form aluminium chloride gas. Significant quantities of this gas, which is responsible for degassing, also react with magnesium to form magnesium chloride, which then floats. Magnesium removal by chlorine is actually considered to be very efficient especially above 710°C as over 90 % of the magnesium can be removed [28]. It, therefore, follows that certain scrap such as the piston and miscellaneous scrap components may have been originally produced from aluminium-silicon-copper-magnesium based alloys in view of the substantial magnesium contents in their samples.

The scrap samples containing trace amounts of magnesium are expected to have lower hardness and strength but relatively higher ductility compared to those containing higher magnesium contents if the composition of other elements is held constant. The situation is, however, complicated because the various scrap samples have variations in other elemental compositions albeit small in certain cases. The magnesium contents in the samples may be considered acceptable because they are below the maximum limit of 1 wt.% magnesium.

The 1 wt% magnesium limit is specified for several commercial hypoeutectic aluminium-silicon-copper-magnesium alloys such as the US 332, 336 and 339.

4.1.4 THE IRON CONTENT

The iron content in the samples is relatively higher for the P, H, M and B alloy groups. The content varies between 0.610 wt. % to 0.900 wt. %. In the C group, however, the iron content is relatively low (i.e., it varies between 0.383 wt. % to 0.710 wt.%). The high iron content associated with the piston and housing scrap component samples suggests that these components were most likely produced via high pressure diecasting. Alloys processed via this process contain higher iron contents deliberately added to mitigate for die soldering. The relatively low iron content in the cylinder head scrap samples suggest that cylinder heads are generally not manufactured via high pressure diecasting. They are, however, possibly produced via other common or proprietary low pressure die casting and precision casting processes.

Efforts were made in this study, during scrap sorting, charging and melting to avoid further contamination with iron and the above arguments are built on this premise. However, some degree of contamination is inevitable during scrap recycling, but the iron level in the samples and its general trend gives credence to the arguments raised.

The deleterious effects of iron on the castability and properties of aluminium-silicon based alloys are well documented in extant literature and are briefly reviewed in chapter two. A more comprehensive coverage of the subject has been extended by Mbuya et al [152] in a recent review.

4.1.5 THE MANGANESE CONTENT

The manganese content in the samples varies within a small range of between 0.188 to 0.326 wt. % except for a few runaway samples, i.e., P1, P2 and H1 whose manganese contents are 0.084, 0.074 and 0.138 wt% respectively. Manganese is usually added in the range of about

0.2 to 0.6 wt. % to ameliorate the effect of iron. The manganese in the samples is therefore within the limits specified for most cast aluminium alloys.

4.1.6 THE CONTENT OF OTHER ELEMENTS

The piston samples contain relatively high nickel (1.726, 1.733 and 1.833 wt. % for P4, P2 and P1 respectively) as would be expected because of the high temperature operating conditions, which pistons are usually subjected to. The P3 piston sample contains a comparatively low nickel content (0.279 wt%), however, but it is apparently an odd sample in the group if its alloy chemistry is compared with the other samples in the group. The rest of the alloys contain a relatively low nickel content with the cylinder head group having the lowest (in the range of <0.1 wt%).

The zinc content in the piston group is relatively low (0.083 to 0.110 wt. %) save for the P3 sample (1.399 wt. %). The cylinder head group also contains relatively low zinc contents (0.101 to 0.146 wt. %) compared to the housing, miscellaneous and blended scrap groups. The detrimental effects of zinc are not very pronounced in aluminium silicon based alloys. It is thus specified in many alloys at higher levels than other impurities, e.g., up to 3 wt. % in some aluminium die casting alloys [34]. The zinc levels in the samples is therefore well within this limit.

The chromium content in the alloys under investigation is of relatively trace amounts across the board (i.e., <0.05 wt.%). Chromium is usually added to correct the effect of iron and improve room and high temperature strength.

In the alloys under investigation, the lead content ranges between 0.043 to 0.166 wt. % while that of tin ranges between 0.052 to 0.180 wt. %. These are generally acceptable ranges applicable to most aluminium-silicon based alloys. Lead and tin are usually added to aluminium-silicon based alloys to improve their machinability.

Titanium is usually added during processing together with boron as Al-Ti-B based master

alloys for grain refinement. The acceptable range of titanium content for grain refinement is between 0.04 to 0.25 wt. %. The titanium content in the experimental alloys is between 0.04 to 0.101 wt. %. This range of residual titanium content is capable of effecting some reasonable degree of grain refinement.

Other important minor alloying elements that are commonly encountered in aluminium-silicon based alloys are strontium, sodium, antimony and calcium for modification of the eutectic silicon. Most of these elements are depleted on remelting except antimony, which is retained even after several remelts. Antimony and calcium are, however, less frequently used for this purpose. The presence and effect of these elements is not investigated as they are deemed to have been lost on remelting. Further investigations on their presence and effect on mechanical properties is, however, encouraged.

Other elements that may be present in aluminium-silicon based alloys are beryllium, vanadium, cobalt, molybdenum, lithium, phosphorus, and tungsten, among others. Some rare earth impurity elements such as lanthanum may also be introduced as constituents of fluxing agents. The presence and effect of these impurities is also not investigated here because their presence is generally rare and their effect is subtle to discern in the presence of the other elements dealt with. The effect of beryllium in the presence of a higher iron content is, however, significant. It is an excellent iron corrector, improves the precipitation kinetics of the strengthening precipitates and even acts as a grain refiner of aluminium. It also raises the melting temperature of the Al_2Cu phase from ~ 515 to ~ 522 °C [64]. This allows a higher solutionizing temperature to be used for aluminium-silicon-copper based alloys without the danger of incipient melting. This element, its benefits notwithstanding, is toxic and its addition is rare and limited to a small group of alloys such as A357, C357, 358, B358 and 364 [13].

4.1.7 COMPARISON WITH COMMERCIAL ALLOYS

A major observation that can be discerned from the chemical compositions of the scrap samples is that there is no significant difference in the composition of the alloys save for

minor variations from group to group and between samples of a similar group. In several cases, samples from different groups exhibit approximate equivalence in composition. For example, it can be discerned that the following samples are approximately equivalent; B1, B4, P3, and M3; P1, P2 and P4; H1, H2, and H3; H4, H5 and B2; C1 and C4; C2 and C3; M1 and B3; M2, M4 and B5; and finally B1 and C2.

Another interesting observation is that the scrap samples are approximately equivalent to a small group of common commercial aluminium alloys. The P3, H1, H2, H3, H4, C2, C3, M1, M2, M3, M4, B1, B2, B3, B4 and B5 are approximately equivalent to the 319-type alloy, its variants (A319, B319 and W319) and its equivalent alloys in other designations (LM4, LM22, EN AC-45200, EN AC- 45400, AC 2A, etc.). This is expected as the 319 group of alloys are secondary aluminium-silicon-copper based alloys whose impurity limits are generally specified high and are extensively used in automotive powertrain applications. The 319 group of alloys are generally used for engine crankcases, cylinder heads, gearbox and rear axle housings, manifolds, engine mounts and other miscellaneous engine parts. It is, therefore, not surprising that most of the scrap samples are approximately equivalent to this group of alloys.

Other comparisons that can be discerned and the chemical composition range of the equivalent commercial aluminium alloys are given in Table 4.2. The 380 alloy, its offshoots and equivalent commercial alloy designations are generally used for gearbox housings, cylinder heads, rear axle housing and other general engineering applications. As would be expected, the housing scrap samples are found to be approximately equivalent to the 380 group of alloys. The overlap in the equivalence of the housing scrap and some of the blended mixtures (B2 and B5) with the 319 and 380 group of alloys is because of the overlap in applications of these two groups of commercial alloys. The same argument applies to other overlaps evident in Table 4.2.

The 332 alloy and its equivalent commercial alloy designations are mostly used for piston applications. The 332 alloy is made almost exclusively from recycled scrap. This is made evident from the observation that the piston scrap samples are generally approximately

equivalent to the 332 and LM26 alloys. The piston samples also seem to be approximately equivalent to the LM27 and AC 2B alloys. Further, the cylinder head scrap samples are approximately equivalent to the 355, LM16 and AC 2D group of alloys, which are commonly used for cylinder head and engine block applications. Finally, 383, LM2 and AD C12 group of alloys is generally used for gearbox housings and the housing scrap sample H5 is observed to be approximately equivalent to these alloys.

Table 4.2 Comparison of scrap samples with equivalent commercial alloys.

Scrap sample	Equivalent commercial alloys	Composition range of the equivalent commercial alloys
P3, H1, H2, H3, H4, C2, C3, M1, M2, M3, M4, B1, B2, B3, B4, B5	319, A319, B319, W319, LM4, LM22, EN AC-45200, EN AC-45400, AC 2A	4.0-8.0Si, 2-4.0Cu, 0.05-0.6Mg, 0.3-1.3Fe, 0.1-0.6Mn, 0.01-0.3Ni, 0.009-3.0Zn, 0.008-0.07Cr, <0.1Pb, 0.05-0.1Sn, 0.12-0.2Ti
M1, B3, B4, B5	308, LM21, EN AC-45000, AC 2A	5.0-7.0Si, 3.0-5.0Cu, 0.1-0.3Mg, <1.0Fe, 0.2-0.6Mn, <0.3Ni, <2.0Zn, 0.2Pb, 0.1Sn, 0.2Ti
H1, H2, H3, H4, H5, B2, B5	380, LM24, EN AC-46500, AC 4B	7.5-9.5Si, 3.0-4.0Cu, <0.35Mg, <1.3Fe, <0.5Mn, <0.5Ni, <3.0Zn, <0.30Pb, <0.2Sn, <0.2Ti
P1, P2, P4, H4	328, 332, 333, LM26	8.0-10.5Si, 1.5-4.0Cu, <1.5Mg, <1.2Fe, <0.5Mn, <1.0Ni, <3.0Zn, <0.2Pb, <0.1Sn, 0.2Ti
C1, C3, C4, M3	355, 305, LM16, EN AC-45300, AC 4D	4.5-5.5Si, 1.0-1.5Cu, 0.4-0.6Mg, <0.6Fe, <0.5Mn, <0.25Ni, <0.35Zn, <0.1Pb, 0.05Sn, <0.2Ti
P1, P3, P4	LM27, EN AC-46600, AC 2B	6.0-8.0Si, 1.5-3.28Cu, <0.35Mg, <0.8Fe, <0.6Mn, <0.3Ni, <1.0Zn, <0.2Pb, <0.1Sn, <0.2Ti
H5, P2	383, LM2, EN AC-46100, AD C12	9.0-11.5Si, 0.7-2.5Cu, <0.3Mg, <1.3Fe, <0.5Mn, <0.5Ni, <2.0Zn, <0.3Pb, <0.2Sn, <0.2Ti

In general, sorting the scrap according to components as done in this investigation could be useful to a limited extent. The ideal situation would be to correct the alloy chemistry of the resulting alloys to appropriate standard alloys using on line facilities such as spectrometers and master alloys or compacted additives. However, since this is not always possible, particularly for Kenyan foundry shops, it would be advisable to sort the scrap component-wise and use the alloy chemistries obtained for one or more samples of the same group as a guide to predict the expected alloy chemistry of alloys recycled from components of that group.

The chemical compositions of some of the scrap categories obtained in this study can be used to predict the alloy chemistry of alloys recycled from components belonging to similar groups. Recycled pistons are likely to result in an alloy containing ~ 8 wt% silicon, 0.4-0.85 wt% magnesium, 0.6-0.9 wt% iron, ~ 1.7 wt% nickel, <0.25 wt% manganese, <0.1 wt % zinc, <0.1 wt % chromium, <0.1 wt % lead, <0.1 wt % tin and <0.1 wt % titanium. However, the copper content may vary from about 1.5 to 3 wt% and cannot easily be predicted as the other elements. Therefore, when recycling pistons, one can have a reasonably good idea as to the expected levels of most elements in the resulting alloy except copper. If the desired application does not require strict chemistry specifications, one will only need to determine the copper content. The same applies to the housings and cylinder head groups. The expected alloy chemistry of an alloy recycled from gear box and rear axle housings is ~ 7-8.5 wt% silicon, ~ 3-3.5 copper, < 0.1 wt% magnesium, 0.8-0.9 wt% iron, ~ 0.2 wt% manganese, ~ 0.1 wt% nickel, <0.1 wt % zinc, <0.1 wt % chromium, ~ 0.1 wt % lead, ~ 0.1-0.2 wt % tin and <0.1 wt % titanium. Recycling cylinder heads would result in an alloy that approximately contains 6 wt% silicon, < 0.1 wt% magnesium, 0.4-0.7 wt% iron, ~ 0.2-0.3 wt% manganese, ~ 0.1 wt% nickel, 0.16-0.27 wt % zinc, <0.1 wt % chromium, < 0.1 wt % lead, < 0.1-0.2 wt % tin and <0.1 wt % titanium. Its copper content is, however, likely to vary from 1.2-3 wt%.

The rest of the assorted scrap including those that are available in small quantities can be lumped together and recycled after which the alloy chemistry of the resulting alloys should be determined for each separate charge. However, if particular scrap components not covered in this study (e.g. cast aluminium wheels) are available in reasonable quantities, they

should also be separated from other scrap and recycled alone. It is likely that the alloy chemistry of different scrap samples belonging to such group will be equivalent for most of the elements.

Table 1. Chemical composition of scrap samples (wt.%)

Sample	Fe	C	Mn	P	S	Si	Al	Ni	Cr	Mo	Cu	Co	Other
1	98.5	0.15	0.4	0.01	0.005	0.05	0.01	0.01	0.01	0.01	0.01	0.01	0.01
2	98.5	0.15	0.4	0.01	0.005	0.05	0.01	0.01	0.01	0.01	0.01	0.01	0.01
3	98.5	0.15	0.4	0.01	0.005	0.05	0.01	0.01	0.01	0.01	0.01	0.01	0.01
4	98.5	0.15	0.4	0.01	0.005	0.05	0.01	0.01	0.01	0.01	0.01	0.01	0.01
5	98.5	0.15	0.4	0.01	0.005	0.05	0.01	0.01	0.01	0.01	0.01	0.01	0.01
6	98.5	0.15	0.4	0.01	0.005	0.05	0.01	0.01	0.01	0.01	0.01	0.01	0.01
7	98.5	0.15	0.4	0.01	0.005	0.05	0.01	0.01	0.01	0.01	0.01	0.01	0.01
8	98.5	0.15	0.4	0.01	0.005	0.05	0.01	0.01	0.01	0.01	0.01	0.01	0.01
9	98.5	0.15	0.4	0.01	0.005	0.05	0.01	0.01	0.01	0.01	0.01	0.01	0.01
10	98.5	0.15	0.4	0.01	0.005	0.05	0.01	0.01	0.01	0.01	0.01	0.01	0.01
11	98.5	0.15	0.4	0.01	0.005	0.05	0.01	0.01	0.01	0.01	0.01	0.01	0.01
12	98.5	0.15	0.4	0.01	0.005	0.05	0.01	0.01	0.01	0.01	0.01	0.01	0.01
13	98.5	0.15	0.4	0.01	0.005	0.05	0.01	0.01	0.01	0.01	0.01	0.01	0.01
14	98.5	0.15	0.4	0.01	0.005	0.05	0.01	0.01	0.01	0.01	0.01	0.01	0.01
15	98.5	0.15	0.4	0.01	0.005	0.05	0.01	0.01	0.01	0.01	0.01	0.01	0.01
16	98.5	0.15	0.4	0.01	0.005	0.05	0.01	0.01	0.01	0.01	0.01	0.01	0.01
17	98.5	0.15	0.4	0.01	0.005	0.05	0.01	0.01	0.01	0.01	0.01	0.01	0.01
18	98.5	0.15	0.4	0.01	0.005	0.05	0.01	0.01	0.01	0.01	0.01	0.01	0.01
19	98.5	0.15	0.4	0.01	0.005	0.05	0.01	0.01	0.01	0.01	0.01	0.01	0.01
20	98.5	0.15	0.4	0.01	0.005	0.05	0.01	0.01	0.01	0.01	0.01	0.01	0.01
21	98.5	0.15	0.4	0.01	0.005	0.05	0.01	0.01	0.01	0.01	0.01	0.01	0.01
22	98.5	0.15	0.4	0.01	0.005	0.05	0.01	0.01	0.01	0.01	0.01	0.01	0.01
23	98.5	0.15	0.4	0.01	0.005	0.05	0.01	0.01	0.01	0.01	0.01	0.01	0.01
24	98.5	0.15	0.4	0.01	0.005	0.05	0.01	0.01	0.01	0.01	0.01	0.01	0.01
25	98.5	0.15	0.4	0.01	0.005	0.05	0.01	0.01	0.01	0.01	0.01	0.01	0.01
26	98.5	0.15	0.4	0.01	0.005	0.05	0.01	0.01	0.01	0.01	0.01	0.01	0.01
27	98.5	0.15	0.4	0.01	0.005	0.05	0.01	0.01	0.01	0.01	0.01	0.01	0.01
28	98.5	0.15	0.4	0.01	0.005	0.05	0.01	0.01	0.01	0.01	0.01	0.01	0.01
29	98.5	0.15	0.4	0.01	0.005	0.05	0.01	0.01	0.01	0.01	0.01	0.01	0.01
30	98.5	0.15	0.4	0.01	0.005	0.05	0.01	0.01	0.01	0.01	0.01	0.01	0.01
31	98.5	0.15	0.4	0.01	0.005	0.05	0.01	0.01	0.01	0.01	0.01	0.01	0.01
32	98.5	0.15	0.4	0.01	0.005	0.05	0.01	0.01	0.01	0.01	0.01	0.01	0.01
33	98.5	0.15	0.4	0.01	0.005	0.05	0.01	0.01	0.01	0.01	0.01	0.01	0.01
34	98.5	0.15	0.4	0.01	0.005	0.05	0.01	0.01	0.01	0.01	0.01	0.01	0.01
35	98.5	0.15	0.4	0.01	0.005	0.05	0.01	0.01	0.01	0.01	0.01	0.01	0.01
36	98.5	0.15	0.4	0.01	0.005	0.05	0.01	0.01	0.01	0.01	0.01	0.01	0.01
37	98.5	0.15	0.4	0.01	0.005	0.05	0.01	0.01	0.01	0.01	0.01	0.01	0.01
38	98.5	0.15	0.4	0.01	0.005	0.05	0.01	0.01	0.01	0.01	0.01	0.01	0.01
39	98.5	0.15	0.4	0.01	0.005	0.05	0.01	0.01	0.01	0.01	0.01	0.01	0.01
40	98.5	0.15	0.4	0.01	0.005	0.05	0.01	0.01	0.01	0.01	0.01	0.01	0.01
41	98.5	0.15	0.4	0.01	0.005	0.05	0.01	0.01	0.01	0.01	0.01	0.01	0.01
42	98.5	0.15	0.4	0.01	0.005	0.05	0.01	0.01	0.01	0.01	0.01	0.01	0.01
43	98.5	0.15	0.4	0.01	0.005	0.05	0.01	0.01	0.01	0.01	0.01	0.01	0.01
44	98.5	0.15	0.4	0.01	0.005	0.05	0.01	0.01	0.01	0.01	0.01	0.01	0.01
45	98.5	0.15	0.4	0.01	0.005	0.05	0.01	0.01	0.01	0.01	0.01	0.01	0.01
46	98.5	0.15	0.4	0.01	0.005	0.05	0.01	0.01	0.01	0.01	0.01	0.01	0.01
47	98.5	0.15	0.4	0.01	0.005	0.05	0.01	0.01	0.01	0.01	0.01	0.01	0.01
48	98.5	0.15	0.4	0.01	0.005	0.05	0.01	0.01	0.01	0.01	0.01	0.01	0.01
49	98.5	0.15	0.4	0.01	0.005	0.05	0.01	0.01	0.01	0.01	0.01	0.01	0.01
50	98.5	0.15	0.4	0.01	0.005	0.05	0.01	0.01	0.01	0.01	0.01	0.01	0.01

4.2 MECHANICAL PROPERTIES

The results obtained in this study for ultimate tensile strength (UTS), percent elongation (El) and brinell hardness (BHN) of the various scrap samples cast under different process conditions are presented in Tables 4.3 - 4.14. Those for P4, H4, H5, C4, and M4 are also presented in Figs 4.1-4.12. Several general observations can be discerned from the results presented in Tables 4.3 - 4.12. These are discussed below.

Table 4.3 As-cast mechanical properties of sand and permanent mould cast piston scrap samples-turbulently filled.

Scrap Sample	Green sand casting				Permanent mould casting			
	Code	UTS (MPa)	El (%)	BHN	Code	UTS (Mpa)	El (%)	BHN
P1	SP1a (R) ¹	--	--	65	PP1a	127	1.8	95
	SP1b	128	1.7	85	PP1b	123	1.5	90
	SP1c (R)	--	--	76	PP1c	160	2.3	90
	Average ²	128	1.7	75	Average	137	1.9	92
P2	SP2a	120	1.4	86	PP2a	146	2.0	95
	SP2b	160	2.2	90	PP2b	166	2.4	90
	SP2c (R)	--	--	--	PP2c	153	2.1	98
	Average	140	1.8	83	Average	155	2.2	94
P3	SP3a (R)	--	--	69	PP3a	138	2.0	95
	SP3b	117	1.2	82	PP3b	127	1.8	95
	SP3c	130	1.8	85	PP3c	200	3.2	90
	Average	123.5	1.5	79	Average	155	2.3	93

1. R represents rejected specimens due to macro-defects.

2. Rejected specimens are not used in computing the averages except for BHN

Table 4.4 As-cast and T6 mechanical properties of sand and permanent mould cast piston scrap sample (P4)-quiescently filled.

Condition	Distance from the gate (mm)	Green sand casting			Permanent mould casting		
		UTS (Mpa)	El (%)	BHN	UTS (Mpa)	El (%)	BHN
As-cast	5	169	2.4	86	196	3.3	99
	25	170	2.4	83	177	2.8	96
	45	167	2.2	83	165	2.4	96
	65	146	2.0	78	156	2.1	94
	85	149	2.0	75	135	1.9	88
	Average	160	2.2	81	166	2.5	95
T6	5	210	2.7	94	270	2.9	106
	25	201	2.4	88	251	2.6	104
	45	174	2.1	85	248	2.4	103
	65	156	2.2	84	243	2.0	104
	85	157	1.8	80	242	1.9	101
	Average	180	2.24	86	251	2.36	104

Table 4.5 As-cast mechanical properties of sand and permanent mould cast housing scrap samples-turbulently filled.

Scrap Sample	Green sand casting				Permanent mould casting			
	Code	UTS (MPa)	El (%)	BHN	Code	UTS (Mpa)	El (%)	BHN
H1	SH1a (R)	--	--	--	PH1a	165	2.2	90
	SH1b	136	2.0	76	PH1b	185	2.4	85
	SH1c (R)	--	--	80	PH1c	182	2.3	87
	Average	136	2.0	78	Average	177	2.3	87
H2	SH2a	118	1.5	69	PH2a	192	2.6	90
	SH2b (R)	--	--	62	PH2b	182	2.4	90
	SH2c	124	1.7	72	PH2c	164	2.1	90
	Average	121	1.6	68	Average	179	2.4	90
H3	SH3a	106	--	80	PH3a	173	2.3	88
	SH3b (R)	--	--	80	PH3b	157	2.1	90
	SH3c (R)	--	0.7	--	PH3c	179	2.4	87
	Average	106	0.7	80	Average	170	2.3	88

Table 4.6 As-cast and T6 mechanical properties of sand and permanent mould cast housing scrap sample (H4)-quiescently filled.

Condition	Distance from the gate (mm)	Green sand casting			Permanent mould casting		
		UTS (Mpa)	EI (%)	BHN	UTS (Mpa)	EI (%)	BHN
As-cast	5	162	2.5	81	203	2.9	90
	25	143	2.1	79	200	2.7	90
	45	136	1.9	74	184	2.3	89
	65	134	2.0	75	178	2.0	89
	85	130	2.0	74	168	2.2	87
	Average	141	2.1	77	187	2.42	89
T6	5	191	2.2	84	284	2.8	99
	25	191	2.1	81	273	2.5	95
	45	189	2.1	81	259	2.2	94
	65	189	1.8	80	240	2.0	94
	85	168	1.3	78	240	2.0	93
	Average	186	1.9	81	259	2.3	95

Table 4.7 As-cast and T6 mechanical properties of sand and permanent mould cast housing scrap sample (H5) -quiescently filled mould, but turbulently handled melt.

Condition	Distance from the gate (mm)	Green sand casting			Permanent mould casting		
		UTS (Mpa)	EI (%)	BHN	UTS (Mpa)	EI (%)	BHN
As-cast	5	122	1.6	76	171	2.4	89
	25	--	--	70	151	2.1	90
	45	105	0.9	69	148	2.0	90
	65	129	1.8	69	134	2.0	88
	85	135	2.0	68	R	-	87
	Average	123	1.6	70	151	2.1	89
T6	5	147	1.8	88	234	2.2	94
	25	142	1.8	86	222	2.0	94
	45	111	0.9	82	213	1.7	92
	65	--	--	--	186	1.5	89
	85	--	--	74	142	1.4	86
	Average	133	1.5	83	199	1.76	91

Table 4.8 As-cast mechanical properties of sand and permanent mould cast cylinder head scrap samples-turbulently filled

Scrap Sample	Green sand casting				Permanent mould casting			
	Code	UTS (MPa)	EI (%)	BHN	Code	UTS (Mpa)	EI (%)	BHN
C1	SC1a	136	1.7	62	PC1a	125	1.5	69
	SC1b	134	1.7	74	PC1b	170	2.0	76
	SC1c	119	1.4	64	PC1c	154	1.9	69
	Average	127	1.6	63	Average	150	1.8	71
C2	SC2a	120	1.5	69	PC2a	190	2.3	80
	SC2b (R)	--	--	72	PC2b	168	2.0	72
	SC2c (R)	--	--	76	PC2c (R)	--	--	76
	Average	120	1.5	72	Average	179	2.15	76
C3	SC3a	122	1.5	76	PC3a	133	1.7	80
	SC3b (R)	--	--	72	PC3b	137	1.8	76
	SC3c (R)	--	--	72	PC3c	145	1.9	80
	Average	122	1.5	73	Average	138	1.8	79

Table 4.9 As-cast and T6 mechanical properties of sand and permanent mould cast cylinder head scrap sample (C4)-quiescently filled.

Condition	Distance from the gate (mm)	Green sand casting			Permanent mould casting		
		UTS (Mpa)	EI (%)	BHN	UTS (Mpa)	EI (%)	BHN
As-cast	5	160	2.1	72	198	2.5	79
	25	145	1.8	68	185	2.1	81
	45	146	1.8	68	180	2.1	75
	65	140	1.7	64	169	1.9	74
	85	138	1.8	65	167	2.0	74
	Average	146	1.84	67	180	2.12	77
T6	5	188	2.0	81	280	2.4	92
	25	182	1.8	82	271	2.0	90
	45	181	1.7	79	246	2.0	85
	65	166	1.4	74	246	2.0	83
	85	149	1.4	76	205	1.5	83
	Average	173	1.66	78	250	1.98	87

Table 4.10 As-cast mechanical properties of sand and permanent mould cast miscellaneous scrap samples - turbulently filled.

Scrap Sample	Green sand casting				Permanent mould casting			
	Code	UTS (MPa)	EI (%)	BHN	Code	UTS (Mpa)	EI (%)	BHN
M1	SM1a	122	1.5	80	PM1a	167	2.5	85
	SM1b	105	0.8	78	PM1b	157	2.0	85
	SM1c	130	1.8	70	PM1c	167	2.4	87
	Average	119	1.4	76	Average	164	2.3	86
M2	SM2a (R)	--	--	76	PM2a	157	2.2	80
	SM2b (R)	--	--	76	PM2b	150	2.1	83
	SM2c (R)	--	--	76	PM2c	137	2.0	80
	Average	--	--	76	Average	148	2.1	81
M3	SM3a (R)	--	--	80	PM3a	172	2.5	87
	SM3b (R)	--	--	72	PM3b	169	2.4	87
	SM3c (R)	--	--	76	PM3c	159	2.3	90
	Average	--	--	76	Average	167	2.4	88

Table 4.11 As-cast and T6 mechanical properties of sand and permanent mould cast miscellaneous scrap sample (M4)-quiescently filled

Condition	Distance from the gate (mm)	Green sand casting			Permanent mould casting		
		UTS (Mpa)	EI (%)	BHN	UTS (Mpa)	EI (%)	BHN
As-cast	5	162	2.7	78	192	3.0	84
	25	152	2.1	78	192	2.8	82
	45	131	1.8	75	185	2.7	82
	65	128	1.4	74	166	2.4	80
	85	135	1.9	75	160	2.4	81
	Average	142	1.98	76	179	2.66	82
T6	5	186	2.7	87	245	2.8	90
	25	182	2.5	86	240	2.8	88
	45	139	1.8	80	233	2.7	86
	65	137	1.7	80	222	2.3	86
	85	144	1.9	81	221	2.0	84
	Average	159	2.12	83	232	2.52	87

Table 4.12 As-cast mechanical properties of sand and permanent mould cast blended scrap samples-turbulently filled.

Scrap Sample	Green sand casting				Permanent mould casting			
	Code	UTS (MPa)	EI (%)	BHN	Code	UTS (Mpa)	EI (%)	BHN
B1	SB1a	132	1.8	72	PB1a	102	0.8	85
	SB1b	96	0.7	75	PB1b	157	2.2	85
	SB1c (R)	--	--	76	PB1c (R)	--	--	88
	Average	114	1.25	74	Average	130	1.5	86
B2	SB2a	142	2.0	76	PB2a	172	2.3	80
	SB2b	145	2.1	76	PB2b	165	2.2	85
	SB2c (R)	--	--	80	PB2c	151	2.2	80
	Average	144	2.05	77	Average	163	2.2	82
B3	SB3a (R)	--	--	80	PB3a	182	2.3	88
	SB3b	140	1.9	70	PB3b	98	0.7	88
	SB3c (R)	--	--	75	PB3c (R)	--	--	86
	Average	140	1.9	75	Average	140	1.5	87
B4	SB4a	123	1.4	76	PB4a	147	2.1	85
	SB4b (R)	--	--	76	PB4b	144	2.0	85
	SB4c (R)	--	--	74	PB4c	159	2.2	82
	Average	123	1.4	75	Average	150	2.1	84
B5	SB5a (R)	--	--	78	PB5a	189	2.3	86
	SB5b	133	1.9	82	PB5b	164	2.2	84
	SB5c (R)	--	--	80	PB5c	159	2.1	88
	Average	133	1.9	80	Average	171	2.2	86

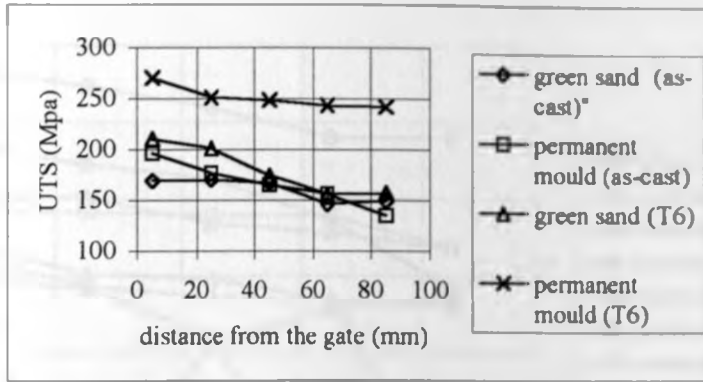


Fig 4.1 As-cast and T6 ultimate tensile strength of sand and permanent mould cast piston scrap sample P4-quiescently filled.

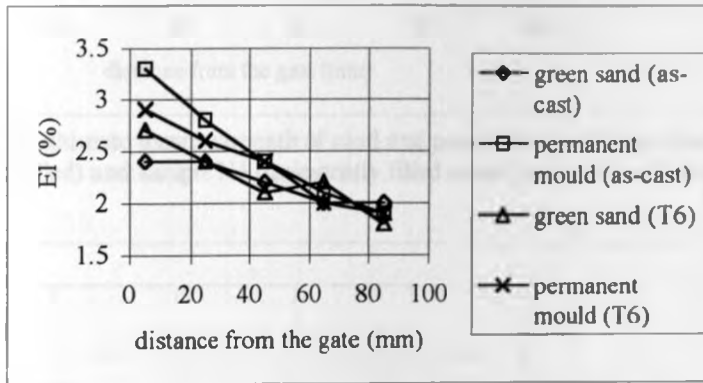


Fig 4.2 As-cast and T6 per cent elongation of sand and permanent mould cast piston scrap sample P4-quiescently filled.

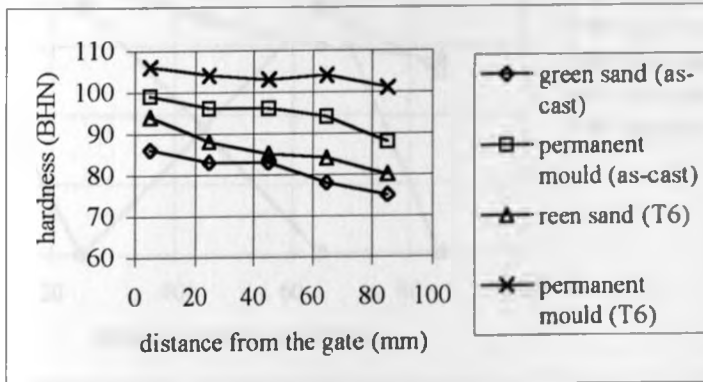


Fig 4.3 As-cast and T6 hardness of sand and permanent mould cast piston scrap sample P4-quiescently filled

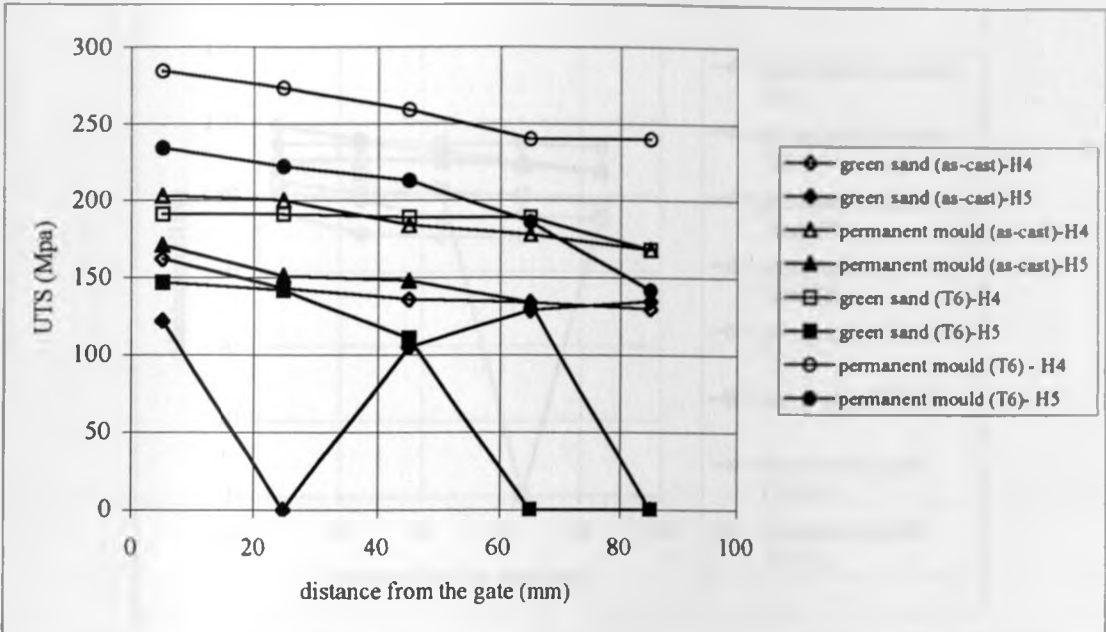


Fig 4.4 As-cast and T6 ultimate tensile strength of sand and permanent mould cast housing scrap sample H4 (quiescently filled) and sample H5 (quiescently filled mould, but turbulently handled melt).

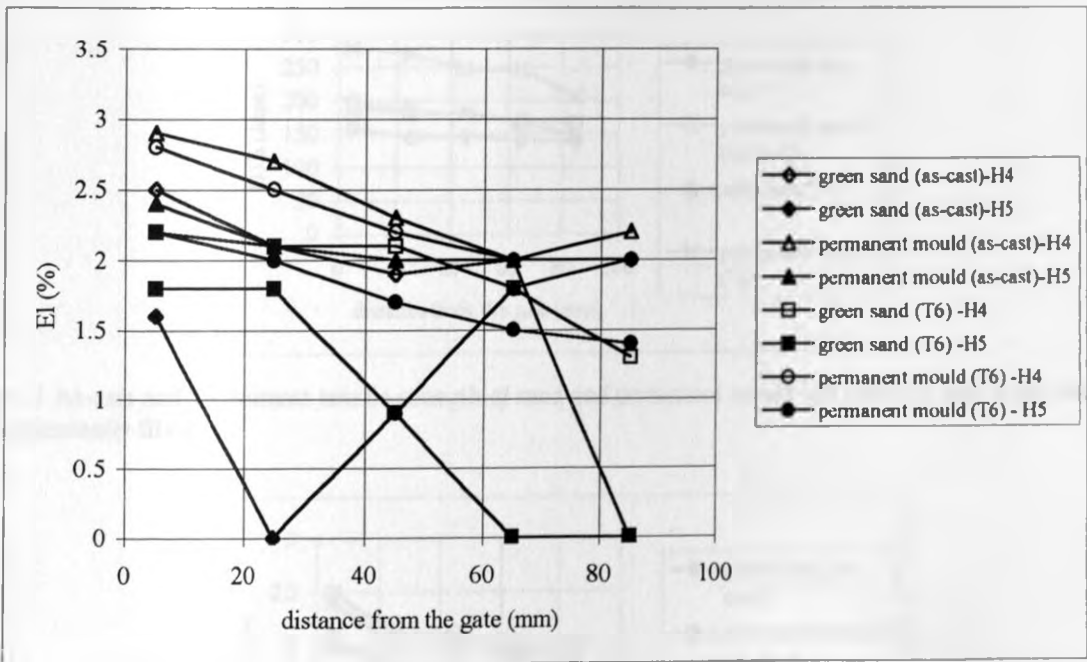


Fig 4.5 As-cast and T6 per cent elongation of sand and permanent mould cast housing scrap sample H4 (quiescently filled) and sample H5 (quiescently filled mould, but turbulently handled melt).

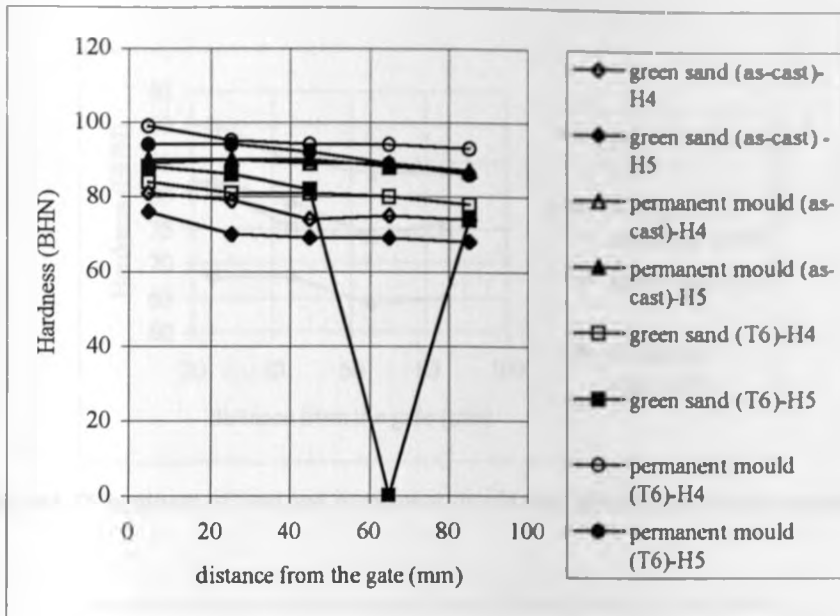


Fig 4.6 As-cast and T6 hardness of sand and permanent mould cast housing scrap sample H4 (quiescently filled) and sample H5 (quiescently filled mould, but turbulently handled melt).

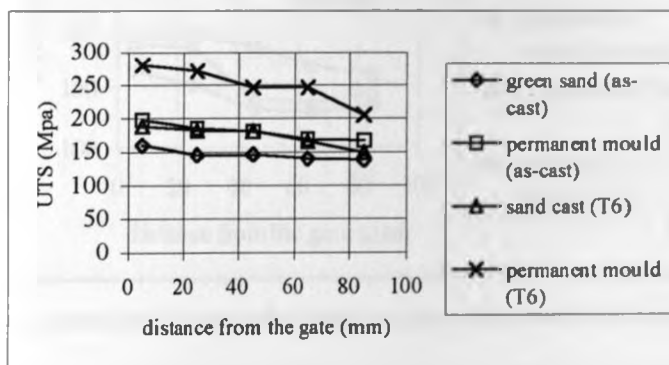


Fig 4.7 As-cast and T6 ultimate tensile strength of sand and permanent mould cast cylinder head scrap sample C4-quiescently filled.

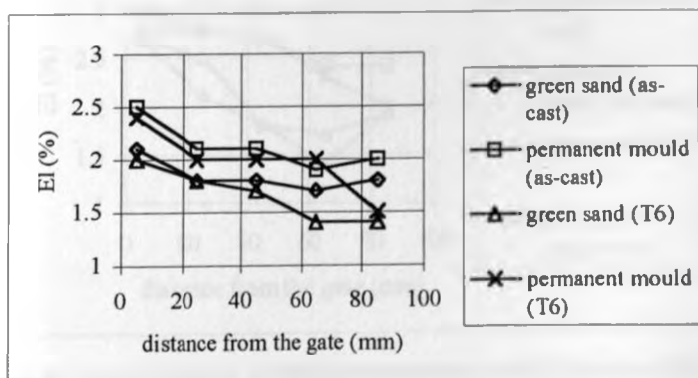


Fig 4.8 As-cast and T6 per cent elongation of sand and permanent mould cast cylinder head scrap sample C4)-quiescently filled.

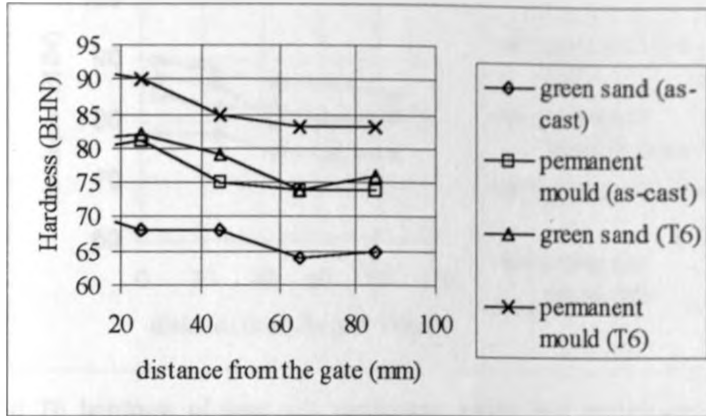


Fig 4.9 As-cast and T6 hardness of sand and permanent mould cast cylinder head scrap sample C4-quietly filled.

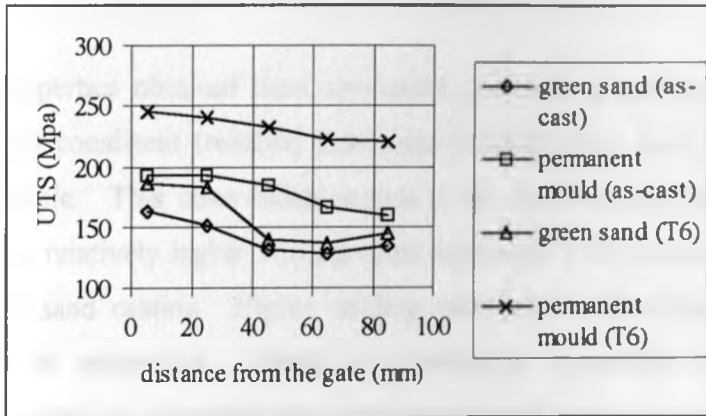


Fig 4.10 As-cast and T6 ultimate tensile strength of sand and permanent mould cast miscellaneous scrap sample M4-quietly filled

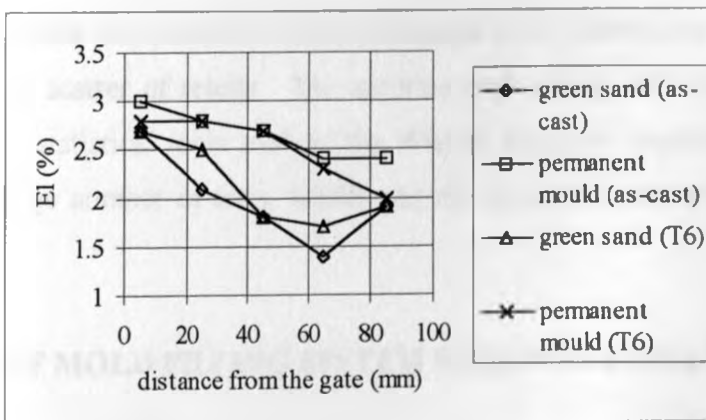


Fig 4.11 As-cast and T6 per cent elongation of sand and permanent mould cast miscellaneous scrap sample M4-quietly filled

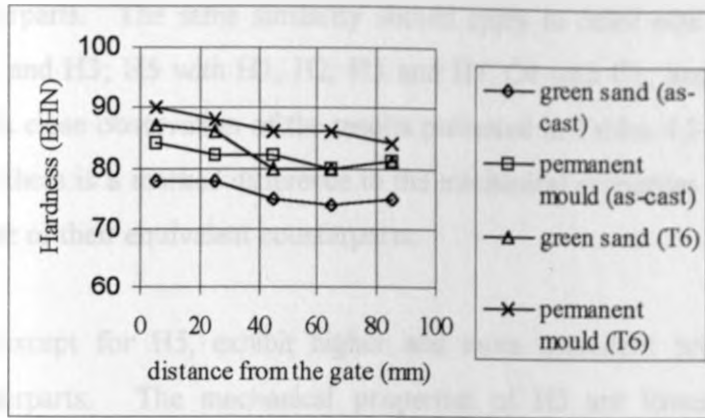


Fig 4.12 As-cast and T6 hardness of sand and permanent mould cast miscellaneous scrap sample M4- quiescently filled

4.2.1 EFFECT OF TYPE OF CASTING PROCESS

The mechanical properties obtained from specimens produced by permanent mould casting are higher and fairly consistent (reliable) than those obtained from sand cast specimens for the same scrap sample. This observation applies to all scrap samples tested. This can be attributed mainly to relatively higher cooling rates associated with permanent mould casting compared to green sand casting. Higher cooling rates lead to decreased SDAS and thus improved mechanical properties. Based on mechanical properties obtained for scrap samples, it is reasonable to conclude that permanent mould casting should be preferred to green sand casting.

Conclusions on whether the observed results are consistent or reliable are at best conjecture that is based on the scatter of results. The accurate methodology of determining reliability would be by using statistical tools such as the Weibull statistical function. However, this would require a large number of tests, which was not possible in this study due to limited finances.

4.2.2 EFFECT OF MOLD FILLING SYSTEM DESIGN AND MELT HANDLING

Based on the fact that sample P4 is approximately equivalent to P1 and P2 (Table 4.2), it would be reasonable to assume that its mechanical properties should be fairly similar to its

equivalent counterparts. The same similarity should apply to other equivalent alloys (e.g., H4 with H1, H2 and H3; H5 with H1, H2, H3 and H4; C4 with C1; and M4 with M1 and M2). However, a close observation of the results presented in Tables 4.3-4.11 and Figs 4.1-4.12 reveals that there is a marked difference in the mechanical properties of P4, H4, H5, C4 and M4 with those of their equivalent counterparts.

These samples, except for H5, exhibit higher and more consistent properties than their equivalent counterparts. The mechanical properties of H5 are lower and inconsistent compared to those of H4 (Figs 4.4-4.6). They are, however, almost equivalent to those of H1, H2 and H3. Samples P4, H4, H5, C4 and M4 were cast using quiescent bottom filled moulds while their equivalent counterparts were cast using turbulent top filled moulds. The higher mechanical properties obtained for H4, C4 and M4 may, therefore, be attributed to the quiescent filling conditions in line with previous reports [128]. For H5, quiescent filling was of no use since the melt handling process prior to pouring was turbulent. It was just as good as pouring into a turbulent top filled system.

4.2.3 VARIATION OF MECHANICAL PROPERTIES WITH CASTING LOCATION

The as-cast and T6 mechanical properties of P4, H4, H5, C4 and M4 given in tables 4.4, 4.6, 4.7, 4.9 and 4.11, respectively and Figs 4.1-4.12 are observed to vary with casting location. It can be discerned from these tables and figures that the UTS, EI and BHN of the scrap samples are higher towards the ingate end of the casting and lower towards the riser end of the casting. The mould design used to make these castings was such that solidification is likely to progress from the ingate end toward the riser end of the casting. The material near the riser is likely to be the last to solidify.

The data clearly shows that the UTS, EI and BHN decreases substantially along the solidification path. This may be attributed to a possible increase in SDAS. Seniw et al [153] also observed a similar trend in UTS and fatigue lifetimes of A356 castings. They attributed the trend to an increase in the amount of aluminium-silicon eutectic and the density of micro-

pores along the solidification path. It is common knowledge that finely spaced SDAS not only reduce the size of interdendritic microconstituents but also promote their uniform distribution. These microconstituents include micropores, eutectic silicon particles, intermetallic compounds and other non-metallic inclusions. This in turn improves mechanical properties. The reverse is true for larger SDAS.

4.2.4 EFFECT OF MOULD THICKNESS AND PREHEAT

Table 4.13 shows the variation of UTS, EI and BHN with mould thickness and preheat. Some of these results are presented graphically in Figs 4.13 - 4.15. It is clearly evident from this data that the UTS, EI and BHN generally improve with increasing mould thickness from 15 to 35 mm at intervals of 5 mm. These properties, however, deteriorate with increasing mould preheat. There is a slight departure from these general trends for both EI and BHN as shown in Figs 4.3 and 4.4 respectively, especially for the specimens cast in moulds of 20 mm thickness. For example, the EI at 350°C mould preheat decreases from 2.4% for a mould thickness of 35 mm to 2.2% at 30 mm mould thickness and remains constant through 25 and 20 mm thickness after which it drops to 2.0% at 15 mm thickness. This deviation may be associated to the scatter in properties normally experienced in castings, especially since the recorded values are averages of three specimen tests. This is a statistically small sample and the average values obtained may not represent the true average if a statistically larger number of samples were tested. With a large number of test samples (say above 30), it is likely that the trend will be clearer.

The increase in UTS, BHN and EI with mould thickness can be attributed to decreased SDAS and decreased grain size. SDAS has a significant influence on both UTS and EI, while grain size significantly affects hardness. SDAS may, however, also have subtle effects on hardness as well. In the current study, there is evidence of microstructural refinement as shown in Table 4.14. Both SDAS and grain size were observed to decrease with increase in the mould thickness. This is expected if the mould is assumed to act as a chill. The ability of the mould to absorb heat is determined by its heat diffusivity (a mould material constant, which is $2.194 \times 10^8 \text{ W}^2\text{M}^{-4}\text{SK}^{-2}$ for mild steel at 625°C [154]), defined as $\rho C_p K$, where ρ is the mould

material density; C_o , its specific heat; and K , its thermal conductivity. However, the amount of heat that can actually be absorbed by the mould before it is saturated with heat is determined by the volumetric heat capacity (VHC_o) of the mould, defined as $\rho C_o V$, where V is the volume of the mould, which is determined by the mould thickness when other dimensions are constant.

Table 4.13 Effect of mould thickness and preheat on mechanical properties.

Mould wall thickness (mm)	MOULD PREHEAT								
	Ambient (25°C)			200°C			350°C		
	UTS (MPa)	EI (%)	BHN	UTS (Mpa)	EI (%)	BHN	UTS (MPa)	EI (%)	BHN
35	240	4.9	90	209	2.8	86	192	2.4	86
30	230	3.5	90	196	2.6	85	177	2.2	85
25	212	2.9	87	183	2.3	82	168	2.2	83
20	191	2.3	86	174	2.3	83	167	2.2	83
15	189	2.3	87	164	2.2	82	159	2.0	81

Table 4.14 Effect of mould thickness and preheat on SDAS and grain size*.

Mould wall thickness (mm)	MOULD PREHEAT					
	Ambient (25°C)		200°C		350°C	
	SDAS (µm)	Grain size (µm)	SDAS (µm)	Grain size (µm)	SDAS (µm)	Grain size (µm)
35	17	180	--	--	20	220
30	--	--	--	--	--	--
25	19	200	--	--	23	300
20	22	280	26	350	--	--
15	--	--	--	--	--	--

* Only selected samples were analysed to determine trends

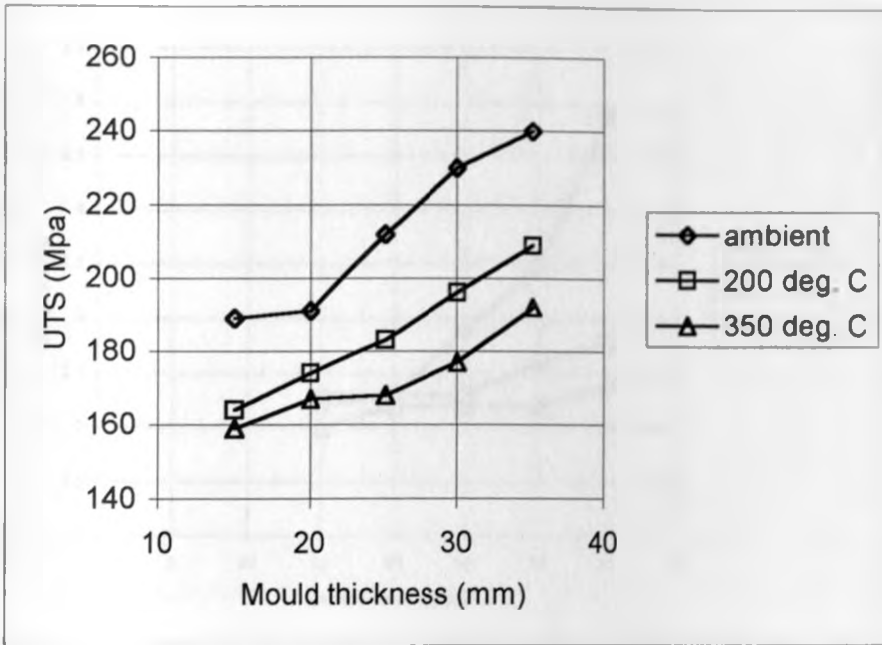


Fig 4.13 Effect of mould thickness and initial mould temperature on ultimate tensile strength.

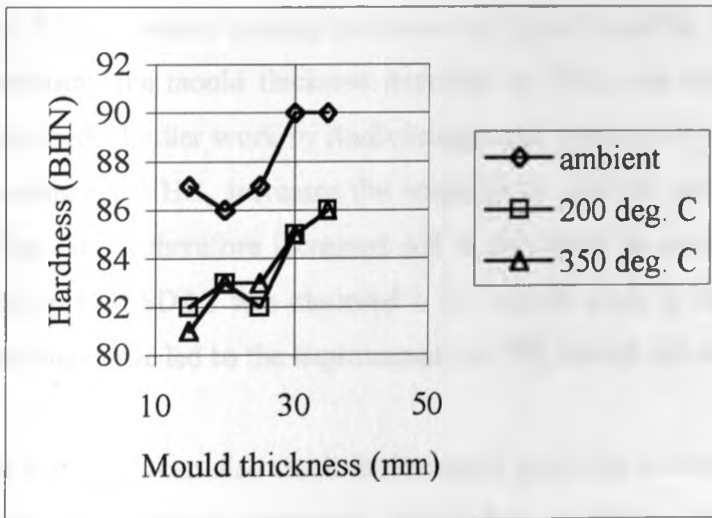


Fig 4.14 Effect of mould thickness and initial mould temperature on hardness.

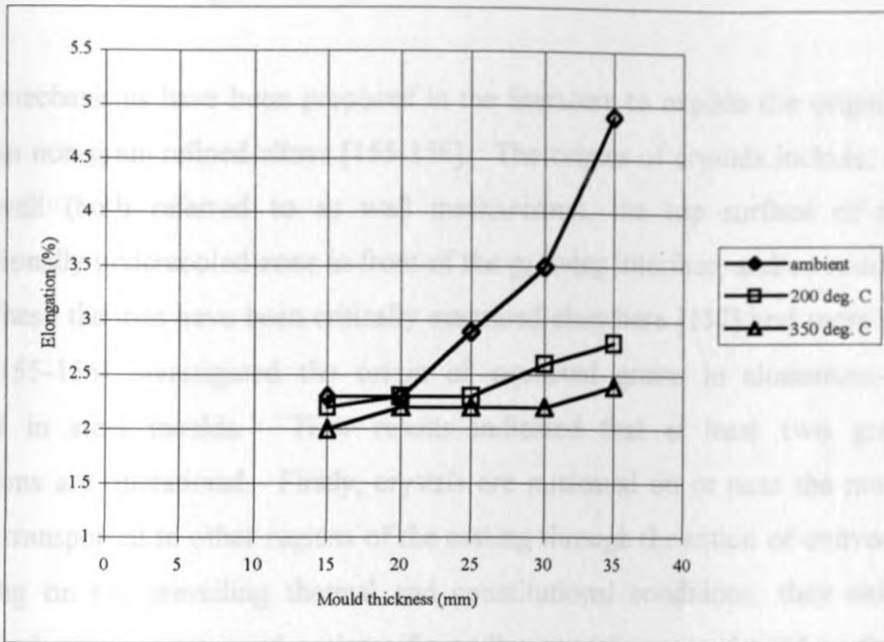


Fig 4.15 Effect of mould thickness and initial mould temperature on percent elongation

Therefore, for a constant casting thickness and mould material, as was the case in current study, increasing the mould thickness increases its VHC_0 and thus the amount of heat that can be absorbed. Earlier work by Radhakrishna and Seshan [147] and Campbell [6] reported that increasing the VHC_0 increases the temperature gradient and lowers solidification time. The cooling rate is therefore increased and is thus likely to result in smaller grain size and SDAS. Decreased SDAS was observed in the current study as has already been mentioned. This in turn may have led to the improvement in UTS, and EI and some extent BHN.

Increasing the VHC_0 can also result in decreased grain size as observed in the current study, which also may lead to improved mechanical properties, particularly hardness. To understand the effect of VHC_0 on grain size, it is necessary to briefly revisit the concept of grain nucleation. In general, there are two factors that influence and control the formation of grains in a solidifying casting. Firstly, suitable substrates that act as sites for heterogeneous nucleation of grains have to be present in sufficient amounts. Secondly, there has to be sufficient undercooling to facilitate the survival and growth of the nuclei. This may be achieved either by rapid cooling generating bulk undercooling or by partition of solute during solidification to generate constitutional undercooling. Both of these criteria have to be

fulfilled to obtain a small grain size [155].

Several mechanisms have been proposed in the literature to explain the origins of equiaxed crystals in non-grain refined alloys [155-156]. The origins of crystals include; at or near the mould wall (both referred to as wall mechanisms), the top surface of the melt, the constitutionally undercooled zone in front of the growing interface, and/or re-melted dendrite arms. These theories have been critically examined elsewhere [157] and more recently, Hutt et al. [155-156] investigated the origin of equiaxed grains in aluminium-silicon alloys solidified in steel moulds. Their results indicated that at least two grain formation mechanisms are operational. Firstly, crystals are nucleated on or near the mould walls and are then transported to other regions of the casting through the action of convective currents. Depending on the prevailing thermal and constitutional conditions, they either remelt or survive and grow as equiaxed grains. Secondly, crystals are nucleated in the bulk of the melt, probably by the constitutional undercooling mechanisms. Recent work on grain refined pure aluminium by Easton and StJohn [158] gave similar results. They asserted that wall mechanisms are a significant contributor to the small grain size, especially when a grain refiner is added in aluminium castings.

A higher VHC_o increases the ability of the mould to absorb heat rapidly from the melt, thus increasing the solidification rate. The rapid solidification rate generates a high undercooling near the mould walls resulting in increased nucleation events. It also increases the cooling rate of the bulk melt, which increases the survival and growth rate of the wall crystals by generating the required bulk undercooling.

The effect of mould thickness on the cooling rate can be controlled by cooling the mould during solidification, for instance by having cooling channels machined into the metal mould, which are carefully positioned so as to remove the right amount of heat from the mould. Thus, a smaller thickness of the mould can be used without appreciably decreasing the cooling rate. However, care should be exercised to avoid a mould thickness that is too small as it would be less resistant to thermal fatigue failure and loss of dimensional stability. It can be inferred from the results and the foregoing discussion that the improvement of mechanical

properties with increasing mould thickness for a given size of casting is also limited to the point where the mould wall is considered infinite and thus acts as an infinite heat sink. In this case, the volumetric heat capacity of the mould ceases to be significant. Metal moulds should therefore be designed to have this infinite thickness while considering the unavoidable preheating of the moulds in continuous high production runs and the cooling effect of the cooling medium (usually running water) in channels usually machined into the moulds. Any extra thickness may be considered for purposes of longer mould life. A chill is, however, designed to extract a smaller amount of heat from a particular location of the casting and its thickness, therefore, affects the mechanical properties of the casting.

The effect of mould preheat on mechanical properties may also be attributed to its perceived influence the nucleation and growth mechanisms during solidification. Hutt et al. [155-156] reported that the grain size increases with increased mould preheat. This is in line with the current observations (Table 4.14). The increase in grain size may be due to a reduction in the imposed temperature gradient, which results in a reduction in the degree of thermal undercooling near the mold wall. This means that fewer crystals are nucleated from the walls or near the walls thus leading to larger grain sizes. At low mould preheat temperatures, the wall mechanisms are dominant and generate more grains which result in reduced grain size.

However, if the bulk volume of the melt increases, the relative proportion of wall crystals decreases due to a decrease in the ratio of the mould surface area to the volume of the melt. This has a similar effect as increasing the mould preheat. It is therefore expected that increasing casting section thickness while holding other parameters constant will increase the grain size. Higher melt superheat (as will be discussed later) would also reduce the number of crystals nucleated on or near the wall, and increase the likelihood of crystals remelting when carried into the bulk liquid. This yields larger grain sizes [6, 156]. Different mould materials and coatings are expected to influence the number of crystals generated by the wall mechanisms. A higher degree of convection and turbulence in the melt can also lead to an increased number of equiaxed grains and thus reduced grain size [6, 156-157].

It therefore seems that if the thermal conditions are such that the likelihood of wall crystal survival is diminished, the constitutional undercooling mechanisms dominate and the grain size is determined by the nucleant potency, the solute concentration and temperature gradient in the liquid. Increased grain sizes result in reduced hardness as depicted by the Hall-Petch relation [6].

Increasing the mould preheat also results in larger SDAS, as shown in Table 4.14, due to the reduced cooling rates. Therefore decreased UTS, BHN and EI with mould preheat may be attributed to the increased SDAS and grain size.

Similar observations of decreased UTS and EI with increased mould preheat were observed by Siaminwe and Clegg [132] for investment castings of Al-Si-Mg alloy. It is, however, reported elsewhere [123] that preheating the mould yields castings with mechanical properties better than those poured in moulds held at ambient temperature. One explanation might be that increased time is available for interdendritic feeding in preheated metallic moulds. On the other hand, it should as well be borne in mind that increased preheat increases the length of the mushy zone which reduces feeding efficiency. Adequate risering ameliorates the feeding inadequacies.

4.2.5 EFFECT OF POURING TEMPERATURE

Table 4.15 shows the variation of UTS, EI and BHN with pouring temperature. This data is presented graphically in Figs 4.16 - 4.18. The data shows that UTS, EI and BHN decrease for both sand cast and permanent mould cast specimens as the pouring temperature is increased from 750°C to 900°C at intervals of 50°C. Table 4.15 also gives variations in density values of sand casting with pouring temperature. The results show a decreasing trend in density with increasing pouring temperature. This indicates that the volume fraction of porosity increased with pouring temperature.

In the current study, increasing the pouring temperature or the melt superheat resulted in a decrease in UTS, BHN and EI for both green sand and permanent mould castings. This trend

is associated with the effects of melt superheat on temperature gradient, solidification time and nucleation [6, 154-156]. Increasing superheat puts more heat energy into the same casting volume and thus more heat has to be extracted by the mould. This leads to decreased cooling rate (i.e. increased solidification time) as reported by Venkataramani et al. [154]. The decreased cooling rate results increased grain size and SDAS as shown in Table 4.16. The increased grain size and SDAS thus resulted in decreased UTS, BHN, and El. Furthermore, increased pouring temperature has been reported to decrease the maximum number of sites available for nucleation, which is attributed to enhanced diffusion of nucleants at higher temperatures, resulting in coalescence of sites [154]. This in turn leads to increased grain size as fewer equiaxed grains are nucleated. Pouring temperature also affects the nucleation and survival of equiaxed crystals from or near the walls as discussed earlier.

Table 4.15. Effect of pouring temperature on Mechanical properties.

Pouring temp. (°C)	Green sand casting				Permanent mould casting		
	UTS (Mpa)	El (%)	BHN	Density (Kg/m ³)	UTS (Mpa)	El (%)	BHN
900	119	1.8	67	2530	159	2.1	82
850	149	2.0	71	2540	165	2.2	85
800	153	2.2	75	2570	189	2.4	87
750	157	2.5	76	2600	200	2.8	89

Table 4.16 Effect of pouring temperature on SDAS and grain size.

Pouring temp. (°C)	Green sand casting	
	SDAS (µm)	Grain size (µm)
900	52	1050
850	49	920
800	45	800
750	42	705

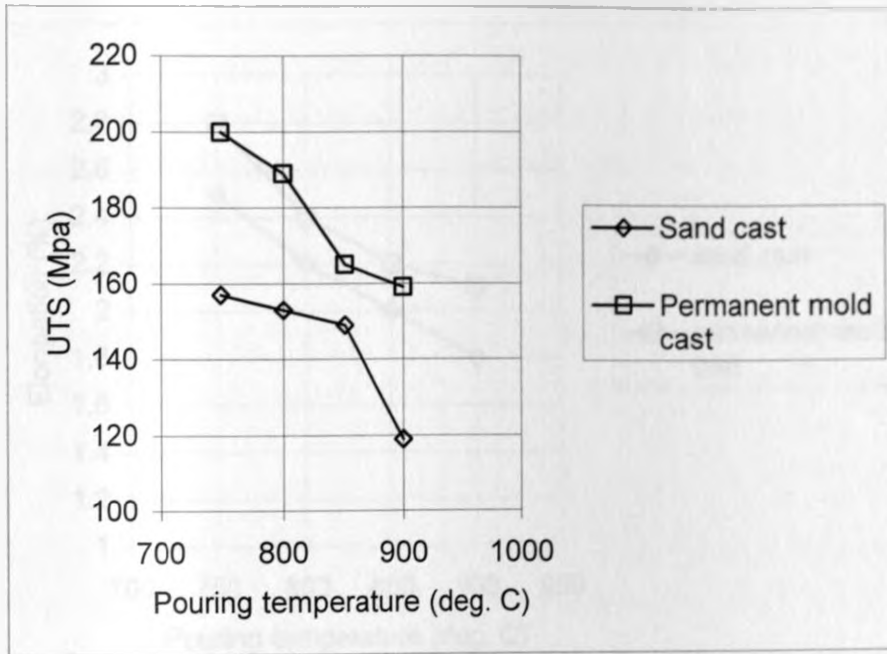


Fig 4.16 Effect of pouring temperature on ultimate tensile strength.

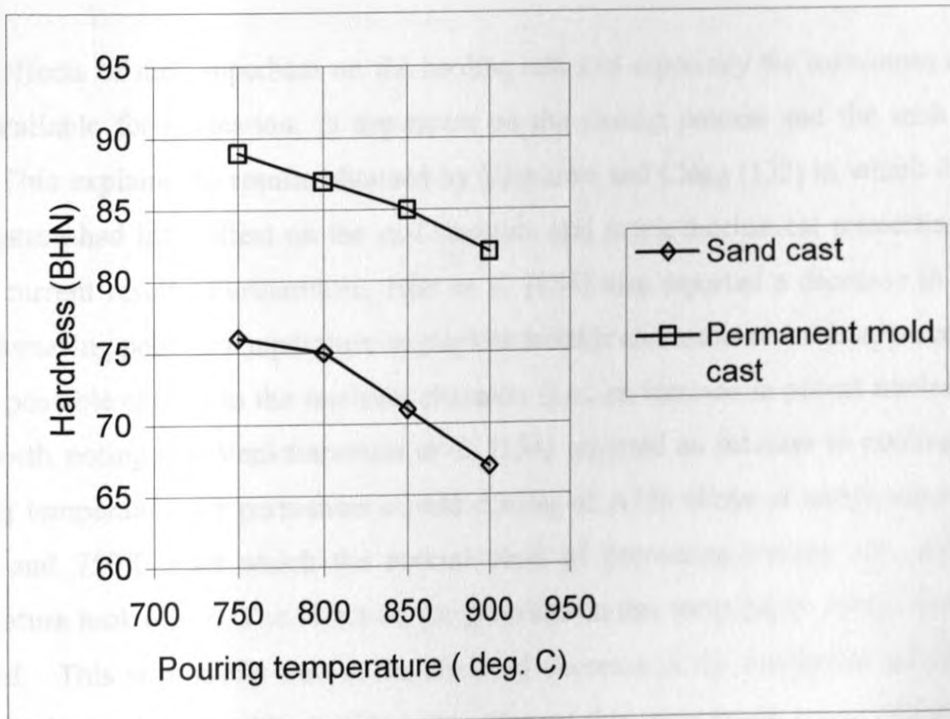


Fig 4.17 Effect of pouring temperature on hardness.

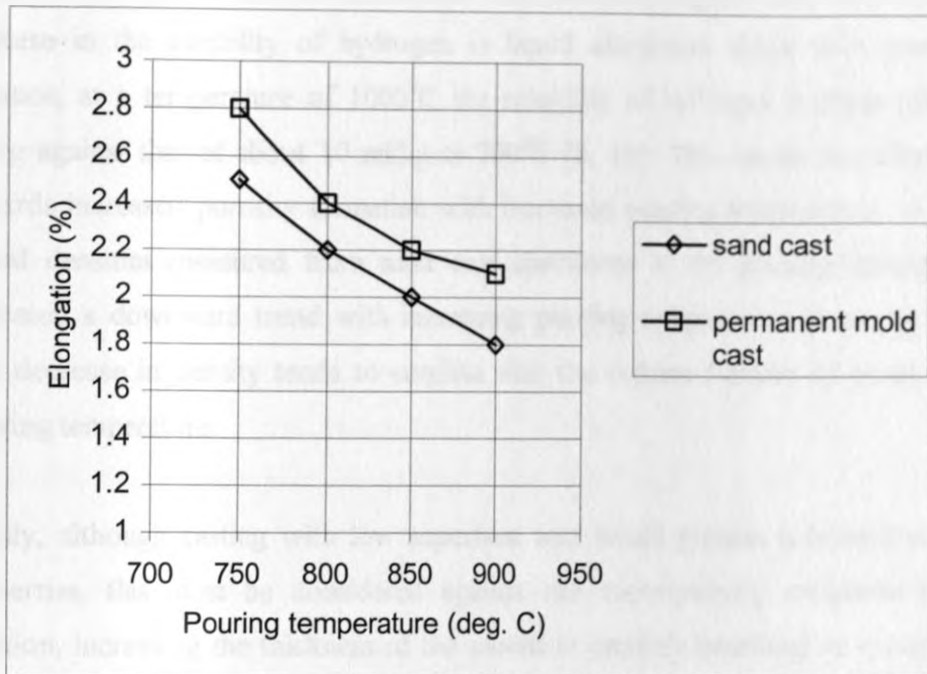


Fig 4.18 Effect of pouring temperature on percent elongation

These effects of melt superheat on the cooling rate and especially the maximum number of sites available for nucleation, is dependent on the casting process and the melt treatment [154]. This explains the results obtained by Siaminwe and Clegg [132] in which the pouring temperature had little effect on the cast structure and hence mechanical properties, contrary to the current results. Furthermore, Hutt et al. [156] also reported a decrease in grain size with increasing pouring temperature in graphite moulds and associated this apparent anomaly with a possible change in the nucleant character (i.e., an increase in potent nucleants). It is also worth noting that Venkataramani et al. [154] reported an increase in cooling rate with pouring temperature for permanent mould casting of A356 alloys at temperatures between 700°C and 750°C after which the normal trend of decreasing cooling rate with pouring temperature took effect. The effect on the grain size at this temperature range was, however, minimal. This is probably due to the observed decrease in the maximum number of sites available for nucleation with pouring temperature at this temperature range, which cancelled the effect of increased cooling rate.

Another explanation as to the decrease in UTS, BHN and EI with increased pouring

temperature, apart from that associated with SDAS and grain size, may be related to the increase in the solubility of hydrogen in liquid aluminium alloys with temperature. For instance, at a temperature of 1000°C the solubility of hydrogen in these alloys is over 40 ml/kg against that of about 10 ml/kg at 700°C [6, 13]. This means that there is a tendency towards increased porosity formation with increased pouring temperature. A comparison of actual densities measured from sand cast specimens at the pouring temperatures studied indicated a downward trend with increasing pouring temperature as shown in Table 4.15. The decrease in density tends to confirm that the volume fraction of pores increased with pouring temperature

Finally, although casting with low superheat and mould preheat is beneficial to mechanical properties, this must be considered against the accompanying reduction in fluidity. In addition, increasing the thickness of the mould is certainly beneficial as it not only improves mechanical properties, but also gives a longer mould operating life. This should, however, be considered against the added cost.

4.2.6 EFFECT OF HEAT TREATMENT

From the results presented in Tables 4.4, 4.6, 4.7, 4.9 and 4.11 and Figs 4.1-4.12, it is evident that heat treatment to the T6 condition resulted in higher UTS and BHN compared to the as-cast properties of the castings tested. The El of the T6 treated castings is, however, generally lower than that of the castings, which were tested in the as-cast condition.

Subjecting the same alloy to different heat treatment parameters results in different mechanical properties. There is not much flexibility on the variation of the solutionizing time and temperature. The aim is normally to use the highest possible temperature allowable without causing incipient melting of the alloy's second phases, and the shortest time possible to saturate the solid solution with as much solute as possible and, perhaps, modify or dissolve certain second phase particles (e.g. eutectic silicon or iron-rich intermetallic particles to make them less deleterious to mechanical properties). The ageing treatment provides enormous flexibility as a wide range of mechanical properties can be obtained by simply subjecting the

same alloy to different ageing parameters (e.g., pre-ageing, underageing, peak-ageing or over-ageing).

The variation of mechanical properties with heat treatment parameters was not investigated in this study. The parameters chosen for the study were, somewhat, arbitrary. The highest temperature possible for solution heat treatment of most aluminium-silicon based alloys (around 540°C) was used in this study while entertaining the danger of possible incipient melting as observed in previous studies [42]. This temperature, however, did result in incipient melting of some second phases (presumably copper-containing phases) as will be discussed later. This may explain why the improvement in UTS and BHN after heat treatment was not as dramatic as would have been expected. The ageing time and temperature used in this study are the average parameters usually used for cast aluminium-silicon based alloys to give peak-ageing (T6). Investigations on the effect of lower solution temperatures and different solution times, ageing times and ageing temperatures on the mechanical properties of these experimental alloys is highly encouraged. Investigations on the possible use of a two-stage solution heat treatment on these alloys is particularly encouraged.

4.2.7 CORRELATION WITH THE CHEMICAL COMPOSITION

The percentage contribution of various alloying elements to mechanical properties of aluminium-silicon-copper (magnesium) based alloys have been established by Wang et al [159] using analysis of variance. The percentages obtained by these authors have been used in this study (Tables 4.17 - 4.18) to determine how the UTS and El is likely to vary with changes in chemical composition from sample to sample. The percentages have been multiplied by their respective element contents in each sample and the products summed. The sums are assumed to be the total weighted contribution of the elements in the samples for the respective mechanical properties. The sums of the various samples are then compared. The sample with the highest value is expected to yield the highest values of UTS or El, whatever the case may be. The elements whose percentage contributions are not known have been left out in the computations assuming that their effect is insignificant.

Similar percentage contributions of elements to BHN are not available, and thus computations for only UTS and EI have been done.

Wang et al [159] established that increasing the silicon content from 7 to 13 wt% decreases the UTS of the aluminium-silicon-copper (magnesium) die casting alloys they studied. The authors, however, pointed out that the difference between these levels was quite large. The predicted decrease in UTS with increasing silicon content may, therefore, not be a steady one, and there is a possibility of an initial increase in tensile strength, followed by a decrease. Since the silicon content in the scrap samples range between about 5 to 9 wt%, it is assumed that increasing its content within this range increases the UTS. Previous reports [34] actually indicate that there is a continuous increase in the UTS of aluminium-silicon alloys with increasing silicon. The percentage contribution of silicon established by Wang et al [159] has, therefore, been used in this study as a positive contribution to UTS. This is, however, an approximation that would require verification through further investigations. As a matter of fact, all these percentage contributions are approximations for the current investigation because the casting parameters used by Wang et al and in the current study are totally different. They are, however, a useful guideline as their use in this study is for comparison only.

Table 4.17 predicts that H4, B3, H5, B2, H1, H3 and M1 are supposed to have the highest values of UTS in decreasing order based on the respective decreasing trend in the total weighted elemental contributions to UTS. They are then supposed to be followed by H2, P3, P4, P2, C2, C3 and B1 with intermediate values of UTS, also in decreasing order. Finally, M4, B5, B4, M2, P1, M3, C1 and C4 are predicted to have the lowest UTS compared to other samples also in decreasing order. The actual UTS values of these samples in Table 4.17, however, show no such trends. Samples H4, C4, H2M4C2, H1, B5, H3 are shown to have the highest UTS in decreasing order (the samples with codes not separated by commas, e.g., H2M4C2, have the same UTS or EI, whatever the case may be). These are followed by M3, P4, M1, B2, H5 and C1B4, which have intermediate values of UTS in decreasing order. Samples M2, B3, C3, P1 and B1 have the lowest UTS in also in decreasing order.

Table 4.18 also predicts that C1, M3, C4, C3, C2, B1, P3 and M1 are supposed to have the highest EI in decreasing order based on the respective decreasing trend in the total weighted elemental contributions to EI. These should then be followed by B4, M2, M4, B5, H2, H1 and B3 also in decreasing order, and finally H3, P1, B2, P4, H4, P2 and H5 should have the lowest EI in that order. Table 4.19, however, indicates that M4, P4 and M3H4H2 have the highest EI. They are then followed by P3H1H3M1, B5B2P2C2 and H5C4M2B4, which have intermediate EI in decreasing order. Finally, P1, C1C2 and B1B3 have the lowest EI in that order.

It is evident that the predicted superiority of certain samples over others in terms of their UTS or EI, as the case may be, are not validated by the actual values obtained in this study. This could be due to two reasons: Firstly, processing conditions have enormous effect on the resulting mechanical properties and when those conditions are not closely controlled, a particular alloy can result in a wide range of mechanical properties. Castings with defects (whether porosity or oxides) complicates the problem as they are extremely unreliable in terms of their failure probability. The process conditions in this study were not closely controlled because it was felt that doing so would not properly simulate what is done in most Kenyan foundry shops. Most foundry shops in the country do not have the necessary foundry facilities to closely control the processing conditions during casting. Secondly, it is possible that the percentage contributions used are not compatible with the alloys and process conditions for this study. It is, therefore, expected that under closely controlled and optimum processing conditions, the UTS and EI of the samples should match the predicted ranking. If not, then a similar study such as that by Wang et al should be done to evaluate the percentage contributions of the various elements in these alloys under closely controlled sand and permanent mould casting conditions.

Table 4.17 Weighted contributions of elements to Tensile Strength of the samples.

Co de	Cu 32.93 ¹	Si 11.64	Mg 12.08	Mn 0.35	Ni -1.99	Zn 2.59	Cr 5.40	Fe+M n+Cr -0.53	Fe+ Mn -2.45	Ti 1.59	Total
P1	52.919	91.735	5.702	0.029	-3.648	0.285	0.086	-0.53	-2.411	0.161	144.328
P2	67.572	99.673	8.456	0.026	-3.449	0.215	0.113	-0.374	-1.676	0.097	170.653
P3	100.50	71.867	1.703	0.083	-0.555	3.623	0.140	-0.496	-2.230	0.064	174.641
P4	75.970	93.376	10.16	0.090	-3.435	0.256	0.124	-0.594	-2.688	0.083	173.341
H1	108.60	83.133	1.015	0.048	-0.273	2.958	0.173	-0.524	-2.324	0.080	192.871
H2	99.580	82.493	0.773	0.067	-0.201	1.704	0.167	-0.568	-2.548	0.067	181.534
H3	105.64	84.704	0.664	0.075	-0.293	2.222	0.173	-0.586	-2.631	0.092	190.119
H4	114.86	94.575	0.834	0.091	-0.291	1.940	0.243	-0.639	-2.844	0.068	208.837
H5	101.16	98.311	0.701	0.082	-0.223	1.756	0.157	-0.616	-2.778	0.068	198.619
C1	57.199	67.722	0.773	0.072	-0.117	0.440	0.027	-0.315	-1.443	0.025	124.383
C2	96.518	68.187	0.713	0.087	-0.080	0.471	0.049	-0.409	-1.867	0.100	163.769
C3	101.69	63.554	0.459	0.100	-0.088	0.707	0.065	-0.534	-2.440	0.089	163.6
C4	40.043	70.480	0.942	0.097	-0.034	0.404	0.043	-0.379	-1.732	0.072	109.936
M1	106.47	78.512	1.522	0.071	-0.464	3.414	0.097	-0.494	-2.242	0.068	186.957
M2	67.111	83.133	1.776	0.077	-0.577	1.593	0.092	-0.504	-2.288	0.086	150.499
M3	62.567	65.405	1.582	0.083	-0.257	3.116	0.140	-0.494	-2.222	0.099	130.019
M4	77.287	85.426	2.223	0.066	-1.170	1.230	0.103	-0.588	-2.666	0.076	161.987
B1	93.883	70.410	1.063	0.087	-0.601	0.531	0.059	-0.492	-2.249	0.091	162.782
B2	106.76	91.432	1.075	0.083	-0.446	1.409	0.151	-0.617	-2.786	0.142	197.202
B3	124.61	81.259	0.556	0.114	-0.159	1.476	0.130	-0.663	-3.004	0.118	204.434
B4	86.112	76.754	0.556	0.074	-0.259	0.888	0.070	-0.504	-2.296	0.070	161.465
B5	78.637	84.343	1.486	0.077	-0.951	1.137	0.108	-0.604	-2.742	0.118	161.609

¹Percent contribution of element

Table 4.18 Weighted contributions of elements to Percent Elongation of the samples.

Co de	Cu	Si	Mg	Fe	Mn	Ni	Zn	Cr	Ti	Total
	-15.35 ¹	-40.01	-7.00	18.47	0.92	-3.14	0.62	-0.93	0.78	
P1	-24.667	-315.319	-3.304	-16.623	0.077	-5.756	0.068	-0.015	0.079	-365.46
P2	-31.498	-342.606	-4.900	-11.267	0.068	-5.442	0.051	-0.070	0.048	-395.566
P3	-46.848	-246.822	-0.987	-12.449	0.217	-0.876	0.867	-0.024	0.031	-306.891
P4	-35.412	-320.960	-5.887	-15.533	0.235	-5.420	0.061	-0.021	0.041	-382.895
H1	-50.624	-285.751	-0.588	-15.108	0.127	-0.430	0.708	-0.030	0.039	-351.657
H2	-46.418	-283.551	-0.448	-15.681	0.176	-0.317	0.408	-0.029	0.033	-345.827
H3	-49.243	-291.153	-0.385	-15.884	0.197	-0.367	0.532	-0.030	0.045	-356.288
H4	-53.541	325.081	-0.483	-16.623	0.240	-0.458	0.464	-0.042	0.034	-395.490
H5	-47.155	-337.924	-0.406	-16.623	0.215	-0.352	0.420	-0.027	0.034	-401.818
C1	-26.663	-232.778	-0.448	-7.074	0.190	-0.185	0.105	-0.005	0.012	-266.846
C2	-44.991	-234.379	-0.413	-9.494	0.228	-0.126	0.113	-0.008	0.049	-289.021
C3	-47.401	-218.455	-0.266	-13.114	0.263	-0.138	0.169	-0.011	0.044	-278.909
C4	-18.666	-242.261	-0.546	-7.942	0.255	-0.053	0.097	-0.007	0.035	-269.088
M1	-54.293	-269.867	-0.882	-17.094	0.816	-0.732	0.817	-0.017	0.034	-314.828
M2	-31.283	-285.751	-1.029	-9.494	0.201	-0.912	0.381	-0.016	0.042	-326.011
M3	-29.165	-224.816	-0.917	-13.114	0.219	-0.405	0.746	-0.024	0.048	-267.428
M4	-36.026	-293.633	-1.288	-7.942	0.173	-1.846	0.295	-0.018	0.037	-340.248
B1	-43.763	-242.020	-0.616	-12.38	0.228	-0.948	0.127	-0.010	0.044	-299.333
B2	-49.765	-314.279	-0.623	-16.623	0.218	-0.703	0.337	-0.026	0.069	-381.395
B3	-58.084	-279.310	-0.322	-16.623	0.300	-0.251	0.353	-0.022	0.058	-353.901
B4	-40.140	-263.826	-0.322	-13.409	0.194	-0.408	0.213	-0.012	0.034	-317.676
B5	-36.656	-289.912	-0.861	-16.623	0.201	-1.502	0.272	-0.019	0.058	-345.041

¹Percent contribution of element

4.2.8 COMPARISON WITH EQUIVALENT COMMERCIAL ALLOYS

Table 4.19 gives a comparison of the average mechanical properties of the scrap samples as obtained in this study with the typical properties of their respective equivalent commercial alloys. The typical properties given for the equivalent commercial alloys have been gleaned

from various publications [13, 101, 160-162]. Where various commercial alloys are equivalent to a particular sample, the lowest and largest values of the typical properties reported for the alloys are given as a range.

As can be discerned from Table 4.19, the UTS and El of the samples cast in turbulent top filled green sand moulds are much lower than those of their commercial counterparts. Furthermore, the mechanical properties of these samples appeared quite unreliable due to the high number of rejected castings. The lower properties are, however, attributed to the design of the mould used rather than the chemical composition as discussed earlier. Turbulently filled castings are generally unreliable as they are riddled with oxides, porosity and other filling related defects.

For samples cast in turbulent top filled permanent moulds, their mechanical properties are fairly closer to their commercial counterparts, but still fairly lower for the same reasons as discussed above. The improvement is attributed to the higher cooling rates experienced in permanent mould casting as compared to green sand casting.

The UTS and El of the quiescently filled samples are much closer to their commercial counterparts, but they lie on the lower end of the range given for commercial alloys. The BHN values of the scrap samples, however, correlate well with those of their commercial counterparts. This is attributed to the fact that hardness is not normally drastically reduced by casting defects.

Table 4.19 comparison of mechanical properties of scrap samples with typical properties of their equivalent commercial.

Code	Green sand casting			Permanent mould casting		
	UTS (MPa)	EI (%)	BHN	UTS (MPa)	EI (%)	BHN
P1	128	1.7	75	137	1.9	92
P1E ¹	150	2	75	234	2	90
P2	140	1.8	83	155	2.2	94
P2E ²	--	--	--	234	2	90
P3	123.5	1.5	79	155	2.3	93
P3E	140-185	2	60-80	160-235	2.5 - 3	70-85
P4	160	2.2	81	166	2.5	95
P4E	150	2	75	234	2	90
P4-T6	180	2.24	86	251	2.36	104
P4E - T6	--	--	--	290	1.5	105
H1	136	2.0	78	177	2.3	87
H1E	140 - 215	1 - 2	60-79	160 - 235	1-2.5	70 - 85
H2	121	1.6	68	179	2.4	90
H2E	140 - 215	1-2	60-79	160 - 235	1 - 2.5	70 - 85
H3	106	0.7	80	170	2.3	88
H3E	140 - 215	1-2	60-79	160 - 235	1-2.5	70 - 85
H4	141	2.1	77	187	2.42	89
H4E	140 - 215	1-2	60-79	160-235	1-2.5	70 - 85
H4 -T6	186	1.9	81	259	2.3	95
H4E - T6	230 - 250	1-2	80-92	259 - 341	<4.52	90-95
H5	123	1.6	70	151	2.1	89
H5E	--	--	--	200	<3	80 - 85
H5 - T6	133	1.5	83	199	1.76	91
H5E - T6	--	--	--	--	--	--

¹Codes with E represent the approximately equivalent alloys for the scrap sample in question.

²Dashes imply that no data could be found for the alloy(s).

³All the sand cast specimens for the sample failed during specimen mounting.

Table 4.19 Continued

Code	Green sand casting			Permanent mould casting		
	UTS (MPa)	EI (%)	BHN	UTS (MPa)	EI (%)	BHN
C1	127	1.6	63	150	1.8	71
C1E	159	3	--	--	--	--
C2	120	1.5	72	179	2.15	76
C2E	140 - 215	1-2	60 - 79	160 - 235	1 - 2.5	70 - 85
C3	122	1.5	73	138	1.8	79
C3E	140 - 215	1-2	60 - 79	160 - 235	1 - 2.5	70 - 85
C4	146	1.84	67	180	2.12	77
C4E	159	3	--	--	--	--
C4 - T6	173	1.66	78	250	1.98	87
C4E - T6	241	3	80	310	2	110
M1	119	1.4	76	164	2.3	86
M1E	140 - 215	1 - 2	60 - 79	160 - 235	1 - 2.5	70-85
M2 ³	--	--	76	148	2.1	81
M2E	140 - 215	1 - 2	60 - 79	160 - 235	1-2.5	70-85
M3 ³	--	--	76	167	2.4	88
M3E	140 - 215	1 - 2	60 - 79	160 - 235	1-2.5	70-85
M4	142	1.98	76	179	2.66	82
M4E	140 - 215	1-2	60 - 79	160 - 235	1-2.5	70-85
M4 - T6	159	2.12	83	232	2.52	87
M4E - T6	230 - 250	1 - 2	80 - 92	259 - 341	<4.52	90-95
B1	114	1.25	74	130	1.5	86
B1E	140-215	1-2	60-79	160-235	1-2.5	70-85
B2	144	2.05	77	163	2.2	82
B2E	140-215	1-2	60-79	160-235	1-2.5	70-85
B3	140	1.9	75	140	1.5	87
B3E	140-215	1-2	60-79	160-235	1-2.5	70-85
B4	123	1.4	75	150	2.1	84
B4E	140-215	1-2	60-79	160-235	1-2.5	70-85
B5	133	1.9	80	171	2.2	86
B5E	140-215	1-2	60-79	160-235	1-2.5	70-85

This indicates that there is room for improvement of the UTS and EI of these scrap samples to at least as much as those of their equivalent counterparts. This is particularly so considering that a poor mould design was used to produce most of the castings and the fact that grain refinement and eutectic silicon modification were not carried out. Furthermore, degassing with hexachloroethane tablets as used in this study is reported to be the most inefficient of available degassing techniques. The level of hydrogen and inclusions in the melt may have, therefore, been relatively high. Facilities are, however, not currently available in Kenya for an online quantitative assessment of the hydrogen and inclusion level in the melt. One can speculate therefore that the as-cast properties of these alloys would be highly improved if they were subjected to grain refinement, eutectic silicon modification, efficient degassing, efficient inclusion removal (e.g. by using ceramic foam filters), quiescent melt handling and quiescent mould filling. Optimum heat treatment of the castings would yield even better mechanical properties.

4.3 MICROSTRUCTURE

Fig 4.19 - 4.30 show the microstructure of the various scrap samples. The microstructure of these alloys is generally similar as illustrated in Figs 4.19-4.30. It consists mainly of α -aluminium dendrites (marked A), eutectic silicon particles (marked B), iron-rich intermetallics (marked C) and in some cases copper-containing phases (marked D). The microstructure for P1 in Fig. 4.19a and b (sand and permanent mould cast) show needle shaped iron-rich intermetallics (probably the β -phase). Similar phases are also observed in Fig. 4.19e, 4.21e, 4.22a, 4.23a, 4.23c, 4.23d, 4.26e, 4.27a, 4.27b, 4.28b and 4.28c. The microstructures containing these β -phases are for those alloys with high iron contents (0.9 wt%). High iron contents and longer solidification times favour the formation of β -phases. The manganese content of P1 is very low (0.084wt%) and is probably the reason for the formation of the β -phase. Certain samples such as H4 and H5 have higher manganese contents and some Chinese script iron-rich phases are observed.

Most of the microstructures contained copper-containing phases, which could probably be Al_2Cu , Al_2CuMg or $\text{Al}_5\text{Cu}_2\text{Mg}_8\text{Si}_6$ phases. The eutectic silicon particles in the as cast microstructures of sand cast specimens are mainly large and acicular shaped as would be expected because the alloys are unmodified and the solidification time is longer. The same applies to permanent mould cast specimens except in some few cases such as in Figs 4.19d and 4.23b where they appear smaller.

Solution treatment at 540°C for 24 h of P4, H4, H5 and C4 modifies the eutectic silicon from acicular to more rounded shapes. Incipient melting of Cu-containing phases is observed in the heat treated microstructures. In some microstructures such as Figs 4.20c and 4.27b for sand cast P4 and M4 respectively, incipient melting is so severe that it has created crack-like defects in the interdendritic regions.

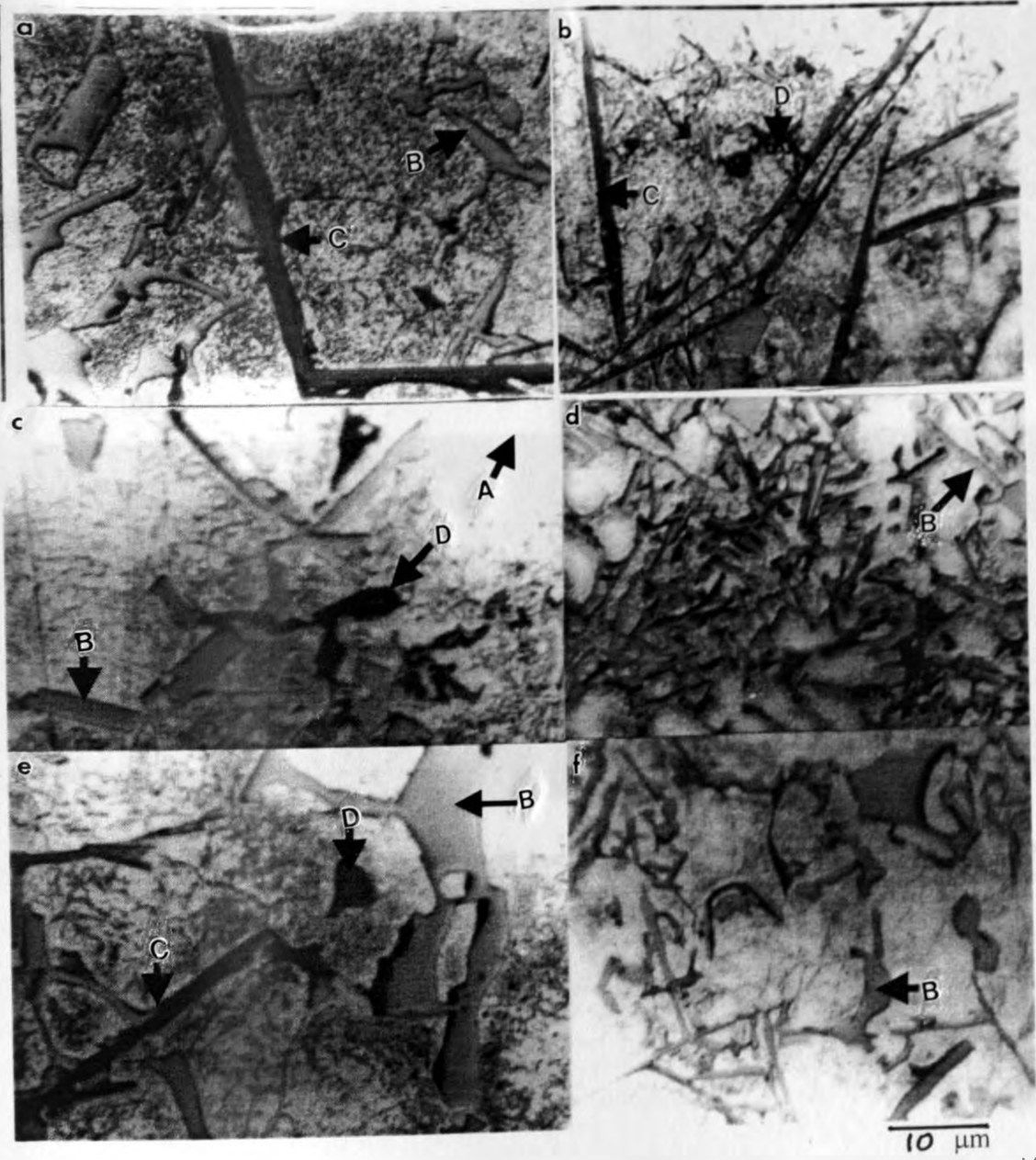
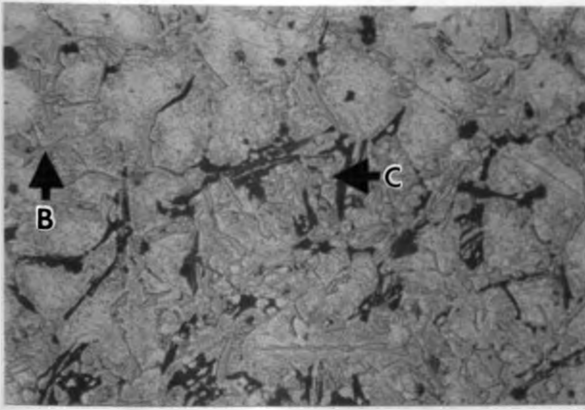
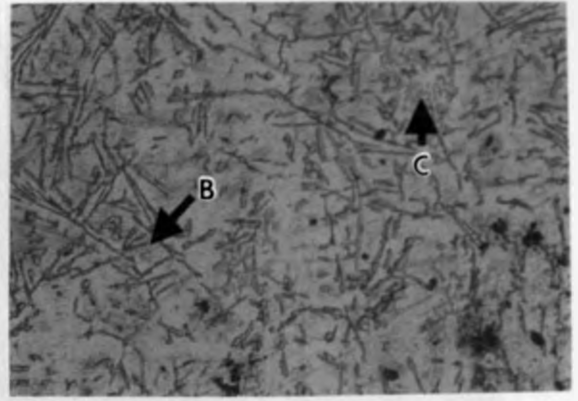


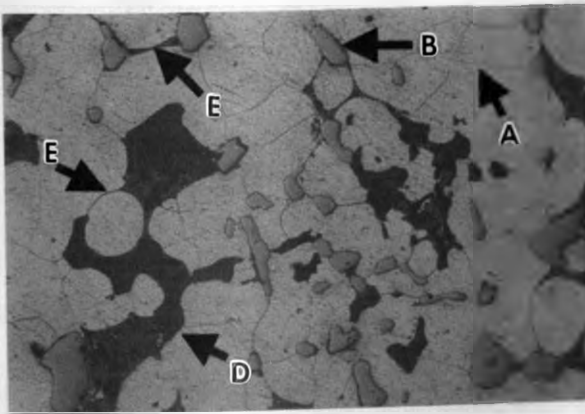
Fig. 4.19 Micrographs for (a) sand cast P1, (b) Permanent mould P1, (c) sand cast P2, (d) Permanent mould P2, (e) sand cast P3, and (f) Permanent mould P3. (A- α -Al dendrites; B-eutectic Si; C-Fe-rich intermetallics and D-Cu-containing phases)



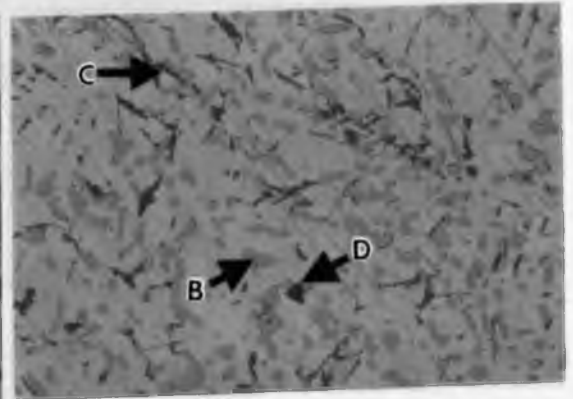
(a)



(b)



(c)



(d)

30 μm

Fig. 4.20 Micrographs for (a) sand cast P4 in as-cast condition, (b) permanent mould P4 in as-cast condition, (c) sand cast P4 - T6, (d) permanent mould P4 - T6. (A- α -Al dendrites; B-eutectic Si; C-Fe-rich intermetallics, D-Cu-containing phases and E-cracks due to local melting)

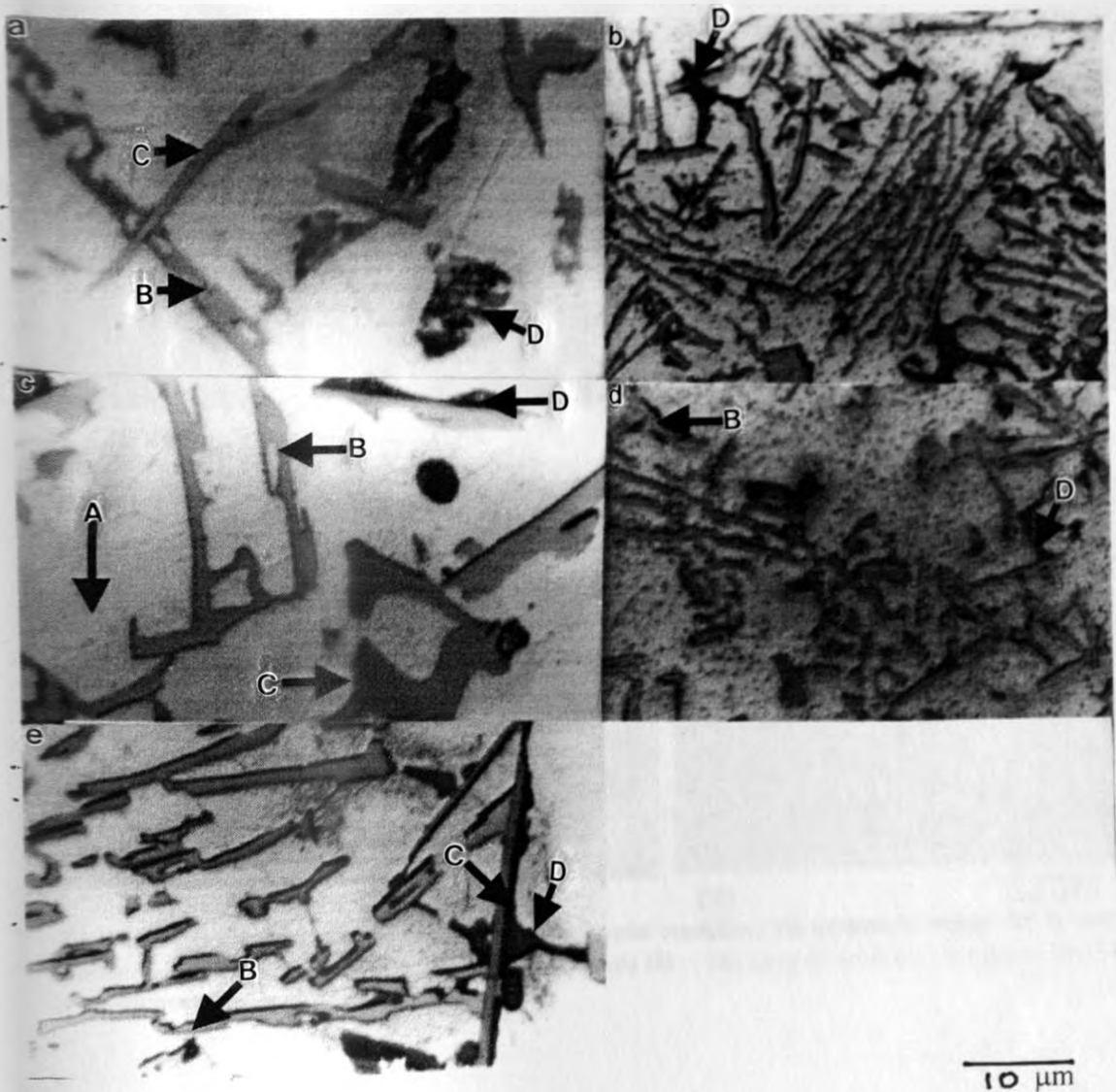


Fig. 4.21 Micrographs for (a) sand cast H1, (b) Permanent mould H1, (c) sand cast H2, (d) Permanent mould H2, and (e) sand cast H3. (A- α -Al dendrites; B-eutectic Si; C-Fe-rich intermetallics and D-Cu-containing phases)

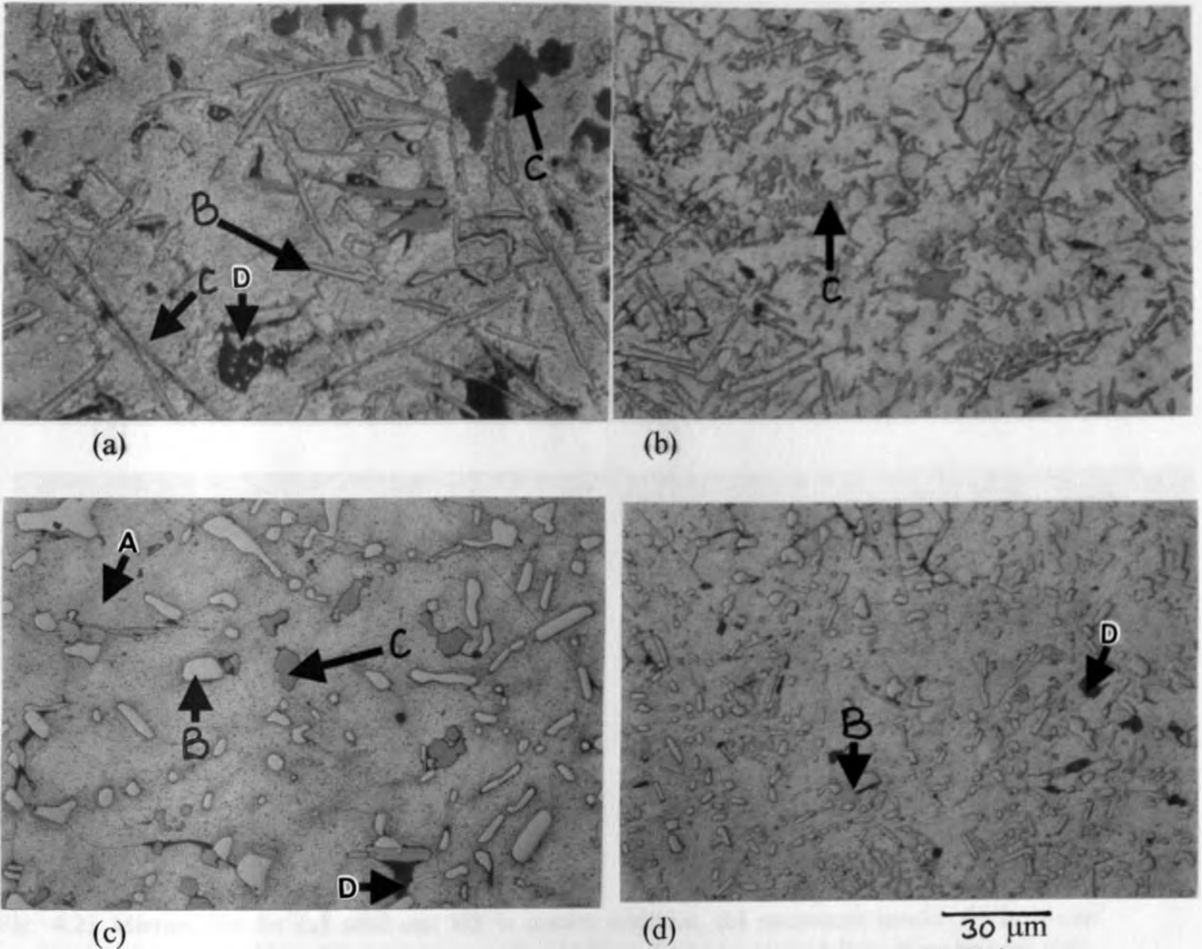


Fig. 4.22 Micrographs for (a) sand cast H4 in as-cast condition, (b) permanent mould H4 in as-cast condition, (c) sand cast H4 - T6, (d) permanent mould H4 - T6. (A- α -Al dendrites; B-eutectic Si; C-Fe-rich intermetallics and D-Cu-containing phases)

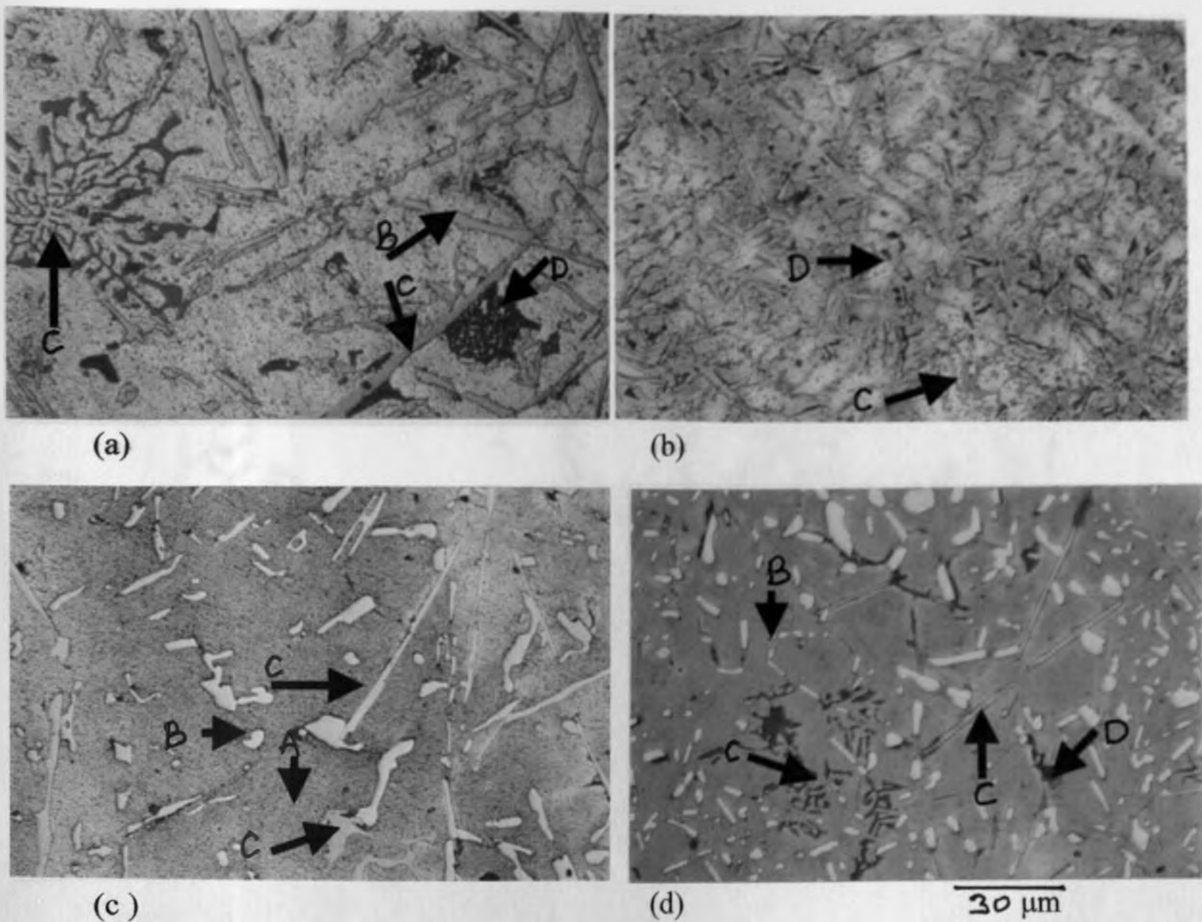


Fig. 4.23 Micrographs for (a) sand cast H5 in as-cast condition, (b) permanent mould H5 in as-cast condition, (c) sand cast H5 - T6, (d) permanent mould H5 - T6. (A- α -Al dendrites; B-eutectic Si; C-Fe-rich intermetallics and D-Cu-containing phases)

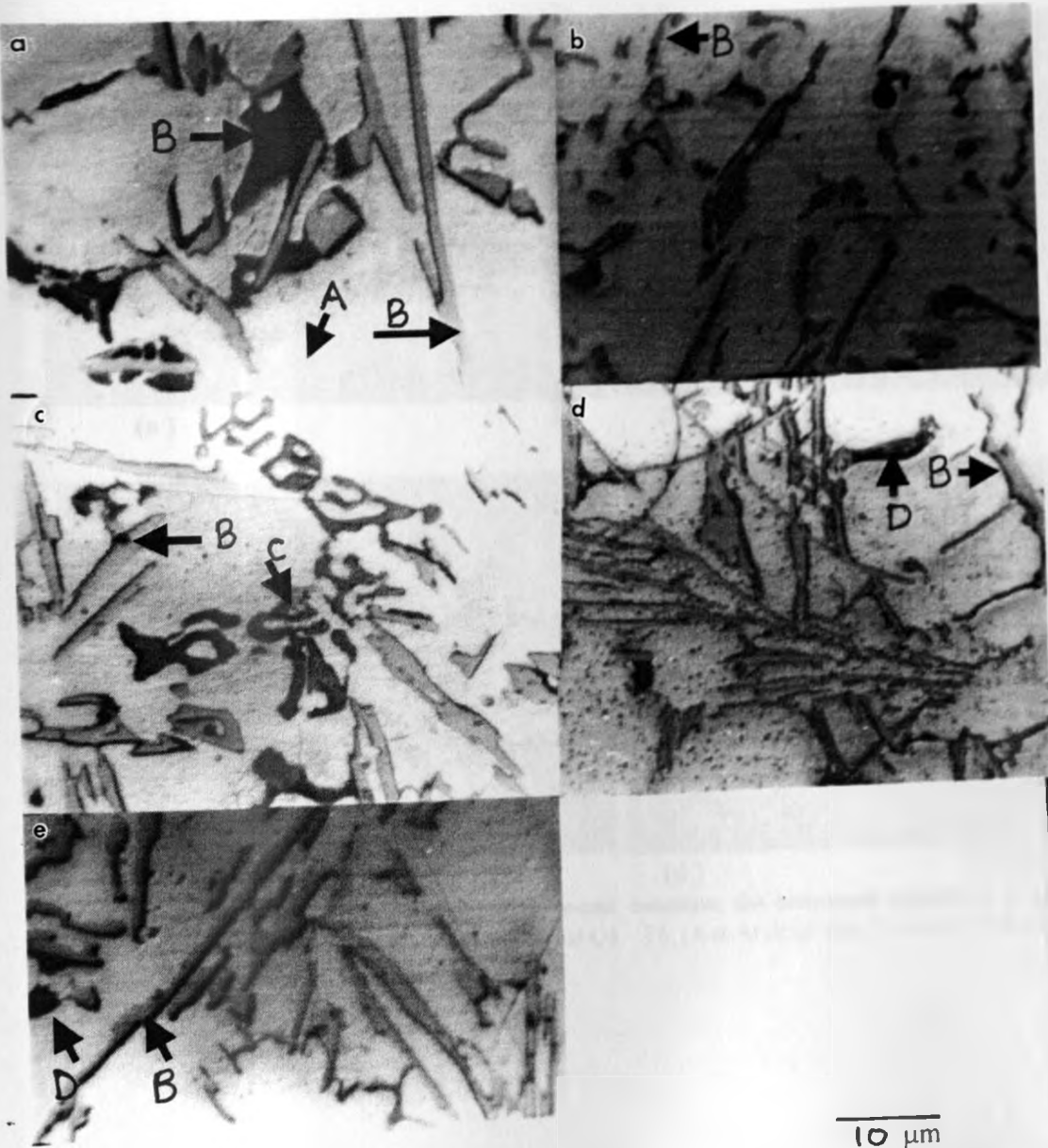


Fig. 4.24 Micrographs for (a) sand cast C1, (b) Permanent mould C1, (c) sand cast C2, (d) Permanent mould C2, and (e) sand cast C3. (A- α -Al dendrites; B-eutectic Si; C-Fe-rich intermetallics and D-Cu-containing phases)

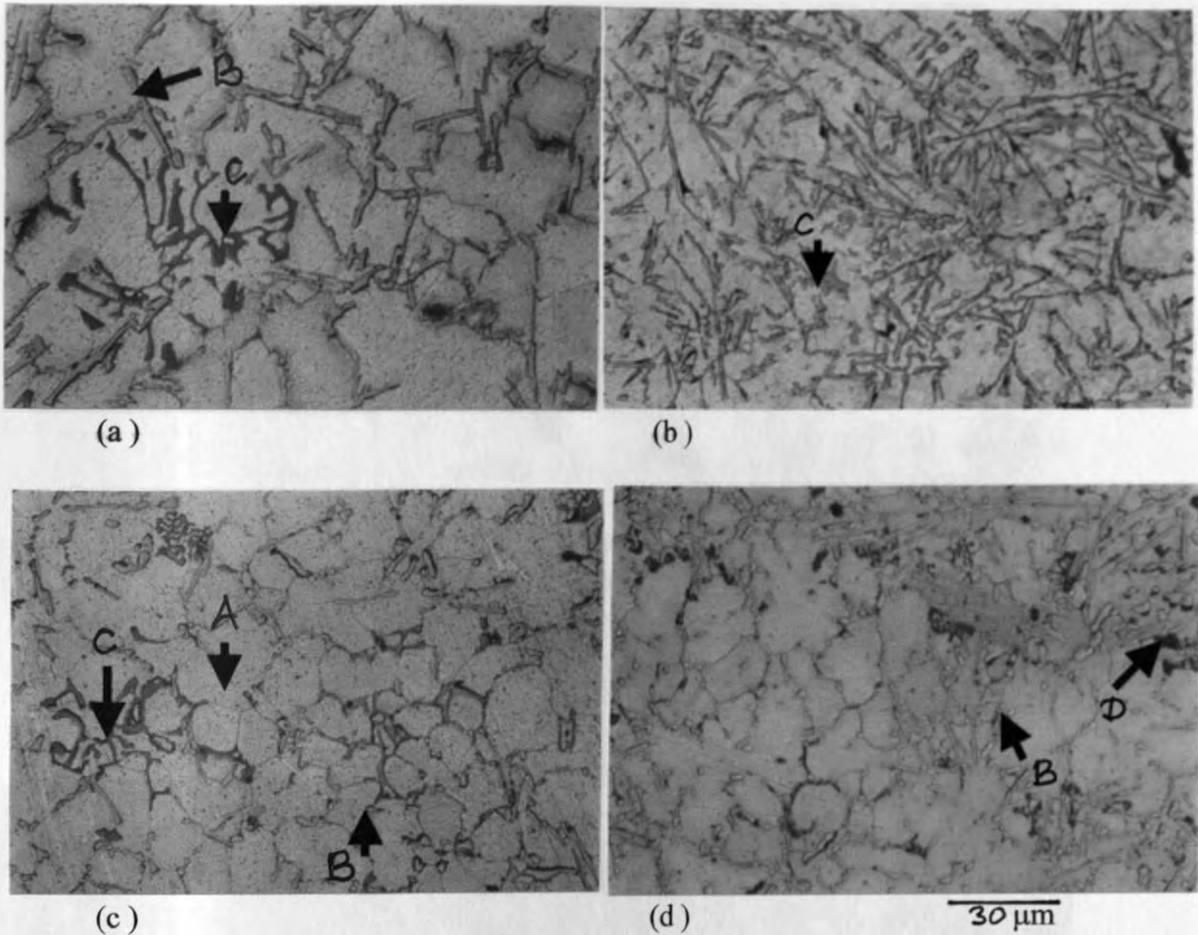


Fig. 4.25 Micrographs for (a) sand cast C4 in as-cast condition, (b) permanent mould C4 in as-cast condition, (c) sand cast C4 – T6, (d) permanent mould C4 – T6. (A- α -Al dendrites; B-eutectic Si; C-Fe-rich intermetallics and D-Cu-containing phases)

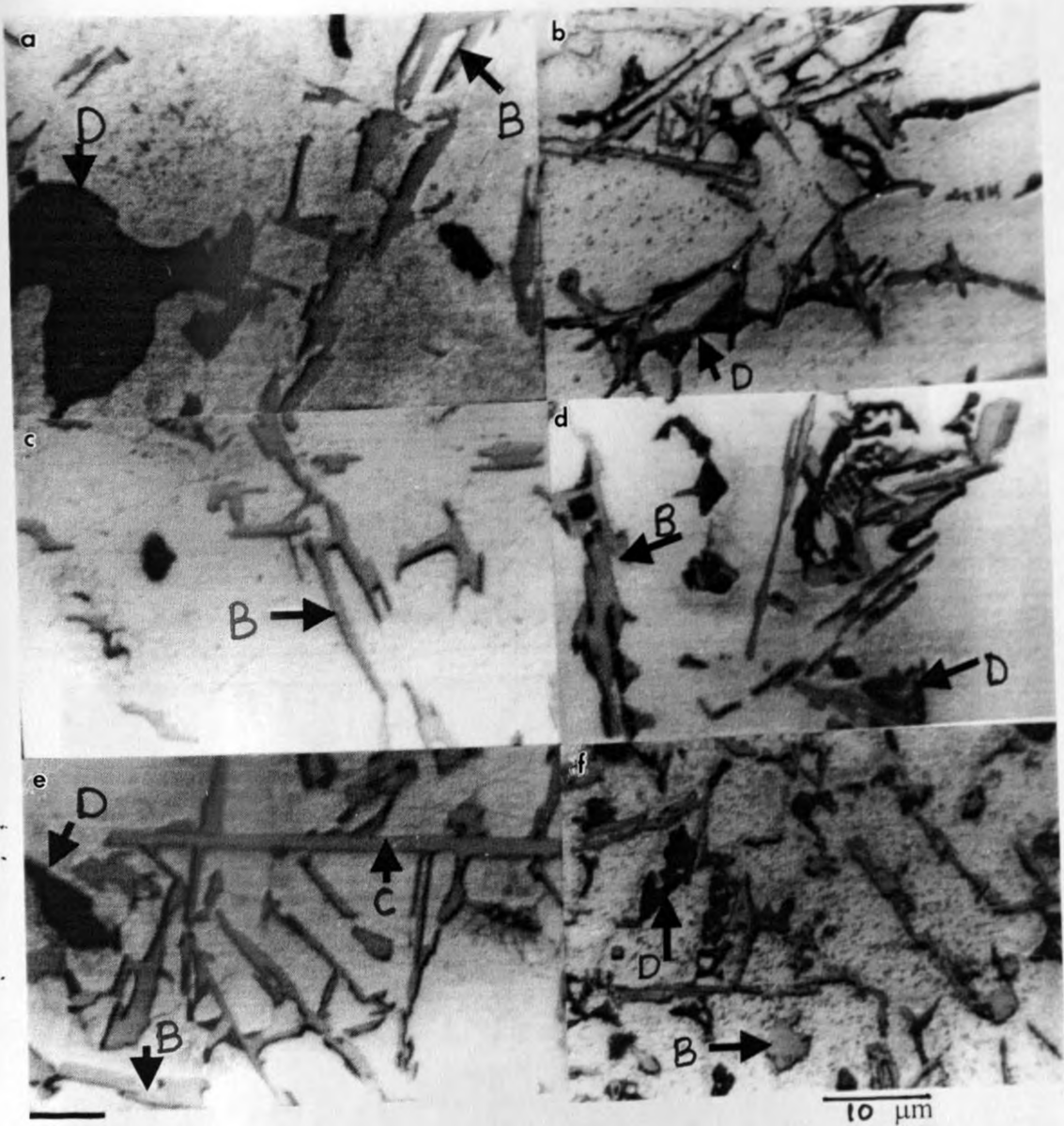
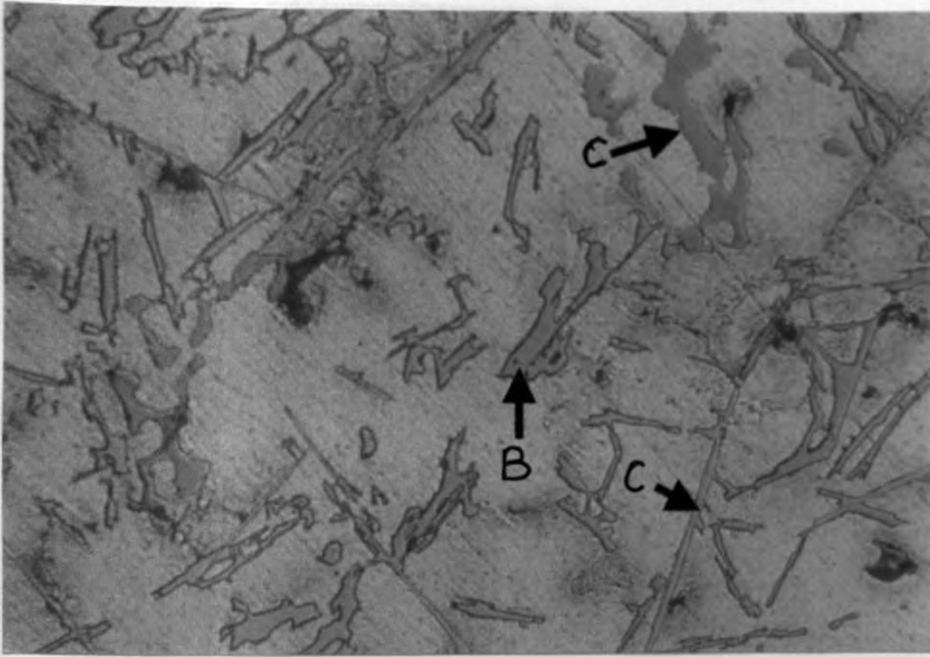
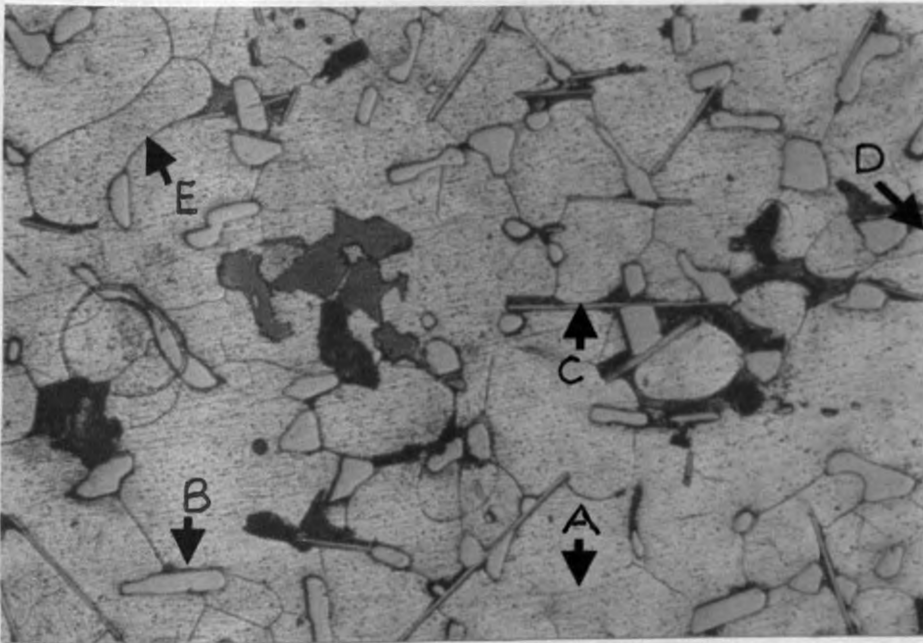


Fig. 4.26 Micrographs for (a) sand cast M1, (b) Permanent mould M1, (c) sand cast M2, (d) Permanent mould M2, (e) sand cast M3, and (f) Permanent mould M3. (A- α -Al dendrites; B-eutectic Si; C-Fe-rich intermetallics and D-Cu-containing phases)



(a)



(b)

45 μm

Fig. 4.27 Micrographs for sand cast M4 in (a) as-cast condition, and (b) T6 condition. (A- α -Al dendrites; B-eutectic Si; C-Fe-rich intermetallics, D-Cu-containing phases and E-cracks due to local melting)

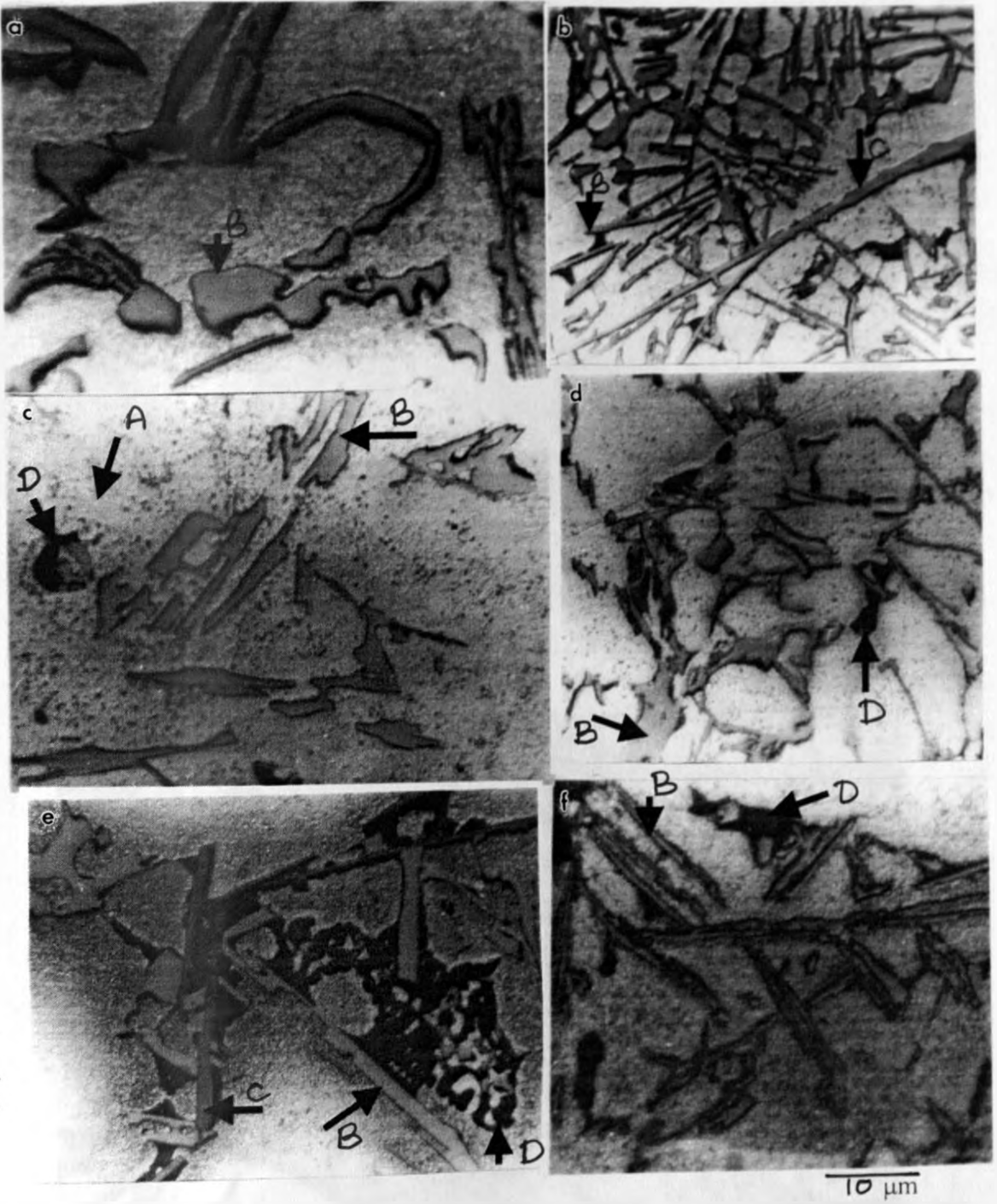
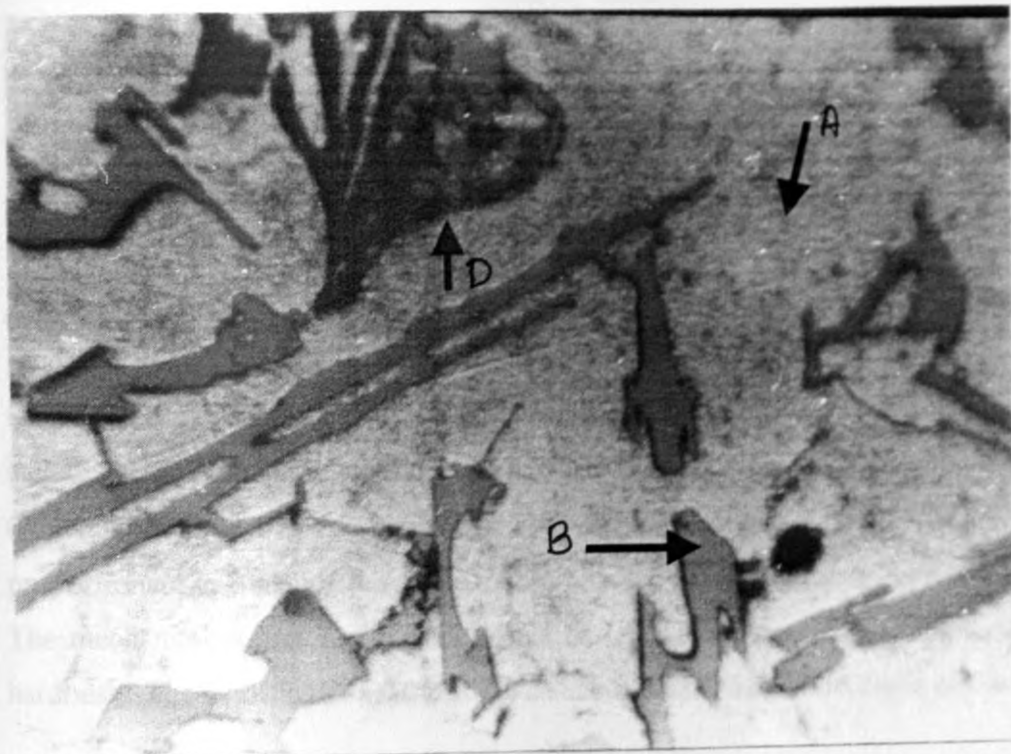
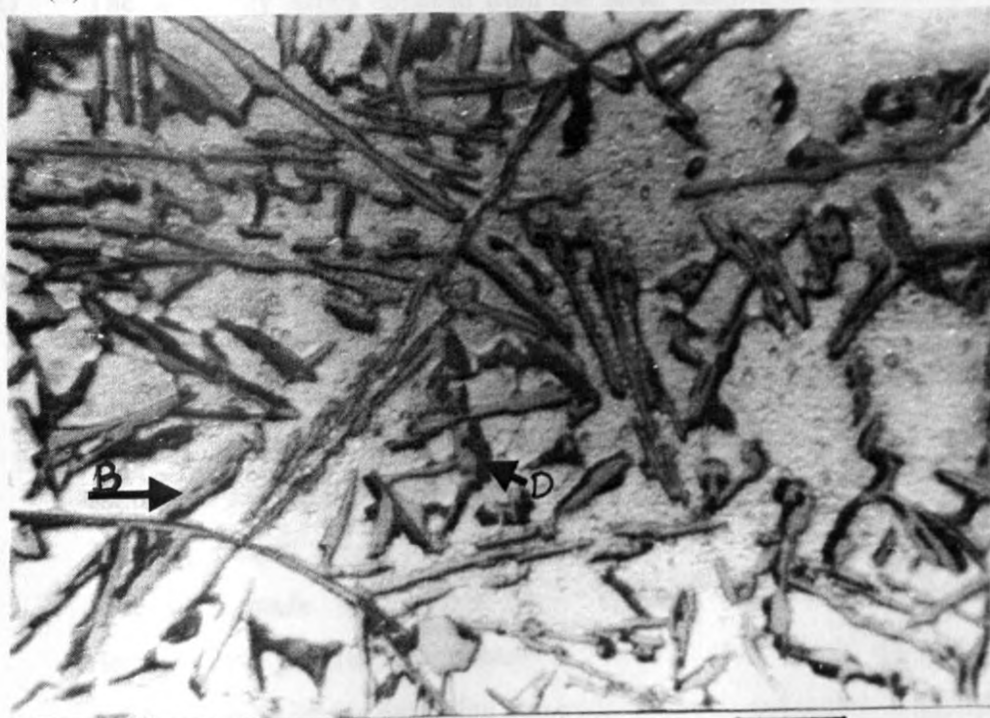


Fig. 4.28 Micrographs for (a) sand cast B1, (b) Permanent mould B1, (c) sand cast B2, (d) Permanent mould B2, (e) sand cast B3, and (f) Permanent mould B3. (A- α -Al dendrites; B-eutectic Si; C-Fe-rich intermetallics and D-Cu-containing phases)



(a)



(b)

15 μm

Fig. 4.29 As-cast micrographs for (a) sand cast B5, and (b) permanent mould. (A- α -Al dendrites; B-eutectic Si; C-Fe-rich intermetallics and D-Cu-containing phases)

CHAPTER 5

CONCLUSIONS AND RECOMMENDATIONS

5.1 CONCLUSIONS

The chemical composition, microstructure and mechanical properties of secondary alloys produced from various categories of cast aluminium scrap components have been investigated in this study. The scrap categories investigated are pistons, housings (which include gearbox casings, rear axle casings and sumps), cylinder heads, miscellaneous scrap (which include all other types of cast aluminium scrap) and blended scrap (which include proportionate mixtures of the above categories to form some form of hybrid scrap samples). The mechanical properties investigated are ultimate tensile strength, percent elongation and hardness. The following conclusions can be inferred from the observations of this study:

- (i) The secondary alloys obtained from the scrap samples are aluminium-silicon-copper based alloys. Some samples such as the housing and cylinder head categories plus some blended scrap samples contain negligible amounts of magnesium. The other samples, especially most of the piston samples, contain substantial magnesium contents.
- (ii) There is no significant difference in the general chemical composition of the alloys save for minor variations between the samples. Most of the samples are actually equivalent in terms of their chemical composition and some defy group boundaries by being equivalent to samples of other groups. However, there are in some cases, significant similarities within a group pertaining to the contents of certain elements. This observation supports the hypothesis that most similar components are likely to have been made from either similar alloys or alloys of equivalent chemistry. However, the general alloy chemistry ceases to be uniquely identified to particular groups because of the possibility that in each group, some few components may have been produced from alloys of significantly different chemistry (e.g. aluminium-copper based alloys compared with aluminium-silicon based alloys). It is also

possible that similar alloys could have been used to make components that belong to different groups.

- (iii) Sorting scrap component-wise is useful to a limited extent as it may allow the use of the alloy chemistry of a representative sample to predict the level of most of elements in other alloys recycled from similar scrap components. For instance, recycled pistons are likely to result in an alloy containing ~ 8 wt% silicon, 0.4-0.85 wt% magnesium, 0.6-0.9 wt% iron, ~ 1.7 wt% nickel, <0.25 wt% manganese, <0.1 wt % zinc, <0.1 wt % chromium, <0.1 wt % lead, <0.1 wt % tin and <0.1 wt % titanium. However, the copper content may vary from about 1.5 to 3 wt% and cannot easily be predicted as the other elements. Therefore, when recycling pistons, one can have a reasonably good idea as to the expected levels of most elements in the resulting alloy except copper.
- (iv) Blending scrap components to obtain hybrid scrap samples does not give any discernible trend in the alloy chemistry.
- (v) The mechanical properties of permanent mould cast specimens are found to be higher than those from sand cast specimens due to, perhaps, their higher cooling rates. The permanent mould casting process is therefore preferred to sand casting if process selection is based solely on mechanical properties.
- (vi) Quiescent bottom filled mould designs yield sounder castings with improved mechanical properties than turbulent top filled mould designs.
- (vii) The mechanical properties of a casting vary from one location of the casting to the other, probably, because of differences in the cooling rates at different casting locations.
- (viii) Increasing the thickness of permanent moulds results increases in mechanical properties.
- (ix) Increasing the mould preheat of permanent moulds results in decreases in mechanical properties
- (x) Increasing the pouring temperature results in decreases in mechanical properties due to decreased cooling rate that results in increased SDAS and grain size.

5.2 RECOMMENDATIONS

In general, sorting the scrap according to components as done in this investigation could be useful to a limited extent. The ideal situation would be to correct the alloy chemistry of the resulting alloys to appropriate standard alloys using on line facilities such as spectrometers and master alloys or compacted additives. However, since this is not always possible, particularly for Kenyan foundry shops, it would be advisable to sort the scrap component-wise and use the alloy chemistries obtained for one or more samples of the same group as a guide to predict the expected alloy chemistry of alloys recycled from components of that group.

The chemical compositions of some of the scrap categories obtained in this study can be used to predict the alloy chemistry of alloys recycled from components belonging to similar groups. Recycled pistons are likely to result in an alloy containing ~ 8 wt% silicon, 0.4-0.85 wt% magnesium, 0.6-0.9 wt% iron, ~ 1.7 wt% nickel, <0.25 wt% manganese, <0.1 wt% zinc, <0.1 wt% chromium, <0.1 wt% lead, <0.1 wt% tin and <0.1 wt% titanium. However, the copper content may vary from about 1.5 to 3 wt% and cannot easily be predicted as the other elements. Therefore, when recycling pistons, one can have a reasonably good idea as to the expected levels of most elements in the resulting alloy except copper. If the desired application does not require strict chemistry specifications, one will only need to determine the copper content. The same applies to the housings and cylinder head groups. The expected alloy chemistry of an alloy recycled from gear box and rear axle housings is ~ 7-8.5 wt% silicon, ~ 3-3.5 copper, < 0.1 wt% magnesium, 0.8-0.9 wt% iron, ~ 0.2 wt% manganese, ~ 0.1 wt% nickel, <0.1 wt% zinc, <0.1 wt% chromium, ~ 0.1 wt% lead, ~ 0.1-0.2 wt% tin and <0.1 wt% titanium. Recycling cylinder heads would result in an alloy that approximately contains 6 wt% silicon, < 0.1 wt% magnesium, 0.4-0.7 wt% iron, ~ 0.2-0.3 wt% manganese, ~ 0.1 wt% nickel, 0.16-0.27 wt% zinc, <0.1 wt% chromium, < 0.1 wt% lead, < 0.1-0.2 wt% tin and <0.1 wt% titanium. Its copper content is, however, likely to vary from 1.2-3 wt%.

The rest of the assorted scrap including those that are available in small quantities can be lumped together and recycled after which the alloy chemistry of the resulting alloys should

be determined for each separate charge. However, if particular scrap components not covered in this study (e.g. cast aluminium wheels) are available in reasonable quantities, they should also be separated from other scrap and recycled alone. It is likely that the alloy chemistry of different scrap samples belonging to such group will be equivalent for most of the elements.

It also recommended greater emphasis be given to the optimising mould designs, particularly the filling systems. Bottom gated quiescent systems should be preferred to top gated turbulent systems for the permanent mould and sand casting processes investigated here. The same should apply even for other casting processes that use gravity filling. Proper melt handling procedures and use adequate equipment will also improve the quality of resulting castings.

5.3 FUTURE WORK

It is recommended that further investigations on scrap recycling be continued, particularly in the following areas:

- The yield strength, fatigue strength and impact energy of these secondary alloys should be investigated.
- The failure behaviour of these alloys under thermomechanical loading conditions should be studied. This will provide insight on their possible application in high temperature operating conditions such as for cylinder heads and engine blocks.
- The effect of grain refining and eutectic silicon modifications of these alloys and the use of efficient degassing and inclusion control techniques on mechanical properties should be studied.
- Optimum heat treatment parameters that can be used to avoid incipient melting and optimise the quality index of these alloys should be investigated.
- The properties of foundry sands available in Kenya and their effect on the soundness and mechanical properties of the resulting castings should be investigated.

REFERENCES

1. J.K. Brimacombe, "The Challenge of Quality in continuous Casting Processes", *Metallurgical and Materials Transactions A*, Vol. 30A (August 1999) pp. 1899
2. J.A. Taylor, "Metal-Related Castability Effects in Aluminum Foundry Alloys", *Cast Metals*, Vol. 8, 4 (1995) pp. 225 – 252.
3. B.L. Tuttle and R.W. Lindsay, "Principles of Solidification Control in Cast Metals", *AFS Transactions*, Vol. (1984) pp. 681-692.
4. T.K. McCluhan, "Technical Challenges in Molten Metal Processing", *AFS Transactions*, Vol. 92 (1984) pp. 661-666.
5. C.W. Meyers, A. Saigal and J.T. Berry, "Fracture Related Properties of Aluminum A357-T6 Cast Alloy and their Interrelation With Microstructure", *AFS Transactions*, Vol. 91 (1983) pp. 281-287.
6. J. Campbell, "*Castings*", Butterworth-Heinemann Ltd., Oxford (1991).
7. J. Campbell, C. Nyahumwa and N.R. Green, "The Concept of the Fatigue Potential of Cast Alloys", *In proceedings from Materials Solutions Conference '98 on Aluminum Casting Technology*, Edited by M. Tiryakioglu and J. Campbell, Rosemont, Illinois, 12-15 Oct., 1998, pp. 225-233.
8. C.C. Chama, "Mechanical Properties of Hot Isostatically Pressed Aluminium-Silicon Castings", *Scripta Metallurgica et Materialia*, 26, 1992, pp. 1153-1156.
9. E.L. Rooy, "Hot Isostatic Process", *AFS Transactions*, Vol. 91 (1984) pp. 607 – 612.
10. S.J. Mashl, J.C. Hebeisen, D. Apelian and Q.G. Wang, "Hot Isostatic Pressing of A356 and 380/383 Aluminum Alloys: An Evaluation of Porosity, Fatigue Properties and Processing Costs", *SAE Technical paper series*, Paper # 2000-01-0062,
11. F. King, "*Aluminum and Its Alloys*", Ellis Horwood Ltd., Chichester (1987).
12. E.A. Starke Jr., "Aluminum: Alloying", *Encyclopedia of Materials: Science and Technology*, Edited by M.C. Fleming and D. Apelian, Elsevier Science Ltd., Vol. 3 (3) 2001.
13. J.E. Hatch, "*Aluminum: Properties and Physical Metallurgy*", ASM, Metals Park, Ohio (1984).

14. E.A. Starke Jr., "Aluminum Alloys: Properties and Applications", *Encyclopedia of Materials: Science and Technology*, Edited by M.C. Fleming and D. Apelian, Elsevier Science Ltd., Vol 3 (2) 2001.
15. G.S. Cole and A.M. Sherman, "Lightweight Materials for Automotive Applications", *Materials characterization*, Vol. 35 (1995) pp. 3-4.
16. A Guide to Aluminium Casting Alloys", AFS Website Technical Article, 2000, (www.castingsource.com)
17. "Aluminum Alloy Selection and Applications", Monograph Published by the Aluminum Association, Inc. (Dec. 1998).
18. J.L. Jorstad, "Applications of 390 Alloy: An Update", *AFS Transactions*, Vol. 92 (1984) pp. 573-578.
19. E.P. Degarmo, J.T. Black, and A.R. Kohser, "Materials and Processes in Manufacturing", 7th Ed., MacMillan Publishing Company, New York (1988).
20. J. Barresi, Z. Chen, C.J. Davidson, M.T. Murray, T. Nguyen, D.H. StJohn and W.R. Thorpe, "Casting of Aluminum Components", *Materials Forum*, Vol. 20 (1996) pp. 53-70.
21. "Status of Jua Kali Sheds in the Country", Republic of Kenya – Ministry of Research and Applied Technology (1992).
22. S.M. Maranga, "Foundry Education and Operations: Aspects for Consideration by the Kenyan Industrial Sector", *In the 6th Mechanical Engineering Seminar – The Focus of Engineering Research for Industrial Development in the New Millenium*, JKUAT, Kenya (June 2000).
23. L.F. Mondolfo, "Aluminum Alloys: Structure and Properties", Butterworths, London (1976)
24. E.A. Starke Jr., "Aluminum Alloys: Alloy, Heat Treatment and Temper Designation", *Encyclopedia of Materials; Science and Technology*, Edited by M.C. Fleming and D. Apelian, Elsevier Ltd, Vol. 3 (3) 2001.
25. D.E. Groteke, "Dross Reclamation at Aluminum Melting Furnaces", *AFS Transactions*, Vol. 108 (2000) pp. 578-583.

26. "Aluminum Recycling Breakthrough Means Potential Boon for Automakers; Laser Separates Aluminum by Alloy, Increases Scrap Value", *The Aluminum Association, Inc., Web Industry News*, Oct. 2000, (www.aluminum.org).
27. E.L. Rooy, "Aluminium Scrap Recycling and its Impact on the Metal Castings Industry", *AFS Transactions*, Vol. 93, 1985, pp. 935-938.
28. J.E. Gruzleski and B. Closset, "*The Treatment of Liquid Aluminum-Silicon Alloys*", American Foundrymen Society, Des Plaines, Illinois (1990).
29. G.K. Sigworth, "Theoretical and Practical Aspects of the Modification of Al-Si Alloys", *AFS Transactions*, Vol. 92 (1984) pp. 7-16.
30. M.M. Makhlof and H.V. Guthy, "The Aluminum Silicon Eutectic: Mechanisms and Crystallography", *Journal of Light Metals*, Vol. 1, 4 (2001) pp. 199-218.
31. D.H. StJohn, A.K. Dahle, M. Easton, J.E.C. Hutt and N.L.M. Veldman, "Solidification of Hypoeutectic Aluminum-Silicon Alloys", *Materials Forum*, Vol. 23 (1999) pp. 137-152.
32. J.B. Andrews and M.V.C Seneviratne, "A New, Highly Wear-Resistant Aluminum-Silicon Casting Alloy for Automotive Engine Block Applications", *AFS Transactions*, Vol. 92 (1984) pp. 209-216.
33. D. Plaza, J. Asensio, J.A. Pero-Sanz and J.I. Verdeja, "Microstructure, a Limiting Parameter for Determining the Engineering Range of Compositions for Light Alloys: The Al-Cu-Si System", *Materials characterization*, Vol. 40 (1998) pp. 145-158.
34. L. Wang, M. Makhlof and D. Apelian, "Aluminum Die Casting Alloys: Alloy Composition, Microstructure and Properties-Performance Relationships", *International Materials Reviews*, 40(6) (1995) 225-252.
35. R. Donahue and P. A. Fabiyi, "Manufacturing Feasibility of All-Aluminum Automotive Engines Via Application of High Silicon Aluminum Alloy", *SAE Paper # 2000-01-0061*.
36. M. Djurdjevic, H. Jiang, and J. Sokolowski, "On-line Prediction of Aluminum-Silicon Eutectic Modification Level Using Thermal Analysis", *Materials characterization*, Vol. 46 (2001) pp. 31-38.
37. Peijie Li, V.I. Nikitin, E.G. Kandalova and K.V. Nikitin, "Effect of Melt Overheating, Cooling and Solidification Rates on Al-16wt%Si Alloy Structure" *Materials Science and Engineering*, Vol. A332, 1-2 (2002) pp. 371-374.

38. M.O. Otte, S.D. McDonald, J.A. Taylor, D.H. StJohn and W. Schneider, "Controlling Porosity-Related Casting Rejects: Understanding the Role of Iron in Al-Si Alloys", *AFS Transactions*, Vol. 107 (1999) pp 471-478.
39. M. Dash and M. Makhlof, "Effect of Key Alloying Elements on the Feeding Characteristics of Aluminum-Silicon Casting Alloys", *Journal of Light Metals*, Vol. 1, 4 (2001) pp. 251-261.
40. C.H. Caceres, M.B. Djurdjevic, T.J. Stockwell and J.H. Sokolowski, "The Effect of Cu Content on the Level of Microporosity in Al-Si-Cu-Mg Casting Alloys", *Scripta Materialia*, Vol. 40, 5 (1999) pp. 631-637.
41. D.L. Zhang and D.H. StJohn, "Effect of Magnesium and Copper Content on the Mechanical Properties of Cast Al-7wt%Si-Mg Alloys", *In Aluminum and Magnesium for Automotive Applications*, Edited by J.D. Bryant, The Minerals, Metals and Materials Society, 1996, pp. 3-15.
42. F.H. Samuel, "Incipient Melting of $Al_5Mg_8Si_6Cu_2$ and Al_2Cu Intermetallics in unmodified and Strontium-Modified Al-Si-Cu-Mg (319) Alloys During Solution Heat Treatment", *Journal of Materials Science*, 33(1998) 2283-2297.
43. W. Reif, J. Dutkiewicz, R. Ciach, S. Yu and J. Krol, "Effect of Ageing on the Evolution of Precipitates in AlSiCuMg Alloys", *Materials Science and Engineering A*, Vols. 234-236 (1997) pp. 165-168.
44. J. Krol, "The Precipitation Strengthening of Directionally Solidified AlSiCu Alloys", *Materials Science and Engineering A*, Vols. 234-236 (1997) pp. 169-172.
45. P. Oeullet, and F.H. Samuel, "Effect of Mg on the Ageing Behavior of Al-Si-Cu 319 Type Aluminum Casting Alloys", *Journal of Materials Science*, 34(1999) 4671-4697.
46. C.H. Caceres, J H Sokolowski and P. Gallo, "Effect of Ageing and Mg Content on the Quality Index of Two Model Al-Cu-Si-Mg Alloys" *Materials Science and Engineering*, A271 (1999) 53-61.
47. Q.G. Wang and C.H. Caceres, "On the Strain Hardening Behavior of Al-Si-Mg Casting Alloys", *Materials Science and Engineering A*, Vols. 234-236 (1997) pp. 106-109.
48. C.H. Caceres, C.J. Davidson, J.R. Griffiths and Q.G. Wang, "The Effect of Mg on the Microstructure and Mechanical Behavior of Al-Si-Mg Casting Alloys", *Metallurgical and Materials Transactions A*, Vol. 30A (October 1999) pp. 2611-2618.

49. C.H. Caceres, L. Wang, D. Apelian and M.M. Makhlof, "Alloy Selection for Die Castings Using the Quality Index", *AFS Transactions*, Vol. 107 (1999) pp. 239-247.
50. A.M. Samuel, P. Ouellet, F.H. Samuel and H.W. Dorty, "Microstructural Interpretation of Thermal Analysis of Commercial 319 Al Alloy With Mg and Sr Addition", *AFS Transactions*, Vol. 105 (1997) pp. 951-962.
51. C.H. Caceres, C.J. Davidson, J.R. Griffiths and Q.G. Wang, "The Effect of Mg on the Microstructure and Mechanical Behavior of Al-Si-Mg Casting Alloys", *Metallurgical and Materials Transactions A*, Vol. 30A (October 1999) pp. 2611-2618.
52. L. Wang, D. Apelian and M. Makhlof, "Iron-Bearing Compounds in Al-Si Diecasting Alloys", Morphology and Conditions Under Which They Form", *AFS Transactions*, Vol. 107 (1999) pp. 231-238.
53. S. Murali, K.S. Raman and K.S.S. Murthy, "The Formation β -FeSiAl₅ and Be-Fe Phases in Al-7Si-0.3Mg Alloy Containing Be", *Materials Science and Engineering A*, Vol. 190 (1995) pp. 165-172.
54. Y-H. Tan, S-L. Lee and Y-L. Lin, "Effects of Be and Fe Additions on the Microstructure and Mechanical Behavior of Al-Si-Mg Casting Alloy", *Metallurgical and Materials Transactions A*, Vol. 26A, (May 1995) pp. 1195-1205.
55. Y-H. Tan, S-L. Lee and H-Y. Wu, "Effects of Beryllium on Fatigue Crack Propagation of A357 Alloys Containing Iron", *International Journal of Fatigue*, Vol. 18, 2 (1996) pp. 137-147.
56. M.M. Makhlof, D. Apelian and L. Wang, "Sludge Formation Tendency of Selected Aluminium Die Casting Alloys", In 2001 Annual NADCA Meeting, Cincinnati, OH, Oct. 29-Nov. 1, 2001, Paper # T01-083.
57. B.S. Murty, S.A. Kori and M. Chakraborty, "Grain Refinement of Aluminium and its Alloys by Heterogeneous Nucleation and Alloying", *International Materials Reviews*, 47, 1, 2002, pp. 3-29.
58. D. Apelian, G.K. Sigworth and K.R. Whaler, "Assessment of Grain Refinement and Modification of Al-Si Foundry Alloys by Thermal Analysis", *AFS Transactions*, Vol. 92 (1984) pp. 297-307.

59. M.A. Easton and D.H. StJohn, "The Effect of Grain Refinement on the Formation of Casting Defects in Alloy 356 Castings", *International Journal of Cast Metals Research*, Vol. 12 (2000) pp. 393-408
60. J.A. Taylor, D.A. Graham and M.A. Easton, "The Redistribution of Shrinkage Porosity in Eutectic Al-Si Alloy by the Addition of Ti-B Grain Refiner", *AFS Transactions*, Vol. 107, 1999, pp. 189-196.
61. A. K. Dahle, P.A. Tondel, C.J. Paradies and L. Arnberg, "Effect of Grain Refinement on the Fluidity of Two Commercial Al-Si Foundry Alloys", *Metallurgical and Materials Transactions A*, 27A, 8, 1996, 2305-2313.
62. M.S. Misra and K. J. Oswalt, "Aging Characteristics of Titanium-Refined A356 and A357 Aluminum Castings", *AFS Transactions*, 90 (1982) 1-10.
63. S. Shankar and D. Apelian, "Mechanism and Preventive Measures for Die Soldering During Al Casting in a Ferrous Mold", *Journal of Metals*, Aug. 2002, 47-54.
64. P.S. Warnig, Y.-J. Liauh, S.-L. Lee and J.-C. Lin, "Effects of Be Addition on Microstructures and Mechanical properties of B319.0 Alloys", *Materials Chemistry and Physics*, 53 (1998) 195-202.
65. G.K. Sigworth, S. Shivkumar and D. Apelian, "The Influence of Molten Metal Processing on Mechanical Properties of Cast Al-Si-Mg Alloys", *AFS Transactions*, 97, 1989, 811-824.
66. A.M. Samuel and F.H. Samuel, "Various Aspects Involved in the Production of Low-Hydrogen Aluminium Castings", *Journal of Materials Science*, 27 (1992) 6533-6563.
67. T.A. Utigard, K. Friesen, R.R. Roy, J. Lim, A. Silny and C. Dupuis, "The Properties and Uses of Fluxes in Molten Aluminium Processing", *Journal of Metals*, Nov. 1998, 38-43.
68. S. Makarov, D Apelian and R. Ludwig, "Inclusion Removal and Detection in Molten Aluminum: Mechanical, Electromagnetic, and Acoustic Techniques", *AFS Transactions*, 107, 1999, 727-735.
69. J.E. Gruzleski, "The Art and Science of Modification : 25 Years of Progress", *AFS Transactions*, 100, 1992, 673-683.
70. Shiukumar, L. Wang and D. Apelian, "Molten Metal Processing of Advanced Cast Aluminum Alloys", *Journal of Metals*, Jan. 1991, 26-32.

71. G.K. Sigworth and T.A. Engh, "Chemical and Kinetic Factors Related to Hydrogen Removal From Aluminum", *Metallurgical Transactions B*, 13B, 1982, 447-460.
72. R. Fuoco, E.R. Correa, M. De Andrade Bastos and L.S. Escudero, "Characterization of Some Types of Oxide Inclusions in Aluminum Alloy Castings", *AFS Transactions*, Vol. 107 (1999) pp. 287-294.
73. X. Li and X. Bian, "Behaviour of Hydrogen in Superheated Aluminium and its Alloys Melt" *Materials Science Forum*, vols. 331-337 (2000) 209-214.
74. C.W. Booth and A.J. Clegg, "Porous Plug Degassing of Aluminium Alloys", *Br. Foundryman*, 77 (1984) 96-106.
75. S. Fox and J. Campbell, "Visualisation of Oxide and Film Defects During Solidification of Aluminium Alloys", *Scripta Materialia*, Vol. 43 (2000) pp. 881-886.
76. D. Shu, B.D. Sun, J. Wang, T.X. Li and Y.H. Zhou, "Study of Electromagnetic Separation of Nonmetallic Inclusions From Aluminum Melt", *Metallurgical and Materials Transactions A*, 30A (1999) pp. 2979-2988.
77. R.W. Lobenhofer and A.T. Spada, "Selecting a Spectrometer for Your Operation", *Modern Casting*, (2000) pp. 42.
78. T. Gudmundsson, T. Sigfussion, D.G. McCartney, E. Wuilloud and P. Fisher, "Efficiency of Holding Time in a Casting Furnace", *Light Metals*, ed. J. Evans, TMS, 1995, pp. 855-858.
79. X. Cao and J. Campbell, "Effect of Precipitation of Primary Intermetallic Compounds on Tensile Properties of Cast Al-11.5Si-0.4Mg Alloy", *AFS Transactions*, 108, 2000, 391-400.
80. M. Maniruzzaman and M. Makhlof, "Modeling of Flotation Process in Aluminum Melt Treatment", *Modeling of Casting, Welding and Advanced Solidification Processes VIII: Edited by B.G. Thomas and C. Beckermann*, The Mineral, Metals & Materials Society, (1998) pp. 705-712.
81. M. Maniruzzaman and M. Makhlof, "Mathematical Modelling and Computer Simulation of the Rotating Impeller Particle Flotation Process: Part I. Fluid Flow", *Metallurgical and Materials Transactions B*, 33B, 4, 2002, 297-303.
82. M. Maniruzzaman and M. Makhlof, "Mathematical Modelling and Computer Simulation of the Rotating Impeller Particle Flotation Process: Part II. Particle

- Agglomeration and Flotation”, Metallurgical and Materials Transactions B, 33B, 4, 2002, 305-314
83. B. Sirrell and J. Campbell, "Mechanism of Filtration in Reduction of Casting Defects Due to Surface Turbulence During Mold Filling", AFS Transactions. Vol. 105 (1997) pp. 645 - 654.
 84. S. Makarov, R. Ludwig and D. Apelian, "Electromagnetic Separation Techniques in Metal Casting. I. Conventional Methods", IEEE Transactions on Magnetics. Vol. 36, 4, 2000, 2015-2121.
 85. S. Makarov, R. Ludwig and D. Apelian, "Electromagnetic Separation Techniques in Metal Casting. II. Separation with Superconducting Coils", IEEE Transactions on Magnetics, vol. 37, 2, 2001, 1024-1031.
 86. G.F. Eskin, "Broad prospects for Commercial Application of the Ultrasonic (Cavitation) Melt Treatment of Light Alloys", Ultrasonics Sonochemistry, 8 (2001) 319-325.
 87. J.L. Roberge and M. Richard, "Instantaneous Evaluation of Inclusion Quantity of Liquid Aluminium Alloys", Materials Science Forum, vols. 217-222 (1996) 135-140.
 88. M.J. Lessiter and W.M. Rasmussen, "To pour or Not to Pour: The Dilemma of Assessing your Aluminum Melt's Cleanliness", Modern Casting, Feb. 1996, 45-48.
 89. V. Thomsen, G. Roberts and C. Otten, "Spectroscopy '97: Not Just for Chemistry Anymore", Modern Casting (1997) pp. 33-35.
 90. P. Cooper, A. Jacob and A. Detomi, "Additive Developments in the Aluminium Industry", 1st International Congress of the Aluminum Industry, November 21st -23rd, 2000 Sao Paulo, Brazil.
 91. P. Cooper and M. Kearns, "Removal of Transition Metal Impurities in Aluminium Melts by Boron Additives", Materials Science Forum, vols, 217-222, 1996, 141-146
 92. A. Flores-V., M. Sukiennik, A.H. Castillejos-E., F.A. Acosta-G., and J.C. Escobedo-B., "A Kinetic Study on the Nucleation and Growth of the $Al_8FeMnSi_2$ Intermetallic Compound for Aluminum Scrap Purification", Intermetallics, 6 (1998) 217 -227.
 93. S.G. Shabestari and J.E. Gruzleski, "Gravity Segregation of Complex Intermetallic Compounds in Liquid Aluminum-Silicon Alloys", Metallurgical and Materials Transactions A, 26A, 5, 1995, 999-10006.

94. J.H. Kim and E-P. Yoon, "Elimination of Fe Element in A380 Aluminium Alloy Scrap by Electromagnetic Force", *Journal of Materials Letters*, 19 (2000) 253-255.
95. N. Unlu and M.G. Drouet, "Comparison of Salt-Free Aluminium Dross Treatment Processes", *Resources, Conservation and Recycling*, 36, 2002, 61-72.
96. R.A. Lindberg, "Processes and Materials of Manufacture", 4th Edition, Prentice Hall, New Jersey (1990).
97. N.B. Luther, "Metal Casting and Molding Processes", *Engineering Casting Solutions*, Web Article (www.castingsource.com) 2002.
98. F. Schleg and P.D. Kanicki, "Guide to Casting and Molding processes", *Modern Casting* (1999) pp. 18-27.
99. G.E. Dieter, "Engineering Design – A materials and Processing Approach", McGraw – Hill Book Company, (1983).
100. J. Campbell, "The Concept of Net Shape for Casting", *Materials and Design*, Vol. 21 (2000) pp. 373-380.
101. J.R. Brown, "Foseco Non-Ferrous Foundryman's Handbook", 11th ed Butterworth-Heinemann, Oxford (1999).
102. A.M. Lovatt, D. Bassetti, H.R. Shercliff and Y. Brechet, "Process and Alloy Selection for Aluminum Casting", *International Journal for Cast Metals Research*, Vol. 12 (1999) pp. 211-225.
103. A.M.K. Esawi and M.F. Ashby, "The Development and Use of a Software Tool for Selecting Manufacturing Processes at the Early Stages of Design", In proceedings of the Third Biennial World Conference on Integrated Design and Process Technology (IDPT), Berlin, Germany, July 5-9, Vol. 3 (1998) pp. 210-217.
104. C.S. Smith III, "The Manufacturing Advisory Service: Web Based Process and Material Selection", Ph.d Dissertation, Mechanical Engineering Department, University of California, Berkeley, USA (1999).
105. Granta Design Ltd., Developers and Distributors of Cambridge Engineering Selector (CES), Trumpington Mews, 40B High Street, Trumpington, Cambridge CB2 2LS, UK, www.grantadesign.com

106. A.M. Lovatt, 'Process Selection in Engineering Design', Ph.D Dissertation, Cambridge University Engineering Department, University of Cambridge, Cambridge, UK (1998).
107. M.M. Akarte, B. Ravi and R.C. Creese, "Casting Process Selection Using AHP and Fuzzy Logic", Presented at the International Seminar on Manufacturing Technology Beyond 2000, Bangalore, November 1999.
108. S.M. Darwish and A.M. El-Tamimi, "The Selection of the Casting Process Using an Expert System", Computers in Industry, Vol. 30 (1996) pp. 77-86.
109. J. Campbell, "Ten Rules for Good castings", Modern Casting, Vol. 87, 4 (1997) pp. 36-39.
110. J. Campbell, "Review: Developments in Filling System Design", CIATF International Technology Forum, (1997) pp. 17.
111. X. Yang, M.R. Jolly and J. Campbell, "Minimization of Surface Turbulence During Filling Using a Vortex-Flow Runner", Aluminum Transactions, Vol. 2, 1 (2000) pp. 67 - 80.
112. S. Guleyupoglu, "Casting Process Design Guidelines", AFS Transactions, Vol.105 (1997) pp. 465 - 471.
113. X. Yang and J. Campbell, "Liquid Metal Flow in A Pouring Basin", International Journal Cast Metals Research, Vol. 10 (1998) pp. 239 – 253.
114. X. Yang, T. Din and J. Campbell, "Liquid Metal Flow in Molds with Off-set Sprue", International Journal of Cast Metals Research, Vol.11 (1998) pp. 1-12.
115. M.R. Jolly, H.S.H. Lo, M. Turan and J. Campbell, "Development of Practical Quiescent Running Systems Without Foam Filters for Use in Aluminum Castings Using Computer Modeling", In modeling of Casting, Welding and Advanced Solidification Processes IX, Edited by P.R. Salim, P.N. Hansen and J.G. Conley, pp. 319 - 323.
116. B. Sirrell and J. Campbell, "Mechanism of Filtration in Reduction of Casting Defects Due to Surface Turbulence During Mold Filling", AFS Transactions. Vol. 105 (1997) pp. 645 - 654.
117. M. Rezvani, X. Yang, and J. Campbell, "Effect of Ingate Design of Strength and Reliability of Al Castings", AFS Transactions, Vol.106 (1998) pp. 181 - 188.

118. C. Nyahumwa, N.R. Green and J. Campbell, "Effect of Mold-Filling Turbulence on Fatigue Properties of Cast Aluminum Alloys", AFS Transactions, Vol. 106 (1998) pp. 215-223.
119. M. Cox, M. Wickins, J.P. Kuang, R.A. Harding and J. Campbell, "Effect of Top and Bottom Filling on Reliability of Investment Castings in Al, Fe and Ni Based Alloys", Materials Science and Technology, Vol. 16 (Dec.2000) pp.1445-1452.
120. F.R. Mollard and N. Davidson, "Experience With Ceramic Foam Filtration of Aluminum Castings", AFS Transactions, Vol. 88 (1980) pp. 595-600.
121. R. Nariman, "Gating Design via Computer Fluid Flow Modeling", Modern Casting, (1999) pp. 43.
122. J. Campbell, "Invisible Macro-Defects in Castings", Journal De Physique IV, Colloque C7, Supplement au Journal de Physique III, Vol. 3, Novembre (1993) pp. 861-872.
123. S.D. Pathak and O. Prabhakar, "Phenomenological Analysis of Feeding in Aluminum Base Alloys", AFS Transactions, Vol. 92 (1984) pp. 671-680.
124. J.T. Berry, R.P. Taylor and R.A. Overfelt, "Porosity Patterns in A356 Bar and Plate Castings and Their Relation to Riser Design", AFS Transactions, Vol. 105 (1997) pp. 465-471.
125. J.T. Berry and R.P. Taylor, "Improving Casting Performance by Extending Feeding Action in Long-Freezing Range Cast Aluminum Alloys", AFS Transactions, Vol. 107 (1999) pp. 203-206.
126. K. Radhakrishna and S. Seshan, "Application of Chills for Aluminum Alloy Castings", AFS Transactions, Vol. 89 (1981) pp.437 - 444.
127. T.C. Wright and J. Campbell, "Enhancing Aluminum Casting Solidification Via Cooling Fins", Modern Casting, Nov.1998, pp. 48-50.
128. M. Cox, R.A. Harding and J. Campbell, "Optimal Running System Design for Bottom Filled Aluminium Alloy 2L99 Investment Castings" Materials Science and Technology, 19 (2003) 613-625.
129. T.C. Midea and D. Schmidt, "1999 Casting Simulation Software Survey", Modern Casting, (1998) pp. 43.

130. M. Nainy-Nejad, R.C. Creese and B. Ravi, "Research Issues in Computer-Aided Parting Design for Casting", AFS Transactions, Vol. 105 (1997) pp. 545-550.
131. O. Vorren, J.E. Evensen and T.B. Pedersen, "Microstructure and Mechanical Properties of AlSi(Mg) Casting Alloys", AFS Transactions, Vol. 92 (1984) pp. 459 - 466.
132. L. Siaminwe and A.J. Clegg, "Effect of processing Variables on Structure and Tensile Properties of Investment Cast Al-Si-Mg Casting Alloy", Materials Science and Technology, Vol. 15 (July 1999) pp. 812-820.
133. Q.G. Wang, D. Apelian and D.A. Lados, "Fatigue Behavior of A356/357 Aluminum Cast Alloys. Part II - Effect of Microstructural Constituents", Journal of Light Metals, Vol. 1 (2001) pp.85-97.
134. C.H. Caceres and B.I. Selling, "Casting Defects and the Tensile Properties of an Al-Si-Mg Alloy", Materials Science and Engineering, Vol. A220 (1996) pp. 109-116.
135. M.K. Surappa, E. Blank and J.C. Jacquet, "Effect of Macro-porosity on the Strength and Ductility of Cast Al-7Si-0.3Mg Alloy", Scripta Metallurgica, Vol. 20, 9 (1986) pp.1281-1286.
136. C.H. Caceres, "On the Effect of Macroporosity on the Tensile Properties of the Al-7%Si-0.4%Mg Casting Alloy", Scripta Metallurgica et Materialia, Vol. 32 (1995) pp.1851-1856.
137. M.H. Lee, J.J. Kim, K.H. Kim, N.J. Kim, S. Lee and E.W. Lee, "Effects of HIPping on High-Cycle Fatigue Properties of Investments Cast A356 Aluminum Castings", Materials Science and Engineering, In Press (2002).
138. C.H. Caceres, J.R. Griffiths and P. Reiner, "The influence of Microstructure on the Bauschinger Effect in an Al-Si-Mg Casting Alloy", Acta Materialia, Vol. 44, 1 (1996) pp.15-23.
139. Q.G. Wang and C.H. Caceres, "The Fracture Mode in Al-Si-Mg Casting Alloys", Materials Science and Engineering, Vol. A241 (1998) pp.72-82.
140. Q.G. Wang, C.H. Caceres and J.R. Griffiths, "Cracking of Fe-Rich Intermetallics and Eutectic Si Particles in an Al-7Si-0.7Mg Casting Alloy", AFS Transactions, Vol. 106 (1998) pp.131-136.

141. C.H. Caceres and J.R. Griffiths, "Damage by the Cracking of Silicon Particles in an Al-7Si-0.4Mg Casting Alloy", *Acta Materialia*, Vol. 44, 1 (1996) pp 25-33.
142. C.H. Caceres, C.J. Davidson and J.R. Griffiths, "The Deformation and Fracture Behavior of an Al-Si-Mg Casting Alloy", *Materials Science and Engineering*, Vol 197 (1995) pp.171 - 179.
143. M.D. Dighe and A.M. Gokhale, "Relationship Between Microstructural Extremum and Fracture Path in a Cast Al-Si-Mg Alloy", *Scripta Materialia*, Vol. 37, 9 (1997) pp.1435 - 1440.
144. C.H. Caceres and Q.G. Wang, "Dendrite Cell Size and Ductility of Al-Si-Mg Casting Alloys: Spear and Gardener Revisited", *International Journal of Cast Metals Research*, Vol. 9 (1996) pp.157-162.
145. J.T. Berry, G.S. Jalewalia and R.G. Kumble, "Anisotropy in Aluminum Castings – 25 Years On", *AFS Transactions*, Vol. 108, 2000, 733-740.
146. K.J. Oswalt and M.S. Misra, "Dendrite Arm Spacing (DAS): A Nondestructive Test to Evaluate Tensile Properties of Premium Quality Aluminum Alloy (Al-Si-Mg) Castings", *AFS Transactions*, Vol. 88 (1980) pp. 845-862.
147. K. Radhakrishna, S. Seshan and M.R. Seshadri, "Dendrite Arm Spacing in Aluminum Alloy Castings", *AFS Transactions*, Vol. 88 (1980) pp. 695-702.
148. G. Atxaga, P. Pelayo and A.M. Irisarri, "Effect of Microstructure on Fatigue Behavior of Cast Al-7Si-Mg Alloy", *Materials Science and Technology*, Vol. 17, 4 (2001) pp 445-450.
149. D.L. Zhang, L.H. Zheng and D.H. StJohn, "Effect of a Short Solution Treatment Time on Microstructure and Mechanical Properties of Modified Al-7wt%Si-0.3wt%Mg Alloy", *Journal of Light Metals*, In press (2002).
150. G. Petzow, "Metallographic Etching", ASM, Metals Park, Ohio (1978).
151. G.F. Vander Voort, "Metallography-Principles and Practice", McGraw-Hill Book Company, USA (1984).
152. T.O Mbuya, B.O. Odera and S.P. Ng'ang'a, "Influence of Iron on Castability and Properties of Aluminum Silicon Alloys", *International Journal of Cast Metals Research* Vol. 16, 5, 2003 (in press).

153. M.E. Seniw, J.G. Conley and M.E. Fine, "The Effect of Microscopic Inclusion Locations and Silicon Segregation on Fatigue Lifetimes of Aluminum Alloy A356 Castings", *Materials Science and Engineering*, Vol. A285 (2000) pp. 43-48.
154. R. Venkataramani, R. Simpson and C. Ravindran, "Effect of Melt Superheat on Maximum Nuclei Density in A356 Alloy", *Materials Characterization*, 35 (1995) 81-92.
155. A.K. Dahle, J.E.C. Hutt, Y.C. Lee and D.H. StJohn, "Grain Formation in Hypoeutectic Al-Si Alloys", *AFS Transactions*, Vol. 107 (1999) pp. 265-270.
156. J.E.C. Hutt, D.H. StJohn, L. Hogan, and A.K. Dahle, "Equiaxed Solidification of Al-Si Alloys", *Materials Science and Technology*, 15 (1999) 495-500.
157. J.E.C. Hutt, D.H. StJohn, "The Origins of the Equiaxed Zone", *International Journal of Cast Metals Research*, 11 (1998) 13-22.
158. M.A. Easton and D.H. StJohn, "The Origin of Equiaxed Crystals in Grain Refined Aluminum Alloys", *Aluminum Transactions*, Vol. 1, 1 (1999) pp.51-59.
159. L.Wang, D. Apelian and M. Makhlof, "Tensile Properties of Aluminum Diecasting Alloys", In *Proceedings of 19th International Diecasting Congress*, Nov. 3-6, 1997, Minneapolis, MN, Published by NADCA, Rosemont Illinois, (1997) pp. 179 – 189.
160. J.H. Sokolowski, X.-C Sun, G. Byczynski, D.O. Northwood, D.E. Penrod, R. Thomas and A. Esseltine, "The Removal of Copper-Phase Segregation and the Subsequent Improvement in Mechanical Properties of Cast 319 Aluminum Alloys by a Two-Stage Solution Heat Treatment", *Journal of Materials Processing Technology*, 53(1995)585-392.
161. J.H. Sokolowski, M.B. Djurdjevic, C.A. Kierkno and D.O. Northwood, "Improvement of 319 Aluminum Alloy Casting Durability by High Temperature Solution Treatment", *Journal of Materials Processing Technology*, 109(2001) 174-180.
162. E. Cerri, M. Cabibbo, P. Cavaliere and E. Evangelista, "Mechanical Behavior of 319 Heat Treated Thixo Cast Bars", *Materials Science Forum*, 331-337 (2000) 259-264.